Pb ve Zn Flotasyon Atıklarından Baz ve Kıymetli Metallerin Entegre Eko-Teknoloji ile Seçimli Kazanımı

Shokrullah Hussaini

DOKTORA TEZİ

Maden Mühendisliği Anabilim Dalı

Mayıs 2022

Integrated Eco-Technology for a Selective Recovery of Base and Precious Metals in Zn and Pb Flotation Tailing

Shokrullah Hussaini

DOCTORAL DISSERTATION

Department of Mining Engineering

May 2022

Integrated Eco-Technology for a Selective Recovery of Base and Precious Metals in Zn and Pb Flotation Tailing

A thesis submitted to the Eskişehir Osmangazi University

Graduate School of Natural and Applied Sciences in partial

Fulfillment of the requirements for the degree of DOCTOR of PHILOSOPHY

In Discipline of Mineral Processing of the Department of Mining Engineering

By

Shokrullah Hussaini

Supervisor: Prof. Dr. Muammer Kaya

This thesis was supported by TÜBİTAK within framework of the project no.217M959

May 2022

APPROVAL OF THE THESIS

The thesis titled "**Integrated Eco-Technology for a Selective Recovery of Base and Precious Metals in Zn and Pb Flotation Tailing**" and submitted by **Shokrullah Hussaini** has been accepted as satisfactory in partial fulfillment of the requirements for the degree of Doctor of Philosophy in Department of **Mining Engineering**.

Supervisor : Prof. Dr. Muammer Kaya

Co-Supervisor : -

Examining Committee Members:

Member: Prof. Dr. Muammer Kaya
Member: Prof. Dr. Haldun Kurama
Member: Assoc. Prof. Dr. Derya Öz Aksoy
Member: Prof. Dr. Hüseyin Koca
Member: Prof. Dr. Ali Uçar

Graduation of Shokrullah Hussaini was approved by the Graduate School Board Decision on ………………with the decision number of ……………………..

Prof. Dr. Hürriyet ERŞAHAN
Director of the Institute

ETHICAL STATEMENT

I hereby declare that this thesis study titled “Integrated Eco-Technology for a Selective Recovery of Base and Precious Metals in Zn and Pb Flotation Tailing” has been prepared in accordance with the thesis writing rules of Eskisehir Osmangazi University Graduate School of Natural and Applied Sciences under academic consultancy of my supervisor Prof. Dr. Muammer Kaya. I hereby declare that the work presented in this thesis is original. I also declare that, Ihave respected scientific ethical pronciples and rules in all stages of my thesis study, all information and data presented in this thesis have been obrained within the scope of scientific and academic ethical principles and rules, all materials used in this thesis which are not original to this work have been fully cited and referenced, and all knowledge, documents and results have been presented in accordance with scientific ethical principles and rules. 11.05.2022

Shokrullah Hussaini

ÖZET

Bu çalışmada, çinko ve kurşun flotasyon atıklarından liç, solvent ekstraksiyon ve elektroliz yöntemi ile baz ve kıymetli metallerin kazanımı incelenmiştir. Laboratuvar ölçeğinde üç kademeli, seçimli ve kesikli liç deneyleri yapılmıştır. Liç testleri en az 25 g temsili numune ile 1/10 katı/sıvı oranında 500 mL'lik ısıtmalı cam balon ve spiral yoğuşturuculu reaktörde yapılmıştır. Birinci aşama Zn liçinde 17 farklı liç reaktifi; ikinci aşama Pb liçinde 10 farklı liç reaktifi ve üçüncü aşama Ag liçinde 2 farklı liç reaktifi test edilerek optimizasyon sağlanmıştır. Birinci aşama liç için H_2SO_4, sitrik asit ve malik asit %90'dan fazla Zn çözünmesini, yüksek Zn-Pb ve Zn-Fe seçimli çözünürlük farkı sağladığından en iyi liç reaktifleri olarak seçilmişlerdir. İkinci aşamada NaOH+KNa-tartart karışımı %85'den fazla Pb çözünümü sağladığı için optimum seçilmiştir. Solvent ekstraksiyonu öncesi, birinci aşama liç yüklü çözeltileri hidrolitik ve H_2SO_4 çöktürme saflaştırmalarına Fe ve As safsızlıklarını gidermek için tabi tutulmuştur. Hidrolitik çöktürme sonunda oluşan Fe'ce zengin atıklar ve jips atık barajına gönderilebilir. Saflaştırma sonrası D2EHPA+hekzan ile pH: 2.6'da solvent ekstraksiyonu (SX) %98 Zn'i organik faza almıştır. Sitrik ve malik asit PLS'leri H_2SO_4 ile çöktürme saflaştırmasına tabi tutulmuş ve 98.9 Pb ile %96.7 Pb, $PbSO_4$ olarak uzaklaştırılmıştır. Saflaştırılan sitrik ve malik asit PLS'leri sırasıyla %20 D2EHPA ile pH: 3.6'da %98.3 Zn ekstraksiyonu ve %10 D2EHPA ile pH: 4.2'de %98 Zn ekstraksiyonu vermiştir. Organiğe aktarılan Zn daha sonra pH: 0.25'te H_2SO_4 PLS'inden %100, sitrik asit PLS'inden pH: 0.25'te %100 ve malik asit PLS'inden pH: 0.5'te %98.7 Zn mertebesinde sıyrılmıştır. Asidik pH'larda yapılan elektroliz ile %99'dan fazla Zn metal kazanımı H_2SO_4 ve sitrik asit PLS'lerinden ve %97 Zn metal kazanımı malik asit PLS'inden %99 saflıkta kazanılmıştır.

Anahtar kelimeler: Flotasyon atıkları, Çinko, Kurşun, Liç, Organik asit, Solvent ekstrasiyon

SUMMARY

In this study, recovery of base and precious metals from zinc-lead flotation tahiling by leaching, solvent extarction and electrowinning was investigated. Three-stage selective and batch laboratory leach tests were performed. A minimum 25 g sample with 1/10 S/L ratio was used. 500 mL balloon flask reactors with glass spiral reflux condensers were employed in leaching. In the first-stage Zn leaching 17 different reagents, in the second-stage Pb leaching 10 different reagents, and in the third-stage Ag leaching 2 different reagents were tested and optimized. In the first-stage leaching, H_2SO_4, citric acid, and malic acid achieved more than 90% Zn dissolution with high Zn-Pb and Zn-Fe dissolution selectivity differences. In the second-stage leach, NaOH+KNa-tartrate provided more than 85% Pb dissolution and was selected as the optimum reagent. Prior to solvent extraction (SX), the first-stage H_2SO_4 leach PLS was purified by hydrolytic precipitation using NaOH+H_2O_2. After hydrolytic precipitation, Fe-rich waste and gypsum were produced. After purification of H_2SO_4 PLS, SX with 20% D2EHPA+hexane at pH: 2.6 achieved 98% Zn extraction to the organic phase. Citric and malic acid PLSs were subjected to the $PbSO_4$ precipitation with 98.9% Pb and 96.7% Pb, respectively using H_2SO_4. Purified citric and malic acid PLSs were subjected to SX using 20% D2EHPA+hexane at pH of 3.6 and 10% D2EHPA+Hexane at pH of 4.2 to obtain more than 98% extraction. 100% Zn was stripped from the organic phase to the aqueous phase at pH of 0.25 from H_2SO_4 and citric acid PLSs. 98.7% Zn was stripped at pH of 0.5 from malic acid PLS. Electrowinning (EW) at acidic pHs, achieved 99% Zn metal recovery from H_2SO_4 and citric acid PLSs and 97% Zn metal from malic acid PLS with 99% Zn purity.

Keywords: Flotation tailing, Zinc, Lead, Leaching, Organic acid, Solvent extraction

ACKNOWLEDGMENTS

I would like to thank my supervisor Prof. Dr. Muammer Kaya for his excellent guidance, patience, motivation, and friendly behaviour. His guidance helped me throughout my time of research and the writing of this thesis. I would like to thank Assoc. Prof. Dr. Sait Kursunoglu for his continuous help, enthusiastic encouragement, and valuable advice during experiments. It would be almost impossible to have completed this task without his contribution.

My special and the biggest thank you goes to my kind parents for their sacrifice, patience, courage, motivation and support during my PhD research.

I would like to express my gratitude and thanks to Yurtdışı Türkler ve Akraba Toplulukar Başkanlığı (YTB) of the Republic of Turkey and TÜBİTAK providing financial support to finish successfully my doctoral studies at ESOGU in Turkey.

Lastly, I would like to thank Angela Manka Tita, Umut Kar and Erkan Gul for helping me in the laboratory experimental works

LIST OF CONTENTS

Page

LIST OF CONTENTS (Continued)

Page

LIST OF CONTENTS (Continued)

LIST OF CONTENTS (Continued)

LIST OF CONTENTS (Continued)

LIST OF FIGURES

LIST OF FIGURES (continued)

Figure **Page**

LIST OF FIGURES (continued)

LIST OF FIGURES (continued)

LIST OF FIGURES (continued)

Figure **Page**

LIST OF FIGURES (continued)

Figure **Page**

LIST OF FIGURES (continued)

Figure **Page**

LIST OF FIGURES (continued)

Figure **Page**

LIST OF TABLES

LIST OF TABLES (continued)

Table **Page**

LIST OF ABBREVIATION AND SYMBOLS

Symbols	**Descriptions**
A/O	Aqueous/Organic
Ag	Silver
Al	Aluminum
AR	Aqua regia
As	Arsenic
ASTM	American Society for Testing and Materials
Au	Gold
Cd	Cadmium
CE	Current density
Cu	Copper
CYNAEX 272	Bis-(2,4,4-trimethylpentyl) phosphinic acid
D2EPHA	Di-(2-ethylhexyl)phosphoric Acid
EAFD	Electric arc furance dust
EDTA	Ethylenediaminetetraacetic Acid
EW	Electrowinning
Fe	Iron
H_2SO_4	Sulfuric acid
HCl	Hydrochloric acid
HNO_3	Nitric acid
IX	Ion Exchange
K	Potassium
Mn	Manganese
mV	Millivolt
Ni	Nickel
O	Oxygen
oC	Celsius
Pb	Lead

LIST OF ABBREVIATION AND SYMBOLS (Continued)

Symbols	**Descriptions**
PLS	Pregnant Leach Solution
PM	Precious Metal
Ppm	Part per Million
rpm	Revolutions per Minute
Sb	Antimony
S/L	Solid/liquid
Sn	Tin
SX	Solvent Extraction
TBP	Tributyl Phosphate
TGA	Thermogravimetric Analysis
t-T	Time Temperature
USGS	United States Geological Survey
W	Watt
Wt	Weight
XRF	X-Ray Fluorescence
XRD	X-Ray Diffraction
Zn	Zinc
ΔG	Difference in Gibbs Free Energy
μm	Micrometer

1. INTRODUCTION AND PURPOSE

During the recovery and processing of nonferrous metal from ores, metal-bearing mining waste is generated. Mining waste, which contains both base and precious metals, might be considered a valuable secondary resource. However, the presence of harmful materials for the environment, such as air, soil, and water, should be considered. The majority of these solid-state mining wastes were dumped into tailing reservoirs with no active control. Still huge capabilities are still being produced. Metals production and recovery from mining waste both require the development of efficient, low-temperature, and environmentally friendly technology.

Due to the formation of acid mine drainage (AMD) and the dispersion of metals into the environment as a result of the exposure of these tailings to atmospheric oxygen, bacteria, and water, which can cause severe degradation of water quality in both subsurface and surface systems, as well as soil in their vicinity, tailings containing metal sulfides present particular challenges for responsible waste management. However, impurities like as clay minerals and pyrite lead the flotation tailings to become more complicated and low-grade, resulting in increased reagent consumption and lower yield of high-grade concentrate. Flotation tailings are typically produced as a byproduct of metal ore beneficiation, specifically froth flotation prior to pyrometallurgical operations. Approximately 90–95 % of the plant's general tailings, such as flotation tailings and cleaning tailings, come from the flotation process and are referred to as flotation tailing.

Greater flotation tailings are expected to be produced in the coming years as a result of increased exploration of nonferrous metal ores and the discovery of lower-grade deposits, potentially causing more environmental issues and disputes. A prospective future metal resource is made up of flotation tailings and low-grade nonferrous metal ores (Antonijević et al., 2008).

Zinc and lead have historically been important base metals, and they are generally found together in Zn–Pb ores and tailing, which are used not only as metals but also as additives in a variety of industries. Grinding is used to concentrate lead-zinc ores, followed by a sequential flotation process in which lead minerals are floated first, followed by flotation of zinc minerals.

There was a wide range of lead and zinc resources, as well as many different types of lead and zinc oxides. Zinc and its companion lead are manufactured in a sequential manner around the world, with pyrometallurgical and hydrometallurgical processes used selectively depending on the raw material. After aluminum and copper, zinc is the most often utilized non-ferrous metal. Apart from its primary use (about 70%) in steel galvanizing, it is also used in sheets, anodes, castings, chemicals, micronutrients, paints, dry cells, and other applications. The gap between demand and availability for zinc is expanding as its use grows. Many of these applications provide opportunities for zinc recycling. Around 30% of the world's annual zinc production or around 10 million tons is produced in the United States. (Asadi et al., 2017; Najiba, 2009) Sunkar, 2005).

Lead and zinc are minerals that are naturally connected with one another. Every lead and zinc deposit has three different types of mineralization:

a) Sulphide ores, which are primarily found in the hypogene primary sulphide ore body, where mineralization occurs over numerous phases, and from which lead and zinc are extracted. The primary sulphide minerals of zinc and lead are sphalerite (ZnS) and galena (PbS), respectively.

b) Hypogene and supergene weathering are two forms of nonsulphide ores. The cap of hypogene oxidized ores usually protects the primary sulphide ore body from supergene weathering. The absence of sulphide minerals and their outcropping at the surface, or their existence near the surface, are signs of supergene oxidation ores.

c) Mixed sulphide–oxide ores with a complex mineralogy that are most commonly found in the transition zones of deposits, but can also be found in the oxidized zones. (Gilg et al., 2006).

Innovative mineral processing and hydrometallurgy approaches are offered for extracting nonferrous metal from flotation tailing. Academics will examine the major phases (pre-concentration, leaching, and high-grade metal recovery) in depth in order to improve the initial relevant process sequences.

Hydrometallurgical separation technologies are now an important aspect of extractive metallurgy, used in a variety of metal refining plants across the world and resulting in lower capital and operational costs. Hydrometallurgical separation techniques are ideal. They're known for being adaptable, highly selective, and ecologically friendly procedures for treating raw materials of various amounts and compositions (Sami, 2013; Yan et al., 2014).

Flotation is the primary method for processing zinc and lead ores, especially those with high sulfur concentration. . The goal of this study is to create novel sustainable ecological and economical procedures for recovering commercially important base metals (Zn and Pb) and precious metal (Ag) from wastes generated from flotation tailing leaching. The flotation tailing sample used in this investigation is made up of oxidized lead and zinc ore taken from Kayseri province.

To achieve this aim, the following objectives were defined:

- Evaluate the leaching of zinc and lead with use of different reagents (organic and inorganic acids and alkaline)

- Determine the effect of reagent concentration, temperature, solid/liquid ratio on the leaching performance

- Perform mass balances using the leaching test results to determine which combination would provide the highest zinc recovery and lower impurity accumulation

- Determine the best purification of leach solution for removal of impurities (Fe, As, Cd, Cu, Ni and Al)

- Electrowinning of zinc solution after purification step for recovery of zinc metal from solution

2. LITERATURE REVIEW

2.1. Introduction

This chapter provides general information about zinc and lead, from their histories to their properties and sources. Lead and zinc production processes are discussed in depth. In addition, several of the uses of lead and zinc are discussed. Finally, prior studies on zinc and lead production in Turkey and around the world are summarized.

2.2. General Information about Zinc

After steel, aluminum, and copper, zinc is the fourth most extensively used metal on the planet. Because it is chemically active and has a high proclivity for forming compounds with other elements, demand for the metal and its alloys has grown. Major application fields can easily be expected and named as galvanizing or coating industries of base metals, die casting of zinc alloys manufacturing of brass, and paint pigments production for chemical industries as a result of its chemical qualities. According to surveys, the value of metallic zinc is predicted to rise if the current economic situation and development continue (Ilzsg, 2020).

2.2.1. Chemical and physical characterasitics of zinc

Zinc has the chemical symbol Zn, an atomic number of 30 and a mass of 65.39 g. There are five stable isotopes of zinc found in nature. Zinc is a transition metal with a hue that is bluish pale gray. It demonstrates excellent thermal and electrical conductivity. Furthermore, it is exceedingly brittle at room temperature yet pliable between 120 and 1500 degrees Celsius. It may be wrapped into sheets between these temperatures because of its property. Other physical, atomic, and other properties of zinc are shown in Table 2.1 (Ruşen et al., 2008).

2.2.2. Minerals of zinc

In nature, sphalerite is the most important zinc metal mineral. Zinc minerals are generally divided into six categories. Table 2.2 shows them all.

Table 2.1. Properties of zinc (Addemir et al., 1994; Wikipedia, 2020)

Solid density (at RT)	7.14 g/cm^3	Ionization energies (1st)	1733.3 KJ/mol
Liquid density(at MP)	6.57 g/cm^3	Ionization energies (2nd)	1733.3 KJ/mol
Melting point	419.5 ^{0}C	Atomic radius	135 picometer
Boiling point	907 ^{0}C	Magnetic ordering	Diamagnetic
Heat of fusion	7.32 KJ/mol	Electrical resistivity (20 ^{0}C)	59 n.Ώ.m
Heat of vaporization	123.6 KJ/mol	Thermal conductivity (20 ^{0}C)	116 W/m.K
Heat capacity (at 25 ^{0}C)	25.390 J/mol·K	Thermal expansion (25 ^{0}C)	30.2 µm/ m.K

Table 2.2. Minerals of zinc (Istanbul mineral exporters association, 1998)

Groups of mineral	Name of mineral	Chemical formulas
Sulfides	Sphalerite (zinc blend)	ZnS
	Vurtzite	ZnS
	ZnS	$4ZnS+ZnO$ Zn_5S_4O-$4ZnS.ZnO$
	Zinc - Teallite	$(Pb, Zn) Sn S_2$
Sulfates	Goslarite (Zincvitriol)	$ZnSO_4.7H_2O$
	Zinc- Melanterit	$(Fe, Zn)SO_4.7H_2O$
	Zinc- Copper Melanterit	$(Fe, Zn)SO_4.5H_2O$
Carbonates	Smithsonite	$ZnCO_3$
	Hidrozincite (Zincblute)	$ZnCO_3$ $3Zn(OH)_2$
	Zincocalsite	$(Ca,Zn)CO_3$ (kind of calcite)
	Nicholsonite	$(Ca,Zn)CO_3$ (kind of aragonite)
	Aurichalcite	$2(Zn,Cu)CO_3.3(Zn,Cu)OH_2$
Silicates	Hemimorphite	$H_2Zn2SiO_5(ZnOH)_2$ SiO_3

Table 2.2. Minerals of zinc (Istanbul mineral exporters association, 1998) (Continued)

Groups of mineral	Name of mineral	Chemical formulas
Silicates	Vilemite	Zn_2SiO_4. 2ZnO. SiO_3
	Hardystonite	$Ca_2ZnSi_2O_7$. 2CaO.ZnO. $2SiO_3$
	Danalite	$3(Fe,Zn,Mn)BeSiO_4ZnS$
Oxides	Zincite	ZnO
	Zincspinel	$ZnO.Al_2O_3$
	Zincdibraunite	$ZnO.2MnO_2.2H_2O$
	Hetaerolite	$ZnO.Mn_2O_3$
	Kreittonite	$(Zn,Fe,Mg)O.(Al,Fe)_2$
	Dysluite	$(Zn,Fe,Mg)O.(Al,Fe)_2O_3$
Other minerals	Franclinite	$(Zn,Fe, Mn). (Fe,Mn_2)O_4$
	Colusite	$(Cu,Fe,Mo,Sn,Zn)_4$ (S,As,Te,Sb)
	Zincaluminite	$Al_6Zn_6S_2O_{221}.8H_2O$
	Hopeite	$Zn_3P_2O_8.4H_2O$
	Tarbuttite	$Zn_3(PO_4)_2$ $Zn(OH)_2$
	Descloizite	$Pb(Zn,Cu)(OH/VO_4)$

2.2.3. Zinc in the world

In 2019, global zinc mine production is expected to reach 13 million tons, up 4% from 2018. Australia, China, and South Africa all saw significant increases in zinc mine production. In Australia, the Woodlawn tailing project began operations in May, and the Dugald River Mine, the Lady Loretta Mine, and two tailing reprocessing projects all saw significant increases in production in 2018. Production rose at the Gamsberg Mine in South Africa, which was commissioned in 2018. Global refined zinc production was anticipated to be 13.49 million tons in 2019, whereas metal consumption was estimated to be 13.67 million tons, resulting in a refined zinc production-to-consumption deficit of around 180,000 tons, according to the

International Lead and Zinc Study Group. Table 2.3 shows global zinc mining production and reserves.

Table 2.3. World Zn mine production and reserves (USGS, 2020)

	Mine production				**Reserves**	
	2018		**2019**			
Country	**10^3 tons**	**%**	**10^3 tons**	**%**	**10^3 tons**	**%**
Australia	1110	8.9	1300	10.0	68000	27.2
Bolivia	480	3.8	460	3.5	4800	1.92
Canada	287	2.3	300	2.3	2200	0.88
China	4170	33.4	4300	33.1	44000	17.6
India	750	6.0	800	6.2	7500	3
Kazakhstan	304	2.4	290	2.2	12000	4.8
Mexico	691	5.5	690	5.3	22000	8.8
Peru	1470	11.8	1400	10.8	19000	7.6
Russia	300	2.4	300	2.3	22000	8.8
Sweden	234	1.9	230	1.8	3600	1.44
United Stated	824	6.6	780	6.0	11000	4.4
Other countries	1840	14.7	1900	14.6	34000	13.6
World total (rounded)	12500	100	13000	100	250000	100

2.2.4. Primary source of zinc (zinc ore deposits)

There are around 55 zinc minerals known, although only a few are economically significant (Thompson, 2006). Table 2.2 contains a list of zinc minerals. Non-sulphide (oxidized, carbonated, etc.) and sulphide zinc ore are the two types of zinc ore deposits. Nonsulfide zinc ores are a valuable resource that may be used to manufacture zinc.

2.2.4.1. Zinc in nonsulphide zinc ores

For hundreds of years, nonsulfide zinc ores were the primary source of zinc metal production, but their importance waned in the early twentieth century due to the development of flotation and smelting procedures for zinc sulfides (Schneider et al., 2008). Non-sulfide ores will be an important alternative source for zinc metal production to fulfill future demand, as the world reserve of sulphide ores is expected to last for several decades. Zinc non-sulphides (often referred to as "zinc oxide") is a broad word that refers to a variety of minerals. The zinc carbonates, such as smithsonite and hydrozincite, and the zinc silicates, hemimorphite and willemite, are the only ones that have been regarded economically important for zinc extraction (Boni et al., 2005; Hitzman et al., 2003; Large, 2001). The most efficient method for recovering zinc from nonsulphide zinc ore is to use a direct acidic or alkaline leaching procedure. Sulfuric acid, in particular, is regarded as the most viable and adaptable of the various processes. Eqs. (2.1) - (2.3) illustrate the process of direct sulfuric acid leaching of oxide minerals for smithsonite, willemite, and hemimorphite, respectively:

$$ZnCO_3 + H_2SO_4 \rightarrow ZnSO_4 + H_2O + CO_2 \tag{2.1}$$

$$Zn_2SiO_4 + 2H_2SO_4 \rightarrow 2ZnSO_4 + Si(OH)_4 \tag{2.2}$$

$$Zn_4Si_2O_7(OH)_2 \,.\, H2O + 4H_2SO_4 \rightarrow 4ZnSO_4 + Si_2O(OH)_6 + 3H_2O \tag{2.3}$$

2.2.4.2. Zinc in sulphide ores

Zinc sulfide ores have been the primary source of zinc metal production for decades, with zinc sulfide (ZnS) concentrates accounting for more than 85 % zinc production (Abkhoshk et al., 2014). Because sulphides are easier to separate from gangue and concentrate using traditional froth flotation techniques, zinc is now produced mostly from zinc sulphide ores (Li et al., 2010). The roast–leach–electrowin (R–L–EW) method is commonly used to generate zinc from zinc sulphide concentrations. Alternatives to the environmentally harmful roasting procedure have been extensively researched. To dissolve in chloride and sulphate solutions, sulphides require the presence of an oxidizing agent such as Fe^{3+}. The roasting–leaching process can be replaced with zinc pressure leaching or atmospheric direct leaching of sphalerite. (Moradi and Monhemius, 2011).

2.2.5. Secondary resource of zinc (wastes)

Zinc is usually manufactured from primary sulphide or nonsulphide in the world. However, as previously indicated, rising metal demand has necessitated metal recovery from secondary resources such as zinc ash, zinc dross, and Electric Arc Furnace (EAF) dust. As seen in Table 2.4, the chemical compositions of these zinc wastes vary. In other words, due to the depletion of high-grade ores and rising demand for these metals, secondary resources have become an increasingly important supply of zinc, as well as other metals. Around 70% of the zinc produced worldwide comes from mined ores, with the remaining 30% coming from recycled or secondary zinc. Each year, the level of recycling rises in conjunction with advancements in zinc production and recycling technologies. Over 80% of the zinc that is now accessible is recycled (Rusen, 2007; IZA, 2011; Jha et al., 2001)

Table 2.4. Different chemical composition of secondary zinc resources (Jha et al., 2001)

Wastes	**Type**	**Composition in wt %**
Galvanizing industry	Zinc ash	60-85 Zn, 0.3-2 Pb, 0.2-1.5 Fe, 2-12 Cl
	Flux skimming	5.6 metallic Zn, 48.1 $ZnCl_2$, 27.4 ZnO, 3.2 Al
	Zinc dross	96 Zn, 4 Fe
EAF	Dust	19.4 Zn, 24.6 Fe, 4.5 Pb, 0.42 Cu, 1.4 Si, 6.8 Cl
Blast furnace	Flue dust	Major component Fe, also contains Zn, Si, Mg
Leaching process	Leach residue	10-12 Zn, 15-17 Pb, 6-7 Fe, 8-10 CaO, 15-16 SiO_2
Flotation tailing	solid residue	5.9-22 Zn, 2-5.3 Pb

2.3. General information about lead

Because of its easy extraction and smelting properties, lead is a well-known metal that has been used by mankind for thousands of years. The oldest lead piece, which dates from 3800 B.C., is in the British Museum. The Chinese are known to have manufactured metallic lead around 3000 B.C. The Romans used lead for plumbing, while the Chinese used it to line tea chests. Egyptians also used it to glaze their ceramics. The majority of the older programs are still in use. The symbol Pb is derived from the Latin word "plumbum," which means "soft metal." Lead is a post-transition metal that is relatively unreactive. Its amphoteric nature exemplifies its weak metallic character; lead and lead oxides react with acids and bases and tend to form covalent bonds. Lead compounds are frequently found in the +2 oxidation state rather than the +4 oxidation state observed in lighter carbon group members (Wikipedia, 2020).

2.3.1. Physical and chemical properties of lead

Lead has an atomic number of 82 and a bluish-white color. There are four stable isotopes of lead in nature. The mechanical strength of pure lead is poor. It's also highly bendable and soft. Furthermore, lead is a dense, ductile metal. Lead has an atomic weight of 207.2. It has a good corrosion resistance but weak electrical conductivity. Because lead is a heavy metal, it is harmful to both humans and the environment. Table 2.5 shows the most important features of lead (Wikipedia, 2020; Lide, 1978).

Table 2.5. Properties of lead (Wikipedia, 2020; Lide, 1978)

Solid density (at RT)	11.34 g/cm^3	Ionization energies (1st)	715.6 KJ/mol
Liquid density (at MP)	10.66 g/cm^3	Ionization energies (2nd)	1450.5 KJ/mol
Melting point	327.5 ^{0}C	Atomic radius	180 picometer
Boiling point	1749 ^{0}C	Magnetic ordering	Diamagnetic
Heat of fusion	4.77 KJ/mol	Electrical resistivity (20 ^{0}C)	208 n.Ω.m
Heat of vaporization	179.5 KJ/mol	Thermal conductivity (20 ^{0}C)	35.3 W/m.K
Heat capacity (at 25 ^{0}C)	26.650 J/mol·K	Thermal expansion (25 ^{0}C)	28.9 µm/ m.K
Crystal structure	Cubic Face Centered	Young's modulus	16 Gpa
Oxidation states	2, 4	Shear modulus	5.6 Gpa
Electronegativity	2.33 (Pauling S.)	Mohs hardness	1.5

2.3.2. Minerals of lead

Galena (PbS), Cerussite ($PbCO_3$), and anglesite are the most important lead minerals ($PbSO_4$). Galena is the most common lead mineral found in mined ore deposits, and it is usually associated with zinc, copper, silver, gold, and iron. Rarely does lead mineralize on its own in ore sources around the world. Table 2.6 shows some of the lead minerals (Onal, 1998).

Table 2.6. Some of lead minerals (Rusen, 2007)

Mineral	**Chemical formula**	**Lead content, %**
Galena	PbS	86.6
Cerussite	$PbCO_3$	77.5
Anglesite	$PbSO_4$	68.3
Jamesonite	Pb_2SbS_5	50.8
Pyromorphite	$PbCl(PO4)_3$	76.4
Vanadinite	$(PbCl)Pb_4(VO4)_3$	Variable
Desclozite	$4(PbZn)O.V_2O_5.H_2O$	Variable

2.3.3. Lead in the world

According to the International Zinc and Lead Study Group, global refined lead production decreased by 0.3 % to 11.76 million tons in 2019, while metal consumption declined by 0.5 % to 11.81 million tons, resulting in a refined lead production-to-consumption deficit of about 50,000 tons due to decreased automobile production and increased lithium-ion battery (LIB) use. Table 2.7 shows global lead mining production and reserves (USGS, 2020).

2.4. Zinc and Lead in Turkey

Zinc and lead are found as smithsonite in Turkey, mainly in the Zamantı and Bolkarlar districts of Central Anatolia and between Balya and Han deresi in the west Anatolia (Figure 2.1). Along the eastern Black Sea shore, significant amounts of sulphides of copper, lead, and zinc are found. Because of the modest size of the mines, Turkish zinc and lead ore reserves vary in chemical composition and characteristics, with typical reserves of 30 – 60 thousand tons of metallic zinc or lead. Furthermore, it can be stated that commercially considerable reserves of typical zinc ore bodies in the Central Anatolia ore basin are in the form of carbonates with siliceous gangue, and that their diversity is due to related and gangue minerals of each separate mineral layer. In the case of lead ores, deposits along the Black Sea coast and in Western Anatolia contain sulphidic type of lead ore bodies with accompanying zinc and copper minerals. Turkey's lead and zinc deposits are estimated to be 861 thousand tons and 2.5 million tons, respectively, according to statistics from the General Directorate of Mineral Research and Exploration (MTA) in 2013. Around 864 thousand tons of Turkey's total lead and zinc reserves are oxide type reserves with a Pb+Zn grade of more than 7%. Table 2.8 shows the locations of these sites, which are mostly in Central Anatolia (SOP, 2001; Onal, 1998).

Table 2.7. World lead mine production and reserves (USGS, 2020)

	Mine production				**Reserves**	
	2018		**2019**			
Country	**10^3 tons**	**%**	**10^3 tons**	**%**	**10^3 tons**	**%**
Australia	432	9.5	430	9.6	36000	40.0
Bolivia	112	2.5	100	2.2	1600	1.8
China	2100	46.1	2100	46.7	18000	20.0
India	192	4.2	190	4.2	2500	2.8
Kazakhstan	86	1.9	90	2.0	2000	2.2
Mexico	240	5.3	240	5.3	5600	6.2
Peru	289	6.3	290	6.4	6300	7.0
Russia	220	4.8	220	4.9	6400	7.1
Sweden	65	1.4	60	1.3	1100	1.2
Turkey	76	1.7	70	1.6	860	1.0
United Stated	280	6.1	280	6.2	5000	5.6
Other countries	468	10.3	430	9.6	5000	5.6
World total (rounded)	4560	100	4500	100.0	90000	100

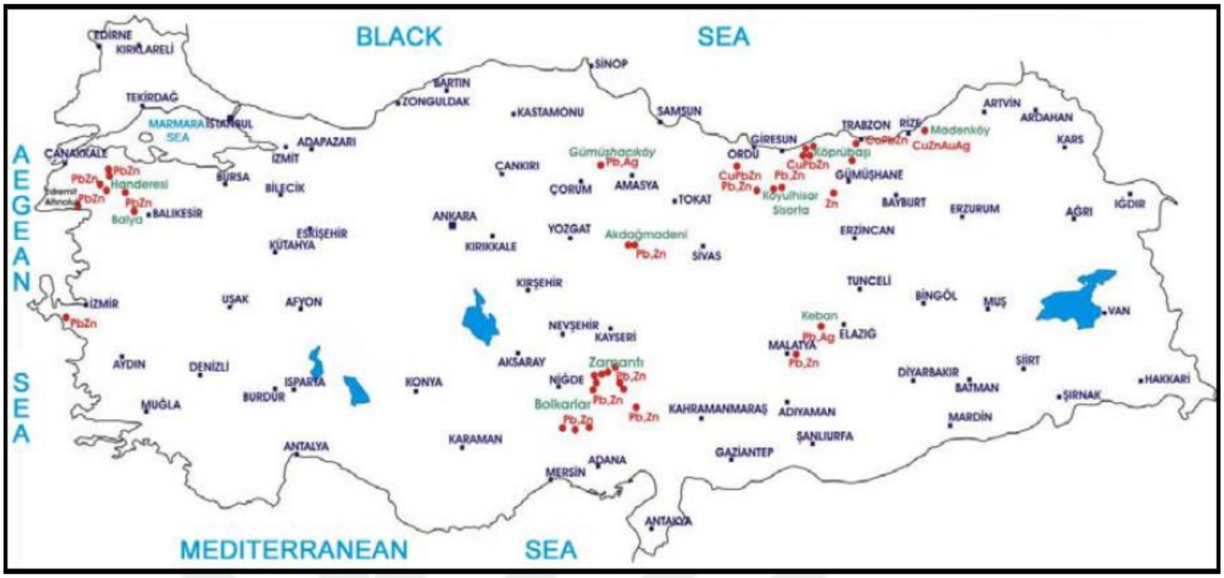

Figure 2.1. Map of zinc and lead ore deposits of Turkey (MTA, 2013).

Table 2.8. Oxide type reserves with Pb+Zn grade greater than 7% in Turkey (SOP, 2001).

Region	**City**	**County**	**Grade (%)**		**Reserve**
			Zn	**Pb**	**10^3 tons**
Oxide type ores Central Anatolia	Kayseri	Yahyali-Aladag	12.9	6.9	397
	Kayseri	Yahyali-Derekoy	25	10	60
	Kayseri	Yahyali-Sucati	25	1	15
	Kayseri	Yahyali-Denizovasi	16	4	10
	Kayseri	Yahyali-Agcasar	22	3	20
	Kayseri	Yahyali-Cadirkaya	20	2	10
	Kayseri	Develi-Havadan	22	1	25
	Kayseri	Zamanti	20.1	3.7	53.5
	Nigde	Camardi-Tekneli (1)	21.5	6	129
	Nigde	Camardi-Tekneli (2)	18	4	25
	Adana	Pozanti-Akdag	22	2	15
	Adana	Tufanbeyli-Besiktas	13.2	4	49
	Adana	Tufanbeyli-Akcal	17.8	2.7	8.5
	Adana	Kozan-Horzum	28	1	20

Table 2.8. Oxide type reserves with Pb+Zn grade greater than 7% in Turkey (SOP, 2001) (Continued)

Region	City	County	Grade (%)		Reserve
			Zn	Pb	10^3 tons
Oxide type ores Central Anatolia	Konya	Bozkir	25	1	15
	Malatya	Yesilyurt-Gorgu	19.8	6	12
Total					**864**

2.5. Method of zinc and lead extraction

Although zinc was initially smelted over 1000 years ago in China and India, it was not until the 18th century that advanced technology for zinc production was created in western civilization. Zinc may currently be produced using a variety of processing processes that can be divided into two categories: pyrometallurgical and hydrometallurgical procedures. The former entails high-temperature smelting of the ore or concentrate, whereas the latter entails low-temperature leaching of the ore or concentrate (Abkhoshk et al., 2014; Bond, 1999).

2.5.1. Pyrometallurgical method of zinc extraction

In the case of non-ferrous extraction, direct smelting is used. Metallurgy is the process of producing metal directly from a sulfide without the use of intermediate chemical reactions that result in the formation of metal oxide (Warner, 2009). The first step in any smelting process is to roast the concentrate to a calcine, which converts the zinc to zinc oxide. Anthracite is commonly used as a source of carbon in furnaces heated with natural gas or electricity to reduce zinc oxide. At a temperature of 920 °C, carbon monoxide generated from anthracite will degrade ZnO at a pressure of one atmosphere. To keep the reaction moving at a reasonable pace, a temperature of 1100 °C is utilized. Because zinc has a boiling point of 907 °C, it is generated as a vapor that must be shielded from reoxidation in order to be collected as liquid zinc. A horizontal retort, a vertical retort, the imperial smelting process (ISP), and an electric furnace are used to reduce zinc oxide with carbon (Gordon et al., 2003). Pyrometallurgical processes have a number of drawbacks, including high energy consumption, significant capital expenditures, and the emission of damaging greenhouse gases. Although pyrometallurgical and hydrometallurgical technologies provided equal percentages of the world's zinc supply in the 1960s, the hydrometallurgical process now dominates zinc extractive metallurgy. (Harmer et al., 2007; Tripathy et al., 2003).

2.5.2. Hydrometallurgical method of zinc extraction

The manufacture of metals or pure chemicals through reactions in water solutions is known as hydrometallurgy. This concept has recently been broadened to encompass the use of organic reagents. It is both a beneficiation and an extraction process. Because of its advantages, hydrometallurgical treatment is commonly used on low-grade ores instead of pyrometallurgical procedures (Najiba, 2009). The three primary steps in the hydrometallurgy method are leaching, solvent extraction (SX), and electrowinning (EW).

2.5.2.1. Leaching

In hydrometallurgical processes, leaching is the most important unit operation. It is the process of dissolving metals from their native ores into a liquid (inorganic, organic, or alkaline) media. The method for leaching metals is classed as hydrometallurgy (chemicals) or bio-hydrometallurgy in leaching processes (microbial mediated leaching) (Sethurajan, 2015).

- **Leaching methods**

Depending on the mineral deposit to be treated, different leaching processes may be used. Some mineral deposits can be handled in place, but others may require to be transported for leaching. (Gupta and Mukherjee, 2020).

- **In-situ leaching or solution mining**, is a method of extracting minerals without transporting them. Metal is retrieved by pumping a solution through fractures. In comparison to other leaching processes, it is a cost-effective approach that also does not require surface disturbance (Habashi, 1970).

- **Heap leaching** method is commonly applied to low and medium grade ores. This method is similar to in-situ leaching, except that ore is collected from the mine and transported to slightly inclined ground in the shape of heaps. The ground beneath heaps is known as a leach pad, and it is made up of many liners. When the ore is carefully and consistently heaped, the pregnant solution is sprayed from the top and allowed to settle in basins at the pile's end. Despite the fact that it is a sluggish process, heap leaching is a common and simple leaching method (Gupta and Mukherjee, 2020; Free, 2013).

- **Dump leaching** is often treated for the treatment of sulfide-bearing ores. The ore is transferred from the mine and put into cones on impermeable ground. The leach solution is poured in from the top and allowed to percolate all the way to the bottom of the dump. The primary parameters that determine the efficacy of dump leaching are effective air circulation, effective bacterial activity, and high solution in particle interaction (Gupta and Mukherjee, 2020; Free, 2013).

- **Vat leaching** method is used in series of rectangular leaching vats with countercurrent principle. The material does not move as much in this process as it does in most countercurrent procedures, and the solution percolates through the material (Gupta and Mukherjee, 2020). Vat leaching has two key advantages: it uses less solvent and produces a high-quality pregnant solution (Habashi, 1970).

- **Agitated leaching** involves treating ore in a succession of agitated vessels. Batch or continuous dissolution is possible (Gupta and Mukherjee, 2020). Compressed air, a mechanical impeller, or a mix of the two can be used to create agitation (Habashi, 1970).

- **Pressure agitation leaching** is accomplished in autoclaves at high temperatures and pressure. Over ambient settings, high pressure acid/autoclave leaching has some advantages, such as high iron removal and low oxygen use (Free, 2013).

2.5.2.2. Purification

Impurity metals dissolved with the zinc during leaching should be eliminated in the purification phase before the EW process. The leachate can be purified in a variety of ways, including cementation, precipitation, or solvent extraction. Fe, Cu, As, Sn, Al, Cl, Si, Mn, Mg, Ni, Cd, Si, Cr, and other elements are commonly found in PLS. If these impurities remain, not only would the zinc produced by following electrolysis be inadequately pure, but their presence will also disrupt the EW process's smooth operation. For the elimination of chlorine from these impurities, two procedures can be used: distilled water washing and calcination. After dissolving the sample in leaching reagent, other impurities can be eliminated using precipitation and cementation procedures (Najiba, 2009).

Precipitation: During leaching, iron is predominantly released as Fe^{2+} into the solution. The most difficult aspect of iron solvent extraction is stripping, which necessitates the use of strong acids and reduction. The use of strong acids exposes the reagent to the risk of breakdown. Furthermore, if the iron concentration is high, the SX's economic feasibility may be harmed due to a large solvent inventory. By oxidation, Fe^{2+} should be transformed to Fe^{3+} for iron precipitation. Fe^{3+} can be precipitated after oxidation by keeping the pH between 2.5 and 4.5.

- **Metal ions precipitation in solution**

According to the solubilities of their compounds, metal cation ions are divided into five major classes (Najiba, 2009):

Group I (Ag^+, Pb^{2+}, Hg^{2+}) all other cations remain in solution while cations create insoluble chlorides that can be precipitated with weak HCl.

$$Ag^+ + Cl^- \rightarrow AgCl_{(s)} \text{ (AgCl is white, turning purple in light)} \quad (2.4)$$

$$Hg_2^{2+} + 2Cl^- \rightarrow Hg_2Cl_{2(s)} \text{ (}Hg_2Cl_2\text{ is white)} \quad (2.5)$$

$$Pb^{2+} + 2Cl^- \rightarrow PbCl_{2(s)} \text{ (}PbCl_2\text{ is white)} \quad (2.6)$$

Group II (Cu^{2+}, Bi^{3+}, Cd^{2+}, Hg^{2+}, As^{3+}, Sb^{3+}, Sn^{4+}) because cations form insoluble sulfides (Ksp values less than 10^{-30}), they can be precipitated with small amounts of sulfide ion, which can be accomplished by adding an acidic H_2S solution. As a result, this group is also known as the Acid Hydrogen Sulfide Group. The ions of this Group will precipitate if the hydrogen ion concentration is kept between 0.1 and 0.3 M (pH = 0.5-1.0). The reactions involved in the precipitation of Group II are as follows (for the ions we're interested in):

$$Pb^{+2} + H_2S \rightarrow PbS_{(s)} + 2H^+ \text{ (PbS is black)} \quad (2.7)$$

$$2Bi^{+3} + 3H_2S \rightarrow Bi_2S_{3(s)} + 6H^+ \text{ (}Bi_2S_3\text{ is brown)} \quad (2.8)$$

$$Cu^{+2} + H_2S \rightarrow CuS_{(s)} + 2H^+ \text{ (CuS is black)} \quad (2.9)$$

Group III (Al^{3+}, Cr^{3+}, Fe^{3+}, Ni^{2+}, Co^{2+}, Mn^{2+}) Because cations form slightly soluble sulfides (Ksp values greater than 10^{-20}), they can be precipitated by large amounts of sulfide ion, which can be accomplished by adding a basic H_2S solution. A basic solution of hydrogen sulfide is used to precipitate the ions of this Group as sulfides or hydroxides. The sulfides of Group III ions are not adequately insoluble to precipitate in the acidic hydrogen sulfide solution of Group II, but they will precipitate in basic hydrogen sulfide solutions. A concentration of hydroxide ions is present in a basic hydrogen sulfide solution. Although this is a little amount, it is enough to precipitate the insoluble aluminum and chromium (III) hydroxides. The following are the equations for the precipitation of Group III ions that we are considering in our laboratory work:

$$Ni^{2+} + H_2S \rightarrow NiS_{(s)} + 2H^+ \text{ (NiS is black)} \quad (2.10)$$

$$Al^{3+} + 3NH_3 + 3H_2O \rightarrow Al(OH)_{3\,(s)} + 3NH^{4+} \text{ (}Al(OH)_3\text{ is white, gelatinous)} \quad (2.11)$$

$$Cr^{3+} + 3NH_3 + 3H_2O \rightarrow Cr(OH)_{3\,(s)} + 3NH^{4+} \text{ (}Cr(OH)_3\text{ is gray-green, gelatinous)} \quad (2.12)$$

It's important not to make the hydrogen sulfide solution excessively basic, because if the hydroxide ion concentration is high enough, undesirable magnesium hydroxide precipitation will occur. An ammonia-ammonium chloride buffer is made by adding ammonia to an ammonium chloride solution to achieve the required hydroxide ion concentration (approximately 10^{-5}M).

Group IV (Mg^{2+}, Ca^{2+}, Sr^{2+}, Ba^{2+}) all of the foregoing groups, including cations, form insoluble carbonates, which can be precipitated by adding carbonate after the previous three groups' ions have been removed.

Group V (Na^{+}, K^{+}, NH_4^{+}) with any of the reagents listed above, cations do not precipitate.

Cementation: Other impurities can be removed by cementation technique. Cementation is the electrochemical precipitation of a metal from solution by another more electropositive metal. The removal of impurities such as Cd, Cu, Co, Ni, etc. from zinc electrolyte is widely conducted through cementation process using zinc powder. As zinc is a highly reactive metal compared to impurity elements, when pure zinc is added to the solution, zinc will be oxidized and dissolves, with the opposite side of the reaction being the reduction of the other dissolved metals back to their metallic state as (2.13) (Najiba, 2009; Pakarinen and Paatero, 2011; Guler et al., 2014):

$$M^{2+} + Zn^{0} = Zn^{2+} + M^{0} \tag{2.13}$$

where M: Cd, Cu, Co, Ni, etc.

2.5.2.3. Solvent extraction

A liquid (organophosphorus) extractant is used for metal extraction in liquid-liquid extraction, or SX. Solvent extraction could be a viable option for producing high-quality zinc from a complicated aqueous stream. Metal ion moved from the liquid to the organic phase. To eliminate impurities, the loaded organic phase goes through a three-stage countercurrent washing process. The first two phases are primarily physical procedures in which the entrained aqueous phase is eliminated, decreasing halide carryover to the strip circuit; the third stage involves chemically scrubbing and removing co-extracted impurities. In a two-stage, countercurrent stripping circuit, the washed organic phase is connected with spent electrolyte (SE) (Abkhoshk et al., 2014; Halli et al., 2020).

In comparison to the classic electrolytic process, the SX technique has two major advantages. (Cole and Sole, 2003; Martín et al., 2002):

a) Metallic impurities (Cd, Cu, Ni, Co, etc.), halogens (Cl, F), alkaline metals (Na, K), and other components such as Ca, Mg, and Mn are all designed to pass through the solvent extraction system.

b) Due to their low zinc concentration and a variety of impurities, many main zinc ores have not been processed using the standard electrolytic technique. The solvent extraction process successfully upgrades the relatively dilute leach liquid (approximately 30 g Zn/L) to an advanced electrolyte that contains 90 g Zn/L and is acceptable for EW, allowing these raw materials to be treated.

c)

- **Solvent extraction of zinc**

Acid leaching and solvent extraction can be used to make an electrolyte from zinc ores. To create metal zinc from the loaded electrolyte, it can be treated in a traditional electrowinning unit. The SX section's goal is to preferentially extract Zn from the cleared pregnant leach solution (PLS) over other metals, resulting in a clean, more concentrated zinc sulphate solution suited for EW. The SX section's key processes include extraction, washing, and stripping (Moradi and Monhemius, 2011):

- **Extraction:** Zinc is carried from the leach solution to the organic phase in a succession of extraction phases as follows:

$$ZnSO_4(\text{Aqueous}) + 2HR(\text{Organic}) \rightarrow H_2SO_4(\text{Aqueous}) + R_2Zn(\text{Organic}) \qquad (2.14)$$

HR, is an organic extractant. Organophosphorus extractants, such as di(2-ethylhexyl) phosphoric acid (D2EHPA), 2-ethylhexyl phosphonic acid mono-2-ethyl hexyl ester (PC88A), and bis(2,4,4-trimethylpentyl)phosphinic acid, are the most often employed SX reagents for Zn extraction (Cyanex 272). D2EHPA has been utilized extensively to extract Zn, as well as other elements such as Fe and V, from these extractants (Halli et al., 2020; Moradi and Monhemius, 2011).

- **Washing**: The following reaction, in which calcium in the organic phase is replaced by zinc, with R again representing a molecule of the organic extractant, is an example of the crowding out mechanism:

$$ZnSO_4(\text{Aqueous}) + CaR_2(\text{Organic}) \rightarrow CaSO_4(\text{Aqueous}) + R_2Zn(\text{Organic}) \qquad (2.15)$$

- **Stripping**. The strip reaction, which occurs in a succession of stripping steps, will be as follows:

$$ZnR_2(\text{Organic}) + H_2SO_4(\text{Aqueous}) \rightarrow 2HR(\text{Organic}) + ZnSO_4(\text{Aqueous}) \qquad (2.16)$$

Filters are used to remove entrained organic phase from the loaded electrolyte, and the filtered electrolyte is sent to the EW step. The SX section's ancillary phases include organic regeneration, organic coalescence, HCl recovery, crude treatment, and electrolyte filtering (Moradi and Monhemius, 2011).

2.5.2.4. Electrowinning

In EW processes the metal is normally in solution in the electrolyte, it is deposited onto the cathode, whereas the anode is an insoluble conductor. This procedure is critical for the production of highly reactive light metals such as aluminum and magnesium, which are virtually entirely created by electrolysis of fused salts. Electrowinning from aqueous solutions is an alternative to the pyrometallurgical method for other metals such as copper and zinc. For the production of high purity copper, zinc, and aluminum, EW with aqueous electrolytes or fused salts is critical. One benefit of employing electrical energy to drive chemical reactions is that no undesired contaminants are introduced into the cell (Najiba, 2009).

Zinc electrolysis is one of the oldest industrial processes, and its relevance is based on the high global demand for this metal, which presently produces 9 million tonnes per year. It is the principal process step in the hydro-&electro-metallurgical pathway for both primary and secondary sources, and it accounts for around 80% of global zinc output. The high over potential of hydrogen production on the zinc layer covering the aluminum cathode enables the process. The temperature of the electrolyte should not be too high, and the electrolyte must be semi pure to achieve this over potential state. It necessitates an electrolyte containing 50–90 g/L Zn^{2+} and 120–200 g/L H_2SO_4, and it is often performed at high current densities of 400–700 A/m^2. Because it does not form alloys with zinc, aluminum is employed as the cathode. The negative influence of metallic impurities on the current efficiency and purity of the zinc deposit is a key challenge during the EW of zinc, which becomes much more critical when the source material is a waste product (Tsakiridis et al., 2010).

- **Impurities in the electrolyte**

The ideal electrolyte is an acid $ZnSO_4$ solution with no additional elements, but in commercial usage, the zinc electrolyte is rather clean and should provide a good zinc deposit at high current efficiency. Iron, cobalt, nickel, copper, arsenic, antimony, germanium, tin, selenium, tellurium, cadmium, lead, chlorine, fluorine, and manganese are all elements that are normally present and are harmful to the electrolyte call's operation.

The influence of a single element impurity on the deposit or action in the cell may be identified, but the effect of a combination of two or three elements is more difficult to identify. A combination of toxic substances is usually far more destructive than the same elements when they are present separately. The impurities found in the electrolysis of zinc sulphate can be classed as cathodic impurities, anodic impurities, or helpful impurities, depending on their general effects on the cells (Adhia, 1969).

- **Cathodic impurities**

The cathodic impurities are further divided into groups based on how they affect electrolysis:

I. Metals whose sulphates breakdown at a higher voltage than zinc sulphate, for example. Al, Na, K, Mg, Mn in terms of reactions at the cathode, these have no influence on electrolysis.

II. Those metals with a hydrogen over-voltage high enough to prevent zinc re-solution but a lower decomposition voltage than zinc.: Pb, Cd These have little effect on the efficiency of zinc breakdown, but they do deposit alongside zinc, resulting in a contaminated product.

III. Metals with a hydrogen over-voltage lower than zinc but a decomposition voltage higher than sulphuric acid.: Fe, Ni, Co. Electrolysis is harmed by these metals, however they rarely contaminate the zinc deposit. They are acid soluble and use energy by alternately depositing on the zinc surface and resolving in the acid electrolyte. When present in combination with other impurities, they are very detrimental to electrolysis.

IV. Metals with a sulphate decomposition voltage lower than that of sulphuric acid and a hydrogen over-voltage low enough to cause zinc re-solution.: Cu, Ge, As, Sb. This category of impurities is the most harmful of all; they are deposited with zinc and generate low hydrogen over-voltage places where hydrogen is evolved at the price of zinc.

- **Anodic impurities**

All anions save those of sulphuric acid are considered anodic impurities. Manganite, permanganate, chloride, chlorate, perchlorate, and fluoride are the most prevalent ions in this group. Although their effect on electrolysis is not as strong as that of metallic impurities, they frequently have a significant impact on the quantity of corrosion that occurs in the cell. Those anions that cause Al-cathode corrosion cause the deposited zinc to "stick" to the Al-cathode. This can get so bad that the only way to get rid of the deposited metal is to dissolve it with acid. An increase in Pb in zinc deposits is caused by anions that enhance corrosion of Pb anodes.

- **Beneficial impurities**

These include all of the additives, such as glue and manganese. They are usually employed to protect against the more severe impacts of other contaminants. To boost the hydrogen over-voltage and create a firm, smooth zinc coating, glue is utilized. Manganese is utilized to prevent corrosion on the anode.

2.5.3. Pyrometallurgical method of lead extraction

Lead is primarily produced from lead sulfide, galena, and pyrometallurgical reduction-extraction processes. The conventional and direct smelting processes are two types of pyrometallurgical lead extraction methods (Rusen, 2007).

2.5.3.1. Conventional Smelting Process

Pyrometallurgical extraction of lead from ore or concentrate is carried out using this method, which involves reduction smelting in a lead blast furnace or a more complicated ISP.

If the deposit contains both zinc and lead minerals, ISP can be utilized to produce both lead and zinc at the same time. The first step in the traditional smelting process is roasting, which converts lead sulphide to lead oxide. A Dwight Lloyd Sintering Machine is utilized to accomplish this goal. The feed for the blast furnace is provided by this unit. Lead sulphide concentrate, returning sintering fines, and limestone flux are among the ingredients in the feed. To reduce lead oxide, a large quantity of heat is required in a lead blast furnace. Carbon combustion provides the majority of the required heat. Carbon monoxide is produced when carbon is burned. Starting at around 400 ^{o}C, the CO created further down in the furnace lowers the lead oxide, resulting in freed lead trickling down over the particles of undecomposed ore, absorbing precious metals as well as a portion of arsenic, copper, and antimony, according to reaction (2.17).

$$PbO + CO = Pb + CO_2 \tag{2.17}$$

Iron oxide in the charge is reduced by CO at around 600-700 ^{o}C, and this iron decomposes lead sulphide and oxide. As seen in reactions, lead is also generated by direct carbon reduction and reactions between lead sulphide and oxide (2.18) -(2.20):

$$2PbO + C = 2Pb + CO_2 \tag{2.18}$$

$$2PbO + PbS = 3Pb + SO_2 \tag{2.19}$$

$$PbSO_4 + PbS = 2Pb + 2SO_2 \tag{2.20}$$

At temperatures above 1000 ^{o}C, metal and slag become fully liquid, and lead is extracted from the furnace (Rusen, 2007).

2.5.3.2. Direct Smelting Processes

Researchers studied to design more inexpensive and less polluting techniques for the manufacturing of lead, taking into account environmental issues and inefficient energy utilization in traditional processes. Some of them aspired to develop methods for converting lead straight from sulphide to metal. The main benefit of these procedures is that PbS changes directly to PbO without any intermediate steps. As a result, various direct smelting techniques have been invented, including Kivcet, QSL (Queneau-Schuhmann-Lurgi), Ausmelt, and Outokumpu (Rusen, 2007).

2.5.4. Hydrometallurgical method of lead extraction

Lead ore (primary resource) and secondary resources are the two types of lead resources that can be extracted using the hydrometallurgical technique.

2.5.4.1. Lead extraction from primary lead resource

The current method of processing lead sulphide concentrates is pyrometallurgical, which involves roasting, smelting, and refining. Lead oxidized minerals are commonly found with zinc oxidized minerals, and during leaching, they react with sulphuric acid. In sulphuric acid, however, lead sulphate is insoluble and will precipitate as $PbSO_4$ in the residue:

$$PbCO_3\text{(Cerussite)} + H_2SO_4 \rightarrow PbSO_4 \downarrow \text{(Anglesite)} + CO_2\uparrow + H_2O \qquad (2.21)$$

$$PbO\text{(Massicot)} + H_2SO_4 \rightarrow PbSO_4 \downarrow \text{(Anglesite)} + H_2O \qquad (2.22)$$

$$2Pb_5Cl(AsO_4)_3\text{(Mimetite)} + 10H_2SO_4 \rightarrow 10PbSO_4 \downarrow\text{(Anglesite)} + 6H_3AsO_4 + 2HCl \qquad (2.23)$$

Typical lead smelting techniques are inadequate for handling low-grade lead containing materials. They aren't usually competent of processing bulk zinc-containing lead concentrates, hence the zinc in lead concentrates is frequently lost in the tailings. The majority of the contained lead values might be recovered through hydrometallurgical treatment of this type of bulk concentrate, as well as residues from zinc procedures. As described in (2.24) (2.25), sodium sulfide precipitation was used to separate lead from zinc as lead sulphide in alkaline leaching solution and lead chloride by brine leaching (Moradi and Monhemius, 2011; Youcai and Stanforth, 2001).

$$PbSO_4 + Na_2S \rightarrow PbS_{(s)} + Na_2SO_4 \quad (2.24)$$

$$PbSO_4 + 2NaCl \rightarrow PbCl_{2(s)} + Na_2SO_4 \quad (2.25)$$

2.5.4.2. Lead in secondary lead resource

Lead is recovered from secondary resources such as lead-acid batteries, zinc leach residues, lead dust, liquid crystal display (LCD) lead glass, and flotation tailing. By the year 2000, recycled materials accounted for more than 60% of the industry's output, due to the big amount of scrapped lead batteries. Furthermore, in recent years, lead recycling in the United States has reached 83 % consumption (UAGS, 2007).

2.6. Previous studies on zinc and lead extraction from flotation tailing

Grinding is used to concentrate zinc-lead ores, which is followed by a sequential flotation approach in which lead minerals are floated first, followed by flotation of zinc minerals. Some lead and zinc are lost as sulphide, oxide, and mixed minerals in the tailings as metal losses during this process, hence zinc and lead flotation tailing might be considered a secondary resource that is processed by hydrometallurgical technology (Moradi and Monhemius, 2011). Some researchers investigated on this process. They used inorganic acid and alkaline reagents for leaching. Asadi et al. (2017) investigated leaching of zinc from a lead-zinc flotation tailing by sulfuric acid and ferric sulphate. Because of ferric ion is widely available at low cost and is a strong oxidizing it was used as oxidant in this study, they used Response Surface Methodology (RSM) for optimization of experiment parameters (Asadi et al., 2017).

The most critical elements determining the zinc leaching rate, according to the mathematical model for response surface analysis, are stirring speed and temperature. It was also shown that the rate of zinc leaching was substantially influenced by the interaction of factors. The biggest interaction impacts between components were temperature and liquid/solid ratio. 320 rpm stirring speed, 1.14 M sulphuric acid concentration, 2.49 acid/ferric sulphate ratio, 10.10 ml/g liquid/solid ratio, and 80 °C temperature were found to be the best dissolve conditions for maximizing zinc leaching rate (approximately 94.3 %).

Another research was investigated by Espiari et al. (2006) that was about zinc extraction from lead floatation tailing. 56.4% of sample was Smithsonite as zinc mineral and Cerussite as lead mineral. The maximum zinc extraction achieved 98% in 2M sulfuric acid, 120 min reaction time, 60 ^{o}C time, 1:4 solid/liquid ratio and 480 rpm stirring speed. The kinetic of leaching indicated this reaction is a physico-chemical desorption. There was filtration problem with polymerization of silicic acid in this study that eliminated by adding lime as a coagulant. Reaction time had a consequential effect on the progress of reaction (Espiari et al., 2006).

Kursun et al. (2017) studied about extraction of lead from lead-zinc flotation tailing with nitric acid. They obtained 44.15% of lead in 2 M nitric acid concentration, more acid concentration had no significant effect in dissolution. Other optimum conditions were 60 ^{o}C temperature, 120 min leaching time and 30% solid ratio. According result nitric acid was not good reagent for extraction lead in this research (Kursun et al., 2017).

A research was studied on zinc and lead flotation tailing by Azizi and Ghasemi, (2017) in alkaline media. Smithsonite and Cerussite were main zinc and lead minerals in sample from XRD pattern. Sodium hydroxide used as leachant. Possible reactions are given on Eq. (2.26) and (2.27) (Azizi and Ghasemi, 2017).

$$PbCO_3 + 4OH^- \rightarrow Pb(OH)_4^{2-} + CO_3^{2-} \qquad (2.26)$$

$$ZnCO_3 + 4OH^- \rightarrow Zn(OH)_4^{2-} + CO_3^{2-} \qquad (3.27)$$

According to the findings, optimum sodium hydroxide determined 4 M cause of the hydroxyl ions are enough due to the further formation of $Zn(OH)_4^{2-}$ and $Pb(OH)_4^{2-}$. The energy available for atomic and molecule collisions increases as the reaction temperature rises from 50 °C to 80 °C, resulting in a considerable increase in leaching rate. Furthermore, as temperature rises, the mass transfer coefficient, reaction constant, and diffusivity all improve. As a result, it was discovered that a high enough temperature is required to activate the reagent, which accelerated the reaction of hydroxyl ions with lead and zinc oxides in the alkaline leaching process. (Rao et al., 2015). Other optimum parameters were liquid/solid ratio 20 ml/g, stirring speed 500 rpm for lead and 400 rpm for zinc. Extraction of zinc and lead obtained 85.52% zinc and 72.15% lead respectively under optimum conditions. The dissolution kinetics of lead and zinc was investigated consistent with the shrinking core models and it was indicated that the leaching process of lead and zinc in sodium hydroxide solution followed the kinetic law of the shrinking core model with the fluid film diffusion as the rate-controlling step. The activation energies were identified to be 13.6 and 13.92 kJ/mol for the leaching of lead and zinc, respectively.

Aykac (2006) investigated extraction of zinc from lead-zinc flotation tailing with alkaline and inorganic reagents. The tailing sample obtained from Aladag, Kayseri and the mineralogical investigation contain Sphalerite, Smithsonite, Zincite as zinc minerals and Cerussite, Galena and Anglesite as lead minerals. At the first, he investigated sodium hydroxide as leaching reagent that 76.6% and 58.6% were dissolution efficiencies for zinc and lead, respectively in 400 g/L sodium hydroxide concentration and 120 minute leaching time. Selectively between zinc and lead was not acceptable in terms of solubility cause of that it was utilized an acidic media by sulfuric acid for following experiments (Aykac, 2006).

At the first roasting after acid leaching, and at the second direct acid leaching, two types of tests were conducted. The ideal temperature for roasting was found to be 400 ^{o}C, followed by acid leaching to achieve maximal dissolution. Zinc dissolution efficiency was 83% at ideal conditions of 60 ^{o}C temperature, 60 minute leaching period, and 50 g/L acid concentration, while lead dissolution was zero and acid consumption was 442.9 kg/t. At the second part of acid leaching, dissolution of zinc obtained 91.5% in 60 g/L of acid concentration, 60 ^{o}C leaching temperature and 360 minutes of leaching time. Iron dissolution was 14.3% and 466.8 kg/t as acid consumption.

Another flotation tailing sample was obtained from Aladag, Kayseri that investigated by Canbazoglu et al, (2010). Acidic leaching experiments was carried out by 125g/L sulfuric acid. 86.26% Zn extraction was obtained in 5 minutes and increased to 89.56% after 45 minutes and it's decreased after 120 minutes so 60 minutes was determined. Optimum weight loss percent was 19.32% as acid consumption in 60 ^{o}C cause of that it was determined as optimum leaching temperature. 89.54% Zn extraction was achieved in 100 g/L as optimum acid concentration by consuming 565 kg/t acid (Canbazoglu et al., 2010).

Talan et al. (2017) investigated extraction zinc from cerussite flotation tailings by ammonia leaching on sample that came from Kayseri-Develi region of Turkey. They observed smithsonite and cerussite were main mineral as predominant species. The maximum 76.66% Zn extraction achived with ammonia concentration of 7 M in 12 hours of leaching time and reaction that occurred in ammonia leaching process was given in (2.28) ((Talan et al., 2017):

$$ZnCO_{3\,(s)} + 4NH_{3\,(aq)} \rightarrow Zn(NH_3)_4^{2+}{}_{(aq)} + CO_3^{2-} \tag{2.28}$$

2.7. Previous studies on zinc and lead extraction from other zinc and lead resources

Zinc and lead can be recovered in a variety of ways from both primary and secondary sources. In general, the hydrometallurgical process is the most practical for this purpose. Different leachants are utilized in hydrometallurgical processes to extract zinc and lead. Inorganic acid, organic acid, and alkaline acids are the three types of leachants. Some of researcher investigated sulphuric acid, hydrochloric acid and nitric acid as inorganic acid leachants for extraction of zinc from zinc ore and secondary resources of zinc.

Some researchers (Abali et al., 2017; Abdel-Aal, 2000; Abdel-Aal et al., 2016; Dhawan et al., 2011; Kaya and Serin Cakir, 2019; Moradi and Monhemius, 2011; Seyed Ghasemi and Azizi, 2016; Wu et al., 2015; Zhang et al., 2016) investigated zinc extraction from zinc-lead ores with inorganic acid. They used sulfuric, nitric, hydrochloric and boric acids as reagent in different leaching conditions. Researches indicated sulfuric acid is most efficient reagent between another reagents. The maximum zinc extraction was obtained by Moradi and Monhenius, (2011) that achieved 99% zinc from mixed sulphide-oxide lead and zinc ore by diluted sulfuric acid. The main zinc minerals of sample were smithsonite, sphalerite and hemimorphite and for lead minerals indicated cerussite and galena. Other optimum conditions were temperature of 60 ^{o}C, pH of 0.61, time of 45 minutes, pulp density of 330 g/L.

Dhawan et al. (2011) obtained 95% zinc extraction by hydrochloride acid from smithsonite mineral. The optimum conditions for leaching were found as 1.5M HCl, 45 ^{o}C temperature, 25 g/L solid-liquid ratio, and 500 rpm stirring speed. They investigated zinc dissolution kinetic also that indicated the dissolution rate controlled by surface chemical reaction and calculated activation energy of process was 59.58 kJ/mol.

Seyed Ghasemi and Azizi. (2016) researched on leaching kinetics of zinc a low-grade ore in inorganic and organic acids. They also investigated dissolution of lead from this sample in another paper (Azizi and Ghasemi, 2017). XRD analyses indicated main minerals of sample were smithsonite and cerussite. They used sulfuric, nitric and hydrochloric as inorganic acids and citric as organic acid. Nitric acid had maximum zinc and lead extraction between other inorganic acid that was 90.76% and 85.52% respectively and extraction with citric acid achieved 88.68% and 73.81% respectively in optimum conditions. Results showed reagent concentration and leaching temperature demonstrated most effects on the rate of zinc leaching. The dissolution kinetics exposed that diffusion through the fluid film was the rate controlling steps for nitric acid with 4.38 KJ/mol as activation energy. There were two parts for dissolution kinetics for sulfuric and hydrochloric acids that firstly was first 20 minutes that controlled by the surface chemical reaction with 50.24 and 60.94 KJ/mol respectively as activation energy and second in range 20-90 minutes that controlled by diffusion process with activation energy of 20.89 and 9.88 KJ/mol respectively. It was indicated that dissolution of zinc in citric acid media controlled by diffusion process with 22.21 KJ/mol as activation energy in 70 minutes but for last 20 minutes controlled by the surface chemical reaction with activation energy of 43.43 KJ/mol. the leaching rate was controlled by the diffusion through the film in nitric and citric acid with activation energy of 7.71 and 11.62 KJ/mol respectively.

Some researchers studied on extraction of zinc from zinc ore by citric acid (Irannajad et al., 2013), citric acid and addition of nitrate, chloride and sulfate (Boukerche et al., 2018;

Larba et al., 2013), trichloracetic acid (Deng et al., 2015), 5-sulphosalicilic acid (Wu et al., 2015), Ida^{2-} -H_2O system (Dou et al., 2011) nitrilotriacetic acid (Yang et al., 2016). Citric acid is one of organic acid that is very popular between organic acids. The sample was investigated by Irannajad et al. (2013) obtained from mining tailings that the main mineral of zinc was smithsonite. They achieved 82% zinc in the optimum conditions that were citric acid concentration of 0.5 mol/L, particle size range of 40-350 µm, temperature of 80 °C, time of 60 min and solid-liquid ratio of 1:10. It was found particle size and leaching time had a negligible effect on the extraction. The reaction between smithsonite and citric acid is given as follows:

$$C_6H_8O_7 \leftrightarrow 2H^+ + C_6H_6O_7^{2-} \quad (2.29)$$

$$ZnCO_3 + 2H^+ \rightarrow Zn^{2+} + CO_2 + H_2O \quad (2.30)$$

$$ZnCO_3 + C_6H_8O_7 \rightarrow Zn^{2+} + C_6H_6O_7^{2-} + CO_2 + H_2O \quad (2.31)$$

The sum of reactions (2.29) and (2.30) is reaction (2.31). Because citric acid is a weak acid, it appears that increasing the amount of citrate with zinc ions produces an increase in the solubility of smithsonite.

Larba et al. (2013) investigated zinc extraction from zinc oxide ore citric acid and addition of anions. Extraction of zinc without any additions was 90.4% in 60 min and 50 °C. They added sodium chloride, sodium nitrate and sodium sulfate to citric acid solution and determined higher effects were found in the presence of chloride that were 98% in 15 min and 40 °C. On another hand they indicated that citric acid when used alone as reagent, the dissolution was controlled by both chemical reaction and diffusion through boundary layer. When chlorides and nitrates were added to citric acid, chemical reaction became the single controlling process over the whole reaction time. It can be speculated that the addition of both anions accelerated the diffusion process. Therefore, the addition of anions affected the kinetic and the mechanism of the dissolution reaction (Larba et al., 2013). Boukerche et al. (2018) achieved completely zinc with 0.5 M citric acid and 2 M nitrates, 91.85% Zn with addition of 2 M chloride. They obtained that dissolution kinetic was controlled by the chemical reaction in entire cases and that activation energy archived 39.3 KJ/mol (Boukerche et al., 2018).

Hursit et al. (2009) studied dissolution kinetics of smithsonite ore with gluconic acid that is organic acid. They determined that dissolution rate was increased with decreased particle size, increased the gluconic acid concentration in range 0.25-1.25 M and decreased it in range of 1.25-2.25 M and independent of stirring speed. The dissolution kinetics pursued a shrinking core model with the surface chemical reaction and 47.92 KJ/mol determined as activation energy (Hurşit et al., 2009).

Some researchers investigated extraction of zinc from smithsonite ore (Ehsani et al., 2018; Youcai and Stanforth, 2000; Zhang et al., 2014, 2013) and from silicate ore (Chen et al., 2009; Santos et al., 2010) with sodium hydroxide. Concentration of sodium hydroxide in all of researches was more than 4 mol/L because of sodium hydroxide does not react extensively with carbonaceous materials and as we know both oxidized zinc ores and residues have high contents of carbonaceous mineral especially smithsonite other hand normally silicate ores needs one step roasting before leaching process or high concentration of reagent (Santos et al., 2010).

Ehsani et al. (2018) investigated extraction Zn from a Turkish smithsonite ore that achieved 70.9% Zn with used 4 M sodium hydroxide but because of the formation of hydrate calcium zincite in the leaching solution that was not acceptable therefore they used 3 M as sodium hydroxide concentration. They observed that when solid/liquid ration was decreased, at constant OH/Zn mole ratio Zn dissolution values decreased and at constant sodium hydroxide concentration the dissolution values of zinc increased (Ehsani et al., 2018).

Extraction zinc from calcined smithsonite with sodium hydroxide was investigated by Zhang et al. (2013). After calcined that was done at 400 ^{o}C for 120 min leaching process was studied. Zinc achieved 92% with sodium hydroxide concentration of 6.25 mol/L leaching time of 240 min at 100 ^{o}C as leaching temperature. Higher calcination temperature resulted in lower zinc dissolution cause of a great deal of undesirable phases of $ZnFe_2O_4$ and $Ca_2ZnSi_2O_7$. Alkaline leaching needs high enough temperature to be speed up and enough time to achieve the equilibrium because zinc oxide combines with hydroxyl ions to form coordination ions $Zn(OH)_4^{2-}{}_{(aq)}$ (Zhang et al., 2013).

Youcai and Stanforth. (2000) studied extraction of zinc and lead from smithsonite ore in a two-step process, at first dissolution zinc and lead and archived more 85% for both with 5.0 M sodium hydroxide and over 95 ^oC as leaching temperature and second lead separation from leach solution with addition of sodium sulfide. They determined when the weight ratio of sodium sulfide added to the lead was over 1.8, lead could be entirely precipitated (Youcai and Stanforth, 2000).

Dissolution of zinc oxides and sulphide zinc ores in ammoniacal solutions (ammonia, ammonium chloride, ammonium sulphate, ammonium carbonate, ammonium hydrogen carbonate and ammonium nitrate) was investigated by (Ding et al., 2010; Feng et al., 2007; Jia et al., 2016; Ju et al., 2005; Ma et al., 2015; Moghaddam et al., 2005; Rao et al., 2015; Song et al., 2018; Wang et al., 2008; Yang et al., 2017).

Ju et al. (2005) investigated zinc dissolution of smithsonite ore in ammonium chloride that reactions were given in following:

$$NH_4Cl \rightarrow NH_{3(aq)} + Cl^- + H \tag{2.32}$$

$$ZnCO_{3(s)} + 2H^+ \rightarrow Zn^{2+} + CO_2\uparrow + H_2O \tag{2.33}$$

$$Zn^{2+} + i(NH3)_{(aq)} \rightarrow Zn(NH3)_i^{2+} \tag{2.34}$$

$$Zn(NH_3)_2^{2+} + 2Cl^- \rightarrow Zn(NH_3)_2Cl_{2(ag)} \tag{2.35}$$

Where i=1, 2, 3, 4.

They achieved 81.2% zinc with 5 mol/L ammonium chloride, leaching temperature of 90 ^oC, 240 min leaching time and 1:10 g/ml as solid/liquid ratio. According to the leaching kinetics diffusion through the inert particle pores and chemical reaction at the new surface together were the rate control steps (Ju et al., 2005).

The zinc extraction can be enhanced by improving the stability of zinc complexes composed of zinc ions and ligand. Therefore, Rao et al. (2015) investigated zinc extraction with combined ammoniacal solution and a new organic ligand–nitrilotriacetic acid (NTA) is added into the $NH_4Cl–NH_3$ solutions. In $NH_4Cl–NH_3$ solutions, Zn ions can combine with chloride ions or ammonia to form soluble $[ZnCl_i]^{2-i}$ complexes or $[Zn(NH_3)_i]^{2+}$ complexes. With NTA added as the leaching agent, some other zinc complexes species are formed, including mono ligand complexes ($[Zn(NTA)_i]^{2-3i}$) and mixed ligand complexes ($[Zn(NTA)(NH_3)_i]^-$)(Rao et al., 2015). The stability constants of zinc complexes according to Feng, et al (2007) $[Zn(NTA)(NH_3)_2]^-$ complexes and $[Zn(NTA)_2]^{4-}$ complexes are more stable due to their larger stability constants. They obtained 90.3% zinc with 2 mol/L ammoniacal solution, 0.1 mol/L NTA concentration, 40 ^oC leaching temperature, 20 ml/g liquid/solid ratio and 400 rpm stirring speed. As a result of leaching kinetic, leaching process control by the surface passing and diffusion through the product layer and the relating activation energy obtained 22.3 KJ/mol (Feng et al., 2007).

Ammonia and citric acid solution as leaching reagent was studied by Ma et al. (2015) for extraction zinc from low grade zinc oxide ore. For determination of citric acid concentration effect on extraction, leaching experiments carried out in two stages. They observed increasing extraction of zinc as citric acid concentration increases was because of the citric acid concentration effect of increasing the $C_5H_7O_5COO^-$ activity that resulted in further dissolution of zinc. They obtained 81.2% zinc in optimum conditions that were ammonia concentration of 6 mol/L, citric acid concentration of 1 mol/L, leaching temperature of 25 ^oC, leaching time of 60 min, stirring speed of 300 rpm and solid: liquid ratio of 1:5. Instead of leaching temperature zinc extraction increased with increasing all of conditions (Ma et al., 2015).

Ammonium sulphate was one of another ammoniacal solution that investigated alone (Feng et al., 2007) or with ammonia solution (Jia et al., 2016; Song et al., 2018; Yang et al., 2017) by some researchers for zinc extraction. According to Jia et al. (2016) the positive effect of ammonia on leaching could be imputed to the favorable stability of zinc amine that stability constant is 9.06. They used ammonium persulfate as oxidant that zinc extraction increase from 85.5% to 98.7% with amount of it from 0.3 mol/L to 0.5 mol/L. leaching temperature had great effect on leaching efficiency, zinc extraction increased from 73.8% to 99% with increasing of temperature from 30 ^oC to 60 ^oC, on the other hand the increase of temperature could Improve the collision between reactant molecules and the rate of mass transfer therefore helping chemical reaction. The optimum conditions with 98.7% extraction zinc determined: ammonia, ammonium sulfate and ammonium persulfate concentrations were 2, 0.25 and 0.5 M respectively, leaching temperature of 50 ^oC and 4 h as leaching time (Jia et al., 2016).

Moghaddam et al. (2005) used the Taguchi method for determination optimum conditions of leaching zinc from nonsulfide zinc ore with ammonium carbonate. Leaching temperature, stirring speed, ammonium carbonate concentration, leaching time and pH were investigated. Before to leaching process, the sample was calcined at 800 ^oC for 1 h for increasing of extraction rate. The optimum conditions achieved as ammonium carbonate concentration of 3 mol/L, leaching temperature of 45 ^oC, stirring speed of 300 rpm, leaching time of 45 min and pH of 10. In these conditions 92% zinc leaching efficiency was obtained. For minimization of the iron and lead dissolutions, some extra experiments carried out. According to results, optimum conditions obtained were 2 mol/L ammonium carbonate concentration and pH of 11 (Moghaddam et al., 2005).

Oustadakis et al. (2010) investigated about zinc extraction from EAF dust in two steps. In the first step, extraction of zinc by sulphuric acid and in the second step purification and EW for metal zinc recovery were investigated. Zinc extraction reached 80% in 3N acid normality, 60 ^oC temperature and 10% solid/liquid ratio. In part two, four unit processes was proposed: first, iron precipitation by 99.9% at 95 ^oC and a pH of 3.5; second, zinc solvent extraction by Cyanex 272 at pH: 3.5, temperature of 40 ^oC with 25% extractant concentration; third, stripping of the loaded organic phase by zinc spent electrolyte (62.5 g/L Zn^{2+}) at temperature: 40 ^oC with diluted sulfuric acid (3 mol/L); fourth, zinc electrowinning from sulphate solutions with 80.37 g/L of Zn^{2+} at 38 ^oC using Al as cathode and Pb as anode and current density was kept constant at 500A/m^2 (Oustadakis et al., 2010)

Zinc extraction from EAF dust was investigated by other investigators (Kukurugya et al., 2015) that highest zinc extraction reached 87% by using 1M sulphuric acid at the temperature of 80 ^oC and solid/liquid ratio 50. Zinc can be present in EAF dust as an oxide (ZnO) and/or as ferrite ($ZnFe_2O_4$), the following reactions describe the possible reactions of zinc in a sulfuric acid solution:

$$ZnO + H_2SO_{4\,(l)} \rightarrow ZnSO_{4\,(aq)} + H_2O\,(l) \tag{2.36}$$

$$ZnFe_2O_4 + 4H_2SO_{4\,(l)} \rightarrow ZnSO_{4\,(aq)} + Fe_2(SO_4)_{3\,(ia)} + 4H_2O_{(l)} \tag{2.37}$$

$$ZnFe_2O_4 + H_2SO_{4\,(l)} + 2H_2O_{\,(l)} \rightarrow ZnSO_{4\,(aq)} + 2Fe(OH)_3 \tag{2.38}$$

Shawabkeh (2010) researched by three inorganic acid as leachant for zinc extraction from EAF dust. He used sulfuric acid, nitric acid and hydrochloric acid for leaching of zinc. Maximum zinc extraction was 72% used by 0.1 M sulfuric acid at 50 ^oC, 900 rpm agitation speed, 10-20 min and -37 μm dust particle. The kinetics study was indicated that zinc extraction has increased with increase acid concentration, solution temperature and mixing speed (Shawabkeh, 2010).

Some researchers investigated extraction of lead and zinc from EAF dust. Halli et al, (2017) used 16 different leachants from inorganic, organic acids and alkaline that four leachants – 10% aqua regia, 1.2 M hydrochloric, 0.94 M citric and 1.5 M nitric acids – resulted in high (>75%) zinc extraction with acceptable Fe selectivity and 1.75 M acetic acid had maximum lead removal (Halli et al., 2017). However Montenegro et al. (2016) carried out two step leach for extraction zinc and lead from EAF dust. Sulfuric acid was used for zinc leaching and sodium sulphide for removal lead from first step leach residue that was achieved 99.7% lead as lead sulphide in 95 ^oC and ambient temperature (Montenegro et al., 2016).

Some researchers investigated extraction zinc and lead from zinc plant residue that used inorganic acid and alkaline for leaching process. Li et al. (2013) investigated extraction if zinc from zinc plant purification residue that used sulfuric acid as leaching reagent. They obtained 91.97% zinc in optimum conditions: 100 g/L sulfuric acid concentration, 70 ^oC temperature for 20 min and 50:1 ml/g as liquid:solid ratio. According to leaching kinetics, dissolution rate of zinc was observed to be controlled by diffusion through a porous product layer and activation energy was 6.69 KJ/mol (Li et al., 2013). Another research was studied about zinc extraction from zinc plant purification filter cake by Behnajady and Moghaddam, (2017) which used Orthogonal Array (OA) of Taguchi’s method to distinguish optimum leaching conditions for maximizing zinc extraction with minimum impurities dissolution. Leaching temperature, leaching time, pH, pulp density and stirring speed utilized for optimization of conditions and sulfuric acid was selected as leaching reagent. Under these conditions: leaching temperature of 60 ^oC, leaching time of 120 min, pH of 5, pulp density of

150 g/L and stirring speed of 625 rpm maximum zinc extraction with minimum impurities obtained that was 95% (Behnajady and Moghaddam, 2017).

Alizadeh et al. (2011) researched on extraction of zinc from leach residues with minimum iron dissolution using oxidative leaching. They used sulfuric acid for reagent and Manganese dioxide and hydrogen peroxide for oxidative agents. Metal extraction in just acidic media were 95% and 72% for zinc and iron respectively in optimum conditions: pH of 1.5, solid: liquid ratio of 1:7, temperature of 75 ^oC and 120 min. Effect of hydrogen peroxide and manganese dioxide was investigated on metal extraction. With used 100 ml/kg hydrogen peroxide iron dissolution decreased from 82% to 5% and also observed no significant effect in different pH in leaching. It was determined that iron dissolution decreased to 0.4% with just 5 g/kg manganese dioxide and it was founded by increasing pH from 1 to 2. The iron dissolution decreased from 3% to 0.45% with no changed in zinc dissolution. Hence the optimum pH was concluded to be 1.5-2. They explained two reasons may be reliable for reduction iron in content. First it may be the effect of oxidants on iron dissolution and second, it may because of different iron species which created in oxidative condition in comparisons with the non-oxidative conditions (Alizadeh et al., 2011).

Turan et al. (2004); Rusen et al. (2008) and Guler et al. (2011) studied extraction zinc and lead from zinc plant residue that samples used in this studies were collected from Cinkur plant leach residue in Kayseri region, Turkey. They carried out two-stage process that for zinc extraction used sulfate roasting followed by water leaching, Rusen et al. (2008) studied direct sulfuric acid leaching as first stage and brine leaching for lead extraction from first stage residue. Achieved zinc from direct acid leaching was 71.9% but in sulfating roasting followed by leaching achieved 86% and 90% zinc at 200 ^oC, 30-60 min roasting time, equal weight ratio of sulfuric acid /sample, 60 min water leaching time at 25 ^oC. Further increasing the temperature up to 500 ^oC had no important effect on the zinc extraction because of the decomposition of metal sulfates and formation of some insoluble compounds such as oxy-sulfates and even ferrites. According to result, roasting process had positive affect in extraction however increased processing cost. Second stage was carried out with residues of first stage by using sodium chloride. Turan et al. (2004) achieved 89% lead at the optimum conditions that were NaCl concentration of 200 g/L, leaching time of 25 ^{o}C in 10 min. At high NaCl concentration, Guler et al. (2011) and Rusen et al. (2008) obtained 92% lead with 315 g/l NaCl concentration and 98.9% lead with 315 g/L NaCl concentration and 30 ml/L HCl concentration respectively. It was found that hydrochloric acid had significant effect in lead extraction along with sodium chloride (Güler et al., 2011; Ruşen et al., 2008; Turan et al., 2004).

Yan et al. (2014); Jiang et al. (2017) and Peng et al. (2012) also investigated extraction of zinc from zinc plant residue with reduction roasting followed by sulfuric acid leaching. They used CO, CO_2 and Ar as reduction agents (Jiang et al., 2017; Peng et al., 2012; Yan et al., 2014). Xie et al. (2020) and Wang et al. (2015) investigated on extraction lead from zinc leach residue with calcium chloride. As a result of XRD, the main mineral of samples was lead sulfate. The main chemical reaction that take place between sample and calcium chloride are as follow:

$$PbSO_{4\,(s)} + Ca^{2+} + 2Cl^{-} \rightarrow PbCl_{2\,(s)} + CaSO_{4\,(s)} \tag{2.39}$$

$$PbCl_{2\,(s)} + Cl^{-} \rightarrow PbCl_4^{2-} \tag{2.40}$$

Wang et al. (2015) obtained 93.79% lead in optimum conditions that were calcium chloride aqueous solution concentration of 400 g/L, at a pH of 1, leaching temperature of 80 ^{o}C, stirring speed of 500 rpm, leaching time of 45 min and liquid: solid ratio of 7:1. But Xie et al. (2019) achieved 85.78% lead on calcium chloride concentration of 3.15 mol/L, leaching temperature of 45 ^{o}C, at a pH of 2, leaching time of 120 min and liquid:solid ratio of 6:1. Leaching time, liquid: solid ratio and calcium chloride concentration had a significant effect on lead extraction. According to the dissolution kinetics, lead leaching rate controlled by the diffusion reaction and activation energy obtained 17.59 KJ/mol (Wang et al., 2015; Xia et al., 2020).

Ashtari and Pourghahramani, (2015) studied on extraction of zinc from zinc plant residue with mechanochemical alkaline leaching. At first they carried out normal chemical alkaline leaching with sodium hydroxide that was achieved 82.4% zinc in sodium hydroxide concentration of 9 M, leaching temperature of 25 ^{o}C, leaching time of 45 min and solid: liquid ratio of 1:10. They used a vertical stirred ball mill with a stainless steel chamber for increasing value of zinc extraction. According to obtained results, zinc extraction achieved 99.9% in sodium hydroxide concentration of 9 M, leaching temperature of 25 ^{o}C, leaching time of 37 min, solid:liquid ratio of 1:6 and Ball:Powder weight ratio of 50. Sodium hydroxide concentration was determined most important parameter despite milling time and milling speed were also statistically significant. As observed results, cause of abrasion and attrition that created in grinding, insoluble layer could be continuously eliminated during through mechanochemical leaching. Therefore the remained unreacted core could be leached totally (Ashtari and Pourghahramani, 2015).

Sodium hydroxide was used in leaching of lead from zinc leaching residue by Sahin and Erdem. (2015). According to XRD result, the main lead minerals in residue sample were anglesite and massicot. The leaching reactions of lead minerals with sodium hydroxide are given as follows:

$$PbSO4_{(s)} + 3NaOH_{(aq)} \rightarrow [Pb(OH)_3]^{-}{}_{(aq)} + SO_4^{2-}{}_{(aq)} + 3Na^{+}{}_{(aq)} \qquad (2.41)$$

$$PbO_{(s)} + NaOH_{(aq)} + H_2O_{(l)} \rightarrow [Pb(OH)_3]^{-}{}_{(aq)} + Na^{+}{}_{(aq)} \qquad (2.42)$$

They achieved 99.6% lead in 11% sodium hydroxide concentration, leaching time of 60 min and leaching temperature of 100 ^{o}C. As dissolution kinetics investigation, lead leaching rate controlled by diffusion process and the activation energy obtained 2.78 KJ/mol. They used sodium sulphide and carbon dioxide for removal lead from PLS as galena and lead carbonate hydroxide. According to chemical analyses, eliminated lead value was 85.16% and 76.27% with sodium sulphide and carbon dioxide respectively (Şahin and Erdem, 2015).

One of secondary resources of lead is spent lead battery paste that some researchers investigated on extraction of lead from it. They used alkaline, organic acid and brine leaching for desulfurization and leaching. Sodium hydroxide (Badanoiu et al., 2013; Chen et al., 2016; Ferracin et al., 2002; Yang et al., 2020; Yu et al., 2019), sodium carbonate (Liu et al., 2019; Yu et al., 2019), ammonium carbonate and ammonium bicarbonate (Liu et al., 2019), sodium potassium tartrate (Ferracin et al., 2002), sodium citrate with citric acid and acetic acid (He et al., 2017; Zhu et al., 2019, 2013), calcium chloride (Xing et al., 2019) and urea acetic (Volpe et al., 2009).

According to investigated XRD pattern of spent lead-acid battery pastes determined lead sulfate was one of main minerals in past. Therefore, desulfurization process carried out by using sodium hydroxide and sodium carbonate that optimum Na/$PbSO_4$ molar ratios obtained 2 and 2.2 respectively. Sodium hydroxide more effective than sodium carbonate for desulfurization. Desulfurization efficiency obtained 99.4% in 10 min with using sodium hydroxide and 96.3% with Na/$PbSO_4$ molar ratio of 2.2 using sodium carbonate in 120 min(Yu et al., 2019).

Ferracin et al, (2002) studied sludge of lead-acid battery solubility with 13 aqueous solution. According to result, only three solution were chosen for process: tetrafluoroboric acid in 200 g/L concentration, glycerol in 92 g/L concentration addition of sodium hydroxide in 120 g/l concentration and sodium potassium tartrate in 150 g/L concentration addition of sodium hydroxide in 150 g/L concentration. In the electrowinning process obtained pure lead from using solution achieved from leaching process in optimum conditions: current density of 150 A/m^2, stainless steel foil was chosen as cathode and graphite as anode (Ferracin et al., 2002). However, Xing et al. (2019) obtained cathode lead powders with a purity of 99.6% via electrowinning with 200 A/m^2 as current density. Current efficiency and power consumption were determined 96.3% and 85.9 kwh/ton respectively. They used iron for cathode and anode both in electrowinning process. Leaching process carried out with calcium chloride that lead dissolution obtained more than 99% under optimum conditions: calcium chloride concentration of 400 g/L, leaching temperature of 90 ^oC, Fe^{2+} concentration of 5 g/L, pH of 1 and leaching time of 120 min. They observed effect of Fe^{2+} concentration on leaching process was significant (Xing et al., 2019).

Sodium citrate and acetic acid were investigated as environmentally acceptable and financial affordable reagents (Zhu et al., 2019, 2013). Three major components ($PbSO_4$, PbO_2 and PbO) in spent lead paste were individually leached in the solution of sodium citrate and acetic acid whose acidity was higher than that of citric acid. The desulfurization efficiency was about 98% in two research and optimum conditions for lead citrate production determined:

sodium citrate 0.67 mol, acetic acid 2.2 mol per mol PbO for 10 min at 25 ^oC and solid: liquid ratio of 1:7 and for a mol of PbO_2 sodium citrate 0.67, acetic acid 2.4, hydrogen peroxide 1.5 mol for 15 min at 25 ^oC with solid: liquid ratio of 1:7, and 2.0 mol sodium citrate , 3.0 mol acetic acid for leaching of 1.0 mol $PbSO_4$ for 60 min with solid: liquid ratio of 1:5. The reactions in this leaching system could be given as (2.43)-(2.46):

$$PbO + 2CH_3COOH \rightarrow (CH_3COO)_2\,Pb + H_2O \quad (2.43)$$

$$PbO + 2CH_3COOH + H_2O_2 \rightarrow (CH_3COO)_2\,Pb + 2H_2O + O_2 \quad (2.44)$$

$$3Pb(CH_3COO)_2 + 2Na_3C_6H_5O_7.2H_2O \rightarrow Pb_3(C_6H_5O_7)_2.3H_2O$$
$$+ 6CH_3COONa + H_2O \quad (2.45)$$

$$3PbSO_4 + 2Na_3(C_6H_5O_7).\,2H_2O \rightarrow Pb_3(C_6H_5O_7)_2.3H_2O + 3Na_2SO_4 + H_2O \quad (2.46)$$

Some researchers investigated purification process for removal impurities metal from PLS of zinc leaching processes before electrowinning. Precipitation, cementation and solvent extraction may be accomplished for this stage. Iron is one of the main impurity metals in hydrometallurgical process because of plenty and easy dissolution (Zhang and Cheng, 2007). For removal other impurities (Cd, Ni, Co, Al, Cu, Mn, and Mg) cementation process could be carried out after precipitation of iron. Pakarinan and Paatero. (2011) studied on iron and manganese removal from zinc sulfate solution with some reagents. They investigated carbonate (sodium bicarbonate, sodium carbonate and calcium carbonate), hydroxide (calcium hydroxide), sulfide (hydrogen sulfide) and oxidative (oxygen and sulfur dioxide) precipitation. According to result, sodium carbonate was the most cost-effective reagent for removal both Mn and Fe, Hydroxide and sulfide precipitations need a long residence time for have increased nucleation and favorable settling and filtration properties (Pakarinen and Paatero, 2011).

Song et al. (2019) studied removal iron, copper, cadmium and cobalt from zinc leach solution. They carried out iron removal with adding hydrogen peroxide as oxidant and controlling pH with sulfuric acid and sodium hydroxide. According to result, 99% iron was removed at a pH of 5, temperature of 80 ^{o}C, time of 90 min and 3% wt hydrogen peroxide. Temperature effect on precipitation reaction was significant to 80 ^{o}C above that was not observed any effect. Because of the fact that iron hydrolysis is an endothermic reaction and more high temperature will make this reaction more complete. Cadmium and copper were removed 99% and reduced to 5 and 1 mg/L respectively in cementation process with zinc powder, on zinc excess coefficient of 1.5, pH of 2-5, temperature of 50 ^{o}C, and time of 30 min. high temperature had positive effect to 50 ^{o}C after that effect was negligible. For precipitation of cobalt from solution sodium ethyl xanthate and potassium manganate (K_2MnO_4) was used. About 88% cobalt removed as xanthate cobalt in this conditions: sodium ethyl xanthate concentration of 8 g/L, potassium manganate concentration of 1 g/L, pH of 4, temperature of 55 ^{o}C and time of 5 h (Song et al., 2019). Guler and Seyrankaya, (2016) used ammonium peroxodisulfate as oxidant for precipitation of iron from zinc leach solution. As result, 99.95%, 100% and 99.87% iron, manganese and arsenic respectively were removed from solution under optimum conditions: 30% ammonium peroxodisulfate (0.5M)/leach solution, pH of 3.5 and temperature of 90 ^{o}C(Güler and Seyrankaya, 2016).

Guler et al. (2014) investigated cementation of nickel, cobalt, copper and cadmium from zinc sulfate solution with zinc dust. As a result of cementation process, remained impurity ions in solution were 0.094 mg/L nickel, 0.084 mg/L cobalt, 0.045 mg/L copper and 0.041 mg/L cadmium. Optimum conditions obtained: zinc dust concentration of 2-3 g/L, zinc dust size of 75-150 microns, temperature of 70-80 ^{o}C, time of 45-60 min. they observed temperature had significant effect on cementation (Guler et al, 2014).

Rudnik. (2019) investigated purification zinc solution and electrowinning for recovery of zinc metal. Purification step carried out with calcium oxide as pH regulator for iron removal that optimum pH determined 4.5. According to EW results, Pb^{2+} ions could be useful for EW of zinc of about 99% purity at high current efficiency. It was indicated the pH of electrolyte was the main influential parameter of zinc electrodeposition. Almost zinc not formed on cathode in very acidic solution (Rudnik, 2019a).

Herrero et al. (2010) investigated purification zinc leach solution for preparing zinc sulfate solution for EW. They carried out cementation step for removal cadmium, copper and lead from solution with zinc dust. As a result, 90 min was enough for removal maximum metal impurities and after analysis was determined that 130 ppm concentration of remained metal impurity in solution. Optimal zinc dust amount was obtained 50 kg/sample ton to be added. Final zinc purity reached around 99.75% (Herrero et al., 2010). Manganese dioxide-hydrogen peroxide were investigated as oxidant for iron removal from zinc solution by Herrero et al. (2011). Iron removal was obtained about 99.6% and iron concentration after precipitation was 0.3 mg/L that was lower than the concentration of 10 mg/L as limit for EW feeds. They determined optimum conditions: hydrogen peroxide 2 ml, manganese dioxide concentration of 1.2 g/L, pH of 4.5 and time of 20 min (Herrero et al., 2011).

Another research was carried out on cementation of cobalt and nickel by Gutknecht et al. (2017). They also used addition of copper and antimony as activator to cementation reaction investigated. They observed copper and antimony form substrate desirable for cobalt cementation by copper forming a larger cathodic area on zinc dust. According to result 56% of cobalt and 90% nickel was removed under optimum conditions: zinc dust concentration of 2 g/L, copper concentration of 0.4 g/L, antimony concentration of 0.8 g/L, pH of 5 and temperature of 20-40 ^{o}C(Gutknecht et al., 2017). For best cobalt removal form zinc solution both copper and antimony were applied by Karlsson et al. (2018). They mentioned that temperature had a positive effect on the kinetics and copper/antimony activators were cemented during the first 90 s and gave synergistic effect on cementation of cobalt (Karlsson et al., 2018). Singh (1996) investigated arsenic and antimony as activator for cementation process. Between antimony and arsenic in the solutions with low cobalt, use of antimony is selected because of environmentally reasons (Singh, 1996).

Solvent extraction of zinc was investigated by some researchers for recovery of zinc from PLS of zinc leaching. D2EHPA (di-2-ethylhexyl phosphoric acid) was investigated as extractant of zinc from solution by Pereira et al. 2007; Hollagh et al. 2010; Halli et al. 2019; Qin et al. 2003. As result, 20% w/w D2EHPA was selected as optimum of organic concertation in extraction step. 5% TBP as modifier with kerosene as diluent added to reaction. They determined different pH for optimum, according to Halli et al. (2020) pH of 5 was optimum for extraction zinc from solution (Halli et al., 2020). Other researcher mentioned pH of 2-2.5. It could be because of Halli et al. (2019) carried out the extraction of zinc from zinc citrate solution. In organic/aqueous ratio of 1/1, temperature of 25 ^oC more that 98% zinc was extracted. As a result of stripping step, in final solution 25-125 g/L of zinc was obtained under optimum conditions: acid concentration of 1.0 M, organic/aqueous ratio of 3-4, temperature of 25 ^oC with three step striping (Hollagh et al., 2010; Pereira et al., 2007; Qin et al., 2003).

Tsakiridis et al. (2010) and Salgado (2003) investigated zinc recovery from zinc leaching solution with Cyanex 272 (bis (2,4,4-trimethylpentyl) phosphinic acid) as extractant. Cyanex diluted with 5% TBP in kerosene. According to results, optimum conditions for zinc solvent extraction obtained as pH of 3.5, temperature of 40 ^oC with 25% Cyanex concentration in extraction step. Stripping of the loaded organic phase carried out with solution of zinc spent electrolyte was carried out in temperature of 40 ^oC, organic/aqueous ratio of 2/1 and 62.5 g/L Zn^{2+} with 3.0 M sulfuric acid. At these conditions zinc stripping efficiency by zinc spent electrolyte obtained 99.5%. Zinc stripping efficiency wan 90% under optimum conditions: pH of 2, 20% Cyanex with kerosene at 50 ^oC. After solvent extraction of zinc, the aqueous solution concluded 80.37 g/L of Zn^{2+}. The acidity of electrolyte was determined at 180 g/L sulfuric acid (Salgado, 2003; Tsakiridis et al., 2010). Rudnik. (2019) fixed acidity of electrolyte on pH of 0.1 with sulfuric acid. Current density determined 500 A/m^2 in 4h, while temperature was 38 ^oC. In this conditions current efficiency reached at 92%. While Rudnik. (2019) found current efficiency range of 84-90% and electrolysis voltage was 3.3 V with 4 kWh/kg as energy consumption (Rudnik, 2019a). Current density also determined 500 A/m^2 by Qin et al. (2003). They indicated the cell potential 3.2 V. Temperature fixed at 40 ^oC and current efficiency was more than 90%. Lu et al. (2013) with comparison of zinc deposit weights before redissolution and energy consumption, selected 650 A/m^2 as current density and zinc deposit weights could be increased expressively while the energy consumption was increased a little (Qin et al., 2003).

3. MATERIALS AND METHODS

3.1. Materials

About 100 kg representative Pb-Zn oxide flotation tailing samples were collected from Oreks Mine tailing dump in Yahyalı-Kayseri. At Oreks Mining, flotation tails send to staged concreate tailing pools where tails are dewatered and solids are settled at the bottom of the concreate pools and then solid material is removed from the pool bases by excavators and stoked in the tailing dump area where tails completely dry and lumpy surface occurs in dry seasons. Figure 3.1a and 3.1b show tailing dump area and surface and Figure 3.2 shows collected sample sacks taken to the ESOGU Mineral Processing Laboratory.

Figure 3.1a and 3.1b. Oreks tailing dump area and surface views.

Samples were firstly roll crushed for deagglomeration and dispersing the sticking fine particles in our Mineral Processing Laboratory and then, dried by spreading in the laboratory floor at room temperature for one week. There were some small lumps/chunks in the samples after drying. During drying also there were caking of some samples; but these lumps were easily broken by squeezing with fingers. Figure 3.2 shows roll crushed samples for drying.

Figure 3.2. Roll crushed flotation tailing during drying.

After drying, all samples were sieved from Russell sieving machine using an 8 mesh (3.175 mm) sieve. Most of the samples were passed the sieve. Small amount oversize fraction was ground in a laboratory ball mill to deagglomerate the coarse lumps for 5 min. Since Russell sieve undersize still contained some agglomerated particles, laboratory ball milling (3 kg sample with 6.7 kg ball) was also applied to this undersize product for 5 min. All ground samples were mixed, homogenized and collected in lidded plastic buckets for the following tests.

3.1.1. Characterization of Materials

3.1.1.1. Moisture Content Measurements

Moisture contents of samples were determined by drying the representative feed stock samples in a drying oven at 105ºC for 3 h. Oreks sample contains 5.29% moisture.

3.1.1.2. Specific Density Determination

Specific density of Oreks sample was determined using Helium Quantachrome Pycnometer at ESOGU Mineral Processing Laboratory. Specific density was determined as 3.456 g/cm^3.

3.1.1.3. Surface Area Determination

As Tek Kimya Blain apparatus in ESOGU Mineral Processing Laboratory was used to determine surface area of Oreks sample. The surface area of the sample was found to be 3678 cm^2/g.

3.1.1.4. Particle Size Distribution Determination

The particle size distribution of the tailing material was determined by Malvern Inst. Mastersizer 2000 in our laboratory. Figure 3.3 shows particle size distribution of flotation tailing sample. d_{10} of sample was around 1 µm, d_{50} 13 µm, d_{80} 57 µm and d_{90} 100 µm. As can be seen from the graph, almost half of the sample is less than 10 µm in size. In general, leaching efficiency increases with increasing fineness of particles. In our case, flotation tails are very fine, there is no need to further grinding the sample. Fine particles may produce aggregation and reduced dispersion problem during leaching. Gravity pre-concentration and/or mechanical flotation concentration of this fine material are very difficult.

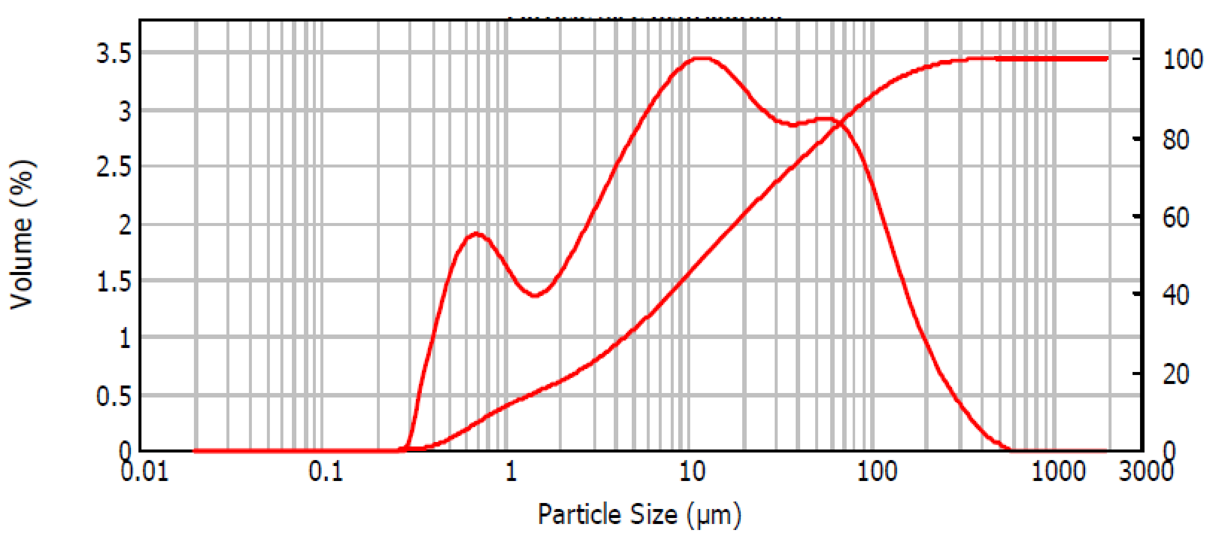

Figure 3.3. Particle size distribution of Turkish tailing sample.

3.1.1.5. XRF and ICP-AES Analysis

Table 3.1 shows major oxide percent of flotation tailing sample using Panalytical Zetium WDXRF. According to the XRF analysis result, Sample contains about 7.12% Zn, 6.77% Pb, 6.12% As, 24.39% Fe, 12.16% $Si0_2$. Small amount of Ce (0.31%) and Co (0.049%) are also found. In this tailing, smithsonite and cerussite (i.e. Zn and Pb) are the important and abundant base metals. Major impurities are Fe_2O_3, SiO_2, As_2O_3, CaO and Al_2O_3. Gangue minerals can be goethite, quartz, calcite and kaolinite.

Table 3.1. XRF results of sample

Report name	Result (%)	Conversion factor	% Metal
L.O.I	12,595		
CuO	0,057	1,2518	0,046
ZnO	8,859	1,2448	7,12
PbO	7,297	1,0772	6,77
NiO	0,064	1,2725	0,05
As_2O_3	8,074	1,3203	6,12
CeO_2	0,380	1,2284	0,31
MnO	0,035	1,2912	0,026
SrO	0,036	1,1826	0,03
BaO	0,572	1,1165	0,51
Fe_2O_3	34,866	1,4297	24,39
P_2O_5	0,055	2,2916	0,024
SO_3	4,531	2,4972	1,81
Co_3O_4	0,066	1,3469	0,049
SiO_2	12,155	2,1392	5,68
Cl	0,126		0,126
TiO_2	0,246	1,6681	0,15

Al_2O_3	3,873	1,8895	2,05
K_2O	0,657	1,2046	0,55
CaO	5,455	1,3992	3,9

Table 3.2 shows sample ICP-AES results. Sample contains 7.50% Pb; 5.77% Zn; 21.3% Fe; 3.91% Ca; 1.92% Al; 1.85% S; 0.66% K; 0.45% Mg; 0.10% Ti; 101 ppp Ag; >10000 ppm As; 420 ppm Ba; 376 ppm St; 306 ppm Cu; 279 ppm Sb; 245 ppm Cd; 63 ppm Cr; 43 ppm V; 20 ppm Tl, U and W; <20 ppm Th; 10 ppm Ga, La and Ni; 9 ppm Mo; <2 ppm Bi; <1 ppm Co and 0.6 ppm Be. Major metals in flotation tailing sample are Pb, Zn, Fe and As. In sample, Cu is very low. Ag is 101 ppm. There are some differences between XRF and ICP analysis results.

Table 3.2. ICP analysis results

Method	Analyte	Units	LOD	Results
WEI-21	Recvd Wt.	Kg	0,02	**<0,02**
ME - ICP61	**Ag**	Ppm	0,5	**>100**
ME - ICP61	**Al**	%	0,01	**1,92**
ME - ICP61	**As**	Ppm	5	**>10000**
ME - ICP61	**Ba**	Ppm	10	**420**
ME - ICP61	**Be**	Ppm	0,5	**0,6**
ME - ICP61	**Bi**	Ppm	2	**<2**
ME - ICP61	**Ca**	%	0,01	**3,91**
ME - ICP61	**Cd**	Ppm	0,5	**245**
ME - ICP61	**Co**	Ppm	1	**<1**
ME - ICP61	**Cr**	Ppm	1	**63**
ME - ICP61	**Cu**	Ppm	1	**306**
ME - ICP61	**Fe**	%	0,01	**21,3**
ME - ICP61	**Ga**	Ppm	10	**10**
ME - ICP61	**K**	%	0,01	**0,66**

ME - ICP61	**La**	Ppm	10	**10**
ME - ICP61	**Mg**	%	0,01	**0,45**
ME - ICP61	**Mn**	Ppm	5	**763**
ME - ICP61	**Mo**	Ppm	1	**9**
ME - ICP61	**Na**	%	0,01	**0,49**
ME - ICP61	**Ni**	Ppm	1	**79**
ME - ICP61	**P**	Ppm	10	**280**
ME - ICP61	**Pb**	Ppm	2	**>10000**
ME - ICP61	**S**	%	0,01	**1,85**
ME - ICP61	**Sb**	Ppm	5	**279**
ME - ICP61	**Sc**	Ppm	1	**4**
ME - ICP61	**Sr**	Ppm	1	**367**
ME - ICP61	**Th**	Ppm	20	**<20**
ME - ICP61	**Ti**	%	0,01	**0,10**
ME - ICP61	**Tl**	Ppm	10	**20**
ME - ICP61	**U**	Ppm	10	**20**
ME - ICP61	**V**	Ppm	1	**43**
ME - ICP61	**W**	Ppm	10	**20**
ME - ICP61	**Zn**	Ppm	2	**>10000**
Ag – AA46	**Ag**	Ppm	1	**101**
Pb – AA46	**Pb**	%	0,001	**7,50**
Zn – AA46	**Zn**	%	0,001	**5,77**

3.1.1.6. XRD analysis

Mineralogical composition and phases of sample were examined using X-Ray Diffraction (XRD). Figure 3.4 shows the XRD pattern of flotation tailing sample. The major mineral phase peaks with 100% intensity were from Smithsonite ($ZnCO_3$), Cerussite ($PbCO_3$), Goethite (FeO(OH)), Calcite ($CaCO_3$), Quartz (SiO_2), Corkite [$PbFe_3[(OH)_6:SO_4:PO_4]$] and Beudantite ($PbFe_3(OH)_6SO_4AsO_4$).

Corkite is a phosphate mineral in the beudantite subgroup of the alunite group. Corkite is the phosphate analogue of beudantite and with it, a complete solid solution range exists. Beudantite is a secondary mineral occurring in the oxidized zones of polymetallic deposits. It is a Pb, Fe, arsenate and sulfate. Beudantite is the arsenate analogue of the phosphate corkite. Corkite and beudantite are readily soluble in warm HCl.

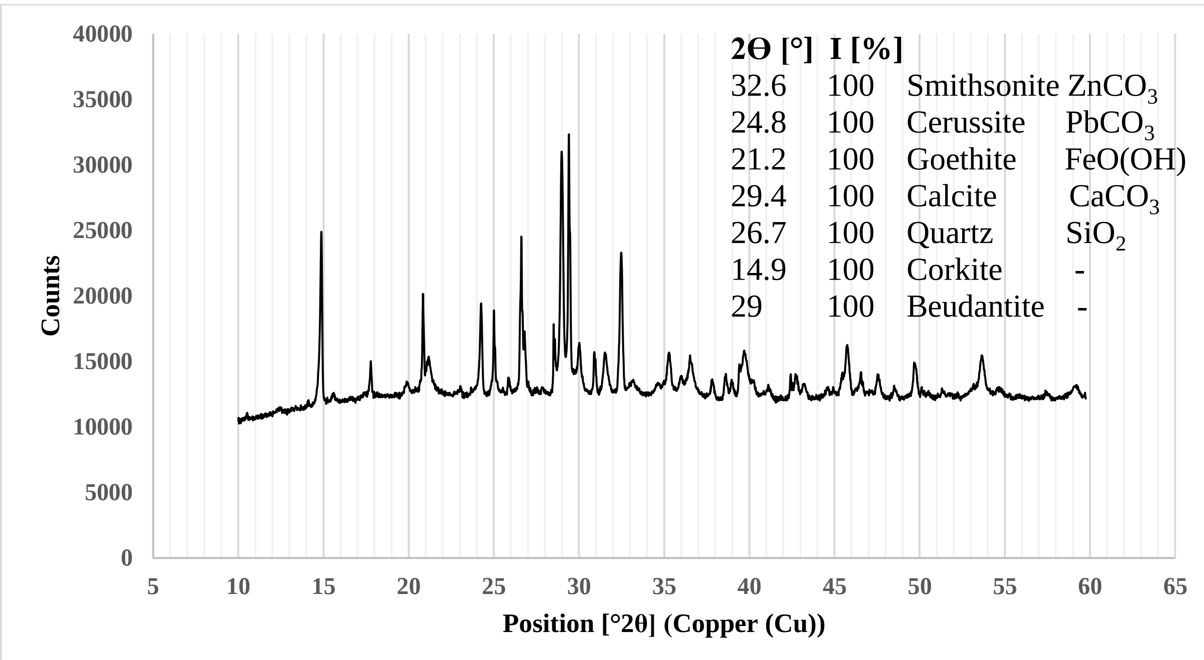

Figure 3.4. XRD pattern of the sample.

3.1.1.7. TGA analysis

Thermogravimetric analysis (TGA) was carried out to find out the thermal behavior of Oreks sample from 30 ºC to 600 ºC. 23 mg of sample was analyzed with a linear heating rate of 10 ºC/min in N_2 atmosphere (flowrate: 20 ml/min and pressure: 2.1 bar) by the Central Laboratory at ESOGU using Perkin Elmer Simultaneous Thermal Analyzer (STA) 8000 equipment. Result of the thermogravimetric analysis is given in Figure 3.5.

Weight loss occurring during thermogravimetric analysis can be explained by evaporation of the moisture, chemically bonded crystal water and several decompositions. Sample contains both moisture and crystal water. There are three endothermic peaks in the TGA graphs. First endothermic peak occurred between 50 and 100 ^oC. Until 100 ^oC moisture content is evaporated. About 1.656% weight loss occurred until 100 ^oC. Second endothermic peak is around 275 ^oC. Between 100 ^oC and 233 ^oC the weight loss is about 1.1%, between 233 ^oC and 315 ^oC, the weight loss is around 2.4% and between 315 and 460 ^oC, the weight loss is about 4.9%. At 600 ^oC, the final weight loss is 11.4%. Between 100^oC and 315 ^oC crystal water evaporates and dehydration occurs. After the loss of water from the compounds, the third endothermic peak appears after 400 ^oC for decomposition of Zn/Pb carbonate. Carbonates decompose, CO_2 evaporates and metal oxides occur ($Zn/PbCO_3 \rightarrow Zn/PbO + CO_{2\,(g)}\uparrow$). Zn, Pb and Cd are volatile fuming metals. Due to low melting points of pure Zn and Pb metals, after 328 ^oC some of Pb and after 427 ^oC some of Zn may evaporate. All three peaks are accompanied by the mass loss as seen in TG curve.

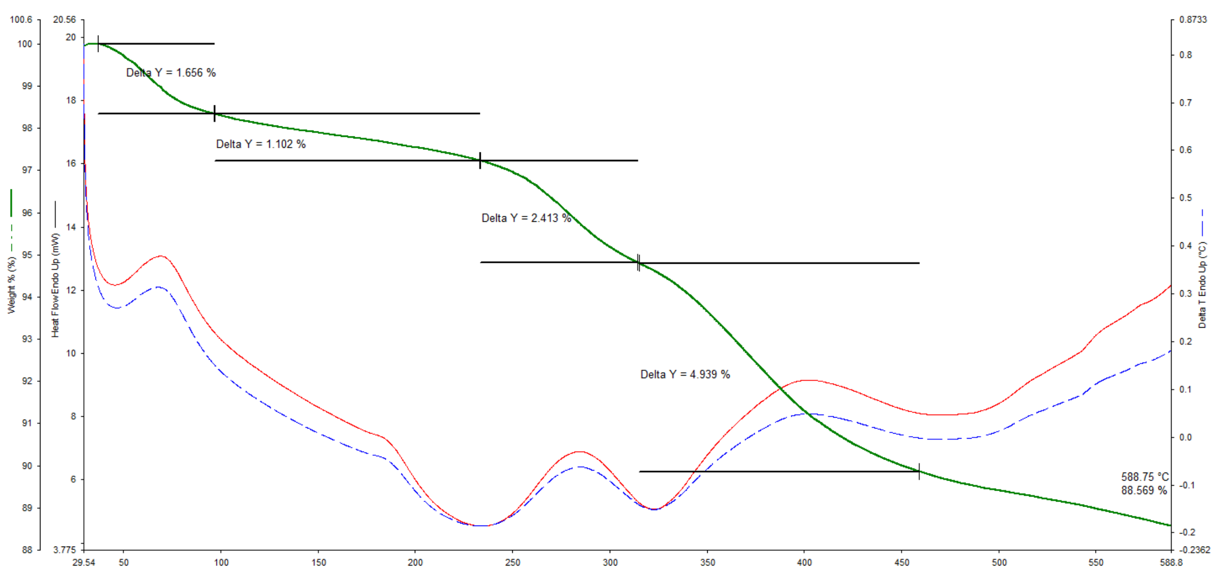

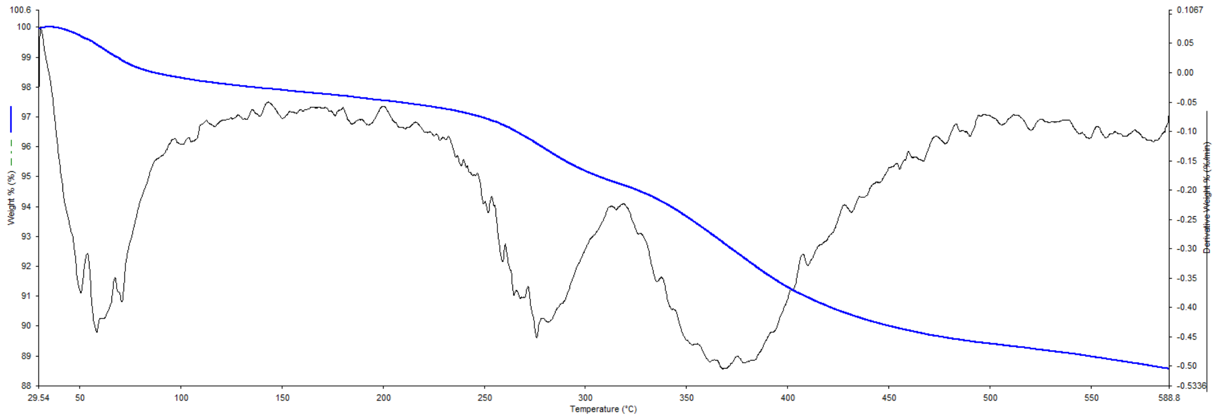

Figure 3.5. DTA and TG curves for Oreks sample.

3.1.1.8. SEM-EDX Analyses

The particle morphology and surface composition of samples were detected by scanning electron microscopy (SEM) and energy dispersive spectrometry (EDS) analyses. SEM and EDX analyses of Oreks samples were carried out at ESOGU. SEM images/micrographs and surface morphologies of some particles are given in Figure 3.6a, b, c and d. Surface morphology of particles are very rough, porous and complex. Different shapes and sizes are observed. Figure 3.7a and b and Table 3.3 and 3.4 show EDX area chemical analysis of the samples. There were three distinct phases. The brightest particles have high level of Pb and O are identified as Cerussite, gray particles with high Zn and O contents can be recognized as Smithsonite and the darkest particles have high amount of O, Ca and Si and likely represent calcite and quartz. Some particles are fine and some particles are agglomerated.

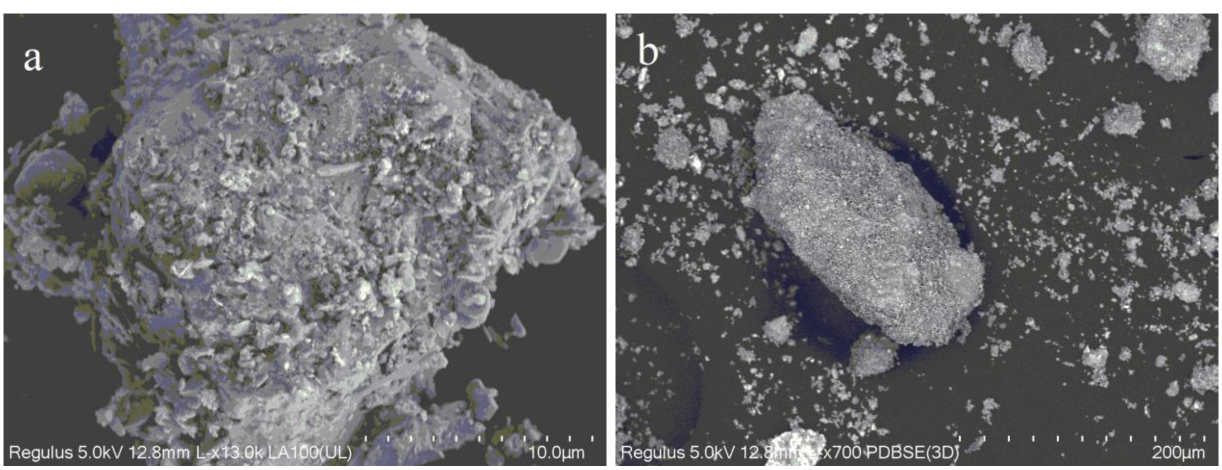

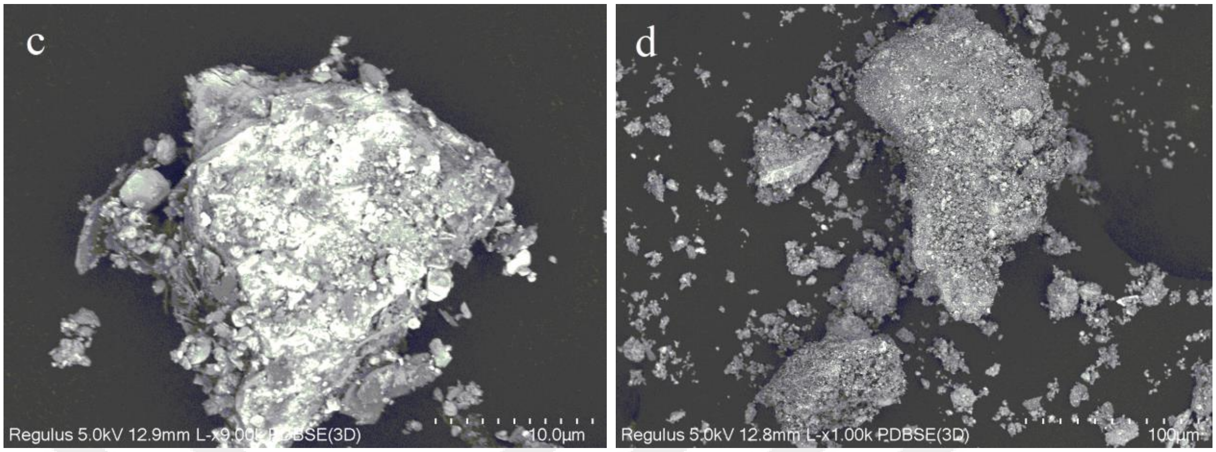

Figure 3.6a, b, c, d. SEM images of Oreks sample

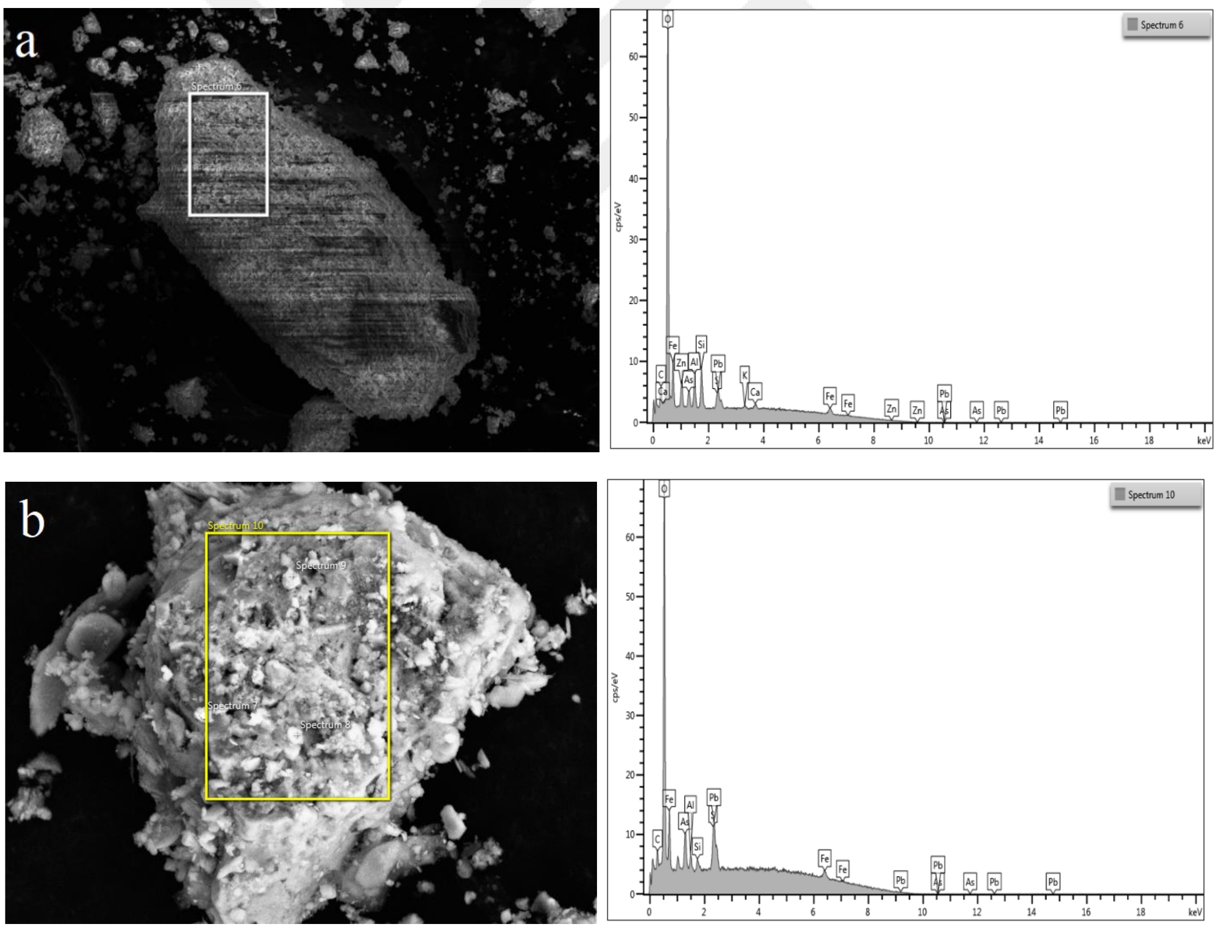

Figure 3.7a and b. SEM-EDX analyses of Oreks sample.

Table 3.3. EDX analyses of Oreks sample a.

Statistics	C	O	Al	Si	S	K	Ca	Fe	Zn	As	Pb
Max	8.01	39.22	4.08	5.10	1.66	0.90	2.01	20.56	6.14	3.68	8.65
Min	8.01	39.22	4.08	5.10	1.66	0.90	2.01	20.56	6.14	3.68	8.65
Average	8.01	39.22	4.08	5.10	1.66	0.90	2.01	20.56	6.14	3.68	8.65
Standard Deviation	0.00	0.00	0.00	0.00	0.00	0.00	0.00	0.00	0.00	0.00	0.00

Table 3.4. EDX analyses of Oreks sample b.

Statistics	C	O	Al	Si	S	Fe	As	Pb
Max	5.96	35.70	1.49	1.26	3.62	22.95	7.49	21.53
Min	5.96	35.70	1.49	1.26	3.62	22.95	7.49	21.53
Average	5.96	35.70	1.49	1.26	3.62	22.95	7.49	21.53
Standard Deviation	0.00	0.00	0.00	0.00	0.00	0.00	0.00	0.00

3.2. Method

3.2.1. Leaching Method

Mtop digital magnetic stirring heated extraction mantle (EAMDS 9603-03) will be used in the leaching tests (Figure 3.8 and Figure 3.9). Stirring speed changes from 100 to 1500 rpms. Digitally controlled (within ± 1^{o}C) temperature changes up to 450 ^{o}C with 3*260W heaters. The reaction temperature maintained constant at the desired temperature. 500 ml three-necked round bottom Pyrex balloon flasks are used in these extraction mantles. Also single stirring mantle will be also used in the leaching tests. NS 29/32 borosilicate glass spiral reflux condensers (40 cm long) are attached to balloon’s center neck for preventing evaporation of leaching agents. Temperature sensor is placed to left neck of the balloon and samples are taken from the right neck (Kaya et al, 2019).

For each selective leaching test, 25 g of solid tailing samples are used with S/L ratio of 1/10 (w/v). 400 rpm stirring speed was used unless otherwise stated. Increasing stirring speed more than 300-400 rpm. Temperature reached the desired value, leach sample was added to 250 mL leach solution. In leaching tests was preferred to use withdrawal method in most of the tests.

Samples of 5 mL were removed from the pulp at defined time intervals. Samples were immediately vacuum filtered, diluted, stored at 4 ^{o}C before analysis and analyzed for Zn, Pb and Fe (three elements) with AAS at ESOGU and/or Zn, Pb, Fe, As and Ag (five elements) with ICP at ALS laboratory . During sampling pH of the solution and at the end of leaching test PLS of the solution was taken and analyzed for Zn, Pb and Fe with AAS in our ESOGU laboratory.

Figure 3.8. Digital leaching experimental set-up.

Figure 3.9. Single experimental leaching set-up

Dissolution of Zn, Pb, As, Ag and Fe was determined as a function of S/L ratio (1:10-1:30), acid concentration (0.25-1.0 M) and temperature (25-80 ^oC).

The leaching rate/efficiency of metals/metal extraction can be calculated from solution according to following formulas:

$$R = \frac{Cm*V}{Co*M} * 10 \quad (3.1)$$

Where R is the leaching recovery percentage of metal of interest (Pb, Zn, Fe, As or Ag); C_m (g/mL) is the concentration of metal ion in leach liquor/filtrate; V (mL) is the leach liquor/filtrate volume; C_o is the metals content of feed sample (wt. %) and M (g) is the mass of the metal oxide ore leached.

At the end of the leaching tests, the solid residue remained in the filter paper was dried in an oven at 105 °C for 2 hours. For some tests, the dried solid residue will be analyzed by the ICP to calculate metal losses and the SEM-EDX to display its structure.

3.2.2. Purification method

3.2.2.1. Precipitation method

Precipitation experiments carried out in 250 ml beaker, 200 rpm mixing speed and 60 min. Mtop digital magnetic stirring heated mantle (EAMDS 9603-03) was used in the purification tests. NaOH and $NH_4(OH)$ were used for pH arrangement. H_2O_2 was used for determined effect of oxidant on precipitation efficiency.

3.2.2.2. Cementation method

After the determination of the optimum condition for precipitation tests, cementation experiments were carried out in 250 ml beaker, 200 rpm stirring speed and 60 min., Zn powder was used in cementation tests. 5.0 M NaOH was used for arrangement of pH.

3.2.4. Solvent extraction method

3.2.4.1. Extraction method

Solvent extraction experiments carried out in 150 ml beaker, aqueous/organic phase ratio (A/O, 25ml/25ml, 1/1) a METOPS mechanical stirrer with a three-blade stainless-steel impeller (35 mm diameter) was used. Mixing speed was 400 rpm and mixing time was 10 minutes. 5.0 M NaOH was used for solution phase pH adjustment. At the end of the experiment, to ensure complete disengagement time of the solution phase and the organic phase. 5 minutes waited. When a complete phase separation was seen, with the help of a syringe 10 mL of the solution was withdrawn from the phase. The pH value of the withdrawn solution was determined and recorded. The solution phase and organic phase mixture was transferred into a 100 mL separatoin funnel. After 1 hour waiting, the solution phase in the separatory funnel was separated from the organic phase and solution phase has been sent to chemical analysis. At the end of the studies, the extraction efficiency was calculated using the formula below:,

$$\% E = [[(C_1 \times V_1) - (C_2 \times V_2)] / (C_1 \times V_1)] \times 100 \qquad (3.2)$$

E: Extraction yield, %

C_1: Metal concentration in synthetic solution, mg/L

V_1: Volume of synthetic solution, mL

C_2: Metal concentration of the synthetic solution after extraction, mg/L

V_2: Total volume of synthetic solution with addition of NaOH, mL

3.2.4.1. Stripping method

Metals remaining in the loaded organic phase after extraction experiments were subjected to stripping. Stripping experiments carried out in 200 mL beaker that loaded with deionized water with organic phase (A:O, 25 mL:25 mL, 1:1) and in the different pH values (0.25, 0.5, 0.75, 1). The temperature was set to 25 °C like extraction experiments and the solutions were expected for 5 minutes to reach the desired temperature. During the stripping process, organic has been observed at which pH values the metals in the phase can be stripped and the stripped organic phase after the process was returned to the solvent extraction circuit.

3.2.5. Electrowinning method

An electrodeposition set-up consisting of a beaker, a D.C. power supply, and a holder was used for electrowinning experiments. A single Mtop digital magnetic stirring heated mantle (EAMDS 9603-03) was used to put the beaker containing the leach solution. A multimeter was used to connect the anode and cathode to the D. C. power supply.

In electrowinning experiments, aluminum sheets (old license plate of the cars) were used as zinc deposition substrates. Lead sheets were utilized as anodes for electrodeposition. The lead anode was 35 mm*40 mm*1 mm in diameter, while the aluminum substrate was 40 mm*35 mm*0.3 mm in diameter. The electrowinning experiments carried out at 20 ^{o}C.

4. RESULTS AND DISCUSSION

4.1. First Step Leaching Study

4.1.1. Inorganic Acid Leaching Study

Pre-leach tests were carried out with inorganic acids of H_2SO_4, HCl, and HNO_3 (0.5 - 1.0 M concentration, 25-80 ^oC leach temperature, and 30-180 min. leach time. Perchloric acid leach was also tested.

4.1.1.1. Sulfuric acid leach study

Solubilization of Zn, Pb, Ag, Fe and As as a function of leaching time was determined at two different H_2SO_4 (0.5 and 1.0 M) concentrations

- **Effect of temperature and time on dissolution with 0.5 M sulfuric acid concentration**

The effect of 0.5 M sulfuric acid concentration and time on metals dissolution was tested. In general, 25 g. Oreks sample with 1/10 S/L ratio at 400 rpm was leached using 0.5 M H_2SO_4 at 25 ^oC, 40 ^oC, 60 ^oC and 80 ^oC for 30, 60, 120 and 180 min. The effect of concentration and time on dissolution efficiency is show in Table 4.1 and Figures 4.1-4.4. In general, as the leaching time and temperature increase, metal dissolutions increase. There is a significant increase in metal dissolution in the first 30 min. and then metal dissolution increase is gradual. Metal dissolution order is Zn>As>Fe>Pb for all leaching temperatures. Most of the time, best leaching results were obtained at 180 min. Sulfuric acid concentration and temperature have a significant effect on the amount of Fe passing into the solution. Leaching with 0.5 M H_2SO_4 at 25 ^oC, 79.4% of Zn dissolution at 30 min. and 84.9% Zn dissolution at 180 min. were achieved. Due to the precipitation of lead as a sulfate formation, lead dissolution was nearly negligible at all examined temperatures and leaching times. As dissolved much higher than Fe, As dissolution was 13.7% at 30 min. and 14.5% at 180 min. Fe dissolution was 3.6% at 30 min and 5.2% at 180 min. In acidic conditions, arsenic appears as As_2O_3. After elapsing a certain time, namely 30 min., the dissolution rate was slow as compared to initial dissolution rate. About 80% Zn dissolution was obtained in short time period (i.e.30 min. leaching time) at room temperature due to fine particle size used (13% -10µm) and fast solubility of our tailing samples. Similar results correspond well with the findings by Jandova et al. (2002). Havlik, et al. (2006) also found that leaching Zn from EAFD using a H_2SO_4 acid lixiviant was a very fast process. Almost all Zn was dissolved almost immediately after combining the solids with the lixiviant (Havlik et al., 2006; Jandová et al., 2002). This study also found that the amount of Zn extracted reduced with reaction time, as the experiment progressed. This is suggested to be a result of the system attempting to achieve dynamic equilibrium.

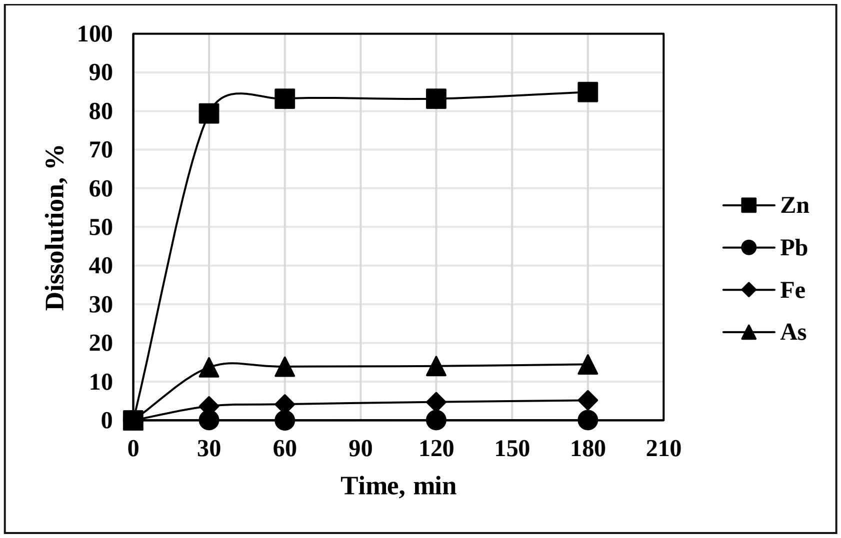

Figure 4.1. Metal dissolution with 0.5 M sulfuric acid at 25 ^oC

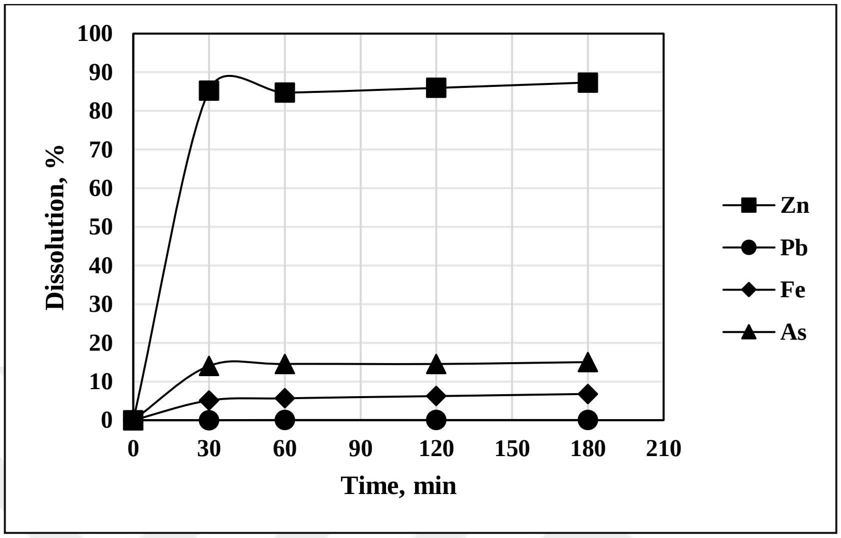

Figure 4.2. Metal dissolution with 0.5 M sulfuric acid at 40 ^oC

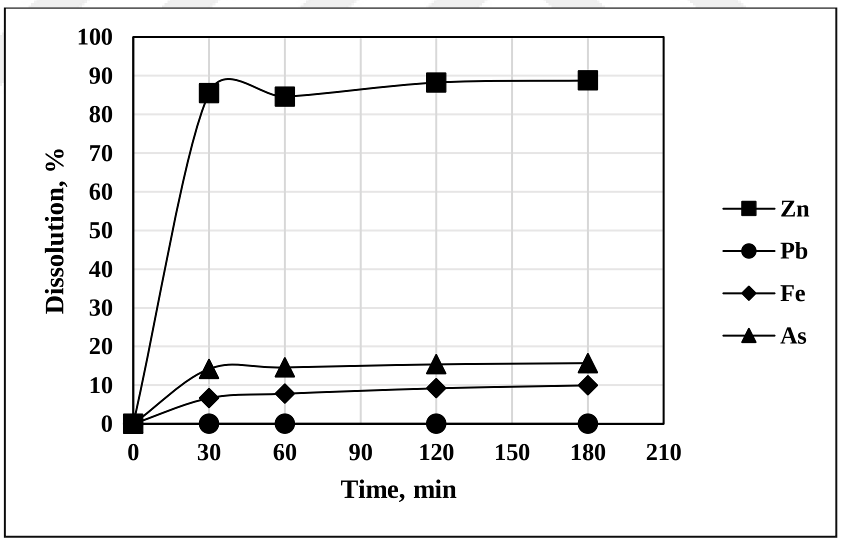

Figure 4.3. Metal dissolution with 0.5 M sulfuric acid at 60 ^oC

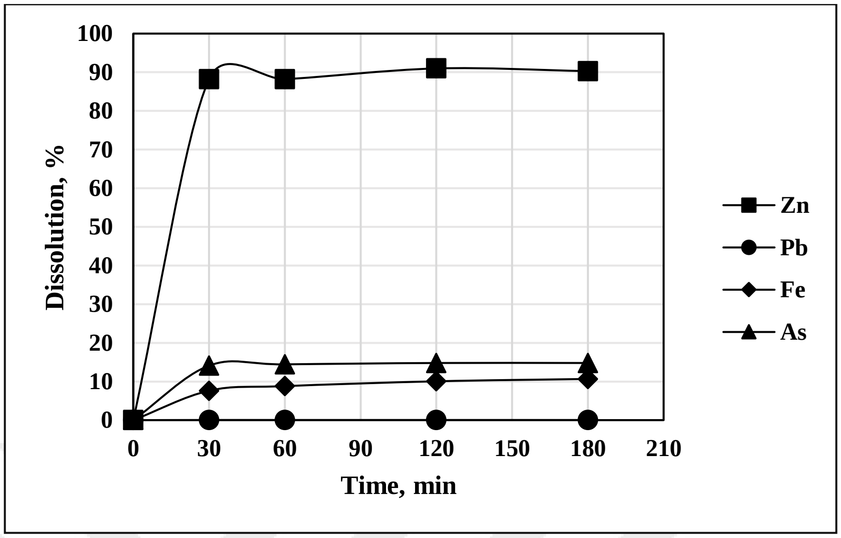

Figure 4.4. Metal dissolution with 0.5 M sulfuric acid at 80 ºC

Table 4.1. Effect of temperature and time on metal dissolution with 0.5 M sulfuric acid.

Time, min	25 ºC				40 ºC			
0	Zn	Pb	Fe	As	Zn	Pb	Fe	As
30	79.4	0.0	3.6	13.7	85.3	0.0	5.1	14.0
60	83.2	0.0	4.2	13.9	84.7	0.0	5.7	14.5
120	83.2	0.0	4.7	14.0	86.0	0.0	6.2	14.5
180	84.9	0.0	5.2	14.5	87.3	0.0	6.8	15.0
	60 ºC				80 ºC			
0	Zn	Pb	Fe	As	Zn	Pb	Fe	As
30	85.4	0.0	6.6	14.2	88.2	0.0	7.6	14.1
60	84.6	0.0	7.8	14.6	88.2	0.0	8.8	14.4
120	88.2	0.0	9.2	15.4	91.0	0.0	10.0	14.8
180	88.7	0.0	10.0	15.7	90.3	0.0	10.7	14.8

With 0.5 M H_2SO_4 leaching, maximum 91% Zn dissolution can be obtained at about 14.8% As and 10% Fe dissolution at 80 ºC leaching temperature and 120 min leaching time. Increase in temperature did not significantly increased As dissolution but, almost doubled the Fe dissolution. Generally, increasing the temperature in a leaching system will result in faster leaching kinetics. This is due to the relationship between the rate constant and the temperature

as described by the Arrhenius equation for chemical reaction rate controlled systems (Lottering, 2016). Increasing leach temperature to 80 ^oC, significantly increases Fe dissolution. At 0.5 M H_2SO_4 concentration, As dissolution was higher than Fe dissolution for all investigated leach temperature and times. Our feed contains goethite ($\alpha FeO(OH).H_2O$), corkite [$PbFe_3[(OH)_6:SO_4:PO_4]$] and bodanite ($PbFe_3(OH)_6SO_4$ AsO_4) as Fe containing minerals.

In H_2SO_4 medium, arsenitic Fe dissolution from bodanite is limited. In our sample, low Fe dissolution was due to complex formation between arsenate and goethite and prevent goethite dissolution. In H_2SO_4 media, arsenic can be leached with Zn, Fe, Cu, Cd, and In, making it difficult not only to separate from important metals, but also to avoid the creation of AsH_3. Simultaneously, a substantial amount of acidic As-containing waste solution is produced, from which As is primarily removed by precipitation, resulting in As-bearing waste residues such as ferric arsenate and calcium arsenate, among others (Zhang et al., 2019).

- **Effect of temperature and time on dissolution with 1.0 M sulfuric acid concentration**

The effect of 1.0 M sulfuric acid concentration and time on the dissolution of metals was investigated. In general, 1.0 M H_2SO_4 was used to leach a 25 g. Oreks sample with a 1/10 S/L ratio at 400 rpm at 25 ^oC, 40 ^oC, 60 ^oC, and 80 ^oC for 30, 60, 120, and 180 minutes, Table 4.2 and Figures 4.5-4.9 show the influence of concentration and time on dissolution efficiency. Leaching with 1.0 M H_2SO_4 at 80 ^oC, 91.9% of Zn dissolution at 30 min. and 96.5% Zn dissolution at 180 min. were achieved. Pb dissolution was negligible even at 180 min. As dissolved higher than Fe at 30 min. leaching time. Fe dissolution was much higher than As after 30 min leaching time. As dissolution was 27.9% at 30 min. and 31.9% at 180 min. At 80 ^oC leaching temperature, Fe dissolution significantly exceeds As dissolution after 60 min. leaching time at more than 95% Zn extraction. With increasing leaching temperature, the energy available for atomic and molecular collusions increases (Asadi et al., 2017). According to Song et al. (2015), with the leaching temperature rising, the spread of lixiviant molecules in leaching solution speeds up, more easily attacks the mineral grains and the stockpile energy of mineral particles increases, so the ability of damage or weakening of the chemical bonds of mineral enhances, and the number of molecules whose kinetic energy is equal to or greater than activation energy increases (Song et al., 2019). While possible reasons for decrease in impact of the temperature may be the pore blocking by solid products, which would cause a barrier for diffusion of reagent into the particles, as well as a barrier for diffusion of products away from the particle (Moradi and Monhemius, 2011). This theory suggests that although chemical reaction control occurs initially, the leaching process may later become diffusion controlled. According to selectivity values, 1.0 M H_2SO_4 concentration at 40 ^oC leaching time and 30 min. leaching time selected as a optimum condition for sulfuric acid leaching.

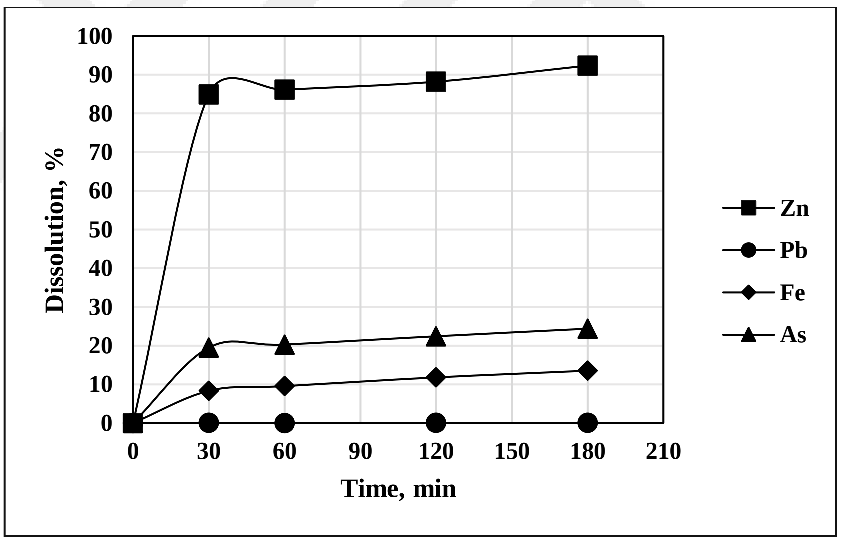

Figure 4.5. Metal dissolutions with 1.0 H_2SO_4 at 25 ^oC.

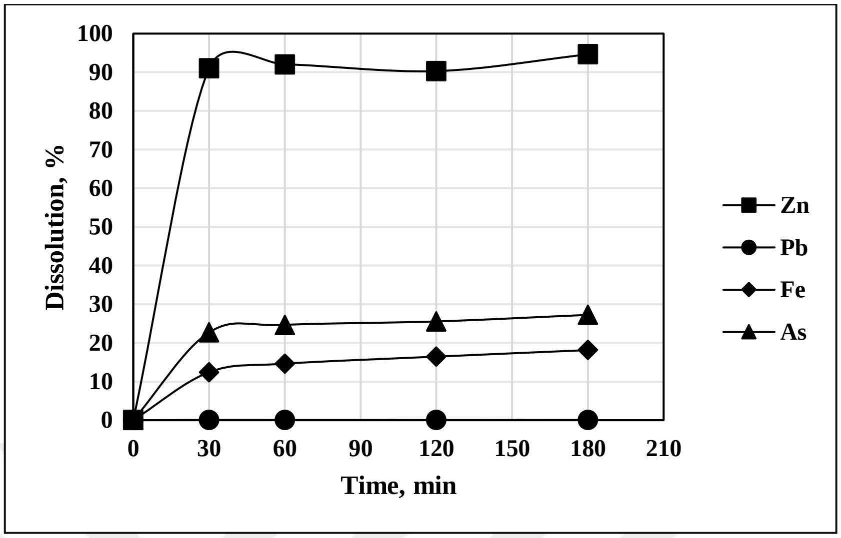

Figure 4.6. Metal dissolutions with 1.0 H_2SO_4 at 40 ^oC.

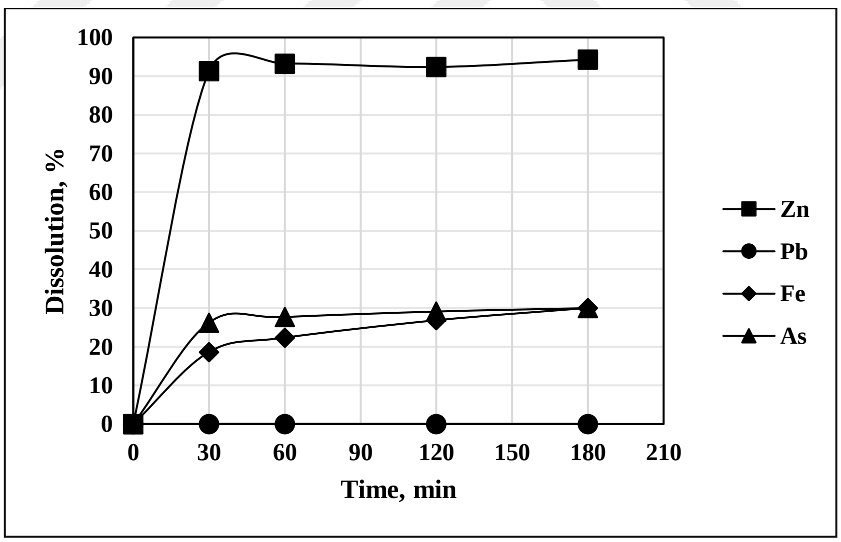

Figure 4.7. Metal dissolutions with 1.0 H_2SO_4 at 60 ^oC.

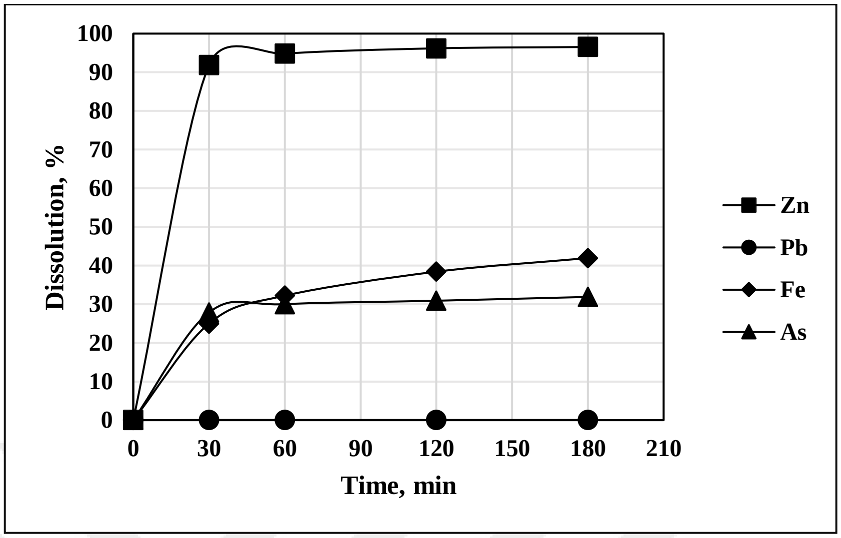

Figure 4.8. Metal dissolutions with 1.0 H_2SO_4 at 80 ^oC.

Table 4.2. Effect of temperature and time on metal dissolution with 1.0 M sulfuric acid.

Time, min	25 ^OC				40 ^OC			
0	Zn	Pb	Fe	As	Zn	Pb	Fe	As
30	84.9	0.0	8.3	19.5	91.0	0.0	12.4	22.7
60	86.1	0.0	9.5	20.3	92.0	0.0	14.6	24.6
120	88.2	0.0	11.8	22.4	90.3	0.0	16.4	25.5
180	92.4	0.0	13.5	24.4	94.6	0.0	18.1	27.2
	60 ^OC				80 ^oC			
0	Zn	Pb	Fe	As	Zn	Pb	Fe	As
30	91.3	0.0	18.6	26.3	91.9	0.0	25.0	27.9
60	93.2	0.0	22.3	27.7	94.8	0.0	32.2	30.0
120	92.4	0.0	26.9	29.1	96.2	0.0	38.4	30.9
180	94.3	0.0	30.0	30.0	96.5	0.0	41.9	31.9

❖ **Effect of Solid/Liquid Ratio on H_2SO_4 Leach**

Effect of solid/liquid ratio on dissolution efficiency has been carried out in 1/10, 2/10 and 3/10 (weight, g/volume, mL) by fixing the temperature at 40 °C and using 1.0 M sulfuric acid. Obtained results were given in Table 4.3 and Figures 4.9-4.11. Increasing the solid-liquid ratio typically increases the total amount of Zn leached, because there is more Zn present in the system. However, the percentage of the Zn leached was found to generally decrease at higher S/L ratios because, at higher S/L ratios, all particles may not be completely surrounded by the solution. In addition, the amount of acid available for leaching would likely be in excess at lower S/L ratios, while the limited acid available per unit of solid at higher S/L ratios may limit the dissolution reactions. In general, an increase in the L/S ratio enhances the leaching rate., but, the higher L/S ratio leads to a dilute solution and high consumption of reaction reagents and therefore it is important to optimize this factor (Asadi et al., 2017).

Table 4.3. Comparison of metal dissolutions with 1.0 M H_2SO_4 using 1/10 2/10 and 3/10 S/L ratios at 40 ^oC.

	S/L: 1/10			S/L: 2/10			S/L: 3/10		
Time (min)	Zn	Fe	As	Zn	Fe	As	Zn	Fe	As
0	0.0	0.0	0.0	0.0	0.0	0.0	0.0	0.0	0.0
30	91.0	12.4	22.7	91.0	11.2	18.4	81.3	3.9	10.9
60	92.0	14.6	24.6	89.3	12.3	18.8	79.0	4.2	10.6
120	90.3	16.4	25.5	91.0	14.5	19.8	81.6	4.9	10.9
180	94.6	18.1	27.2	91.4	14.8	19.9	87.8	5.8	11.5

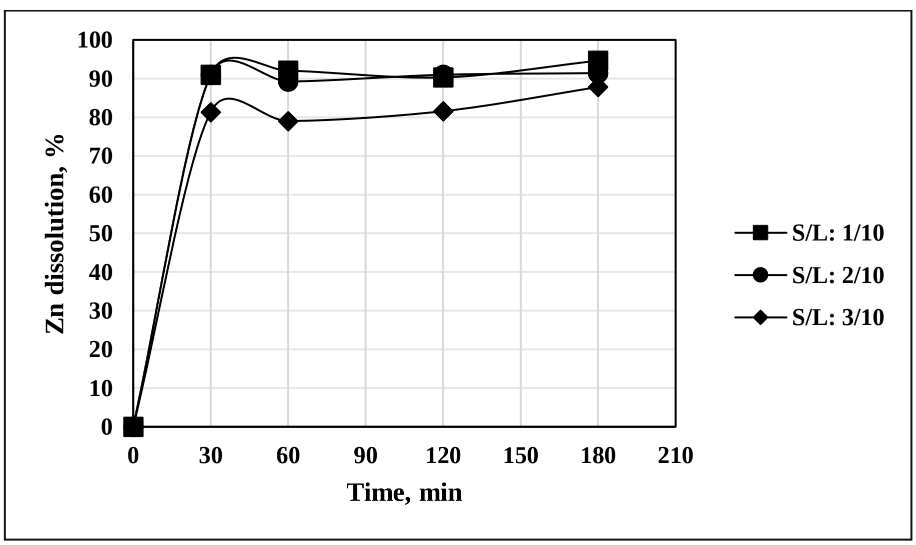

Figure 4.9. The effect of solid/liquid ratio on Zn dissolution.

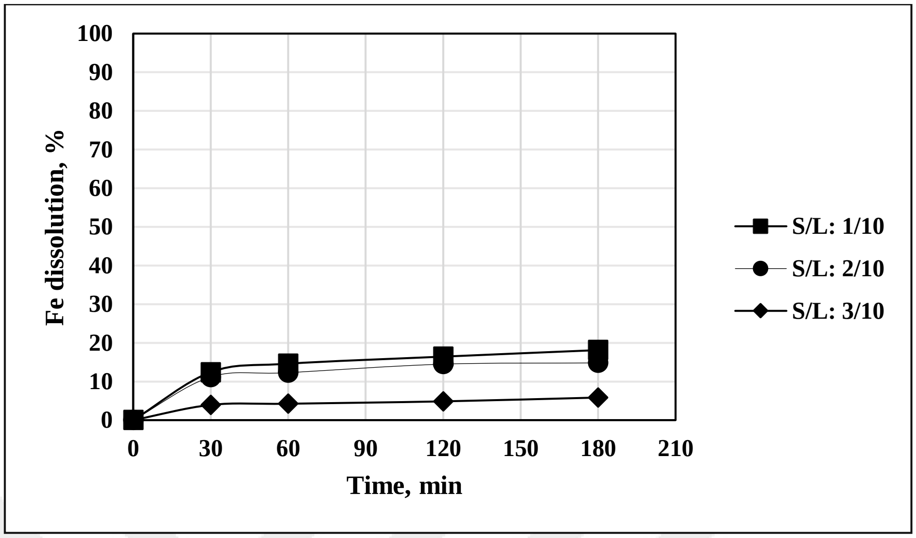

Figure 4.10. The effect of solid/liquid ratio on Fe dissolution.

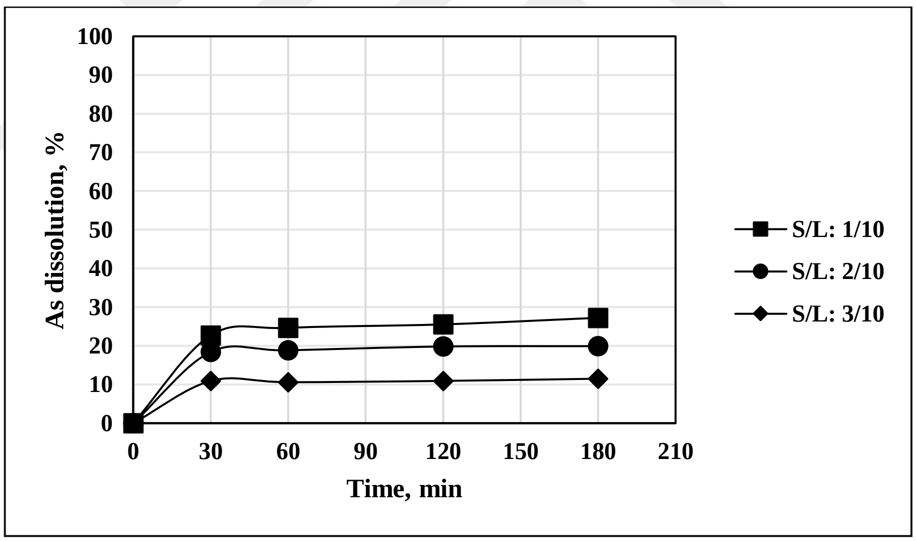

Figure 4.11. The effect of solid/liquid ratio on As dissolution

As a result, at 1/10 S/L ratio, about 95% Zn dissolution was obtained at 18% Fe and 27% As co-dissolution. When the solid amount doubled for the same amount of acid concentration, Zn dissolution decreased to 91.4% at 15% Fe and 20% As co-dissolutions. At 3/10 S/L ratio, 88% Zn dissolution is achieved at 180 min with 6% Fe and 11.5% As co-dissolution. Increasing the mass of sample (i.e. S/L ratio) per unit solution increases the Zn extraction due to increased surface area of solids available for contact with solution and therefore, the larger amount of Zn available for potential extraction (Lottering, 2006). Here, the reason for this divergence from other studies probably related to the acid concentration/the amount of H^+ ions, which was probably sufficient to dissolve the increased amount of Zn. But after optimum of S/L ratio zinc dissolution decreased because of the loss of H^+ ion in the solution. The optimum S/L ratio was determined to be 2/10 in this study. Langová, et al. (2007) also suggested that for a maximum Zn recovery, a S/L ratio of at least 2/10 is necessary.

Pulp density has significant effect on Zn, Fe and As dissolutions. With increasing S/L ratio, viscosity of slurry increases and consumption of leaching reagent decreases. Therefore, it is better and economical to use high S/L ratio in leaching. At high S/L ratio, H_2SO_4 selectively attacked to Zn rather than Fe and As. However; at low S/L ratio, some of the H_2SO_4 also attacks to Fe and As; because, the total Zn amount is low. High S/L ratio increased competing reactions for the Zn and Fe-As particles. Both Fe and As are difficult to leach at given operational conditions. Kukurugya et al., (2015) also proposed these theses. Pulp density significantly affects the ionic strength and increases pulp viscosity of the solution. The higher L/S ratio leads to a dilute solution and high consumption of leaching reagents (Kukurugya et al., 2015).

Table 4.4 shows the pH change with S/L at different leaching times. pH changes between 0.4 and 1.0. As the S/L ratio and leaching time increase, the pH of the leach solution increases. The highest pH was obtained at 3/10 S/L ratio. Increased pH means decreased H^+ ion concentration and more metal dissolution in the pulp. Since the pH was not kept constant in our batch tests, Zn, As and Fe metals compete for H^+ ion for dissolutions. The longer the leaching time, more H^+ ions were consumed from the medium by metals and pH of the medium increases. At constant leaching time, higher S/L ratio means more metals are available for dissolution; thus, metal dissolution increases. The higher the final pH means, the more metals were dissolved during leaching. The lower Fe and As dissolutions at high S/L ratio was related to the higher final pH which may start to precipitate these metals partially. The optimum conditions were determined to be 1.0 M sulfuric acid concentration, 40 °C leaching temperature, 2/10 solid to liquid ratio, and 30 minutes of leaching time.

Table 4.4. pH change with 1.0 M H_2SO_4 leach at different S/L ratios and 40 ^oC leaching temperature.

	pH		
Time, min	S/L: 1/10	S/L: 2/10	S/L: 3/10
30	0.35	0.77	0.88
60	0.53	0.79	0.95
120	0.62	0.84	0.99
180	0.65	0.88	1.04

Figure 4.12 shows the XRD spectra of sulfuric acid leached residue at the optimum conditions. Segnitite is a series from beudantite ($PbFe_3(AsO_4)(SO_4)(OH_6)$), which is the arsenate of corkite with which a complete solid-solution range exists, to $PbFe_3AsO_4(AsO_3OH)(OH)_6$ and difficult to distinguish since the sulfate and arsenate anions readily exchangeable with each other. According to the XRD results, H_2SO_4 leach residue contains 18.6% Fe, 17.8% Pb, 11.6% As, 4% Ca, 3.8% S, 5.4% Si, 0.2% Al, 37.6% O and 1.1% H. The residue contained 1.67 % ZnO, 13.2 % PbO, 6.27 % As_2O_3, 39.2 % Fe_2O_3, and 6.29 % CaO, according to XRF analysis.

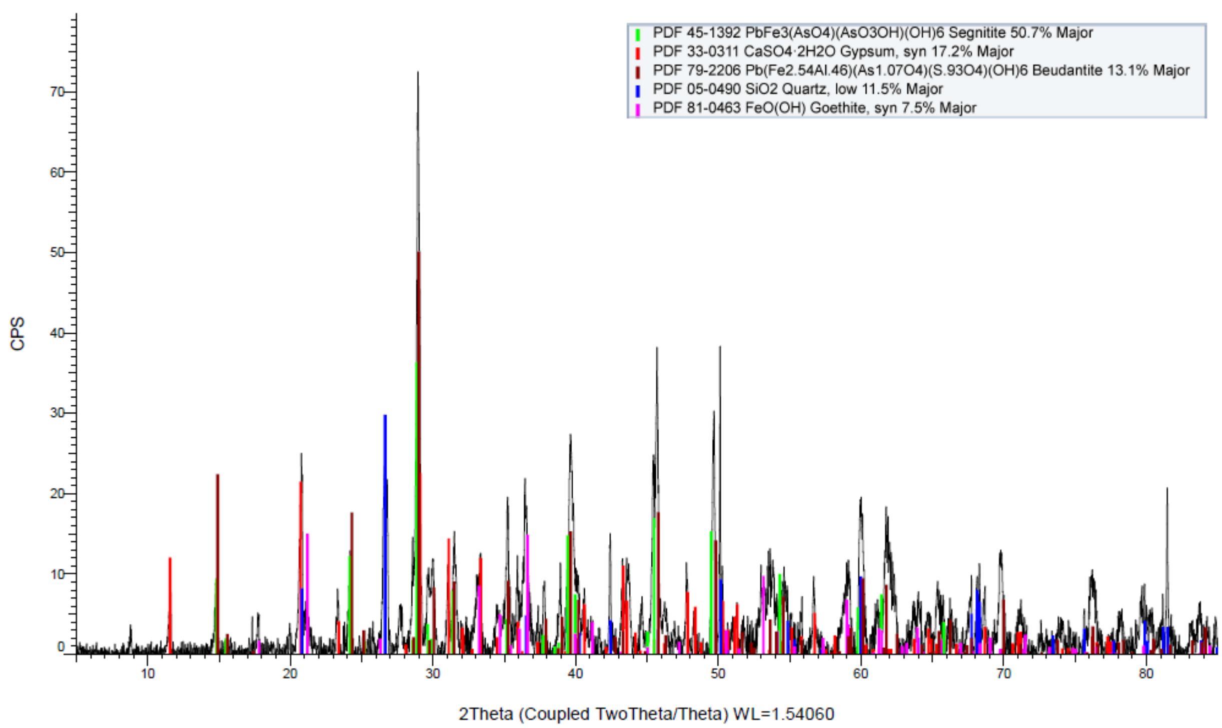

Figure 4.12. XRD spectra of sulfuric acid leached residue at the optimum conditions.

4.1.1.2. Hydrochloric acid leach study

Table 4.5 and Figures 4.13-4.21 show metal dissolution in different time, leaching temperature and acid concentration. Up to 0.5 M, the metal dissolution was determined to be Zn > Pb with no Fe dissolution. The rate of zinc dissolution increases as the leaching temperature increases, resulting in faster leaching kinetics. This effect was particularly noticeable for hydrochloric acid concentrations below 1.0 M. Metal solubility in hydrochloric acid increased, allows for faster metal leaching. With temperature increase, the slurry's viscosity and diffusion resistance reduced. Yoshida (2003) discovered that increasing the concentration of hydrochloric acid and the leaching temperature increased zinc dissolution from a zinc oxide powder, and the activation energy of the zinc oxide leaching by hydrochloric acid was 11.6 kJ/mol, which is consistent with the current study's finding that leaching time has no beneficial effect on zinc dissolution from flotation tailing (Yoshida, 2003). However, for the leaching of zinc ferrite, hydrochloric acid is a particularly effective lixiviant (Kaya et al., 2020a).

As results from Figure 4.21, with using 1.0 M hydrochloric acid solution at 80 °C temperature and a solid to liquid ratio of 1/10, 30 minutes of leaching appears to be sufficient to dissolve 93% zinc, 8.8 % lead, and 9.3 % iron. Increases in leaching temperature and time, on the other hand, had little effect on iron dissolution. For the optimum selecting of metal dissolution with hydrochloric acid, 0.5 M hydrochloric acid concentration, 80 °C leaching temperature, and 30 min. leaching time (Figure 4.18) or 1.0 M hydrochloric acid concentration, 80 °C leaching temperature, and 30 min. leaching time (Figure 4.21) were chosen as the optimal conditions based on these tests. However, the former is chosen as the ideal conditions for the hydrochloric acid leaching process because of the acid consumption and PLS neutralization in the downstream process. The hydrochloric acid leach should be carried out at a pH of less than 1.0. To precipitate Fe, the leach solution might be chlorinated. SX/EW in chloride solutions is expensive and complicated for small operations, and chlorine handling is challenging. The creation of Cl_2 gas rather than HCl during the EW process, as well as corrosion of anodes and cathode substrates, are some of the issues with HCl leaching–EW. because of these problems hydrochloric acid is not optimum agent for this research (Kaya et al., 2020a; Mackinnon et al., 1983; Majima et al., 1990; Mirza, 2016). The following are some of the possible reactions between $ZnO/ZnCO_3/PbO$ and hydrochloric acid (Hussaini et al., 2021a):

$$ZnO(s) + 2HCl(aq) \rightarrow ZnCl_2(aq) + H_2O \tag{4.1}$$

$$ZnCO_3(s) + 2HCl(aq) \rightarrow ZnCl_2(aq) + CO_2(g) + H_2O \tag{4.2}$$

$$PbO(s) + 2HCl(aq) \rightarrow PbCl_2(s) + H_2O \tag{4.3}$$

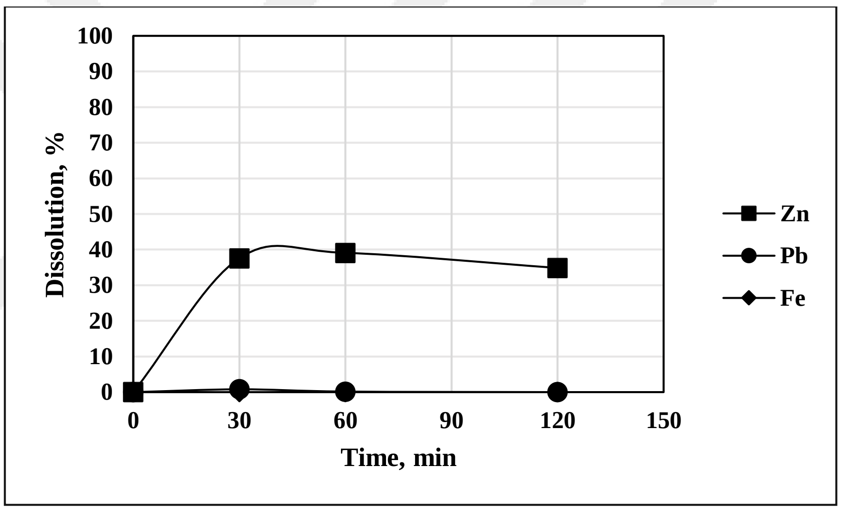

Figure 4.13. Metal dissolution with 0.25 M HCl at 40 ^oC and S/L: 1/10.

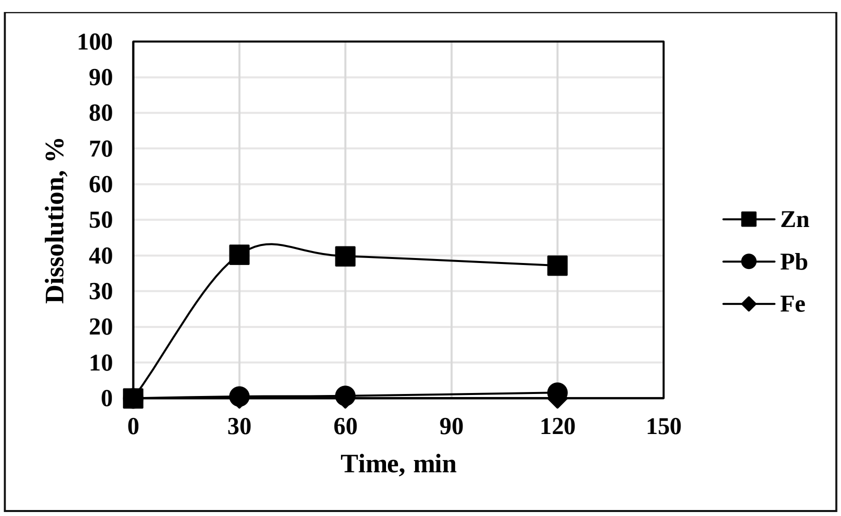

Figure 4.14. Metal dissolution with 0.25 M HCl at 60 ^oC and S/L: 1/10.

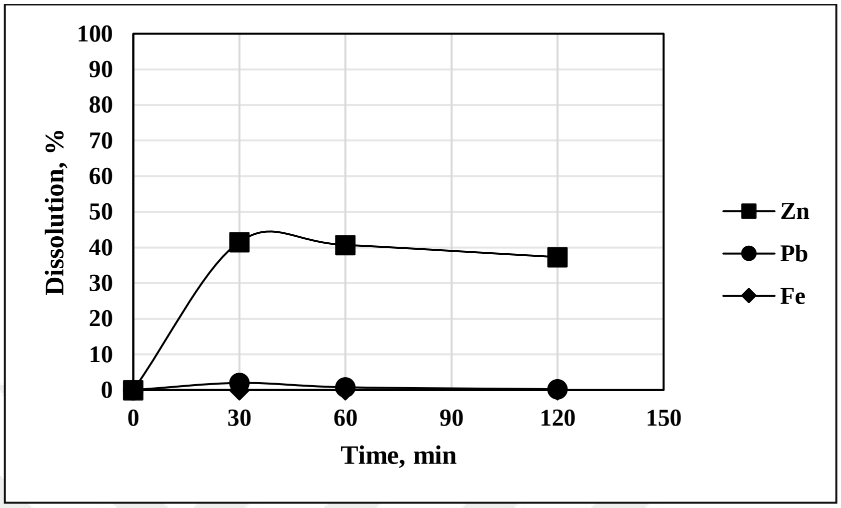

Figure 4.15. Metal dissolution with 0.25 M HCl at 80 ^{o}C and S/L: 1/10.

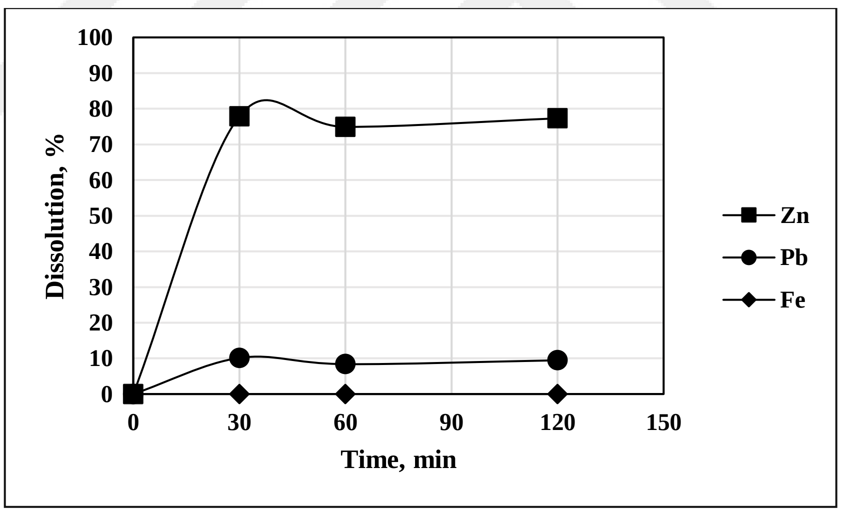

Figure 4.16. Metal dissolution with 0.5 M HCl at 40 ^{o}C and S/L: 1/10.

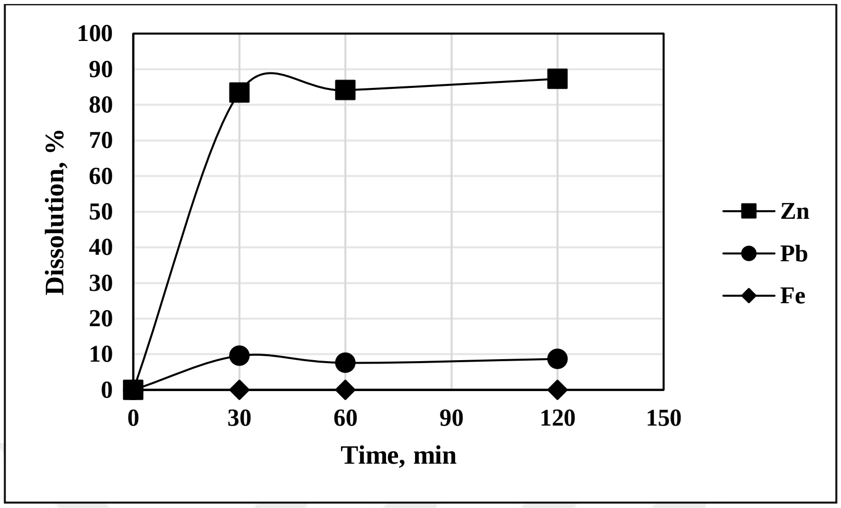

Figure 4.17. Metal dissolution with 0.5 M HCl at 60 °C and S/L: 1/10.

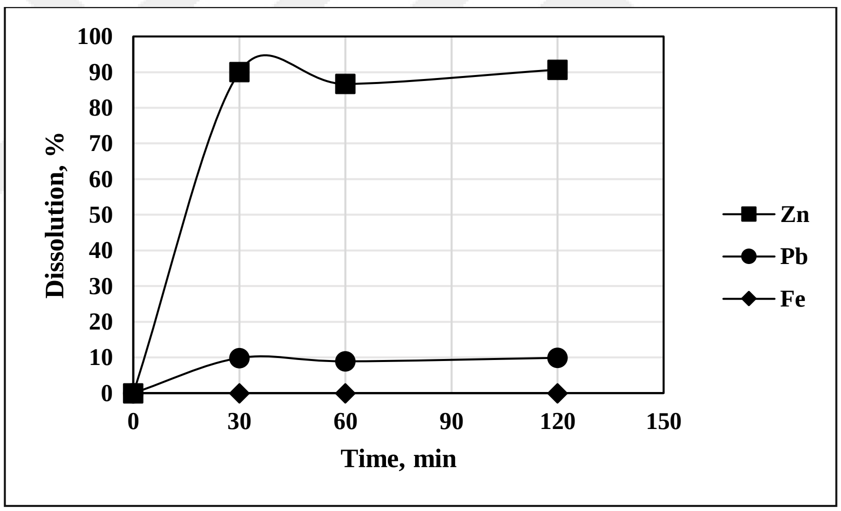

Figure 4.18. Metal dissolution with 0.5 M HCl at 80 °C and S/L: 1/10.

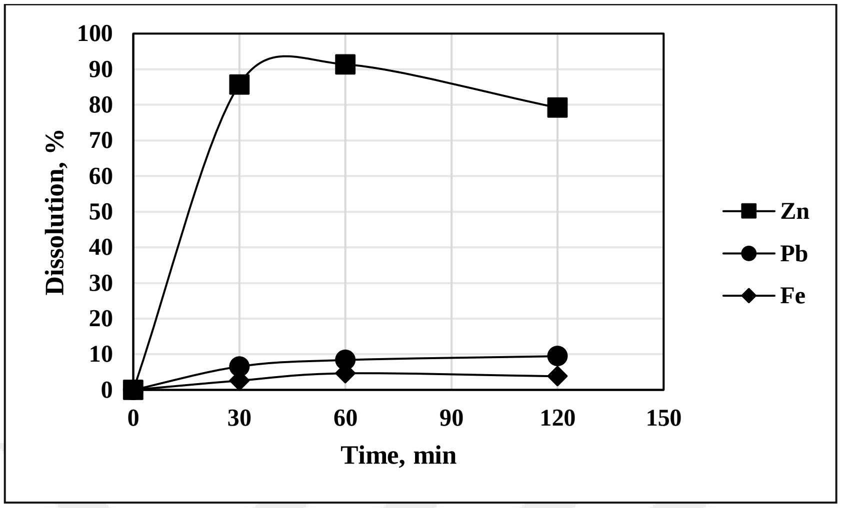

Figure 4.19. Metal dissolution with 1.0 M HCl at 40 ^{o}C and S/L: 1/10.

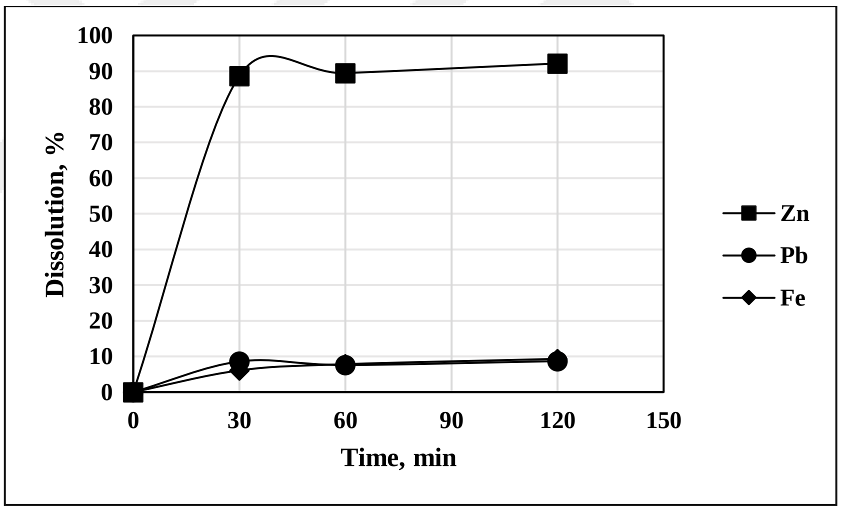

Figure 4.20. Metal dissolution with 1.0 M HCl at 60 ^{o}C and S/L: 1/10.

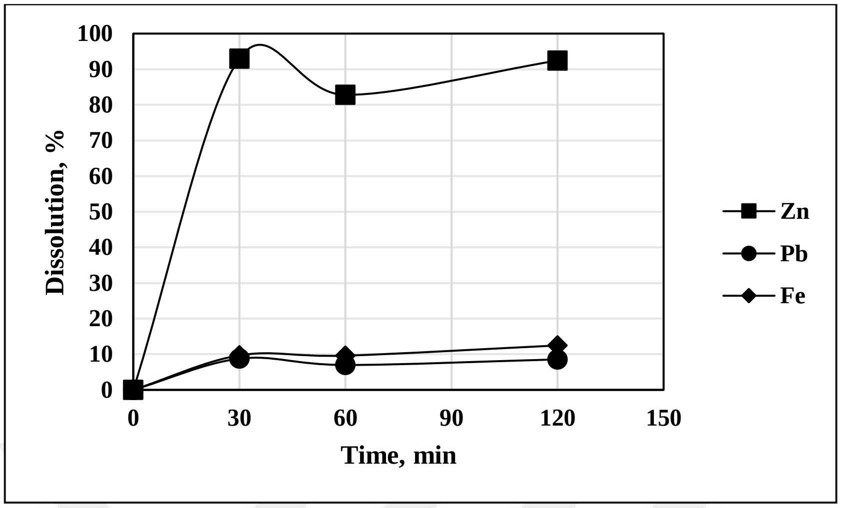

Figure 4.21. Metal dissolution with 1.0 M HCl at 80 ^{o}C and S/L: 1/10.

Table 4.5. Effect of leaching temperature and time on metal dissolutions at different HCl concentrations

HCl	Zn (%)			Pb (%)			Fe (%)		
0.25 M	40ºC	60ºC	80ºC	40ºC	60ºC	80ºC	40ºC	60ºC	80ºC
30 min	38	40	41	0	0	2	0	0	0
60 min	39	39	40	0	1	1	0	0	0
120 min	37	38	39	0	2	1	0	0	0
0.50 M	40ºC	60ºC	80ºC	40ºC	60ºC	80ºC	40ºC	60ºC	80ºC
30 min	78	82	90	10	10	10	0	0	0
60 min	75	83	88	9	9	10	0	0	0
120 min	76	88	90	10	10	10	0	0	0
1.0 M	40ºC	60ºC	80ºC	40ºC	60ºC	80ºC	40ºC	60ºC	80ºC
30 min	86	90	92	8	10	10	2	5	10
60 min	91	90	83	9	9	11	3	8	8
120 min	80	91	91	10	10	13	4	10	10

4.1.1.3. Nitric acid leach study

Table 4.6 and Figures 4.22-4.30 show the effect of leaching time from 30 to 120 min and leaching temperature from 40 ^{o}C to 80 ^{o}C at a S/L ratio of 1/10 on base metal dissolutions employing 0.25-1.0 M HNO_3 as lixiviant. As shown in Figures 4.22-4.30, increasing the nitric acid concentration from 0.25 to 1.0 M enhanced zinc dissolving from 38% to 70%, while increasing the time and leaching temperature decreased zinc dissolution. This could be owing to the fine mineral particles passivizating the mineral surfaces. Because the metals have been exposed to nitric acid, they can no longer be oxidized, and the reaction rate has slowed. Lead co-dissolution increased from 7% to 23% when the concentration of nitric acid was increased. There was no iron co-dissolution under any of the conditions that were examined. It was discovered nitric acid dissolved both zinc and lead at the same time. It is cost-effective, can be regenerated and re-used, and is a powerful oxidizing agent, resulting in the least precipitation after the leaching process; nevertheless, the rate of leaching is rather low. The metals disintegrated in the following order: Zn > Pb > Fe. During the nitric acid leaching process, the following processes occur (Hussaini et al., 2021a; Kaya et al., 2020b):

$$ZnO(s) + 2HNO_3(aq) = Zn(NO_3)_2(aq) + H_2O \quad (4.4)$$

$$PbO(s) + 2HNO_3(aq) = Pb(NO_3)_2(aq) + H_2O \quad (4.5)$$

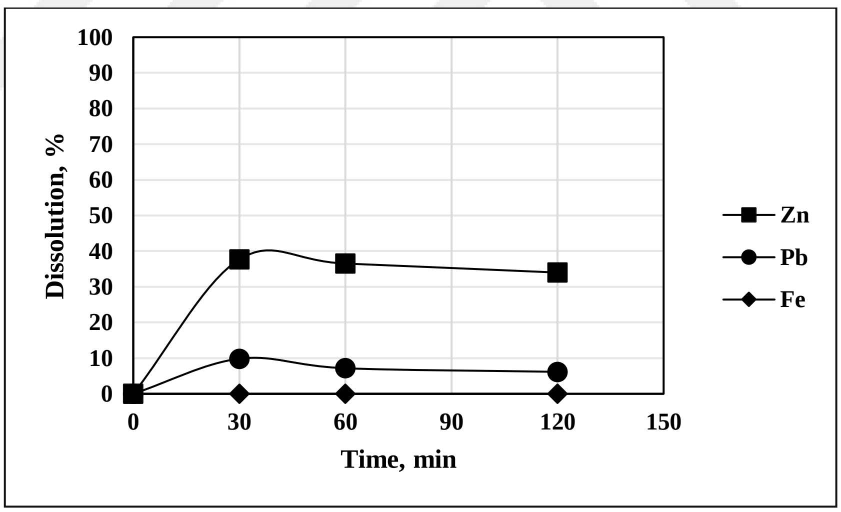

Figure 4.22. Metal dissolution with 0.25 M HNO_3 at 40 ^{o}C and S/L: 1/10.

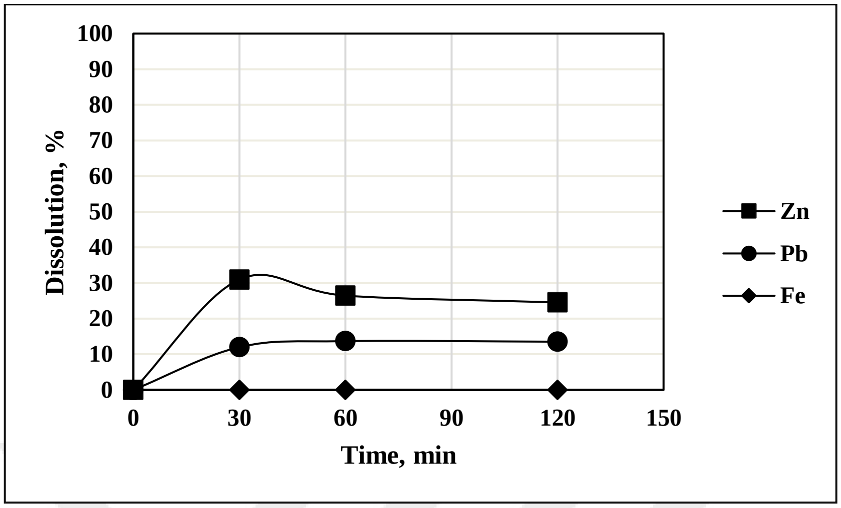

Figure 4.23. Metal dissolution with 0.25 M HNO_3 at 60 ^oC and S/L: 1/10.

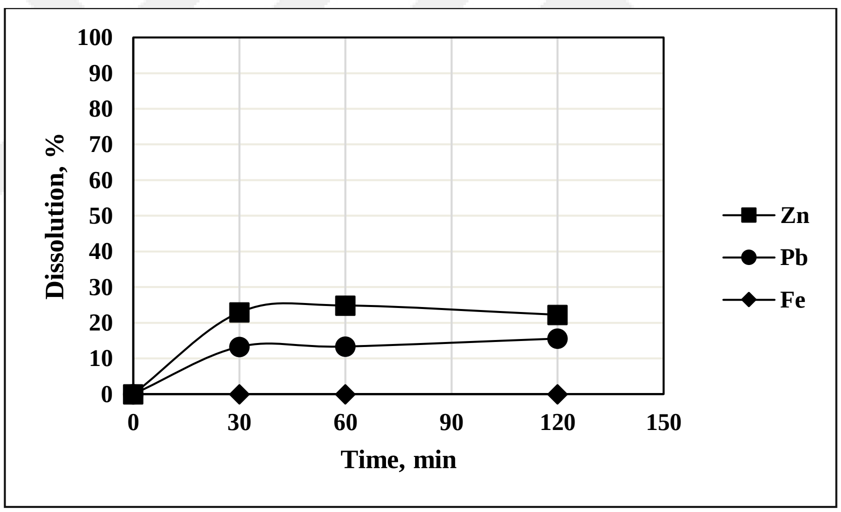

Figure 4.24. Metal dissolution with 0.25 M HNO_3 at 80 ^oC and S/L: 1/10.

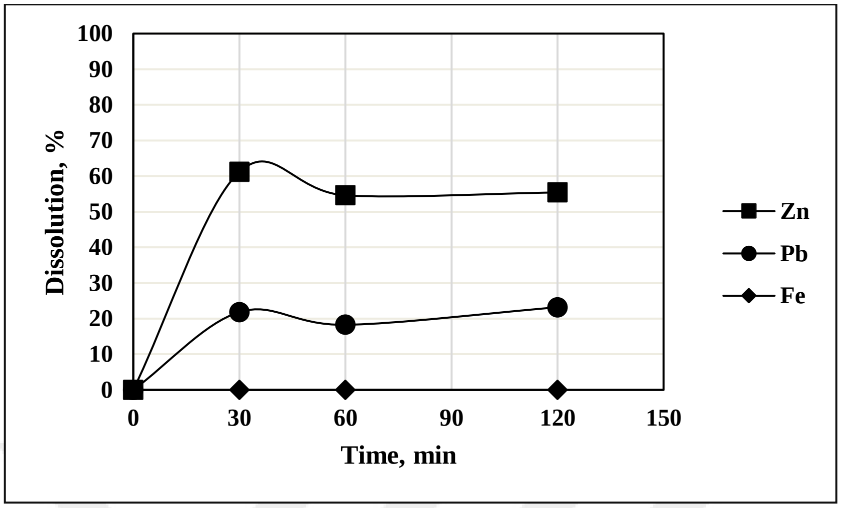

Figure 4.25. Metal dissolution with 0.5 M HNO_3 at 40 ^oC and S/L: 1/10.

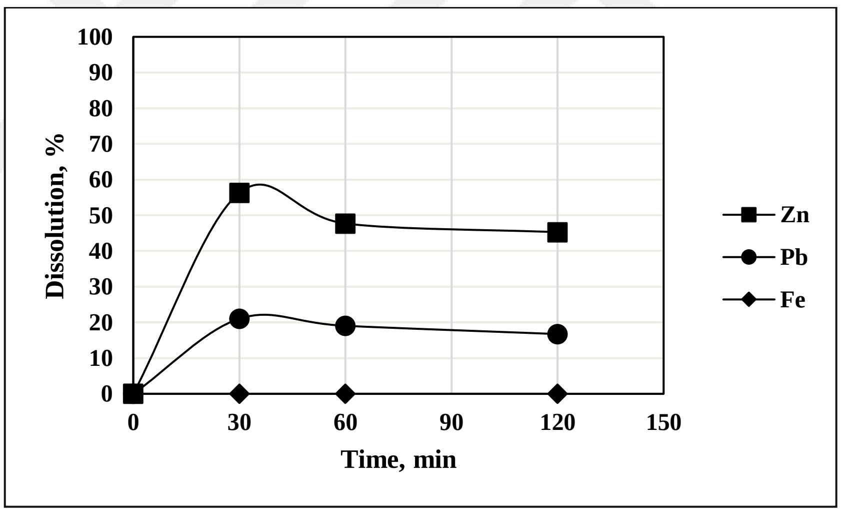

Figure 4.26. Metal dissolution with 0.5 M HNO_3 at 60 ^oC and S/L: 1/10.

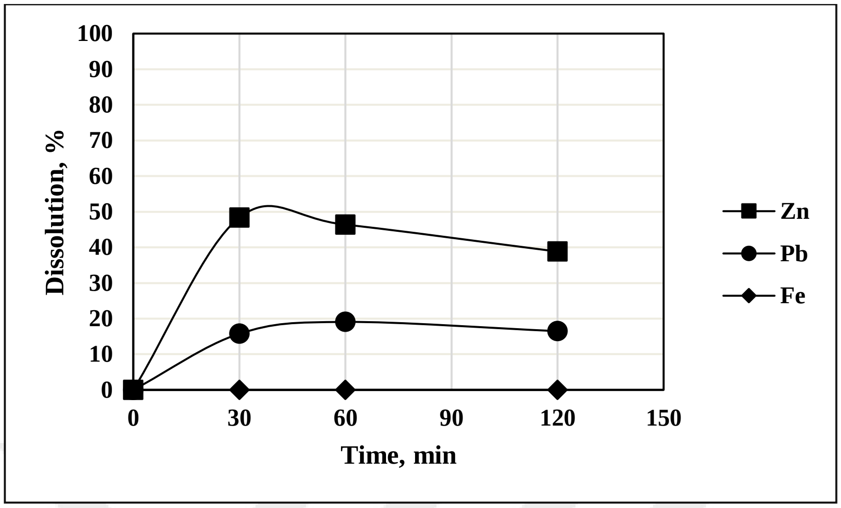

Figure 4.27. Metal dissolution with 0.5 M HNO_3 at 80 ^oC and S/L: 1/10.

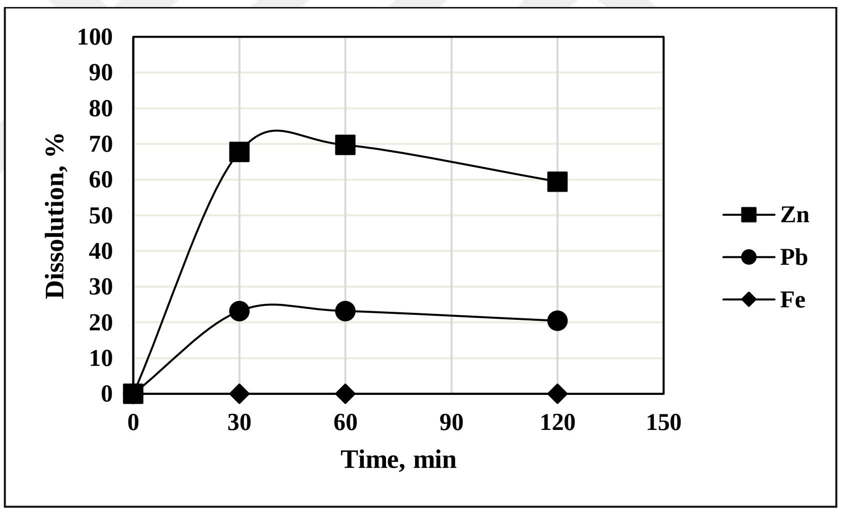

Figure 4.28. Metal dissolution with 1.0 M HNO_3 at 40 ^oC and S/L: 1/10.

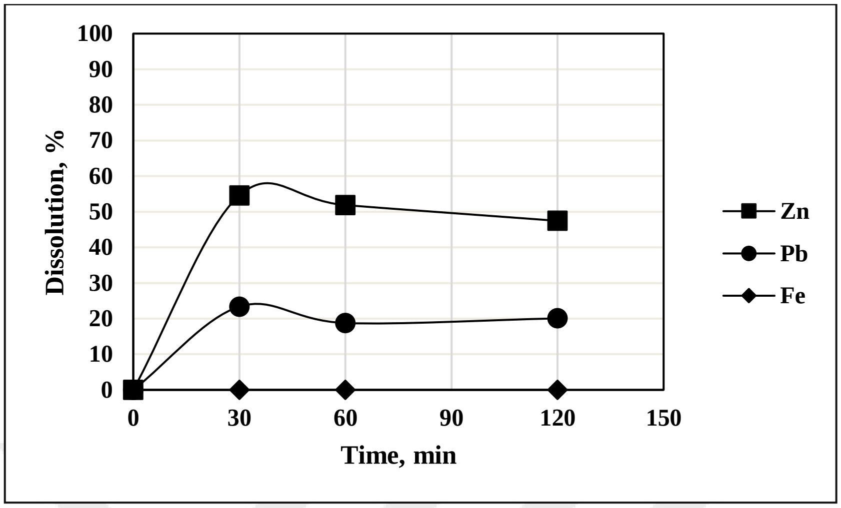

Figure 4.29. Metal dissolution with 1.0 M HNO_3 at 60 ^oC and S/L: 1/10.

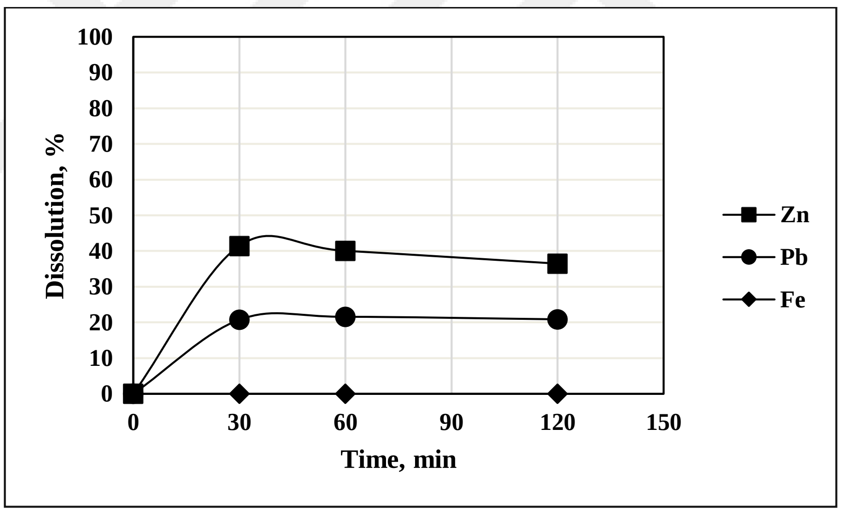

Figure 4.30. Metal dissolution with 1.0 M HNO_3 at 80 ^oC and S/L: 1/10.

Table 4.6. Effect of leaching temperature and time on metal dissolutions at different HNO_3 concentrations

HNO_3	Zn (%)			Pb (%)			Fe (%)		
0.25 M	40^{o}C	60^{o}C	80^{o}C	40^{o}C	60^{o}C	80^{o}C	40^{o}C	60^{o}C	80^{o}C
30 min	38	31	24	11	12	12	0	0	0
60 min	37	27	22	8	14	12	0	0	0
120 min	34	25	21	7	14	13	0	0	0
0.50 M	40^{o}C	60^{o}C	80^{o}C	40^{o}C	60^{o}C	80^{o}C	40^{o}C	60^{o}C	80^{o}C
30 min	61	57	49	22	21	13	0	0	0
60 min	55	49	48	19	20	14	0	0	0

120 min	54	47	39	21	18	13	0	0	0
1.0 M	40ºC	60ºC	80ºC	40ºC	60ºC	80ºC	40ºC	60ºC	80ºC
30 min	70	55	42	23	22	22	0	0	0
60 min	69	52	40	21	19	19	0	0	0
120 min	60	48	37	20	20	20	0	0	0

4.1.1.4. Perchloric acid leach study

Perchloric acid is an inorganic acid that is both a strong oxidizer and a stronger acid than sulfuric and nitric acid. Using 1.0 M perchloric acid at 80 °C and a 1/10 solid-to-liquid ratio for 60 minutes, this is able to achieve a maximum of 89.3% zinc dissolution and 10.7% lead dissolution. Figure 4.31 shows metal dissolution with perchloric acid.

Table 4.7 compares the different types of inorganic acids and the best conditions for dissolving zinc and lead from flotation tailing. The optimal leaching conditions were found to be 1.0 M sulfuric acid concentration, 40 °C leaching temperature, 30 minute leaching time, and a 2/10 solid to liquid ratio. The dissolution of zinc was found to be 91 %, with dissolutions of 11.2 % Fe and 18.4 % As. At a concentration of 0.5 M hydrochloric acid, an 80 °C leaching temperature, a 30 min leaching time, and a 1/10 solid to liquid ratio, % Zn and 9.6 % Pb dissolution was accomplished. Using nitric acid as a solvent, 69.7% Zn and 23.2 % Pb were dissolved in the leach solution under the following conditions: 1.0 M nitric acid concentration, 40 °C leaching temperature, 60 min leaching time, and 1/10 solid to liquid ratio. The following inorganic agent order resulted in the highest zinc selectivity between lead: sulfuric acid > hydrochloric acid > perchloric acid > nitric acid.

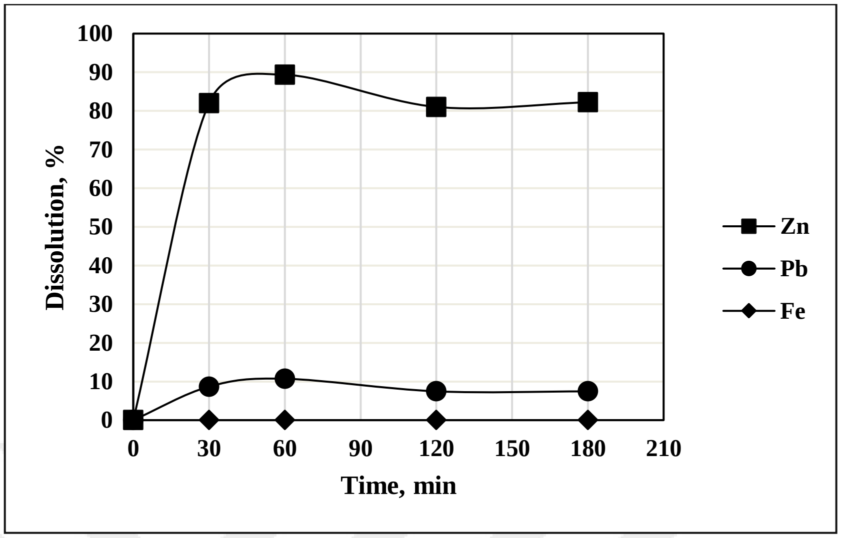

Figure 4.31. Metal dissolution with 1.0 M perchloric acid at 80 °C and S/L: 1/10.

Table 4.7. The comparison of inorganic acid types and optimum conditions for metal dissolutions

Reagent	Dissolution			Optimum parameters
	Zn (%)	Pb (%)	Fe (%)	
Sulfuric acid	91	0	10.2	Con.: 1 M, t: 30 min., T: 40 ◦C, S/L: 2/10
Hydrochloric acid	90	9.8	0	Con.: 0.5 M, t: 30 min., T: 80 ◦C, S/L: 1/10
Nitric acid	69.7	23.2	0	Con.: 1 M, t: 60 min., T: 40 ◦C, S/L: 1/10
Perchloric acid	89.3	10.7	0	Con.: 1 M, t: 60 min., T: 80 ◦C, S/L: 1/10

4.1.2. Organic Acid Leaching Study

In the organic acid leaching studies, citric acid, malic acid, oxalic acid, formic acid, tartaric acid, ascorbic acid and sulfosalicylic acid in different times and temperature was investigated.

4.1.2.1. Citric acid leaching study

- **Effect of temperature and time on metal dissolution with 0.5 M citric acid**

The citric acid leaching tests were performed using 0.5 M citric acid concentration with 25 gr Oreks samples at S/L ratio of 1/10 at 25, 40, 60 and 80 ºC temperature and 30, 60 and 120 min for leaching time. Results of leaching experiments shown in Figures 4.32-4.35.

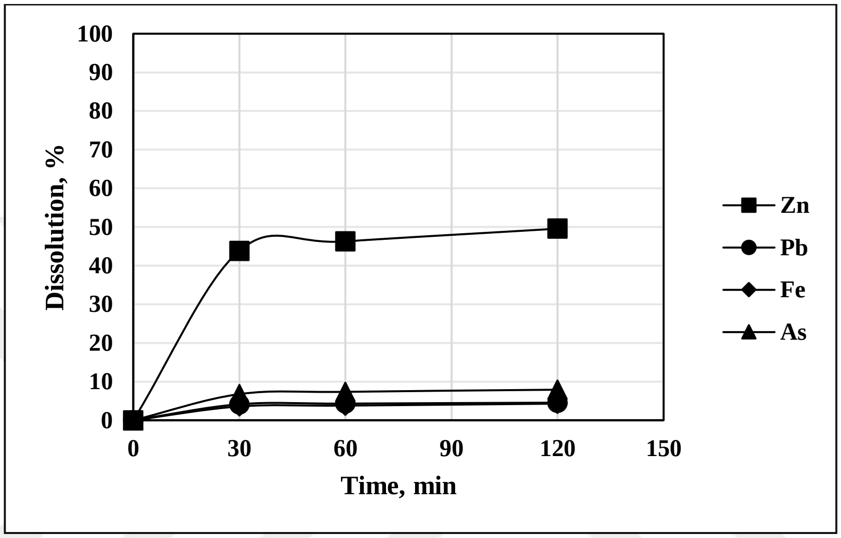

Figure 4.32. Metal dissolutions with 0.5 M citric acid at 25 ºC and S/L ratio of 1/10.

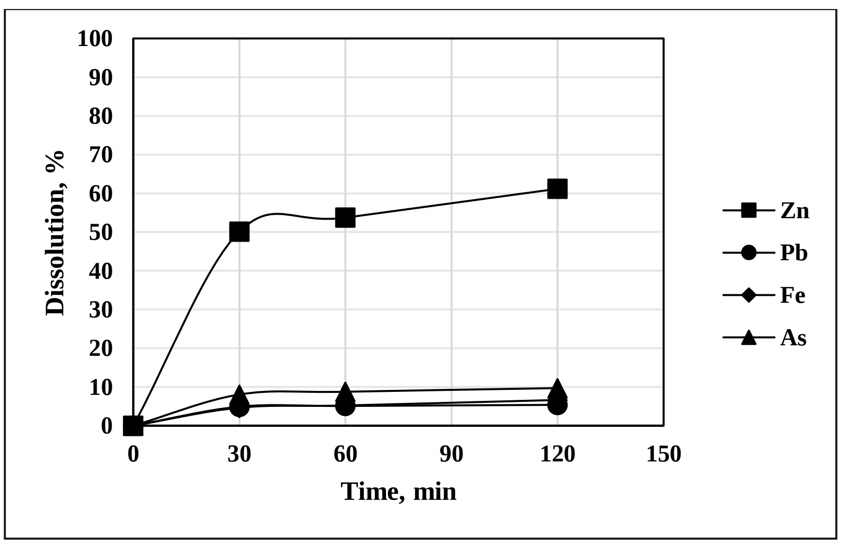

Figure 4.33. Metal dissolutions with 0.5 M citric acid at 40 ºC and S/L ratio of 1/10.

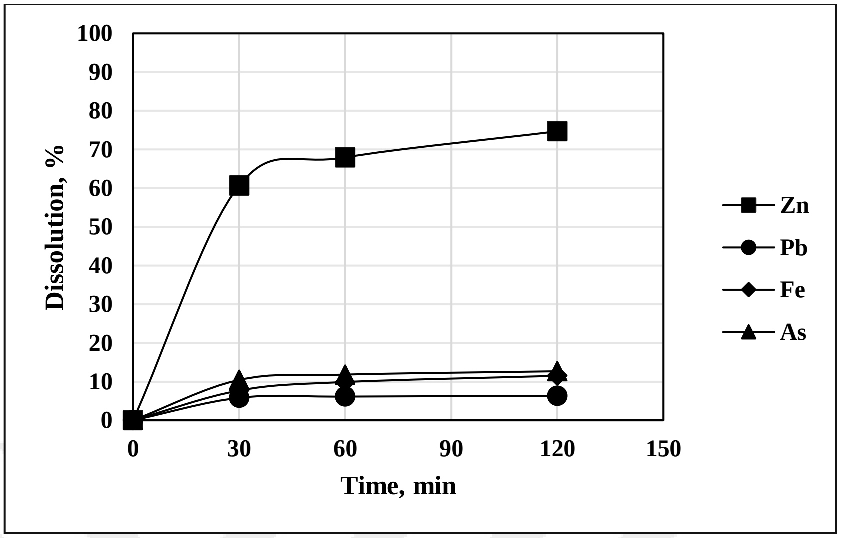

Figure 4.34. Metal dissolutions with 0.5 M citric acid at 60 ºC and S/L ratio of 1/10.

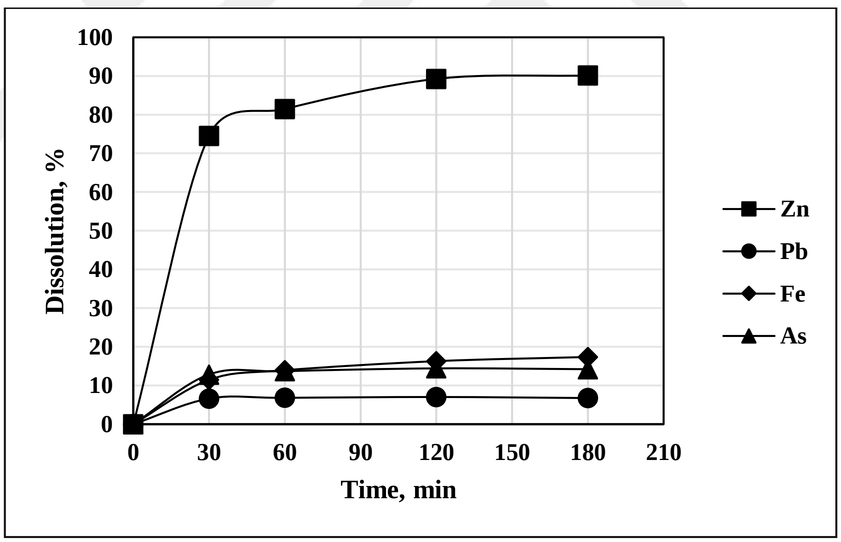

Figure 4.35. Metal dissolutions with 0.5 M citric acid at 80 ºC and S/L ratio of 1/10.

Figure 4.35 shows metal dissolutions at 0.5 M citric acid concentration at 80 ºC and 1/10 S/L ratio. Zn dissolution was 75% at 30 min. and 90% at 180 min. leaching time. At 80 ºC metal dissolution order was Zn>Fe>As>Pb>Ag after 60 min. leaching time. Maximum 90% Zn dissolution was obtained at 17% Fe and 14% As co-dissolutions. Pb co-dissolution was maximum 7%. After 120 min. leaching time Zn dissolution reached almost a plateau. The same result observed by Halli et al., (2018). They extracted about 78% Zn with 9% Fe from EAF with direct leaching using 0.4 M citric acid at 40 ^oC leaching temperature, 1/10 S/L ratio for 120 min leaching time (Halli et al., 2018).

As the leaching time and temperature increase, Zn dissolution significantly, and Fe and Pb dissolutions slightly increased. Increase in Zn dissolution was highest in the first 30 min, after that; there was a slight increase in the Zn dissolution. The diffusion speed and chemical reaction rate during leaching process can be accelerated by an increase in temperature, finally leading to a rapid leaching process. An increase in temperature from 25^oC up to 80°C was beneficial for Zn dissolution. The pH values obtained during the batch leaching experiments at this concentration were 3–4.5, keeping Fe in the solids. The reaction steps between zinc oxide and citric acid can be written as follows (Demir et al., 2006; Larba et al., 2013):

$$C_6H_8O_7(s) + H_2O(l) \leftrightarrow H_3O^+(aq) + C_6H_7O_7^- (aq) \tag{4.6}$$

$$C_6H_7O_7^- (aq) + H_2O(l) \leftrightarrow H_3O^+(aq) + C_6H_6O_7^{2-} (aq) \tag{4.7}$$

$$C_6H_6O_7^{2-}(aq) + H_2O(l) \leftrightarrow H_3O^+(aq) + C_6H_5O_7^{3-} (aq) \tag{4.8}$$

$$3ZnO(s) + 2C_6H_8O_7(aq) \rightarrow 3Zn^{2+}(aq) + 2C_6H_5O_7^{3-}(aq) + 3H_2O(l) \tag{4.9}$$

The pKa values presented in the literature are $pK_1 = 3.128$, $pK_2 = 4.761$, and $pK_3 = 6.396$. The pKa values presented in the literature are $pK_1 = 3.128$, $pK_2 = 4.761$, and $pK_3 = 6.396$. Because the pH of the reaction medium was less than 4, Pb-citrate ($Pb_3(C_6H_5O_7)_2$) is almost insoluble. Citric acid is often used because of high efficiency in binding Zn cations (Boukerche et al., 2018).

- **Effect of solid/liquid ratio on 0.5 M citric acid leach**

Table 4.8 and Figures 4.36-4.37 show metal dissolutions at 0.5 M citric acid concentration at 80 ^oC and 2/10 and 3/10 S/L ratio. Zn dissolution was 53% at 30 min. and 84% at 180 min. leaching time. At 80 ^oC metal dissolution order was Zn>Fe>As>Pb>Ag after 60 min. leaching time. Maximum 84% Zn dissolution was obtained at 17% Fe and 12% As co-dissolutions. Pb co-dissolution was maximum 5%. The maximum zinc dissolution was 50% at 120 min leaching time in 3/10 S/L ratio. Zinc dissolution decreases with increasing S/L ratio because of increasing sample volume in the solution, which means more acid will be needed to dissolve zinc metal. Those are consistent with the results of Chen et al., (2009) and Espiari et al., (2006) in the treatment of the zinc oxide ore by alkaline and acidic leaching respectively (Chen et al., 2009; Espiari et al., 2006).

Table 4.8. Comparison of metal dissolutions with 0.5 M citric acid using 1/10 2/10 and 3/10 S/L ratios at 80 ^oC.

	S/L: 1/10				S/L: 2/10				S/L: 3/10			
Time, min	Zn	Pb	Fe	As	Zn	Pb	Fe	As	Zn	Pb	Fe	As
0	0.0	0.0	0.0	0.0	0.0	0.0	0.0	0.0	0.0	0.0	0.0	0.0
30	74.5	6.6	11.5	12.8	53.3	4.3	10.6	10.2	40.0	1.2	9.9	7.1
60	81.5	6.8	13.9	13.7	63.0	4.4	12.5	10.8	43.1	3.0	10.1	7.3
120	89.3	7.0	16.3	14.4	74.8	4.6	14.8	11.7	49.5	1.5	11.6	7.3
180	90.1	6.8	17.4	14.2	84.0	4.8	17.2	12.4	46.9	0.9	11.1	7.3

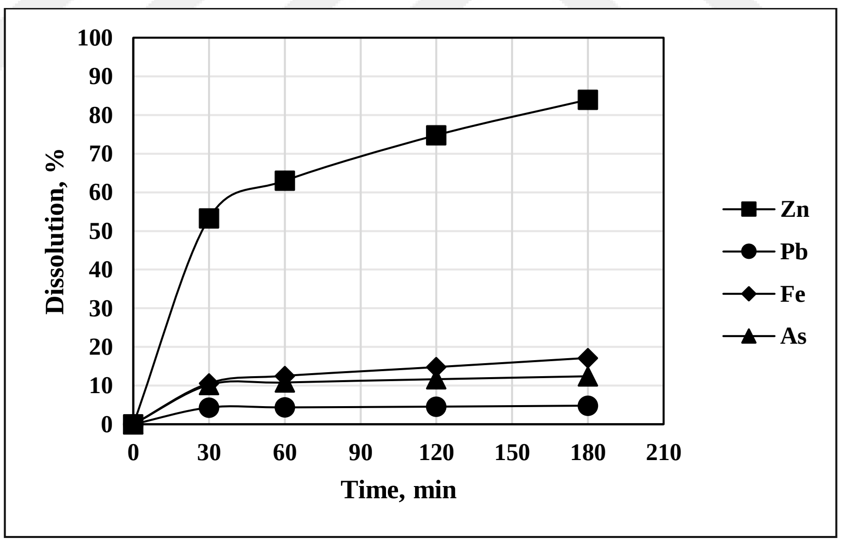

Figure 4.36. Metal dissolutions with 0.5 M citric acid at 80 ^oC and S/L ratio of 2/10.

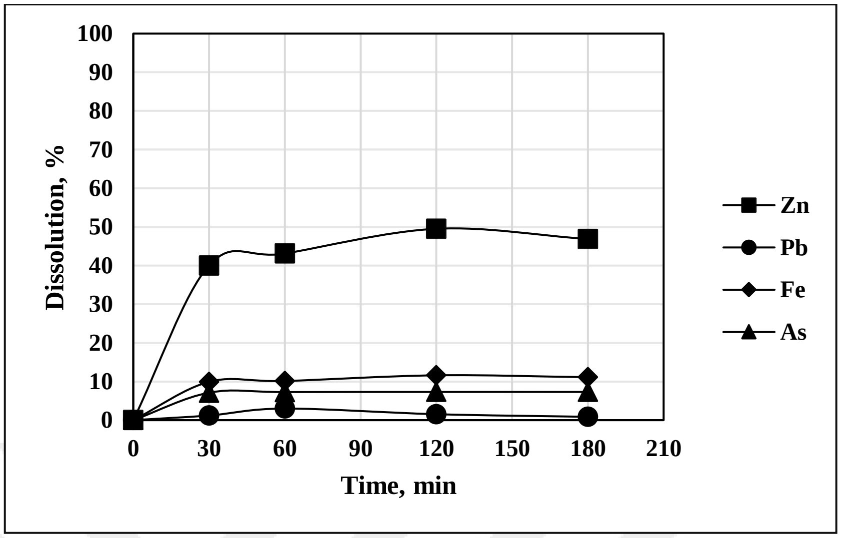

Figure 4.37. Metal dissolutions with 0.5 M citric acid at 80 ^{o}C and S/L ratio of 3/10.

❖ **Metal dissolution studies with 1.0 M citric acid**

According to result of metal dissolution with 0.5 M citric acid, temperature of 80 ^{o}C selected for 1.0 M citric acid leaching. Figure 4.38 shows the effect of leaching time on metal dissolutions with 1.0 M citric acid at 80 ^{o}C and 1/10 S/L ratio. At 30 min. leaching time 84% Zn and at 180 min. leaching time 91% Zn dissolutions were obtained at 19% Fe, 17% As and 12% Pb co-dissolutions. As the citric acid concentration increased from 0.5 to 1.0 M, pH of medium decreased from 3.7 to 2.2 at 80 ^{o}C zinc dissolution. The final pH did not differ significantly when applying the same citric acid concentration at different leaching temperature. Moreover, when increasing the concentration of citric acid, the final pH decreases and eventually the final pH is below 2.5 (1.0 M citric acid concentration) which favors the dissolution of Fe (Pourbaix, 1974).

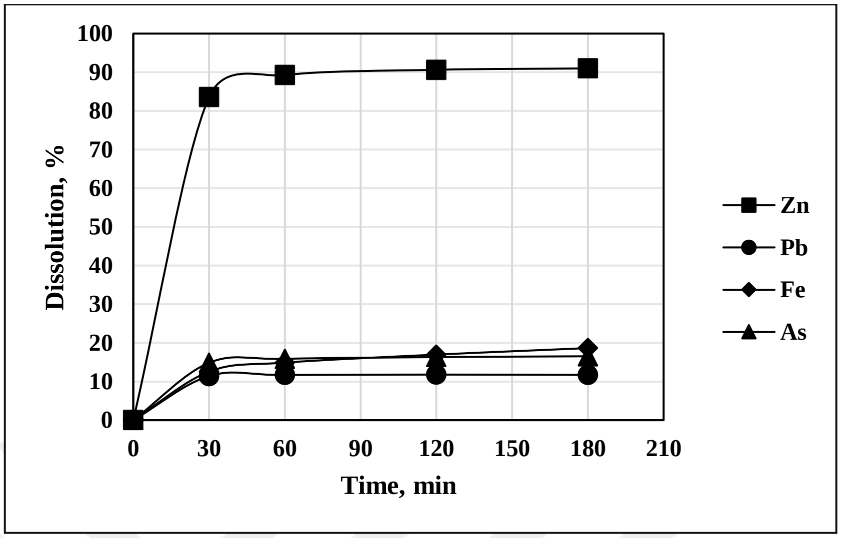

Figure 4.38. Metal dissolutions with 1.0 M citric acid at 80 ºC and S/L ratio of 1/10.

❖ **Effect of solid/liquid ratio on metal dissolution with 1.0 M citric acid leach**

Effect of solid/liquid ratio on metal dissolution was carried out with different S/L ratio, 1/10, 2/10 and 3/10. Table 4.9, Figure 4.39, and 4.40 show result of effect of solid/liquid ratio on metal dissolution.

Table 4.9. Comparison of metal dissolutions with 1.0 M citric acid using 1/10 2/10 and 3/10 S/L ratios at 80 ºC

	S/L: 1/10				S/L: 2/10				S/L: 3/10			
Time, min	Zn	Pb	Fe	As	Zn	Pb	Fe	As	Zn	Pb	Fe	As
0	0.0	0.0	0.0	0.0	0.0	0.0	0.0	0.0	0.0	0.0	0.0	0.0
30	83.5	11.4	12.5	14.8	72.0	7.5	12.5	12.9	54.0	5.4	11.0	10.4
60	89.3	11.7	14.9	15.9	79.4	7.6	14.6	13.5	64.7	5.5	13.3	11.1
120	90.6	11.8	16.9	16.3	88.0	7.9	17.4	14.2	73.1	5.6	15.6	11.4
180	91.0	11.7	18.6	16.5	90.6	9.3	19.2	14.5	73.4	5.3	16.2	11.0

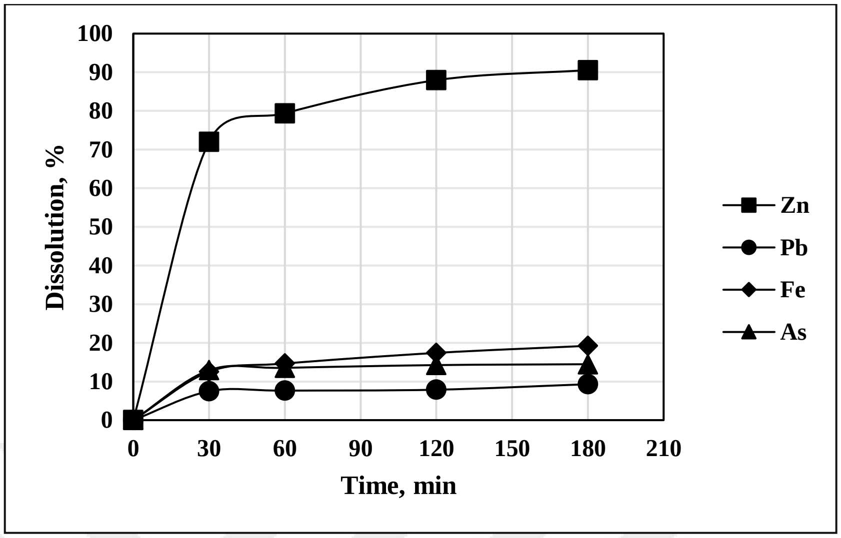

Figure 4.39. Metal dissolutions with 1.0 M citric acid at 80 ºC and S/L ratio of 2/10.

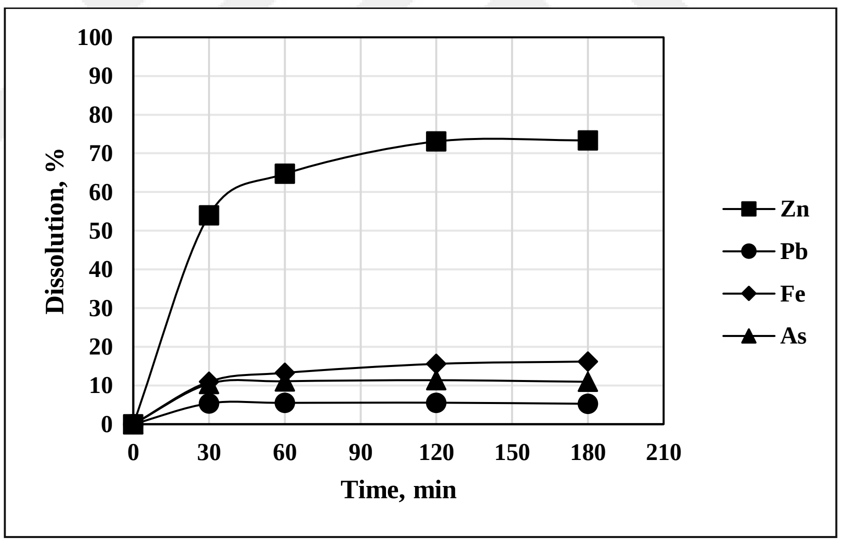

Figure 4.40. Metal dissolutions with 1.0 M citric acid at 80 ºC and S/L ratio of 3/10.

The ionic strength (concentration of total ions in the solution) of the resulting solution increases when bigger quantities of Zn were leached at higher S/L ratios. The ionic strength of a solution affects its solubility; as the ionic strength of the solution increases, solubility decreases. As the ions were leached from the solids at greater S/L ratios, the solubility drops. Because there are more ions to leach (due to the presence of more solids), a lesser percentage of the ions can be leached, because the solution's ionic strength and viscosity will increase as more ions are leached.(Lottering, 2006).

Herrero et al., 2010 discovered that decreasing the S/L ratio enhanced the percentage of metal leached because there was more lixiviant per unit of solids and therefore a higher possibility of solid-liquid interaction. Furthermore, at larger S/L ratios, this study revealed that the solution became saturated with Zn as a result of the high Zn amounts leached for the quantity of solution available, preventing more Zn from being leached and reducing overall Zn recovery (Herrero et al., 2010). Increased solution density reduces the proportion of Zn that was dissolved, according to studies employing EAFD leaching (Havlik et al., 2006).

Table 4.10 shows the pH of the medium at 80 ^oC using 1.0 M citric acid concentration at different S/L ratios and leaching times. The pH of the medium was between 2.0 and 3.0. As the S/L ratio increases, pH of the medium increases, but Zn dissolution decreases. The pH of the medium is less acidic with citric acid leach than H_2SO_4 leach.

Table 4.10. Effect of S/L ratio on solution pH in 1.0 M citric acid leaching at 80 ^oC.

	pH		
Time, min	S/L: 1/10	S/L: 2/10	S/L: 3/10
30	2.12	2.42	2.57
60	2.14	2.31	2.52
120	2.13	2.3	2.56
180	2.14	2.28	2.77

Figure 4.41 shows the XRD spectra of citric acid leached residue at the optimum conditions. Precipitate contains 48% Segnitite ($PbFe_3(AsO_4)(AsO_3OH)(OH)_6$) 48%, beudantite $PbFe_3^{3+}[(As,S)O_4]_2(OH)_6$) 43.5% and quartz 8.5% as the major phases. The XRD results indicate that segnitite and beudantite are the most common minerals in the residue. The citric acid leach residue comprises 14.8% PbO, 2.25% ZnO, 44.1% Fe2O3, 8.12% As_2O_3, and 0.78% CaO, according to XRF analysis. In comparison to the sulfuric acid leaching method, where calcium precipitated as gypsum, no calcium precipitate was found in the residue, according to XRF data (Hussaini et al., 2021a).

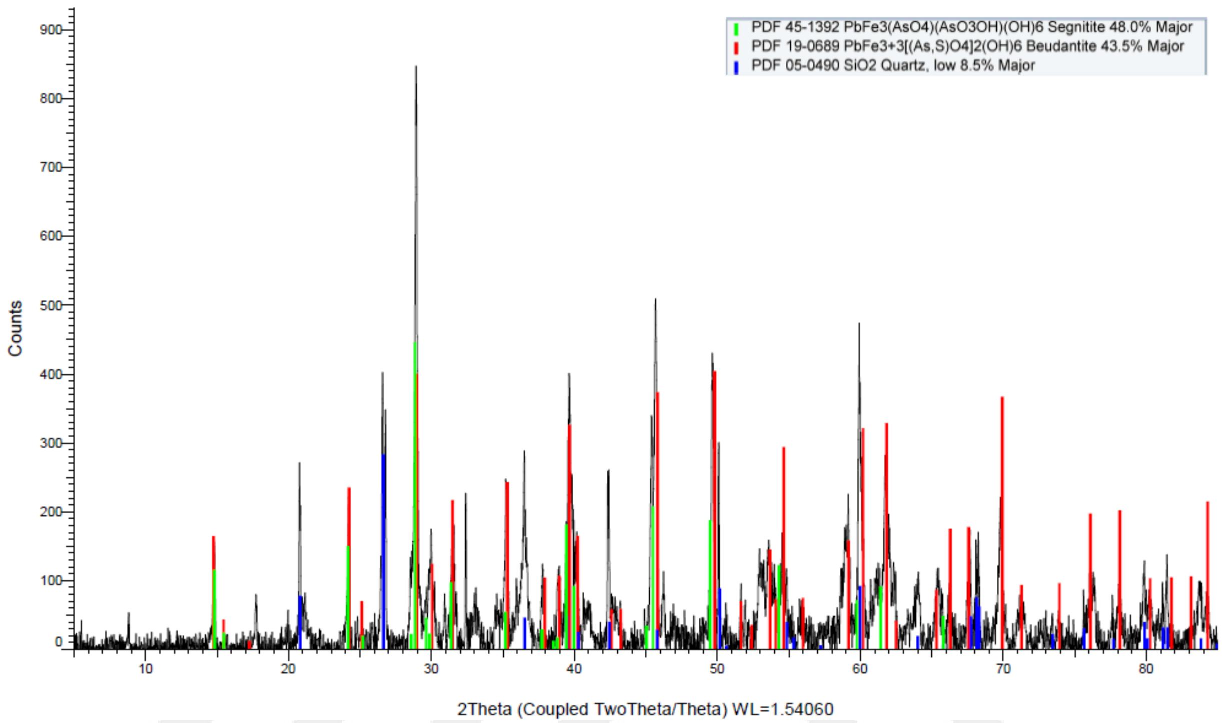

Figure 4.41. XRD spectra of citric acid leached residue at the optimum conditions.

4.1.2.2. Malic acid leaching study

❖ **Effect of time on metal dissolution with 1.0 M malic acid**

Metal dissolutions with 1.0 M malic acid at 80 ^{o}C and 1/10 S/L ratio were given in Figure 4.42. Metal dissolution order was Zn>Pb>Fe. More than 92% Zn dissolution was achieved after 60 min. leaching time. At 60 min. leaching 8.5% Pb and 3.2% Fe co-dissolutions were obtained. At 180 min leaching time Zn dissolution reaches to 92.7% at 10.4% Pb and 6.1% Fe co-dissolutions. Medium pH (2.0-2.4) was less acidic than H_2SO_4 leaching (0.5-1.0). Table 4.11 presents Zn-Pb and Zn-Fe selectivity with respect to leaching time and medium pH. As the leaching time increases pH of the medium increases from 2.04 to 2.39. The selectivity between Zn and Pb or Fe increased up to 84% and 85% with increasing leaching period. It seems that malic acid is a very good solvent for Zn leaching with quite low Pb and Fe co-dissolution.

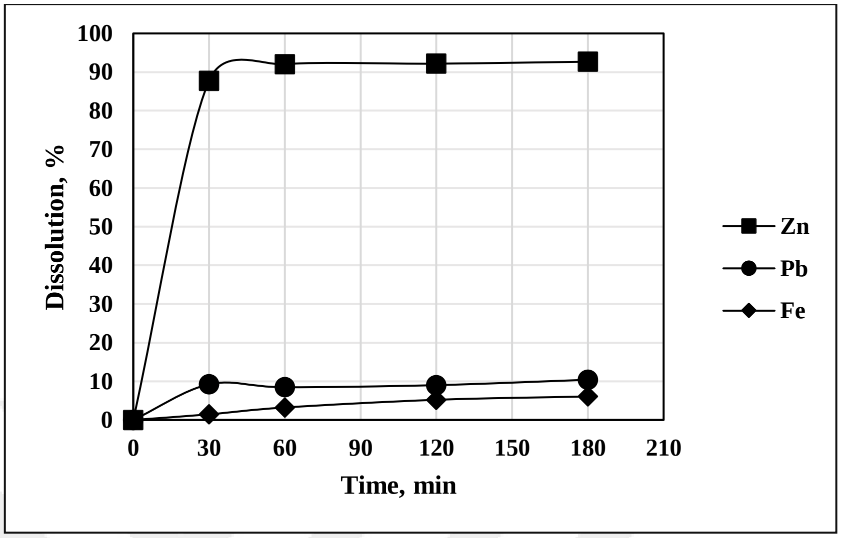

Figure 4.42. Metal dissolution with 1.0 M malic acid leach at 80 ^{o}C and 1/10 S/L ratio.

Table 4.11. Selectivity difference with malic acid leach as a function of leaching time and medium pH.

Time, min	Zn-Pb selectivity (%)	Zn-Fe selectivity (%)	pH
0	0	0	2,04
30	64	76	2,12
60	76	79	2,26
120	76	79	2,22
180	84	85	2,39

❖ **Effect of solid/liquid ratio on metal dissolution with 1.0 M malic acid leach**

Metal dissolutions at 1.0 M malic acid concentration, 80 ^{o}C leaching temperature and S/L ratios of 1/10, 2/10 and 3/10 were determined (Table 4.12, and Figures 4.43 and 4.44). Metal dissolution order was Zn > Pb > Fe. The maximum 92.7% Zn dissolution was achieved at S/L ratio of 1/10 in 180 min. With increasing S/L ratio, Zn dissolution decreased to 82% and 63%. Both Pb and Fe dissolutions were less than 10%. pH of the medium changed from 2.68 to 3.06. With rising pulp viscosity and a high solid ratio, stirring problems exist, and particles may not be completely covered by the solution. When a result, as the solid ratio increased, the zinc dissolution decreased (Hussaini et al., 2021a). According to result, zinc leach efficiency with malic acid is lower than citric acid. Yan et al., 2014 observed the same result. According to them, citric acid is supposed to have a stronger leaching potential than malic acid from polluted sediment (Yan et al., 2014). When lead and zinc were leached using citric acid and malic acid, similar results were obtained. Li et al., (2010), indicated that citric acid had a greater leaching ability than malic acid, which was consistent with our findings that citric acid has a greater leaching ability than malic acid. The ionization of malic acid was given by the following equation:

$$HCO_2H(aq) + H_2O(l) \leftrightarrow H_3O^+(aq) + HCO^-_2\,(aq) \qquad (4.10)$$

The organic acid with a zinc oxide reaction can be written as (Song and West Chester, 2004):

$$2H_XA + XZnO \rightarrow XZnA_{2/X} + XH_2O \qquad (4.11)$$

Where A is an organic acid, and X is a number between 1 and 2.

Table 4.12. Comparison of metal dissolutions with 1.0 M malic acid using 1/10 2/10 and 3/10 S/L ratios at 80 ^oC.

	S/L: 1/10			S/L: 2/10			S/L: 3/10		
Time, min	Zn	Fe	Pb	Zn	Fe	Pb	Zn	Fe	Pb
0	0.0	0.0	0.0	0.0	0.0	0.0	0.0	0.0	0.0
30	87.8	1.5	9.2	66.5	0.7	5.1	49.4	0.7	3.9
60	92.0	3.2	8.5	69.5	1.0	4.9	55.7	0.9	3.5
120	92.2	5.2	9.0	70.5	1.2	4.4	61.4	1.2	3.4
180	92.7	6.1	10.4	82.1	1.7	4.9	63.5	1.4	3.4

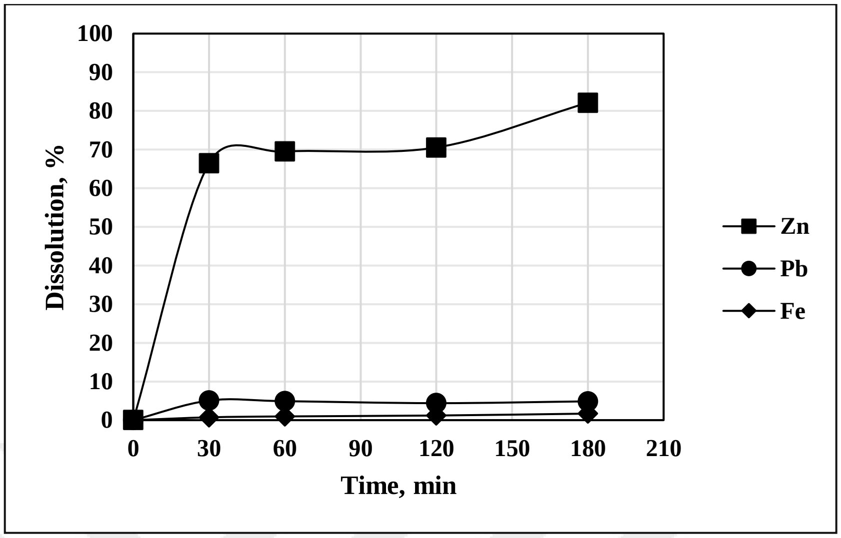

Figure 4.43. Metal dissolutions with 1.0 M malic acid at 2/10 S/L ratio and 80 ^{o}C leaching temperature.

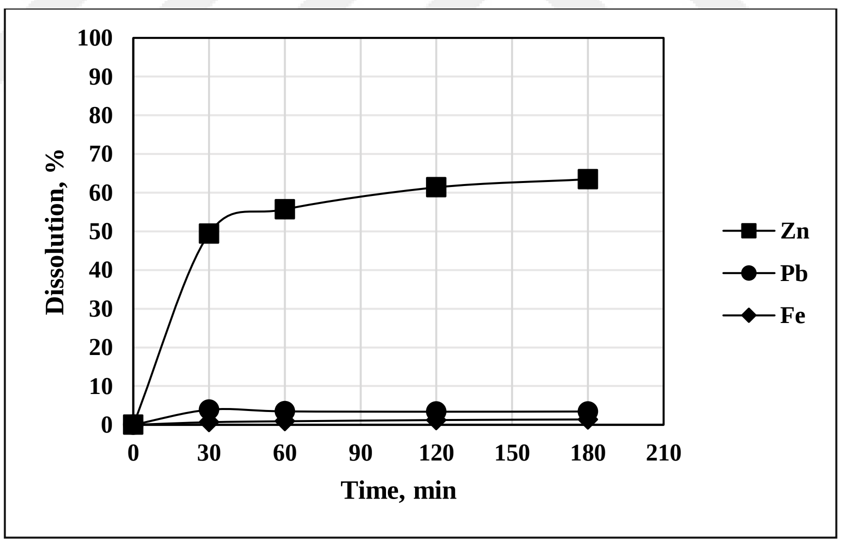

Figure 4.44. Metal dissolutions with 1.0 M malic acid at 3/10 S/L ratio and 80 ^{o}C leaching temperature.

Figure 4.45 shows the XRD spectra of malic acid leach residue at the optimum conditions. Precipitate contains 39% segnitite, 30.3% beudantite, 25.4% silicon oxide and 5.3% quartz as major phases. The leach residue contains 2.89 % ZnO, 16.4 % PbO, 9.8 % As_2O_3, 52.8 % Fe_2O_3, and 0.85 % CaO, according to XRF data (Hussaini et al., 2021a).

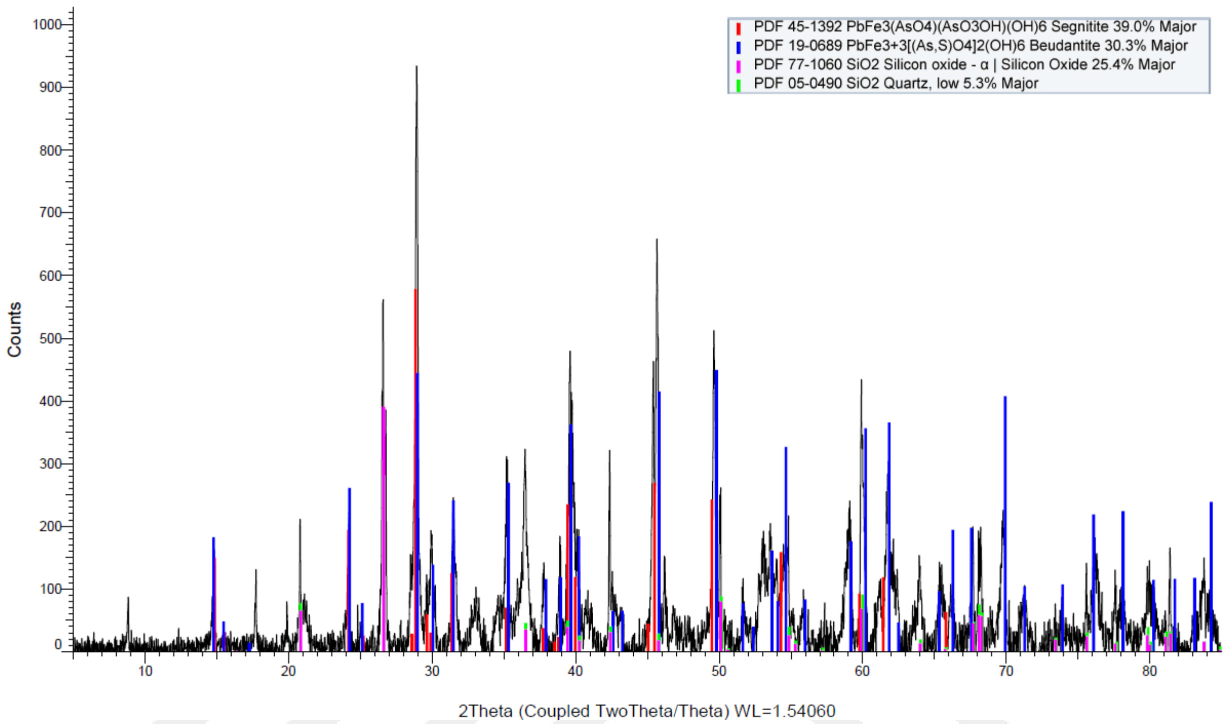

Figure 4.45. XRD spectra of malic acid leached residue at the optimum conditions.

4.1.2.3. Oxalic acid leaching study

❖ **Effect of temperature and time on metal dissolution with 1.0 M oxalic acid**

The effects of 1.0 M oxalic acid on metal dissolutions at 25, 40 and 60 ^{o}C leaching temperatures were tested at 1/10 S/L ratio. Figures 4.46 - 4.48 show metal dissolutions as a function of leaching time. Fe and As dissolve while Zn, Pb and Ag did not dissolve with oxalic acid. Fe and As dissolutions are about 50% in the first 30 min. and then, remained almost constant up to 180 min. at 25 ^{o}C. The iron and arsenic have a slightly concave form at 25 ^{o}C, which is indicative of a long induction age. With increasing leaching temperature to 40 ^{o}C, Fe and As dissolutions slightly increased between 50% and 70%, demonstrating that the reaction proceeds via an autocatalytic process. At 60 ^{o}C, 96% Fe and 69% As dissolutions were obtained at 180 min. with 2.9% Zn and 3.2% Pb co-dissolutions. These findings suggest that the temperature at which iron and arsenic were dissolved is particularly important. There was no significant pH variation in the solution medium at different leaching temperature with oxalic acid. pH was changed between 0.7 and 0.9. Oxalic acid can be used to dissolve impurities Fe and As without dissolving valuable Zn and Pb metals. For the metallic cations, oxalic acid functions as a powerful complexing agent. Oxalic acid has the strongest ability to dissolve Fe and As.. The major mineral phase in our sample, goethite (α- FeOOH), has a somewhat different free energy of production. Cornell and Schwertmann (1996) looked on the thermodynamics of goethite breakdown. The dissolution of Fe complexes in oxalic acid can be expressed as (Kaya et al., 2020b; Kursunoglu et al., 2021; Nworie et al., 2017):

$$H_2C_2O_4 \rightarrow H^+ + HC_2O_4^- \rightarrow 2H^+ + C_2O_4^{2-} \quad (4.12)$$

$$Fe^{2+} + C_2O_4^{2-} + 2H_2O \rightarrow FeC_2O_4{\cdot}2H_2O \quad (4.13)$$

$$Fe_2O_3 + 2HC_2O_4^- + 4H^+ \rightarrow 2Fe\ (C_2O_4)^+ + 3H_2O \quad (4.14)$$

$$FeOOH + HC_2O^-{}_4 + 3H^+ = [FeHC_2O_2]^{2-} + 2H_2O \quad (4.15)$$

Nworie et al., 2017 was determined that oxalic acid dissolved metals in the following order Fe>As>Mn>Pb>Cu>Zn. Zn-oxalate ($ZnC_2O_4.2H_2O$) has a very low solubility of 1.38×10^{-9} at 20 °C. Pb-oxalate ($PbC_2O_4/(Pb(C(COO)_2)_2)$) solubility product at 18 °C is 2.74×10^{-11} and 8.5×10^{-10} at 25 °C which is insoluble (Nworie et al., 2017).

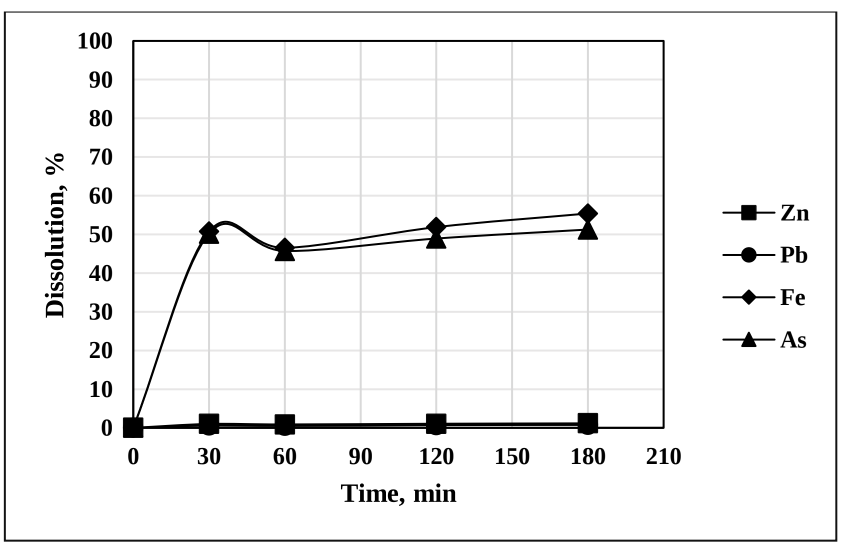

Figure 4.46. Metal dissolutions with 1.0 M oxalic acid at 25 °C and S/L ratio of 1/10.

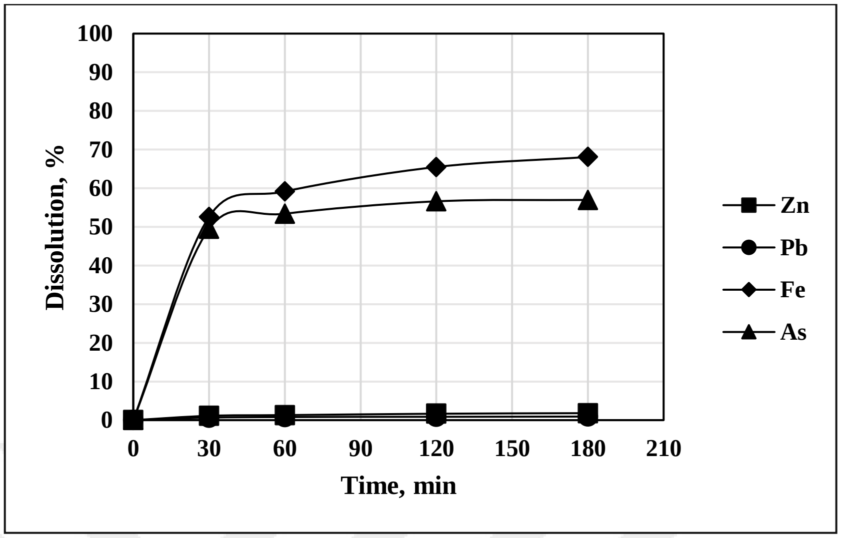

Figure 4.47. Metal dissolutions with 1.0 M oxalic acid at 40 ^{o}C and S/L ratio of 1/10.

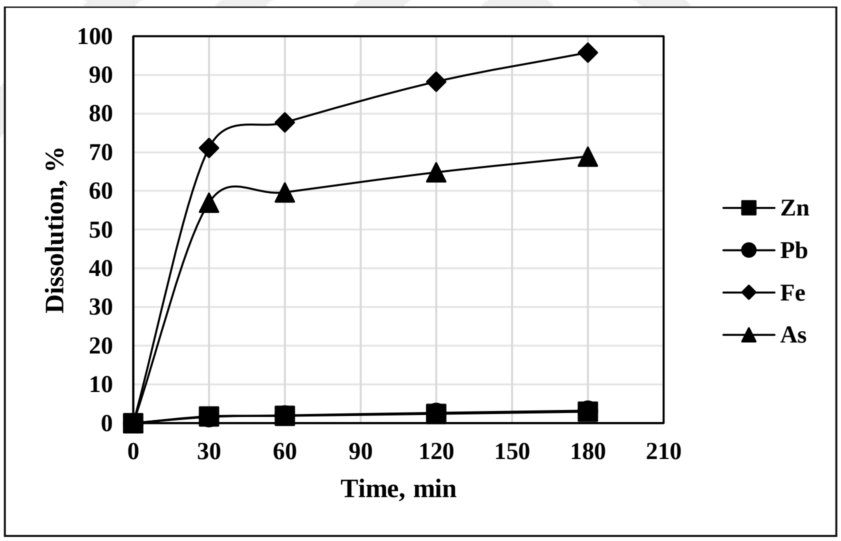

Figure 4.48. Metal dissolutions with 1.0 M oxalic acid at 60 ^{o}C and S/L ratio of 1/10.

❖ **Effect of solid/liquid ratio on metal dissolution with 1.0 M oxalic acid leach**

Table 4.13 and Figures 4.49 and 4.50 show the Fe and As dissolutions at 1.0 M oxalic acid concentration at 2/10 and 3/10 S/L ratios. According to result, Fe and As dissolutions significantly decreases with increasing S/L ratio. In dilute solution, 96% Fe and in high percentage solid solution, only 30% Fe dissolves. Arsenic dissolution also dropped from 69%

down to 25% with S/L ratio of 3/10. Increasing S/L ratio slightly increased Zn dissolution at almost constant Pb dissolution without any Ag dissolution. Metal dissolution order was Fe>As>Zn>Pb>Ag. Zn, Pb and Ag did not dissolve significantly with oxalic acid. The best S/L ratio at 60 ^{o}C and 1.0 M oxalic acid is 1/10.

Table 4.13. Comparison of metal dissolutions with 1.0 M oxalic acid using 1/10 2/10 and 3/10 S/L ratios at 60 ^{o}C

	S/L: 1/10				S/L: 2/10				S/L: 3/10			
Time, min	Zn	Fe	Fe	As	Zn	Fe	Fe	As	Zn	Fe	Fe	As
0	0.0	0.0	0.0	0.0	0.0	0.0	0.0	0.0	0.0	0.0	0.0	0.0
30	1.7	1.6	71.1	57.0	3.2	2.6	52.6	45.0	3.3	1.3	30.3	30.1
60	1.9	2.0	77.7	59.6	3.5	2.5	50.7	42.1	5.1	1.6	30.6	29.2
120	2.4	2.6	88.3	64.8	4.5	3.9	54.2	44.6	7.1	1.7	30.0	26.9
180	2.9	3.2	95.8	68.9	5.0	4.3	55.9	45.4	8.7	1.7	30.0	25.2

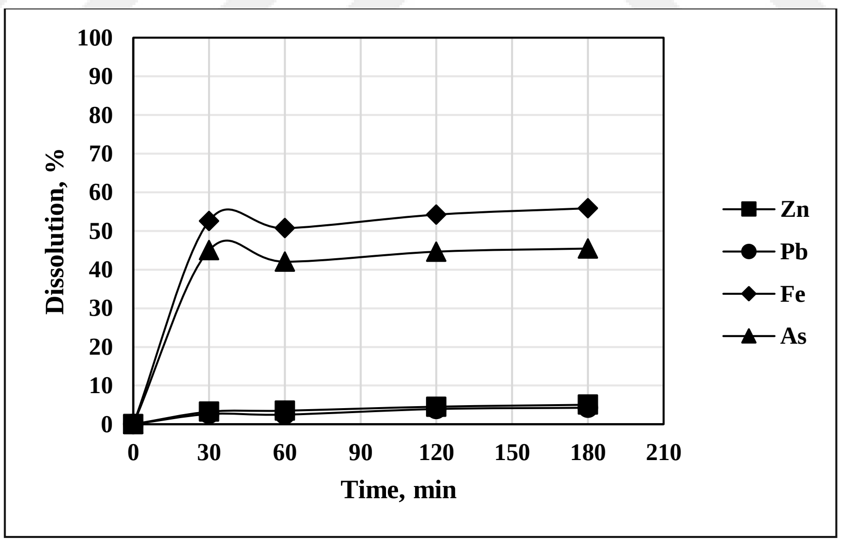

Figure 4.49. Metal dissolutions with 1.0 M oxalic acid at 2/10 S/L ratio and 60 ^{o}C leaching temperature.

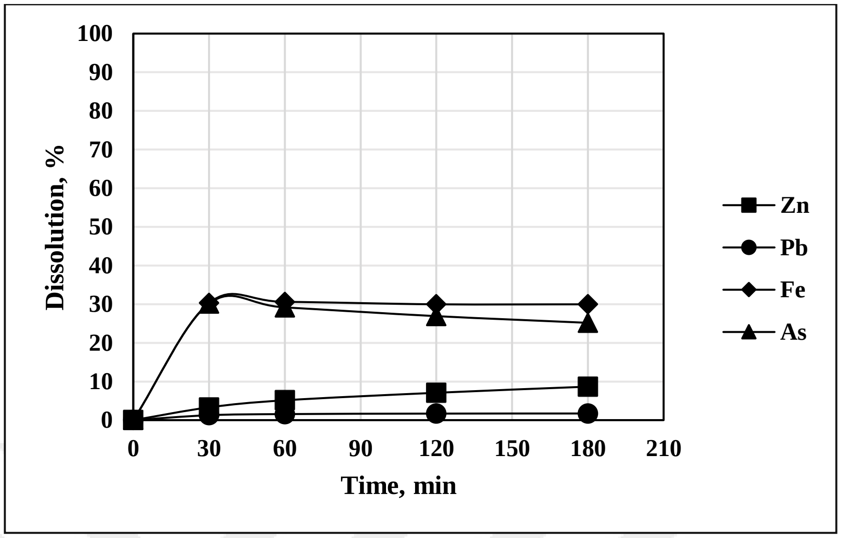

Figure 4.50. Metal dissolutions with 1.0 M oxalic acid at 3/10 S/L ratio and 60 ^{o}C leaching temperature.

4.1.2.4. Formic acid leaching study

❖ **Effect of temperature and time on metal dissolution with 1.0 M formic acid**

Leaching with formic acid at 1.0 M concentration at 40, 60 and 80 ^{o}C were performed at S/L: 1/10 ratio. For 40 ^{o}C leaching temperature, at 30 min. leaching time 62% and at 120 min. leaching time 78% Zn dissolution was obtained. At 180 min. leaching time Zn dissolution was 76%. Metal dissolution order was Zn>Pb>Fe. Solution pH changed between 2.8 and 3.0 with formic acid. The zinc dissolution increased somewhat as the leaching duration and temperature increased. At 80 ^{o}C leaching time, Zn dissolution increased from 76% to 82% at 4.3% Pb co-dissolution with increasing leaching time from 30 min. to 180 min. Solution pH was around 3.0. Under the tested all-leaching conditions, lead dissolution was less than 5%, whereas no iron dissolution was observed. The zinc was extracted from the flotation tailing quite selectively, leaving a significant amount of lead and iron in the residue (Hussaini et al., 2021a). Figures 4.51- 4.53 show the result of metal dissolution with 1.0 M formic acid. 1.0 M formic acid concentration, 60 °C leaching temperature, 120 min.leaching time, and 1/10 solid to liquid ratio were shown to be the optimum leaching conditions. The reactions for formic acid ionization and diffusion of H^+ ions are as follows (Hussaini et al., 2021a):

$$CH_2O_2 \leftrightarrow H^+ + CHO^-2 \tag{4.16}$$

$$2H^+ + ZnCO_3 \leftrightarrow H_2CO_3 + Zn^{2+} \tag{4.17}$$

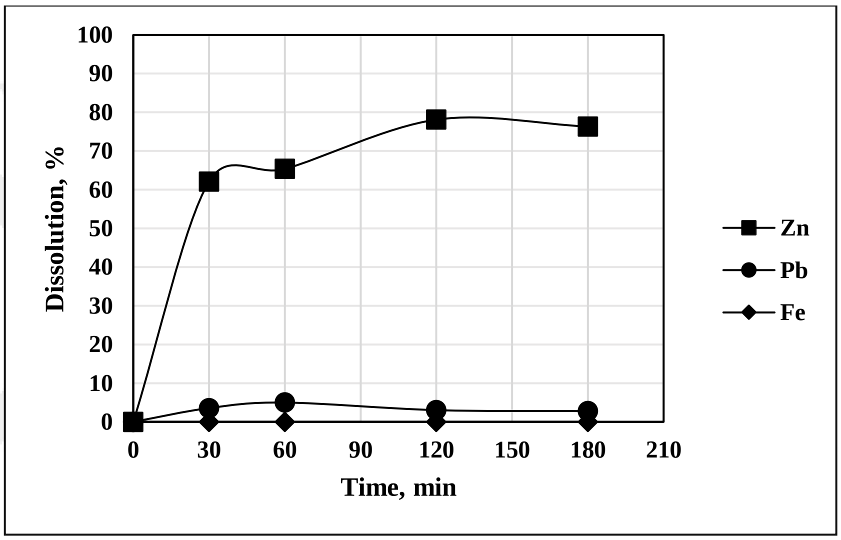

Figure 4.51. Metal dissolutions with 1.0 M formic acid at 40 ^oC and S/L ratio of 1/10.

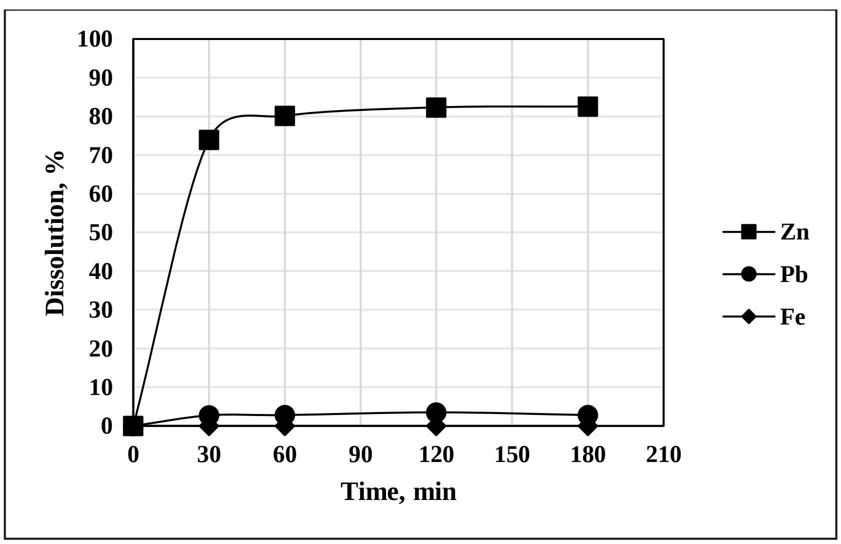

Figure 4.52. Metal dissolutions with 1.0 M formic acid at 60 ^oC and S/L ratio of 1/10.

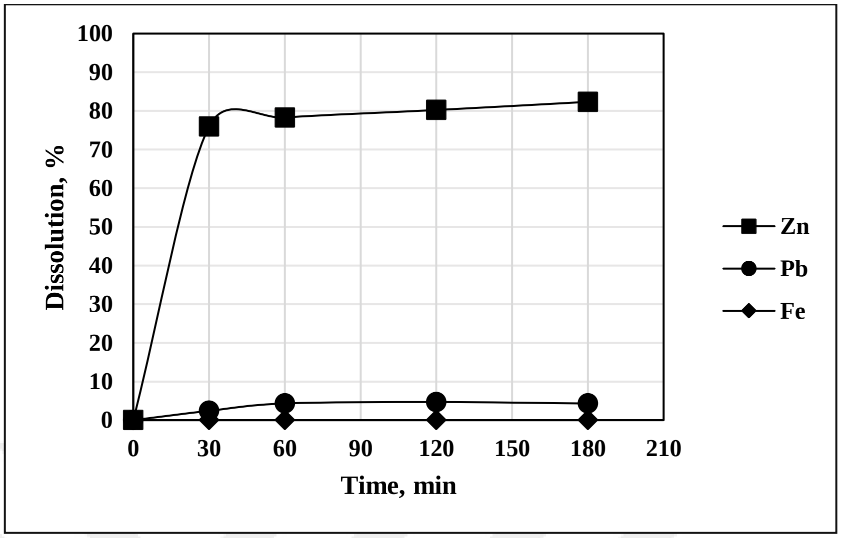

Figure 4.53. Metal dissolutions with 1.0 M formic acid at 80 ºC and S/L ratio of 1/10.

4.1.2.5. Other organic acid leaching study

Tartaric acid was used as an organic agent to investigate the dissolution of metals. The zinc, lead, and iron dissolutions were rather stable when tartaric acid was utilized as lixiviant. Zinc dissolutions were discovered to be less than 35%. Under the tested conditions, lead dissolutions increased to 11.7%, while iron dissolutions were less than 7%. The order of metal breakdown was Zn > Pb > Fe. The pH of the solution was around 2. The results of metal dissolution with tartaric acid are given in Figure 4.54.

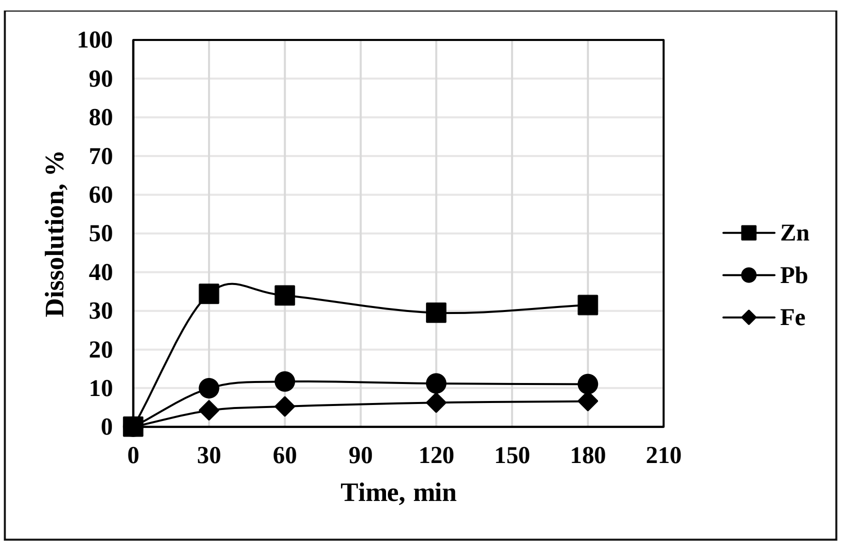

Figure 4.54. Metal dissolutions with 1.0 M tartaric acid at 80 ^{o}C and S/L ratio of 1/10.

Ascorbic acid was used as another lixiviant in the dissolution of metals from our sample. Under the tested conditions, zinc, lead, iron, and arsenic all showed the same dissolution tendency when ascorbic acid was utilized as an organic agent. Figure 4.55 show the results of metal dissolution with ascorbic acid. During the zinc dissolution, there were some minor changes. With 1.0 M ascorbic acid, an 80 °C leaching temperature, a 1/10 solid-to-liquid ratio, and a 30 minute leaching period, 34.4% zinc dissolution was achieved. Under the tested all-leaching conditions, lead dissolution was less than 12%, but iron dissolution increased to 18.3%, with 12.1 % arsenic dissolution for 180 min. When ascorbic acid was utilized as an organic agent, it was discovered that there was no good selectivity between zinc and other impurities such as iron and arsenic. The order of metal dissolution was discovered to be Zn > Fe > As > Pb. The solution had a pH of roughly 3.5(Hussaini et al., 2021a; Kaya et al., 2020b).

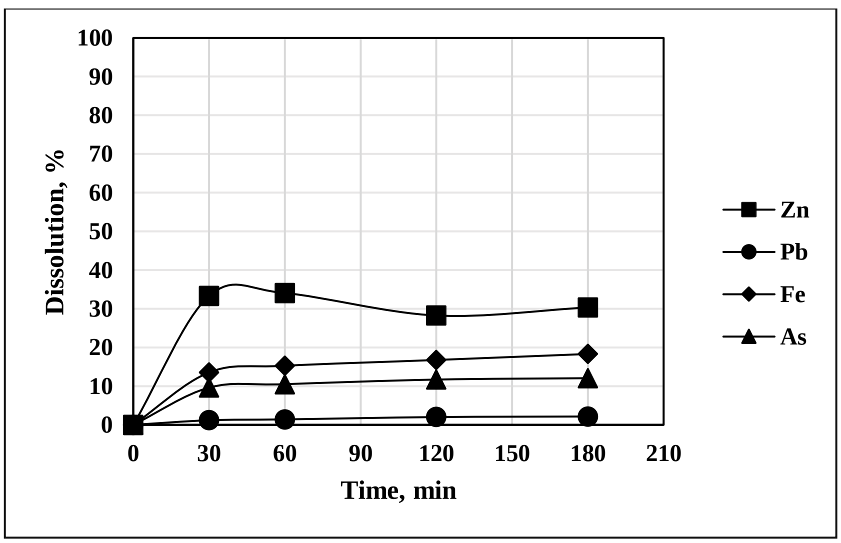

Figure 4.55. Metal dissolutions with 1.0 M ascorbic acid at 80 ^{o}C and S/L ratio of 1/10.

Sulfosalicylic acid as another organic agent was used to dissolve metals (Figure 4.56). The zinc dissolutions remained generally constant under the investigated conditions when sulfosalicylic acid was used. With 1.0 M sulfosalicylic acid, an 80 °C leaching temperature, a 1/10 solid-to-liquid ratio, and a 30 minute leaching time, more than 87 % Zn dissolutions were accomplished. Within 30 minutes of leaching, 88.7% Zn dissolution was achieved, while 6.4% Fe was recovered. Under the tested conditions, no lead co-dissolution was found during the leaching process. With using sulfosalicylic acid from a copper oxide ore, Deng et al., 2017 discovered that when reaction duration and temperature increased, copper leaching rates increased. As seen in the reaction equations (4.18 and 4.19), sulfosalicylic acid is totally ionized. The current investigation found that when sulfosalicylic acid was utilized as an organic agent, there was a fair amount of selectivity between lead and zinc, as well as iron. The order of metal dissolution was found to be Zn > Fe > Pb (Deng et al., 2017; Hussaini et al., 2021a).

$$C_7H_6O_6S(s) \rightarrow C_7H_3O_6S_3^- (aq) + 3H^+(aq) \tag{4.18}$$

or

$$C_7H_6O_6S(s) + 3H_2O(aq) \rightarrow C_7H_3O_6S_3^- (aq) + 3H_3O^+(aq) \tag{4.19}$$

The effect of several organic acids on the dissolution of metals from flotation tailing is shown in Table 4.14. Citric and malic acid were shown to be superior leachates to the other organic acids tested, with zinc dissolution percentages greater than 90% under the conditions studied. Citric acid > malic acid > sulfosalicylic acid > formic acid > tartaric acid > ascorbic acid.

Table 4.14. The effect of organic acid on the dissolution of zinc and lead (Hussaini et al., 2021a).

Agent	Dissolution		Optimum parameters
	Zn (%)	Pb (%)	
Citric acid	90.6	9.3	Con.: 1 M, t: 180 min., T: 80 ◦C, S/L: 2/10
Malic acid	90.0	9.3	Con.: 1 M, t: 60 min., T: 80 ◦C, S/L: 1/10
Sulfosalicylic acid	88.7	-	Con.: 1 M, t: 30 min., T: 80 ◦C, S/L: 1/10
Formic acid	82.7	2.8	Con.: 1 M, t: 180 min., T: 60 ◦C, S/L: 1/10
Tartaric acid	34.4	10	Con.: 1 M, t: 30 min., T: 80 ◦C, S/L: 1/10
Ascorbic acid	34.1	1	Con.: 1 M, t: 60 min., T: 60 ◦C, S/L: 1/10

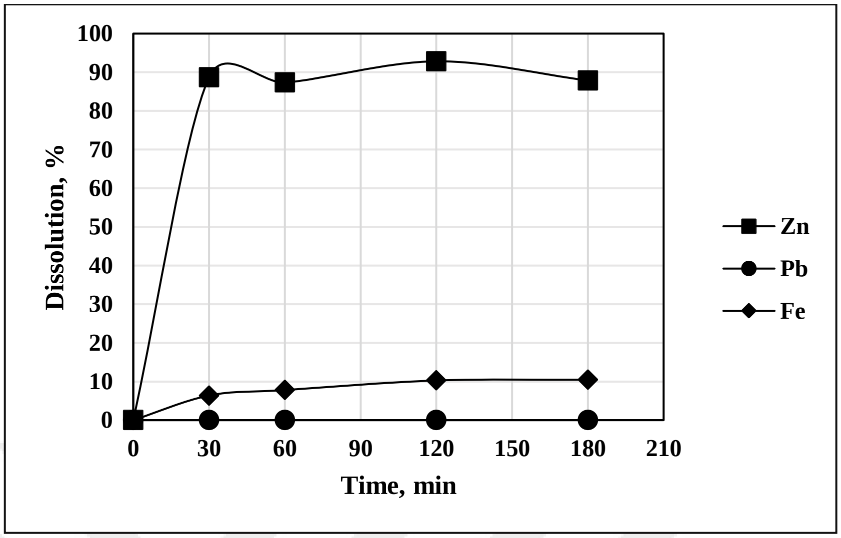

Figure 4.56. Metal dissolutions with 1.0 M sulfosalicylic acid at 80 ^oC and S/L ratio of 1/10.

4.1.3. Alkaline Leaching Study

4.1.3.1. Sodium hydroxide leaching study

- **Effect of NaOH concentration and time on metal dissolution at 80 ^oC**

In the metals leaching process, the alkaline concentration is quite significant. To investigate the effect of NaOH concentration at 1.0, 3.0, 5.0 and 7.0 M dosages at 80 ^oC and S/L ratio 1/10 on the leaching rate of Zn and Pb metals, experiments were carried out. Figures 4.57-4.60 show metal dissolution in different NaOH concentration and time at 80 ^oC and S/L: 1/10. According to Figure 4.40, Using 5.0 M sodium hydroxide for 180 minutes, 81.4 % Zn and 47.5 % Pb were simultaneously transferred to the leach solution without any Fe co-dissolution, which is consistent with the of Zhao and Stanforth, (2000) findings. For the production of zinc powder by alkaline treatment of smithsonite ores, they discovered that the best leaching results were obtained in 5.0 M NaOH at 90–95 °C with a reaction time of 90 minutes (Zhao and Stanforth, 2000). Liu et al., (2011) observed in an alkaline solution, Fe, Al, Mg, Ca, etc would not dissolve.

As a result, leaching agent consumption will be reduced to a minimum, and a leach solution comprising only Zn and Pb as main elements will be achieved (Liu et al., 2011). Zinc and lead metal ion dissolution is acceptable in alkaline leaching and at the same time, Fe does not dissolve in alkaline solutions, which increases selectivity in the solution, making this leaching very convenient for, BOF dust, EAF dust and galvanized steel scrap. This method, on the other hand, necessitate highly concentrated solutions, which presents certain technological challenges. Furthermore, because Zn in the ferritic form is not leached out during alkaline leaching, pyrometallurgical reduction is required as an intermediate step (Kaya et al., 2020a). Because high concentrations of sodium hydroxide have a strong oxidation characteristic and transform a portion of PbO into PbO_2, which has a low solubility in sodium hydroxide solution, lead dissolution decreased slightly at 7.0 M sodium hydroxide concentration (Badanoiu et al., 2013). ZnO transforms to $NaZn(OH)_3$ at high alkali concentrations, and the solubility of $NaZn(OH)_3$ drops with increasing alkali concentration at the same temperature. At 4.0 M sodium hydroxide concentration, Seyed Ghasemi and Azizi (2018) discovered that the hydroxyl ions are sufficient due to the creation of $Zn(OH)_4^{2-}$ and $Pb(OH)_4^{2-}$. The sequence of metal dissolution was discovered to be Zn > Pb. The following is a description of how cerrusite and smithsonite dissolve in sodium hydroxide solution (Hussaini et al., 2021a; Seyed Ghasemi and Azizi, 2018):

$$ZnCO_3(s) + 4OH^-(aq) \rightarrow Zn(OH)_4^{2-}(aq) + CO_3^{2-}(aq) \tag{4.20}$$

$$PbCO_3(s) + 4OH^-(aq) \rightarrow Pb(OH)_4^{2-}(aq) + CO_3^{2-}(aq) \tag{4.21}$$

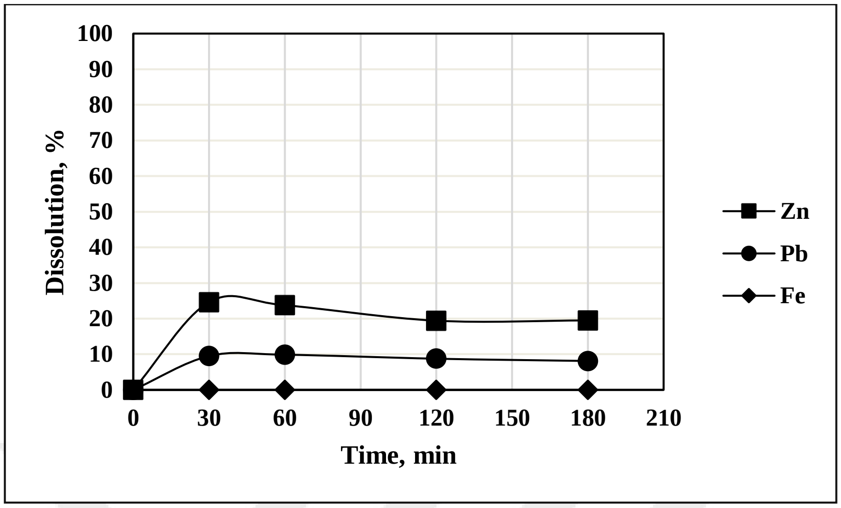

Figure 4.57. Metal dissolution with 1.0 M NaOH at 80 ºC and S/L: 1/10.

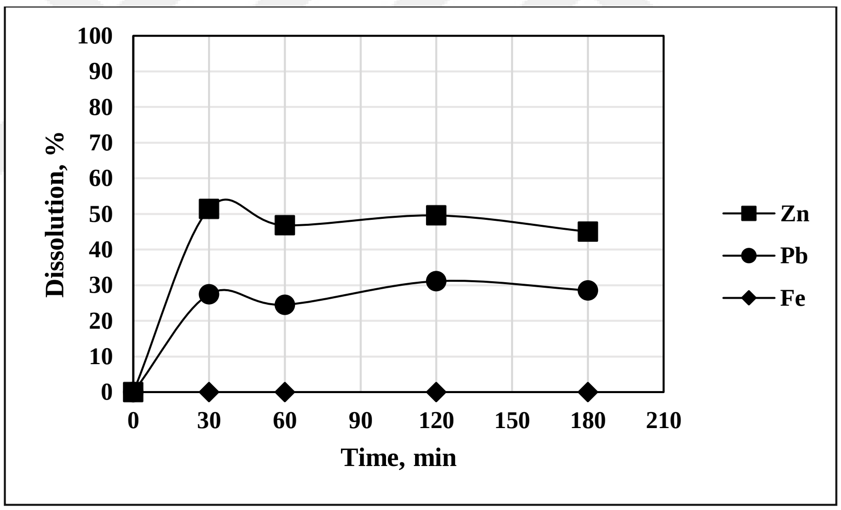

Figure 4.58. Metal dissolution with 3.0 M NaOH at 80 ºC and S/L: 1/10.

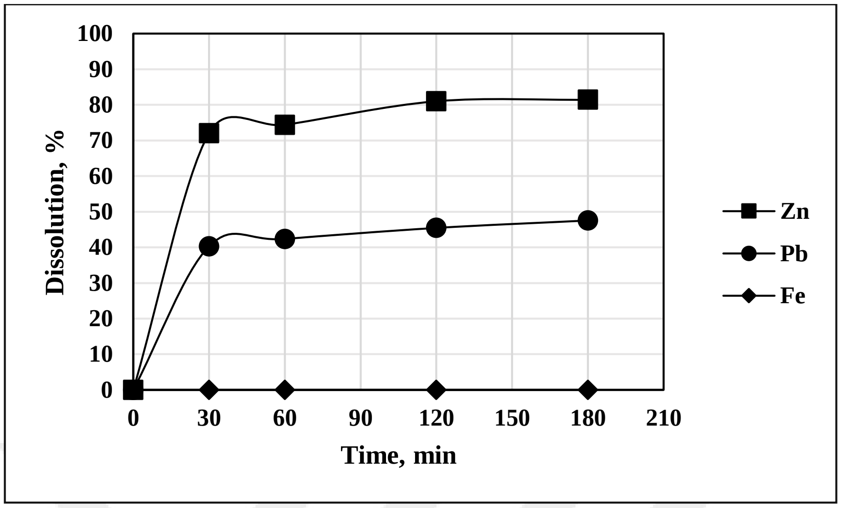

Figure 4.59. Metal dissolution with 5.0 M NaOH at 80 ^oC and S/L: 1/10.

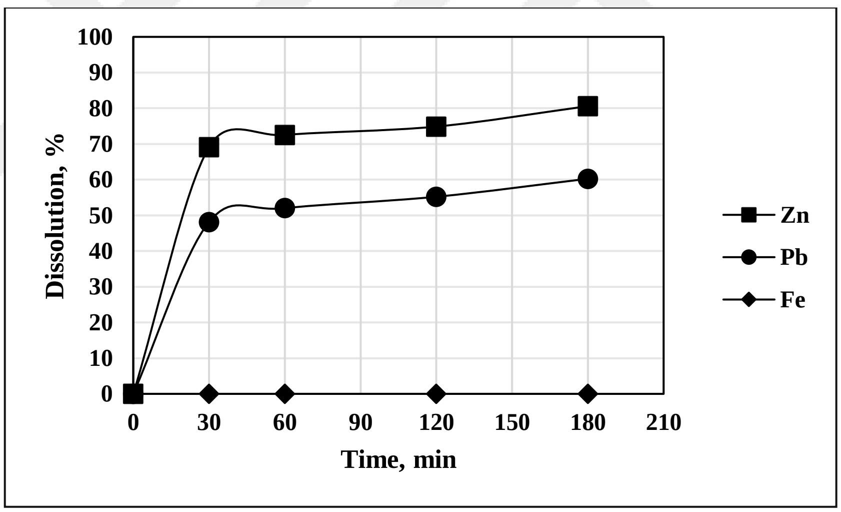

Figure 4.60. Metal dissolution with 7.0 M NaOH at 80 ^oC and S/L: 1/10.

4.1.3.2. Ammoniacal leaching study

❖ **Ammonia leaching study**

The metals dissolution with ammonia solution was researched at 80 ^oC temperature and S/L: 1/10. The metal dissolution result in different ammonia concentration and time are given in Figures 4.61-4.63. Under the tested conditions, the zinc dissolution remained reasonably consistent. During the leaching process, no iron or lead co-dissolutions were found. According to Wang et al., (2008). Zinc dissolution from a low grade zinc oxide ore increased with increasing of ammonia concentration, which conflict with present findings. This could be related to the high rate of ammonia volatilization at the current study's high leaching temperature. According to Figure 4.63, within 180 minutes, 61.3 % zinc dissolution was obtained at a 50% ammonia concentration, leaving all iron and lead in the leach residue. Due to the extremely high pH value of the process, high acid consumes $MgCO_3$ and $CaCO_3$, and contaminants, SiO_2, MgO, CaO, and Fe_2O_3 are insoluble in ammonia leaching (Abkhoshk et al., 2014). In an aqueous solution, the reactions between ammonia and smithsonite are as follows(Hussaini et al., 2021a; Wang et al., 2008):

$$ZnO(s) + 2NH_3(aq) + H_2O = [Zn(NH_3)_2]^{2+}(aq) + 2OH^- \quad (4.22)$$

$$ZnO(s) + 2NH_4^+ (aq) + 2NH_3(aq) \Leftrightarrow Zn(NH_3)_4^{2+} (aq) + H_2O \quad (4.23)$$

$$ZnCO_3(s) + 4NH_3(aq) = [Zn(NH_3)_4]^{2+}(aq) + CO_3^{2-} \quad (4.24)$$

$$ZnSO_4(s) + iNH_3(aq) = [Zn(NH_3)_i]^{2+}(aq) + SO_4^{2-} \quad (4.25)$$

where i: 1, 2, 3, 4.

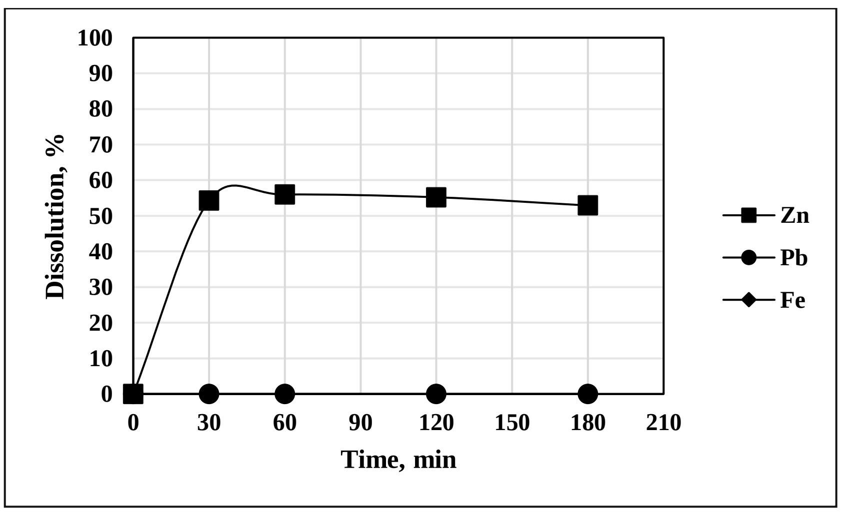

Figure 4.61. Metal dissolution with %20 ammonia at 80 ^oC and S/L: 1/10

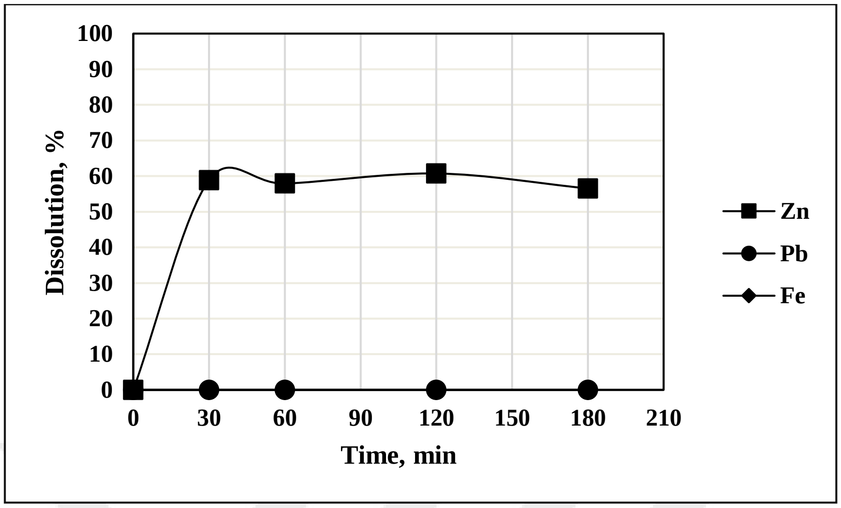

Figure 4.62. Metal dissolution with %30 ammonia at 80 ^{o}C and S/L: 1/10

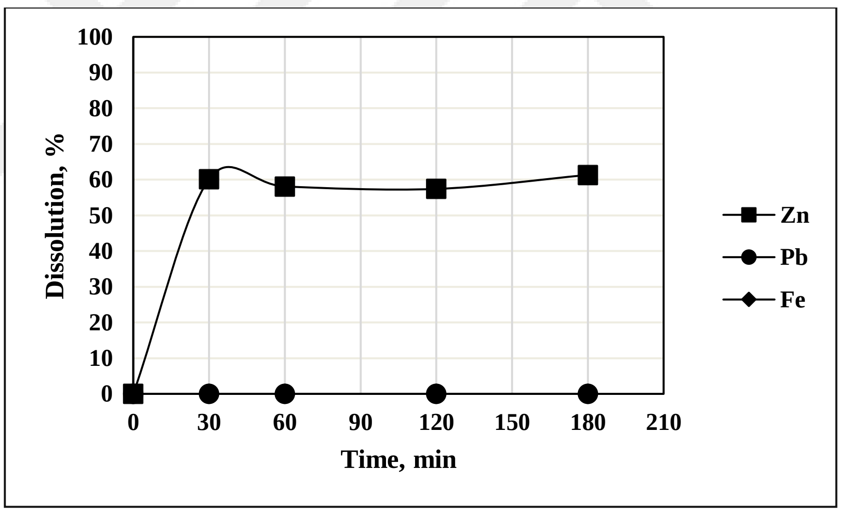

Figure 4.63. Metal dissolution with %50 ammonia at 80 ^{o}C and S/L: 1/10

- **Ammonium chloride leaching study**

The effects of 5.0 M NH_4Cl on metal dissolutions at 25, 40, 60 and 80 ^{o}C at 1/10 S/L ratio were given in Figures 4.64-4.67. Only Zn and Ag metals dissolved in NH_4Cl while Fe and As did not dissolve. At 80 ^{o}C leaching temperature, maximum Zn dissolution was 73% and Ag dissolution was 35% at 120 min. leaching time. According to Ju et al.(2005) with increasing leaching temperature, dissolution of zinc increased in ammonium chloride solution. This is most likely due to the firstly sublimation of NH_4Cl into hydrochloric acid and ammonia at high temperatures and in second high activation energy of a surface chemical reaction. No lead, iron, or arsenic dissolutions were found when the leaching temperature increased from 60 to 80 ° C. At 80 °C, dissolution of 73% Zn and 34.8% Ag was obtained at 120 minutes. The order of metal dissolution was Zn > Ag. The solution's pH ranged between 6.4 and 6.9 which, because of that, impurities such as, SiO_2, Fe_2O_3, CaO etc. are not suitable in leaching solutions (Ju et al., 2005; Kaya et al., 2020a; Rao et al., 2015).

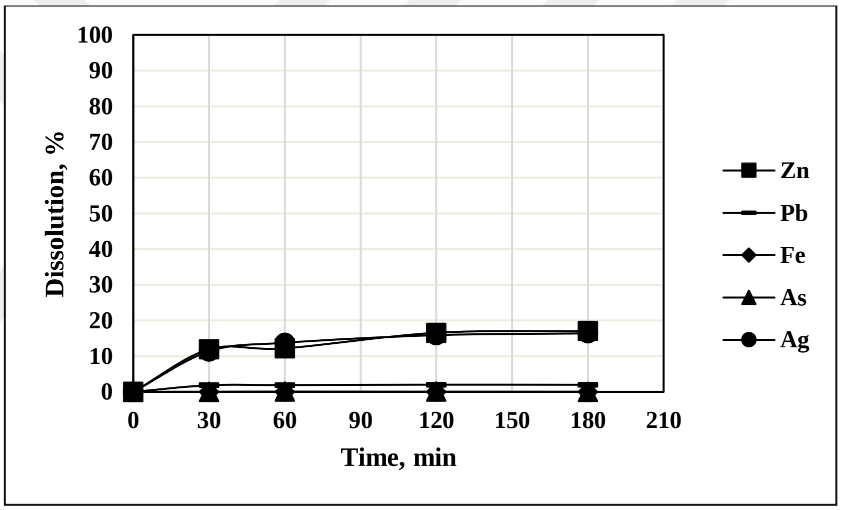

Figure 4.64. Metal dissolution with 5.0 M NH_4Cl at 25 ^{o}C and S/L: 1/10

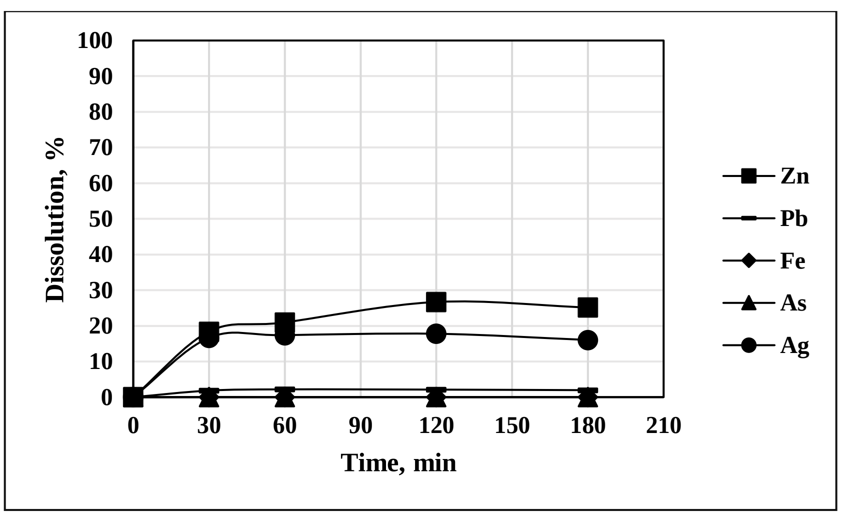

Figure 4.65. Metal dissolution with 5.0 M NH_4Cl at 40 ^{o}C and S/L: 1/10

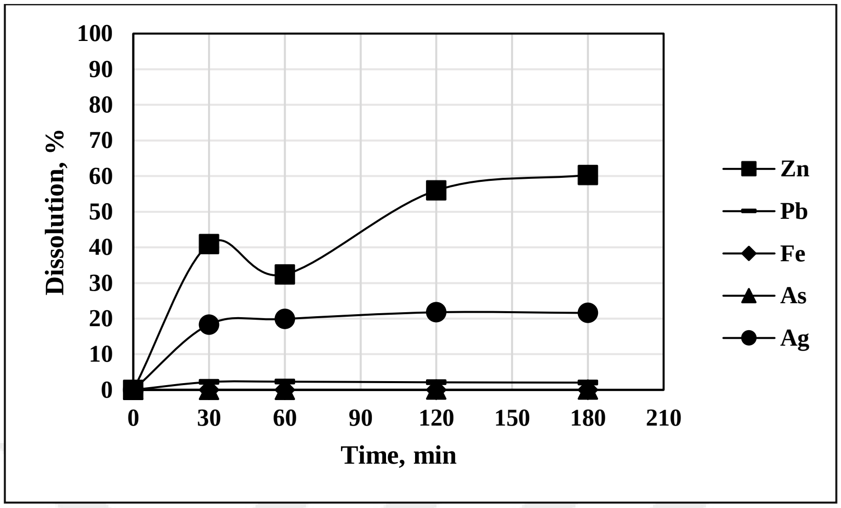

Figure 4.66. Metal dissolution with 5.0 M NH_4Cl at 60 ^oC and S/L: 1/10

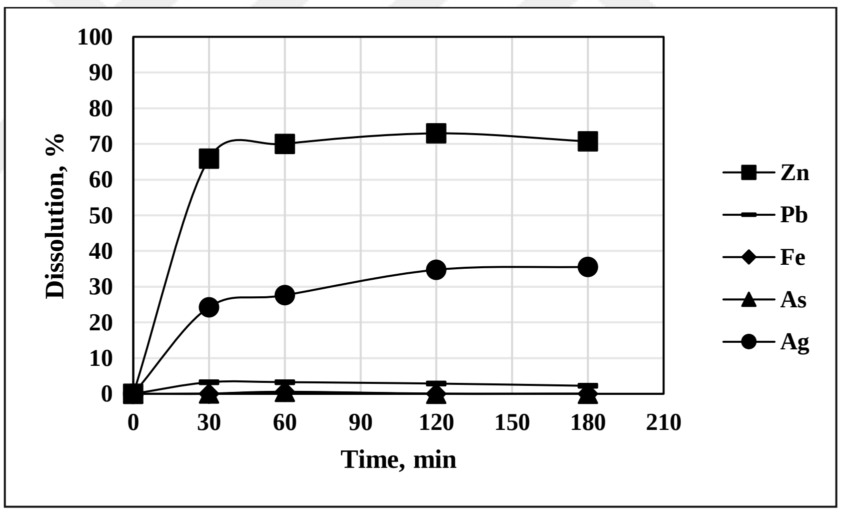

Figure 4.67. Metal dissolution with 5.0 M NH_4Cl at 80 ^oC and S/L: 1/10

- **Others ammoniacal leaching study**

The metal dissolution with ammonium oxalate ($(NH_4)_2C_2O_4$) at various leaching times is shown in Figure 4.68. The dissolution of zinc was rather than 20% using 1.0 M ammonium oxalate at 80 °C, 180 minutes of leaching time and S/L: 1/10, as shown in Figure 4.68. Under the tested conditions, less than 3% Pb dissolution was achieved. There was no evidence of iron co-dissolution. During ammonium oxalate leaching pH of the medium changed between 7.4 and 7.7.

The effect of leaching time and ammonium acetate ($C_2H_7NO_2$) on the metal dissolution was researched at 80^{o}C and S/L: 1/10 (Figure 4.69). According to Figure 4.69 with increasing leaching time, dissolution of zinc slightly increased. 3.0 M ammonium acetate was used for 180 minutes to achieve maximum zinc dissolution (39 %). time for leaching. Metal dissolution order was Zn>Pb>Fe. %. There is some selectivity between Zn and Pb-Fe dissolutions. However, Zn dissolution rates were very low. Thus, the use of ammonium acetate was not considered from now on.

Figure 4.70 shows the metal dissolution using 3.0 M ammonium sulfate ($(NH_4)_2SO_4$) at 80 ^{o}C and S/L: 1/10. As a result, 23.1% zinc dissolution was archived after 180 min. The co-dissolutions of iron and lead were found to be less than 5%. Metal dissolution order changed Zn>Fe>Pb. Since Zn dissolution was very low, the use of ammonium sulphate was neglected for the latter tests. According to Feng et al.(2007) leaching of zinc oxide pellets using ammonium sulfate controlled by the diffusion of the leach solution through the gangue layer in the entire leaching procedure.

The effect of ammoniacal agents on zinc and lead dissolution was summarized in Table 4.15. Because high selectivity or recovery between lead and zinc were not obtained, ammoniacal agents were not considered as a lixiviant for the dissolution of lead and zinc.

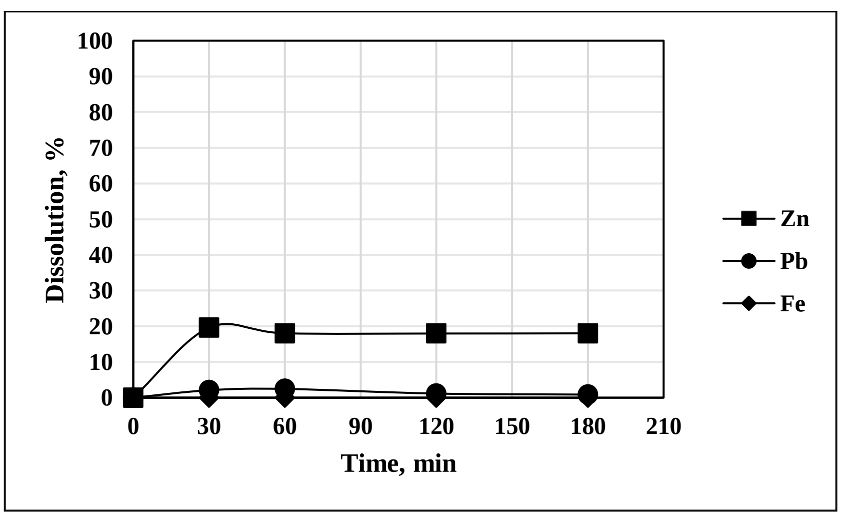

Figure 4.68. Metal dissolution with 1.0 M ammonium oxalate at 80 ^{o}C and S/L: 1/10.

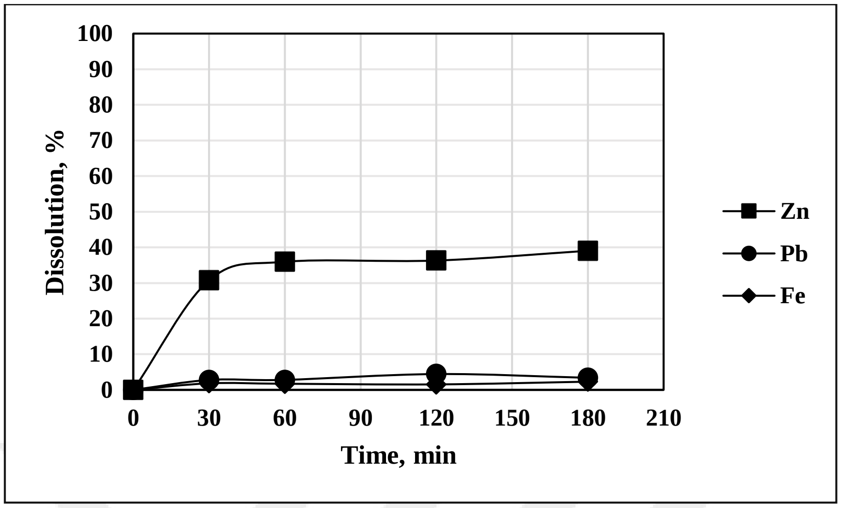

Figure 4.69. Metal dissolution with 3.0 M ammonium acetate at 80 ^{o}C and S/L: 1/10.

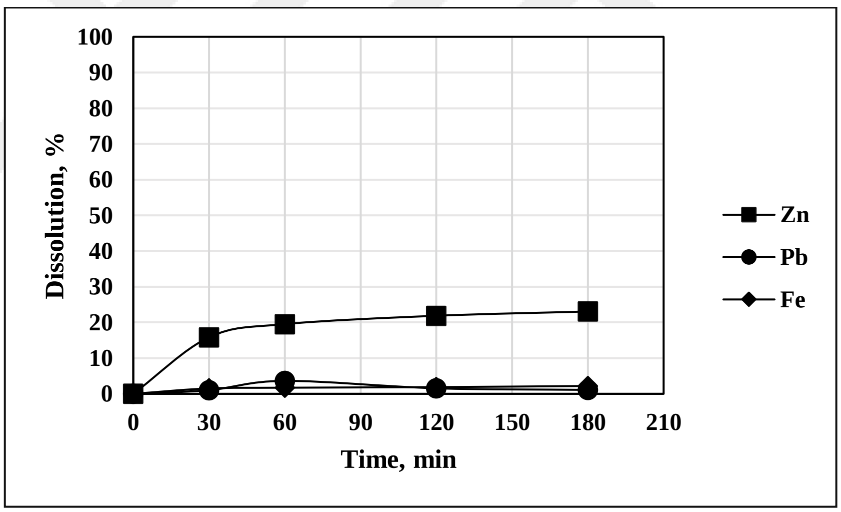

Figure 4.70. Metal dissolution with 3.0 M ammonium sulfate at 80 ^{o}C and S/L: 1/10.

Table 4.15. The effect of ammoniacal solution on the dissolution of Zn and Pb.

Agent	Disolution		Optimum parameters
	Zn (%)	Pb (%)	
Ammonia	61.3	0	Con.: 50%, t: 180 min., T: 80 ◦C, S/L: 1/10
Ammonium oxalate	19.6	2.1	Con.: 1 M, t: 30 min., T: 80 ◦C, S/L: 1/10
Ammonium acetate	39	3.4	Con.: 3 M, t: 180 min., T: 80 ◦C, S/L: 1/10
Ammonium sulfate	23.1	1.1	Con.: 3 M, t: 180 min., T: 80 ◦C, S/L: 1/10
Ammonium chloride	73	0	Con.: 5 M, t: 120 min., T: 80 ◦C, S/L: 1/10

4.1.4. EDTA (ethylenediaminetetraacetic acid ($C_{10}H_{16}N_2O_8$)) leaching study

The effect of 0.375 M EDTA concentration on Zn, Pb and Fe dissolution at 40, 60 and 80 ^oC and with S/L: 1/10 were investigated (Figures 4.71-4.73). According to Figure 4.73 at 80 ^oC, about 83% Zn dissolution was obtained at 30 min. and 97% Zn dissolution at 180 min. leaching time. At 27% Pb and 20% Fe co-dissolutions. The EDTA obtained over 90% zinc dissolution, as well as lead and iron co-dissolutions, which is consistent with Sun et al., 2001 results. The researcher determined at low EDTA concentrations, recovery of zinc from contaminated surface soils collected from four different places is more than recovery of lead (Sun et al., 2001). The order of metal dissolution was determined to be Zn > Pb > Fe. pH changed from 5 to 6 during all experiments which were close to the neutral pH and less corrosive. Due to the relatively low EDTA affinity for Zn^{2+} than Pb^{2+}, EDTA cannot interact with zinc oxide if lead oxide is found in the flotation tailing, as shown in Eq 4.26. When EDTA concentrations over a specific level, excess EDTA can bind with zinc, resulting in a significant increase in zinc concentration (Hussaini et al., 2021a; Liu et al., 2014).

$$Zn - EDTA + PbO + H_2O = Pb - EDTA + Zn(OH)_2 \tag{4.26}$$

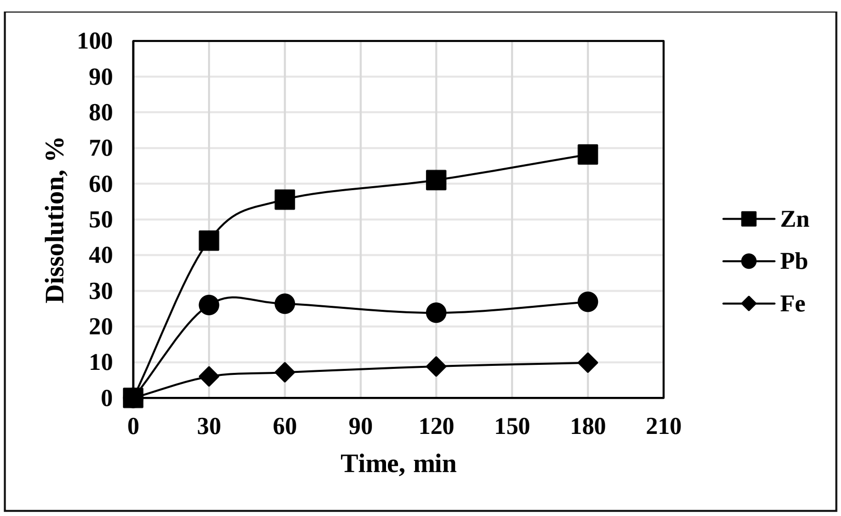

Figure 4.71. Metal dissolution with 0.375 M EDTA at 40 ^oC and S/L: 1/10.

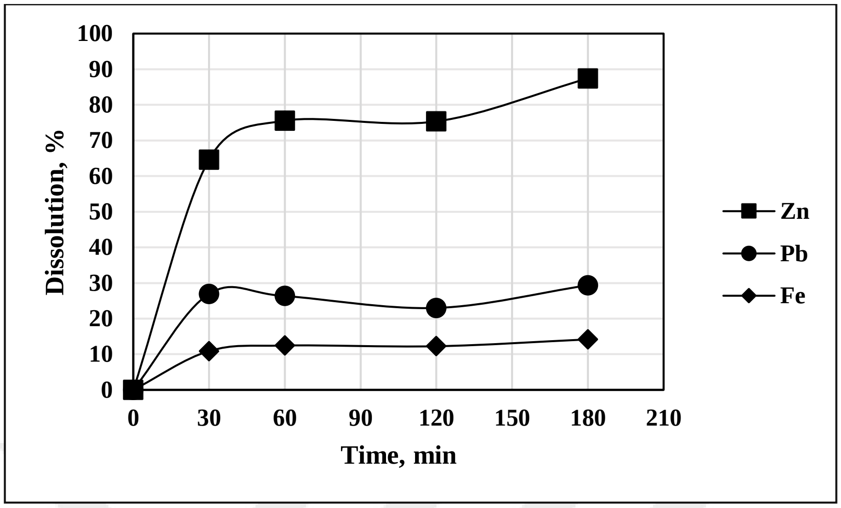

Figure 4.72. Metal dissolution with 0.375 M EDTA at 60 ^oC and S/L: 1/10.

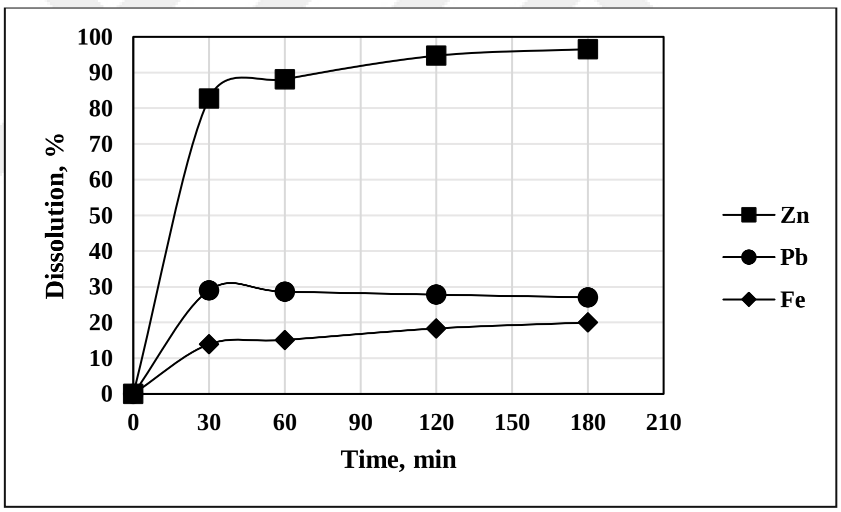

Figure 4.73. Metal dissolution with 0.375 M EDTA at 80 ^oC and S/L: 1/10.

4.2. Second Step Leaching Study

In the first stage leach tests, inorganic H_2SO_4 (1.0 M, 40 ^oC, 30 min., and 2/10 S/L ratio) and organic citric (1.0 M, 80 ^oC, 180 min., and 2/10 S/L ratio) and malic (1.0 M, 80 ^oC, 60 min. and 1/10 S/L ratio) acids were chosen as the optimum lixiviant for highest Zn dissolution. The second step leaching were studied with these leaching residues.

4.2.1. Second step leaching of sulfuric acid residue for lead recovery

Sulfuric acid leach residue has 1.38% Zn, 9.91% Pb, 23.3% Fe, more than 10000 ppm As and 142 ppm Ag. In addition, 2.01% Al, 3.19% Ca, 0.65% K, 0.22% Mg, 0.09% Na, 4.19% S, 0.09% Ti, 70 ppm Ba, 0.5 ppm Be, <2 ppm Bi, 35.7 ppm Cd, <1 ppm Co, 56 ppm Cr, 214 ppm Cu, 10 ppm Ga, 10 ppm La, 80 ppm Mn, 12 ppm Mo, 29 ppm Ni, 180 ppm P, 322 ppm Sb, 3 ppm Sc, 390 ppm Sr, <20 ppm Th, 10 ppm Tl, 10 ppm U, 37 ppm V and 10 ppm W were found in the sulfuric acid leach residue.

Chloride leaching is the most recognized and widely used recovery method. Chloride leaching processes have been employed using either NaCl, or $MgCl_2$ and $CaCl_2$, or $FeCl_3$ along with HCl (Behnajady et al., 2012).

4.2.1.1. NaCl leaching study

In the first brine leaching test, 6.25 g H_2SO_4 leach residue was leached with 75 g NaCl in 250 mL (300 g/L NaCl) distilled water at 80 ^oC leaching temperature for 30 min which results are given in Figure 4.74. Metal dissolution order was Pb>Zn>Fe. At 10 min. leaching time, Zn dissolution was 5.6% and Pb dissolution was 26.7%. At 30 min leaching time Zn dissolution was 7.7% and Pb dissolution was 28%. There was no Fe dissolution in 30 min. leaching time. At S/L ratio of 1/40 (0.025), we used about 5.13M NaCl concentration and Pb dissolution was less than 30% and Zn dissolution was less than 8%. pH was around 4 and 5. The theoretical reaction between lead sulfate and NaCl was given Eq 4.27.

$$PbSO_4 + iCl^- = [PbCl_i]_{2-i} + SO_4^{2-} \quad (4.27)$$

Where (i =1, 2, 3, 4)

Most metal chlorides are considerably more soluble than sulfate salts, and brine leaching is the most recognized and widely used recovery method. Both pulp density and NaCl concentration significantly affect Pb extraction. Our results were different from other investigations (Farahmand et al., 2009; Guo et al., 2010; Rusen, 2007; Turan et al., 2004; Ye et al., 2017). It could be due to the complexity of the lead compound in our residue sample as shown in Figure 4.12. Another reason could be that while we used just NaCl for leaching excrement, they used other regents together with NaCl. For example, Gue et al., 2010 and Turan et al., 2004 used sulfuric acid with NaCl for leaching experiments and recovered more than 90% lead.

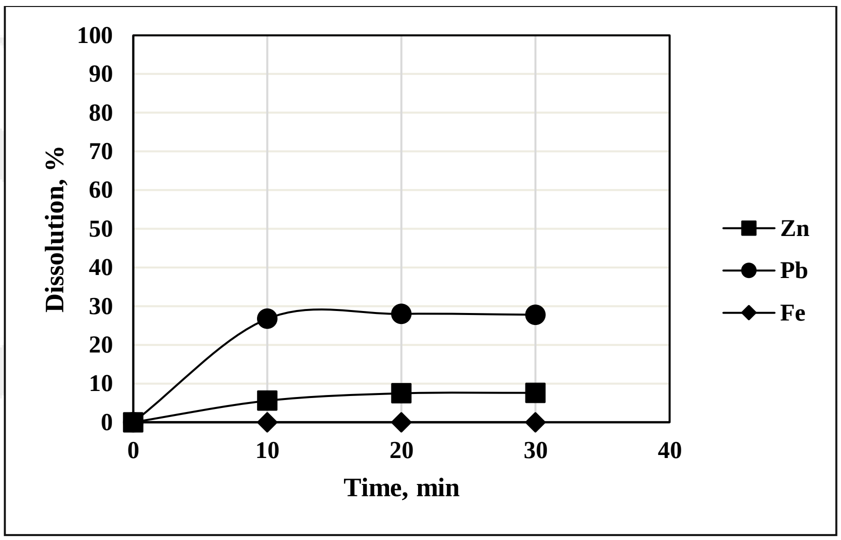

Figure 4.74. Metal dissolution with 300 g/L NaCl at 80 °C and S/L: 1/40.

4.2.1.2. $CaCl_2$ leaching study

In the second brine leaching test, 400 g/L $CaCl_2$ was used at 1/7 S/L ratio, 80 °C leaching time for 90 min. leaching time. Figure 4.75 shows the results of metal dissolution with $CaCl_2$. Metal dissolution order was Pb > Zn > Fe. Zn dissolution was 13.2% at 30 min. and 17.3% at 90 min. leaching time. Pb dissolution was 21.9% at 30 min. and 25.5% at 90 min. leaching time. After 30 min. leaching time metal dissolutions were remain constant. The other exprement was carried out with same conditions but pH was adjusted at 1.0 with HCl. Metal dissolution order was Pb>Zn>Fe. Zn dissolution increased with increasing leaching time from from 30 min. to 90 min. But, the increase in Zn dissolution was changed from 13.6% to 16.3%. Pb dissolution decreased from 23.2% to 21.4% at 90 min. leaching time. Fe dissolution was zero. With $CaCl_2$ brine, less than 24% Pb and 17% Zn dissolutions were achieved. After 30 min. leaching time metal dissolutions were remain constant. The results of metal dissolution in second test are shown in Figure 4.76. Wang et al., 2015 and Xie et al., 2019 were taken 94% and 86% lead respectively, which these were different from our results. It was possible that the low recovery was due to the same reasons as indicated in leaching with NaCl (Wang et al., 2015; Xie et al., 2019). According to results pH not significant effect on Pb dissolution.

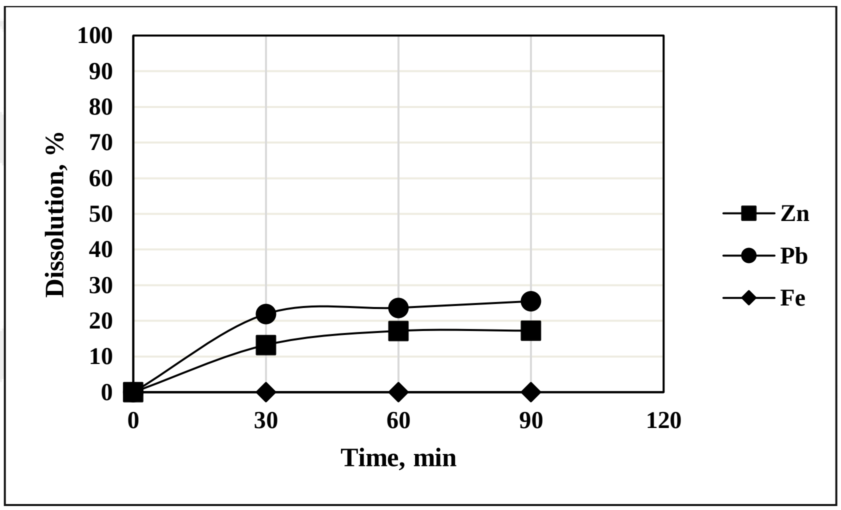

Figure 4.75. Metal dissolution with 400 g/L $CaCl_2$ at 80 ^oC and S/L: 1/7.

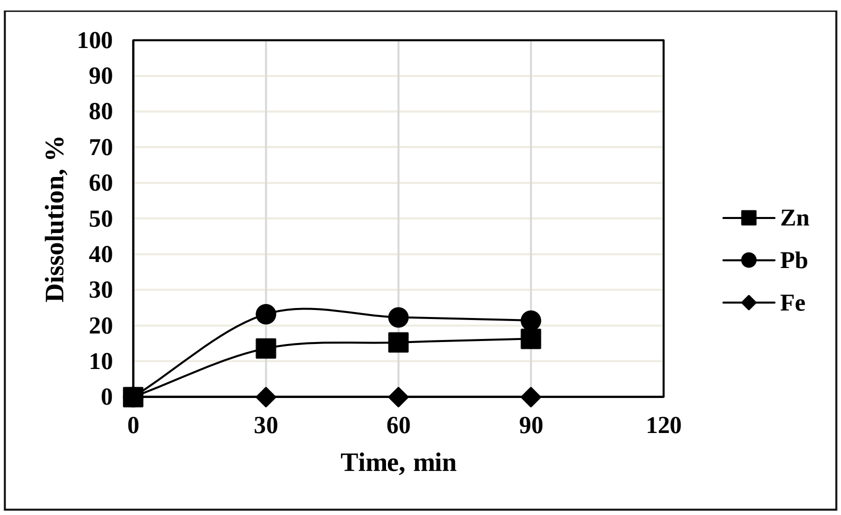

Figure 4.76. Metal dissolution with 400 g/L $CaCl_2$ at pH 1.0, 80 ^oC and S/L: 1/7.

4.2.1.3. NaOH leaching study

The second step leaching continued with 5.0 NaOH at 80 ^oC and 1/10 S/L ratio. Metal dissolution order is Pb > Zn > Fe. At 30 min. leaching time 50.2% Pb and 16.3% Zn and at 180 min. leaching time 74% Pb and 35.8% Zn dissolutions were obtained (Figure 4.77). Both Pb and Zn dissolved together without Fe dissolution. Maximum Pb dissolution was obtained at 180 min. leaching time. About 27.6% of the feed material was dissolved and the pH of the medium was between 9.0 and 9.1. The desulphurization of $PbSO_4$ occurs in two steps(Yu et al., 2019):

$$PbSO_{4(s)} + 2NaOH_{(aq)} \rightarrow PbO_{(s)} + Na_2SO_{4(aq)} + H_2O_{(l)} \tag{4.28}$$

PbO also dissolve in NaOH:

$$PbO_{(s)} + NaOH_{(aq)} \rightarrow NaHPbO_{2(aq)} \tag{4.29}$$

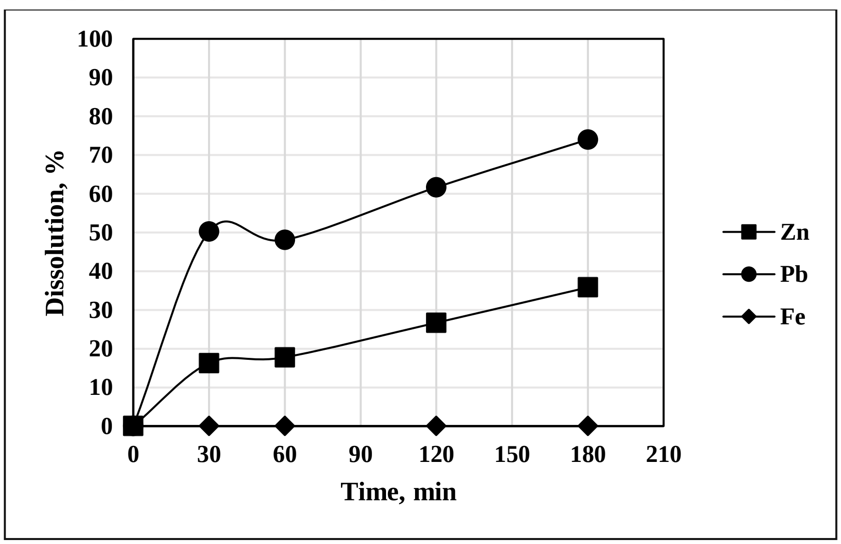

Figure 4.77. Metal dissolution with 5.0 M NaOH at 80 ^oC and S/L: 1/10.

4.2.1.4. NaOH and NaCl leaching study

5.0 M NaOH and 2.0 M NaCl used for second step leaching of sulfuric reside at 80 ^oC and S/L: 1/10. Figure 4.78 shows the results of metal dissolution. Metal dissolution order is

Pb>Zn>Fe. At 30 min. leaching time 75.6% Pb and 26.1% Zn and at 180 min. leaching time 96.2% Pb and 46.8% Zn dissolutions were obtained. Both Pb and Zn dissolved together without Fe dissolution. Maximum Pb dissolution was obtained at 180 min. leaching time. The pH of the medium was between 8.6 and 9.0. NaCl addition significantly increased both Pb and Zn dissolutions. This significant increase with NaCl was also observed by Chmielewski et al., 2017. They recovered 96% Pb in two steps and 180 min. leaching time at 90 ^oC (Chmielewski et al., 2017).

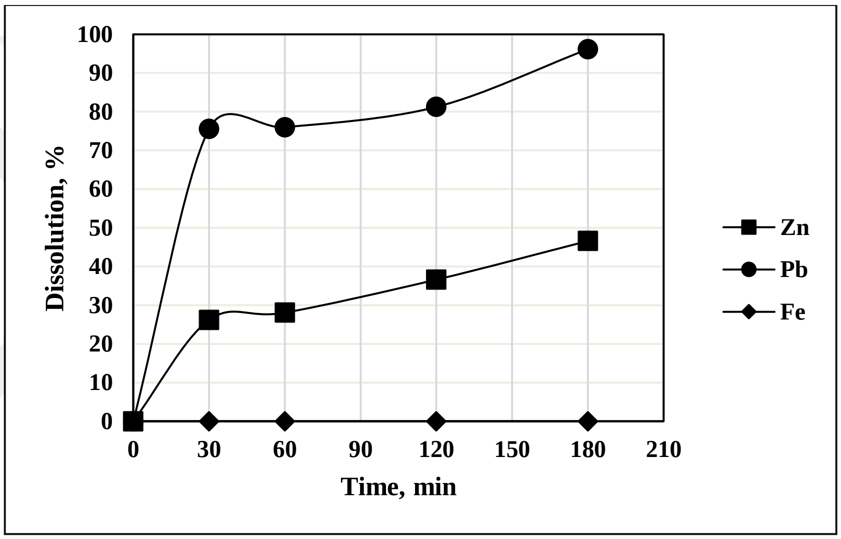

Figure 4.78. Metal dissolution with 5.0 M NaOH and 2.0M NaCl at 80 ^oC and S/L: 1/10.

4.2.1.5. NaOH and potassium-sodium tartrate leaching study

150 g/L NaOH (3.75M) and 150 g/L sodium-potassium tartrate (1.88 M) were used for H_2SO_4 leach residue leach at 25, 40, 60 and 80 ^oC and 1/10 S/L ratio in 30, 60, 120 and 180 min. leaching time. The results of metal dissolution were given in Figures 4.79-4.82. According to Figure 4.79 metal dissolution order was Pb > Fe > Zn. At 30 min. leaching time, Pb dissolution was 79.1% at 22.5% Fe and 4.9% Zn co-dissolutions. Maximum Pb dissolution of 90.4% at 26.4% Fe and 8.6% Zn co-dissolution was obtained at 120 min. leaching time. Potassium sodium tartrate increased both Pb dissolution and Fe and Zn co-dissolutions significantly. As a results increasing the temperature did not have any effect on the metal dissolution. Then the second step leaching at 25 ^oC leaching temperature and 120 min. leaching time at was the

selected optimum. Ferracin et al., 2002 also studeid 13 aquoes solution for recovery of lead from waste of lead acid battery. They obtained the best lead dissolution with 150 g/L NaOH and 150 g/L KNaTartrate at 25 ^{o}C, 60 min leacnihg time and S/L: 1/10(Ferracin et al., 2002). The reactions of the leaching process are shown in Reactions 4.30-4.33. Our suggestion in leaching process is that the $PbSO_4$ is first desulfurized by NaOH to create PbO in the residue sample and then lead compounds are leached with $KNaC_4H_4O_6$ solution (Li et al., 2019):

$$2PbSO_4(s) + 2KNaC_4H_4O_6(aq) + 2NaOH(aq) \rightarrow 2Pb(C_4H_4O_6)(aq) + 2Na_2SO_4(aq) + 2KOH(aq) \quad (4.30)$$

$$2PbSO_4(s) + 3KNaC_4H_4O_6(aq) + 2NaOH(aq) \rightarrow KNaPb_2(C_4H_4O_6)_3(aq) + 2Na_2SO_4(aq) + 2KOH(aq) \quad (4.31)$$

$$2PbO(s) + 2KNaC4H4O6(aq) + 2NaOH(aq) \rightarrow Pb_2(C_4H_4O_6)_2(aq) + 2Na_2SO_4(aq) + 2KOH(aq) \quad (4.32)$$

$$2PbO(s) + 3KNaC_4H_4O_6(aq) + 2NaOH(aq) \rightarrow KNaPb_2(C_4H_4O_6)_3(aq) + 2Na_2SO_4(aq) + 2KOH(aq) \quad (4.33)$$

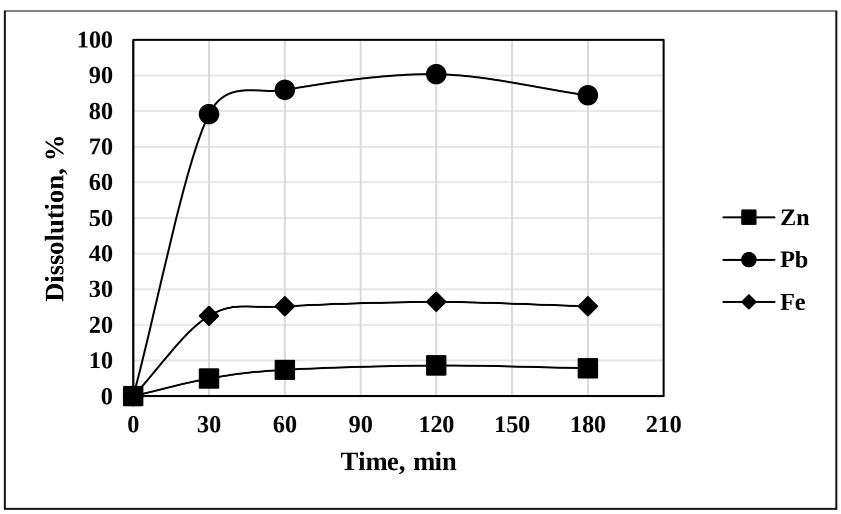

Figure 4.79. Metal dissolution with 150 g/L NaOH and 150 g/L KNaTartrate at 25 ^{o}C and S/L: 1/10.

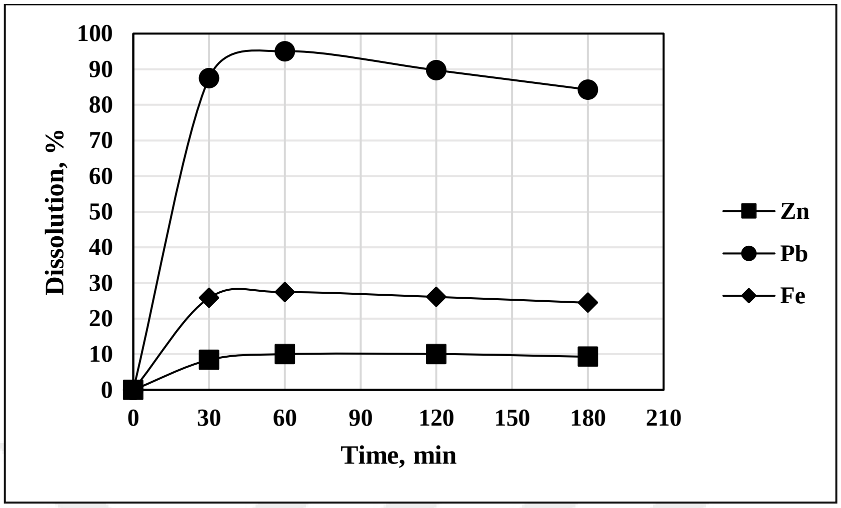

Figure 4.80. Metal dissolution with 150 g/L NaOH and 150 g/L KNaTartrate at 40 ^oC and S/L: 1/10.

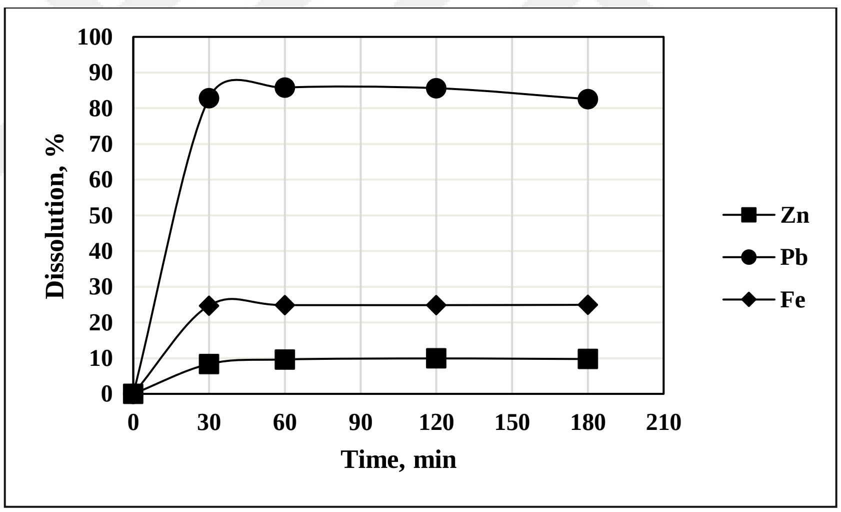

Figure 4.81. Metal dissolution with 150 g/L NaOH and 150 g/L KNaTartrate at 60 ^oC and S/L: 1/10.

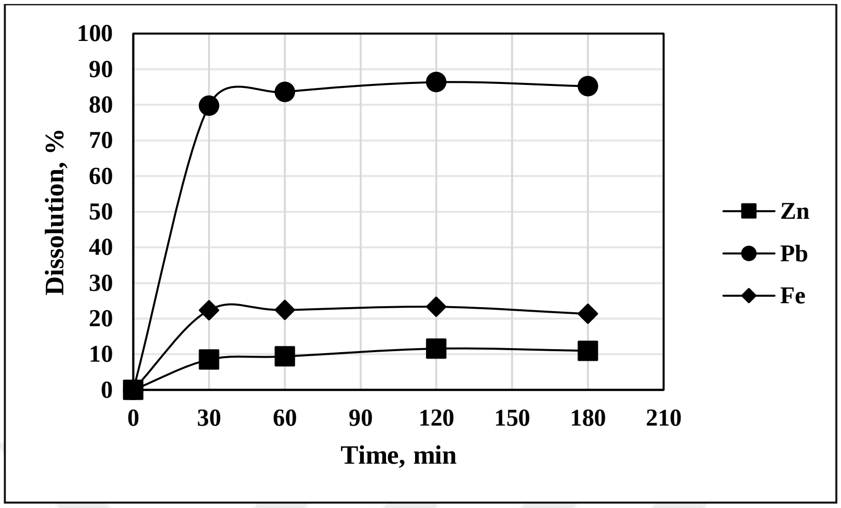

Figure 4.82. Metal dissolution with 150 g/L NaOH and 150 g/L KNaTartrate at 80 ^{o}C and S/L: 1/10.

Figure 4.83 shows the XRD spectra of NaOH and KNaTartrate leached residue at the optimum conditions. Muscovite, quartz, gypsium and celestine (more than 78%) are the mineral impiurities in residue but kintoreite ($PbFe_3(PO_4)1.46(AsO_4)0.32(SO_4)0.22(OH)_6$) and beudantite ($Pb(Fe_{2.54}Al_{.46})(As_{1.07}O_4)(S_{.93}O_4)(OH)_6$) were also obsereved in XRD spectra. Compared with Figure 4.12, it could be seen that segnitite is not present in the residue. On the other hand, sodium hydroxide and potassium sodium tartrate had no effect on the lead dissolution in beudantite. Table 4.16 shows the concentration of the metals in NaOH and KNaTartrate leached solution (PLS). It could be seen that 8270 mg/L lead was transferred to the solution. 248 mg/L zinc and 5630 mg/L iron observed in the solution.

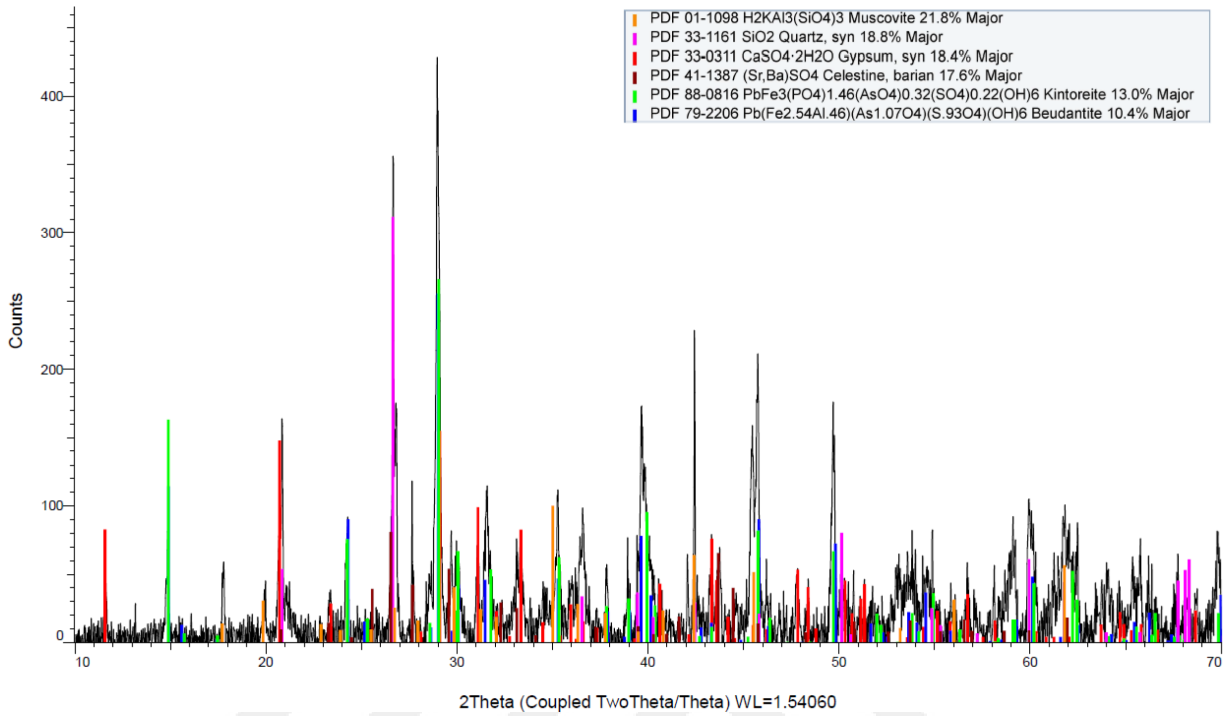

Figure 4.83. XRD spectra of NaOH and KNaTartrate leached residue from sulfuric acid residue at the optimum conditions.

Table 4.16. Concentration of the metals in NaOH and KNaTartrae leached solution.

Elements	mg/L	Elements	mg/L	Elements	mg/L
Ag	0.04	Cu	2.88	Pb	8270
Al	66.6	Fe	5630	S	4600
As	2540	K	17450	Sb	14.25
B	2.03	Li	0.05	Se	48.6
Ba	6.6	Mg	6.83	Sn	261
Bi	0.2	Mn	1.48	Sr	9.09
Ca	3130	Mo	0.41	Tl	<0.03
Cd	0.13	Na	80100	Zn	248
Co	0.24	Ni	1.32	Zr	0.2
Cr	0.41	P	1320		

4.2.1.6. Oxalic acid leaching of sulfuric acid leach residue for iron recovery

As we know oxalic acid has significant effect on iron dissolution (Kaya et al., 2020b; Kursunoglu et al., 2021). Sulfuric acid leach residue was leached with 1.0 M oxalic acid at 80

^{o}C and 1/S/L: 1/10 ratio for 180 min. Metal dissolution order was Fe > Zn > Pb. At 30 min. leaching time 74.4% Fe dissolved at 52.2% Zn and 2.6% Pb co-dissolution. With increasing leaching time Fe dissolution increased up to 86.8% at 120 min. leaching time (Figure 4.84). Table 4.17 shows the concentration of the metals in oxalic acid leached solution (PLS). It could be seen that 23500 mg/L iron was transferred to the solution. 395 mg/L lead and 231 mg/L zinc observed in the solution at optimum conditions.

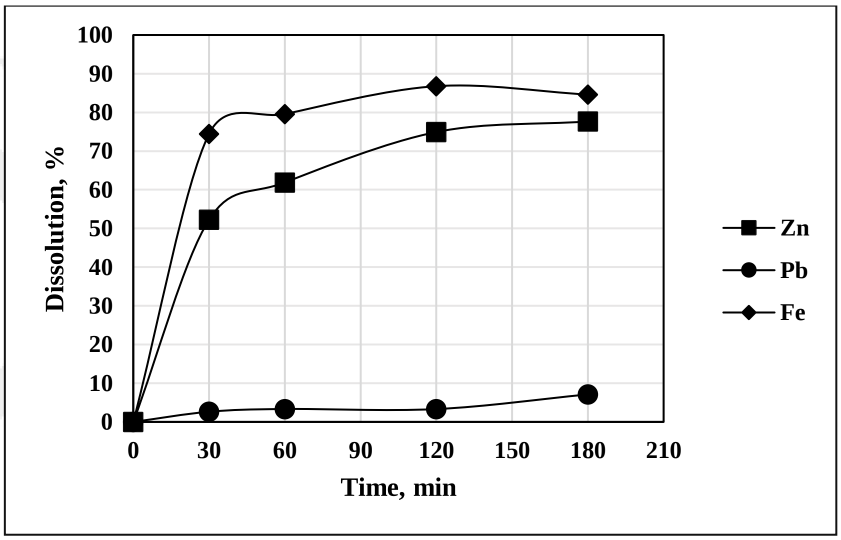

Figure 4.84. Metal dissolution with 1.0 M oxalic acid at 80 ^{o}C and S/L: 1/10.

Table 4.17. The concentration of the metals in oxalic acid leached solution.

Elements	mg/L	Elements	mg/L	Elements	mg/L
Ag	0.004	Cu	0.287	Pb	395
Al	286	Fe	23500	S	2680
As	3540	K	74.7	Sb	24.8
B	0.2	Li	0.93	Se	42.8
Ba	0.163	Mg	54.9	Sn	0.01
Bi	0.6	Mn	4.01	Sr	3.24
Ca	2230	Mo	0.771	Tl	0.07
Cd	3.02	Na	27.1	Zn	231
Co	0.698	Ni	1.16	Zr	0.2
Cr	0.914	P	9.17		

4.2.1.7. Other agents leaching study

Some agents were studied for lead dissolution from sulfuric residue, such as malic acid, acetic acid, NaOH with glycerol, and NaOH with glycerol and ascorbic acid. There was no indication of significant lead dissolution.

4.2.2. Second step leaching of citric acid leach reside

Citric acid leach residue has 1.805% Zn, 11.25% Pb, 24.8% Fe, more than 10000 ppm As and 171 ppm Ag. In addition, 2.4% Al, 0.47% Ca, 0.77% K, 0.31% Mg, 0.1% Na, 2.16% S, 0.1% Ti, 120 ppm Ba, 0.6 ppm Be, <2 ppm Bi, 95.2 ppm Cd, <1 ppm Co, 63 ppm Cr, 301 ppm Cu, 10 ppm Ga, 10 ppm La, 96 ppm Mn, 12 ppm Mo, 32 ppm Ni, 10 ppm P, 331 ppm Sb, 4 ppm Sc, 361 ppm Sr, <20 ppm Th, <10 ppm Tl, <10 ppm U, 50 ppm V and 10 ppm W were found in the citric acid leach residue.

4.2.2.1. NaOH and potassium-sodium tartrate leach of citric acid leach residue

150 g/L NaOH (3.75M) and 150 g/L sodium-potassium tartrate (1.88 M) were used for citric acid residue leach at 25 ºC and 1/10 S/L ratio for 180 min leaching time. The results of leaching were given in Figure 4.85. Metal dissolution order was Pb>Fe>Zn. At 30 min. leaching time, Pb dissolution was 85.2% at 30.6% Fe and 28.8% Zn co-dissolutions. Maximum Pb dissolution of 86.64% at 30.9% Fe and 29.9% Zn co-dissolution was obtained at 120 min. leaching time. Figure 4.86 shows the XRD spectra for NaOH and KNaTartaret leached residue. Quartz, muscovite and goethite minerals were observed in XRD spectra which means NaOH and KNaTartrate leaching could be beneficial to lead dissolution.

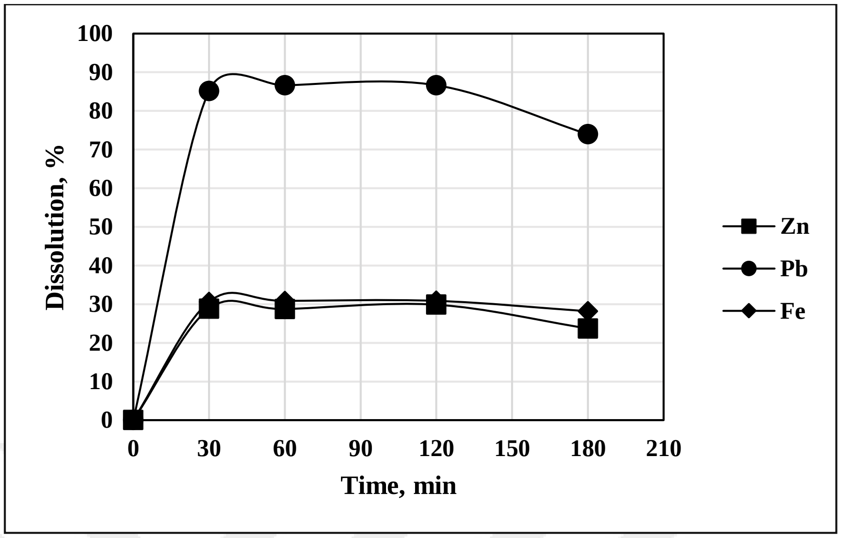

Figure 4.85. Metal dissolution with 150 g/L NaOH and 150 g/L KNaTartrate at 25 ^{o}C and S/L: 1/10.

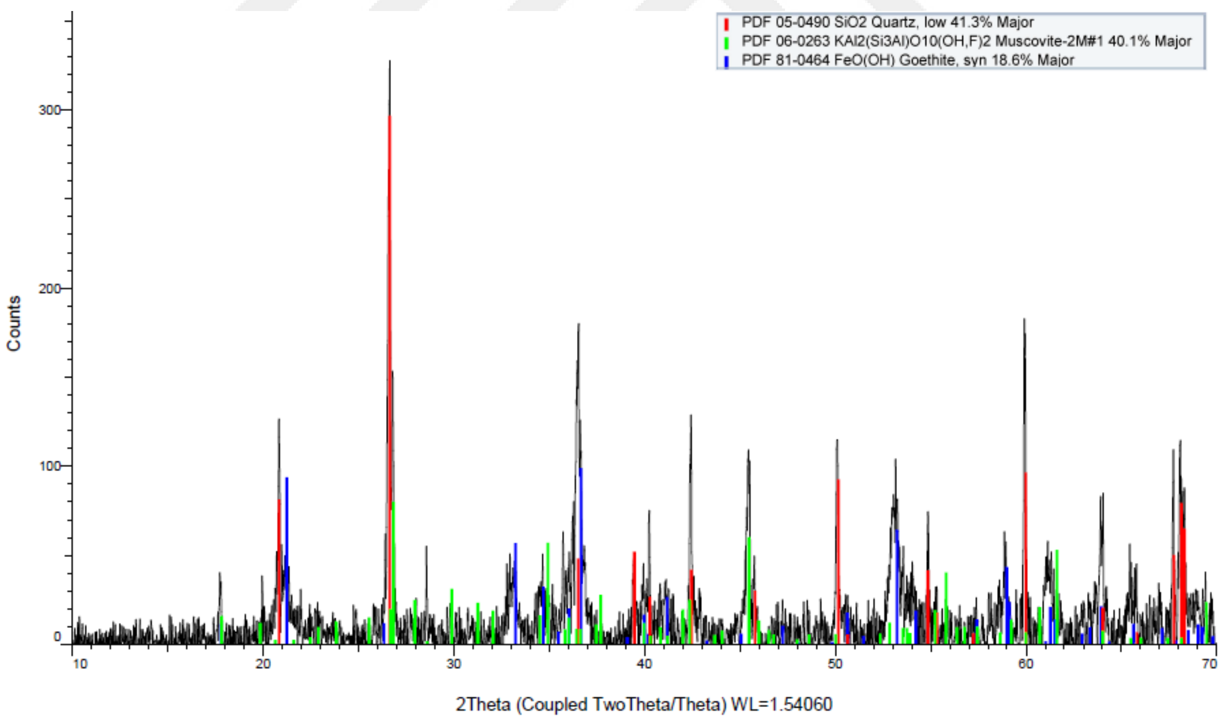

Figure 4.86. XRD spectra of NaOH and KNaTartrate leached residue from citric acid residue at the optimum conditions.

4.2.2.2. Oxalic acid leach of citric acid leach residue for iron recovery

Citric acid leach residue was leached with 1.0 M oxalic acid at 80 ^{o}C and 1/10 S/L ratio for 180 min. Metal dissolution order was Fe > Zn > Pb. At 30 min. leaching time 70.6% Fe dissolved at 16.9% Zn and 4% Pb co-dissolution. With increasing leaching time Fe dissolution increased up to 88% at 180 min. leaching time (Figure 4.87). Table 4.18 shows the concentration of the metals in oxalic acid leached solution (PLS). It could be seen that 24600 mg/L iron was transferred to the solution. 965 mg/L lead and 335 mg/L zinc also observed in the solution.

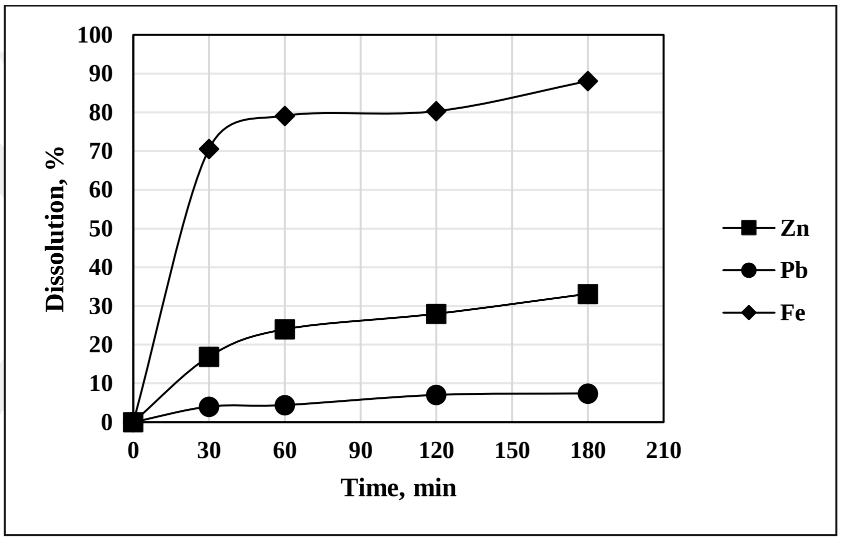

Figure 4.87. Metal dissolution with 1.0 M oxalic acid at 80 ^{o}C and S/L: 1/10.

Table 4.18. The concentration of the metals in oxalic acid leached solution.

Elements	mg/L	Elements	mg/L	Elements	mg/L
Ag	0.024	Cu	0.106	Pb	965
Al	314	Fe	24600	S	1290
As	4310	K	82.1	Sb	27.1
B	0.09	Li	1	Se	49.5
Ba	0.366	Mg	88.6	Sn	106
Bi	0.8	Mn	5.14	Sr	7.62
Ca	271	Mo	0.708	Tl	0.29
Cd	8.37	Na	32.3	Zn	335
Co	0.674	Ni	1.545	Zr	0.2
Cr	0.97	P	18.9		

4.2.2.3. Other agents leach of citric acid leach residue

For the recovery of lead from citric acid leach residue, 3.0 M NaOH, 250 g/L NaCl, 6.0 M Acetic acid, and Urea were utilized as agents. There was no evidence of significant lead recovery.

4.2.3. Second step leaching of malic acid leach reside

Malic acid leach residue has 1.97% Zn, 10.10% Pb, 27.2% Fe, 4.52% As and >100 ppm Ag. In addition, 2.22% Al, 0.43% Ca, 0.72% K, 0.29% Mg, 0.1% Na, 1.93% S, 0.09% Ti, 250 ppm Ba, 0.6 ppm Be, <2 ppm Bi, 99 ppm Cd, <1 ppm Co, 58 ppm Cr, 250 ppm Cu, 10 ppm Ga, 10 ppm La, 96 ppm Mn, 12 ppm Mo, 37 ppm Ni, 290 ppm P, 340 ppm Sb, 4 ppm Sc, 352 ppm Sr, <20 ppm Th, <10 ppm Tl, <10 ppm U, 45 ppm V and 50 ppm W were found in the malic acid leach residue.

4.2.3.1. NaOH and potassium sodium tartrate leach of malic acid leach residue

As specified, NaOH and KNaTartrate have significant result for recovery of lead then metal dissolutions with 3.75 M NaOH and 1.88 M potassium sodium tartrate studied at 1/10 S/L ratio and 25 ^{o}C leaching temperature. The results are given in Figure 4.88. Metal dissolution order was Pb > Fe > Zn. Metal dissoltions were rapid for the first 30 min. Then there was a maximum at 120 min. leaching time. 85.1% Pb was dissolved wiyh 28.3% Fe and 20.3% Zn co-dissolutions at 120 min. leaching time. Figure 4.89 shows the XRD spectria of NaOH and KNaTartare leach residue. According to the XRD spectria, Muscovite, Quartz and Goethite minerals observed in the secons step leaching residue and there was no lead determind in this residue.

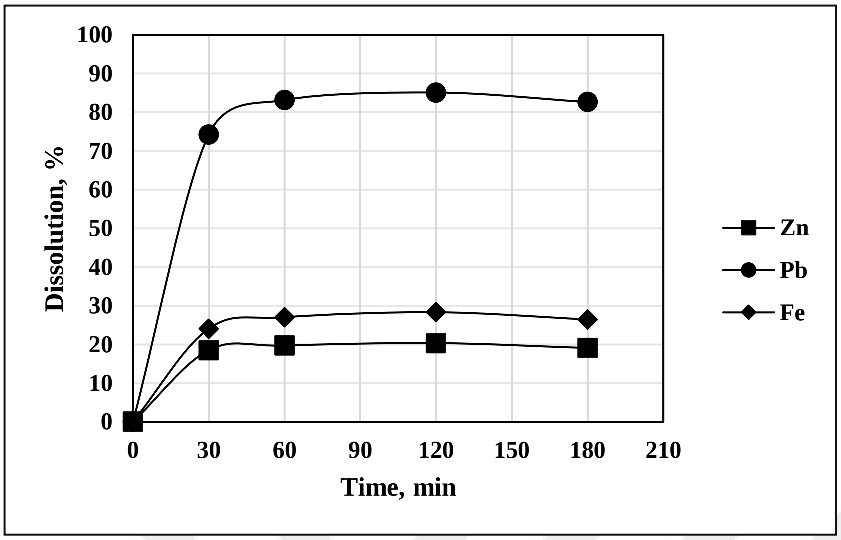

Figure 4.88. Metal dissolution with 150 g/L NaOH and 150 g/L KNaTartrate at 25 ^oC and S/L: 1/10.

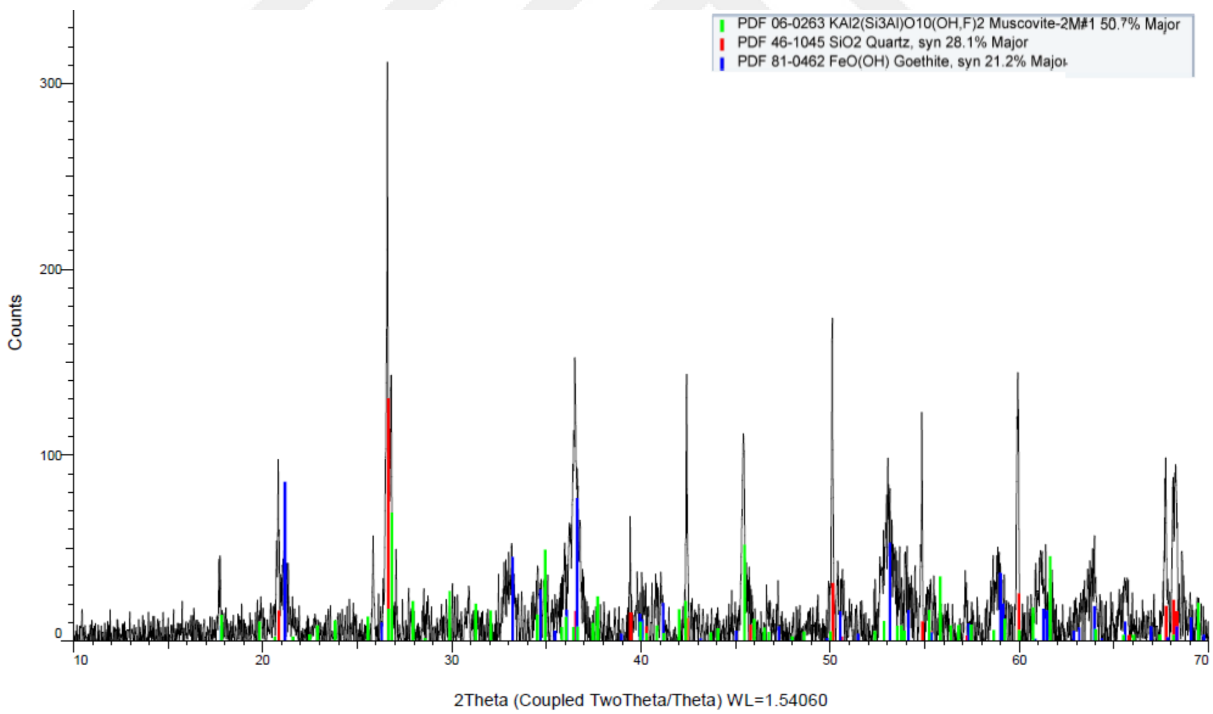

Figure 4.89. XRD spectra of NaOH and KNaTartrate leached residue from malic acid residue at the optimum conditions.

<u>4.2.3.2. Oxalic acid leach of malic acid leach residue for iron recovery</u>

Malic acid leach residue leached with 1.0 M oxalic acid at 80 ^oC leach temperature, 1/10 S/L ratio for 180 min. leaching time. Metal dissolution order was Fe > Zn > Pb. At 30 min. leaching time 64.3% Fe, 15.5% Zn and 4.5% Pb dissolved. With increasing leaching time metal dissolutions increased to 80.3% Fe, 30.4% Zn and 8.3% Pb. The results of oxalic acid leaching are given in Figure 4.90. Table 4.19 shows the concentration of the metals in oxalic acid leached solution (PLS). It could be seen that 26100 mg/L iron was transferred to the solution. 1125 mg/L lead and 451 mg/L zinc also observed in the solution.

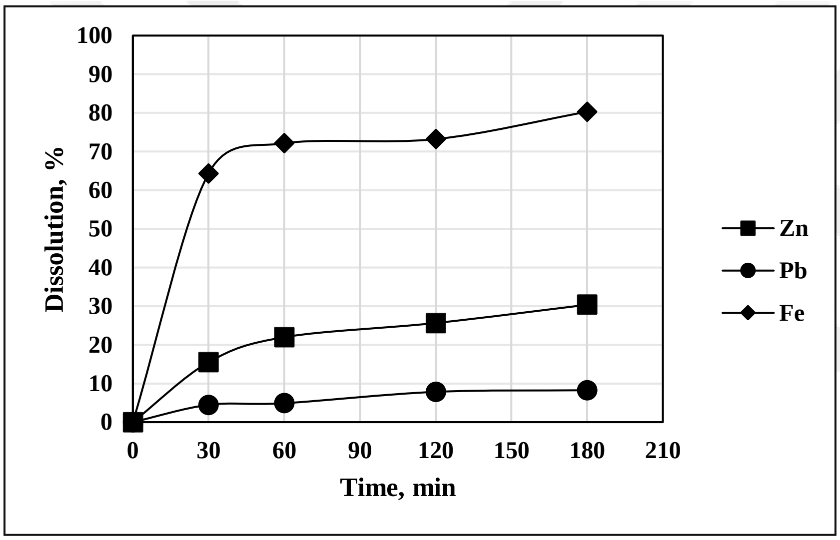

Figure 4.90. Metal dissolution with 1.0 M oxalic acid at 80 ^oC and S/L: 1/10.

Table 4.19. The concentration of the metals in oxalic acid leached solution.

Elements	mg/L	Elements	mg/L	Elements	mg/L
Ag	0.019	Cu	0.178	Pb	1125
Al	340	Fe	26100	S	1120
As	4380	K	76.6	Sb	25.6
B	0.17	Li	0.95	Se	42.5
Ba	0.341	Mg	110.5	Sn	77.5
Bi	1.0	Mn	5.92	Sr	8.07
Ca	300	Mo	0.665	Tl	0.09
Cd	9.63	Na	25.5	Zn	451
Co	0.729	Ni	1.915	Zr	0.2
Cr	1.065	P	20.7		

4.3. Third Step Leaching Study

4.3.1. Third step leaching of sulfuric acid leach residue study

The leach residue was collected for the third step leaching studies, which were done utilizing the cupric-ammonium thiosulfate system, after two-step leaching with sulfuric acid followed by sodium potassium tartrate. The feed sample (the second step leaching residue) had a mean content of 194 ppm Ag, 17950 ppm Zn,100 ppm Cr, 270 ppm Cu, 18900 ppm Pb, 10200 ppm Ba, 14900 ppm As and 29.2 % Fe, according to the chemical analysis.

4.3.1.1. The effect of the thiosulfate type on the dissolution of silver

The experiments were done with 0.5 g/L $CuSO_4$ and 20 g/L ammonium or sodium thiosulfate concentrations. These experiments were carried out at a temperature of 25 ^oC. Figures 4.91 and 4.92 show the leaching times, which range from 1 to 6 hours. Silver and copper were found in the ammonium thiosulfate leaching as amine and thiosulfate complexes. According to Eqs. 4.34 and 4.35 the cupric-tetrammine complex $[Cu(NH_3)_4]^{2+}$ serves as the main oxidant (Aylmore and Muir, 2001; Zipperian et al., 1988). Because of the dissolution of silver in thiosulfate leaching media is slowed down copper sulfate used as a catalytic system to solve this problem (Banijamali et al., 2021).

$$\mathrm{Ag} + \mathrm{S_2O_3^{2-}} + [\mathrm{Cu(NH_3)_4}]^{2+} \rightarrow [\mathrm{Ag(S_2O_3)_2}]^{3-} + 2\mathrm{NH_3} + [\mathrm{Cu(NH_3)_2}]^{+}$$

$$\Delta G^\circ = -581.2\ \mathrm{kJ/mol} \tag{4.34}$$

$$\mathrm{Ag} + 5\mathrm{S_2O_3^{2-}} + [\mathrm{Cu(NH_3)_4}]^{2+} \rightarrow [\mathrm{Ag(S_2O_3)_2}]^{3-} + 4\mathrm{NH_3} + [\mathrm{Cu(S_2O_3)_3}]^{5-}$$

$$\Delta G^\circ = -16.1\ \mathrm{kJ/mol} \tag{4.35}$$

According to Figure 4.91, when the leaching time was increased from 1 to 4 hours, the silver dissolution increased dramatically from 59.8% to 77.1 % with ammonium thiosulfate. Higher leaching times result in greater Ag dissolution, whereas lower times result in lower dissolution percentages, which can be related to the necessity for longer leaching times since the thiosulfate concentrations are insufficient. According to Bae et al., 2020, when the solid-to-liquid ratio is reduced from 0.5 to 0.2, the maximum dissolution of Ag can be obtained by increasing the leaching time up to 4 hours. Unlike ammonium thiosulfate, Ag dissolution in sodium thiosulfate solution (Figure 4.92) has remained reasonably steady at roughly 51% up to 4 h, then declined somewhat to 45.5 % when the leaching time was increased to 6 h (Bae et al., 2020). Li et al., 2018, showed the same results, they reported when the pH was high; the hydrogen ion content was insufficient to complete the complexation reaction, resulting in a decrease in the leaching rate. They achieved almost 74% silver with sodium thiosulfate in 2 h leaching time at pH 5. On the other hand, higher leaching Ag efficiency could be obtained at higher temperatures, according to Banijamali et al., 2021. They used sodium metabisulfite and sodium thousulfate togheter for improve the siddolution of silver at 25 ^{o}C. Furthermore, this is because the presence of ammonium ions in the solution likely disguised or suppressed the recovery of other metal ions in the PLS, such as copper. In terms of dissolution percentages of silver from the leach residue under the conditions investigated, ammonium thiosulfate was found to be a better leaching agent than sodium thiosulfate (Banijamali et al., 2021; Li et al., 2018).

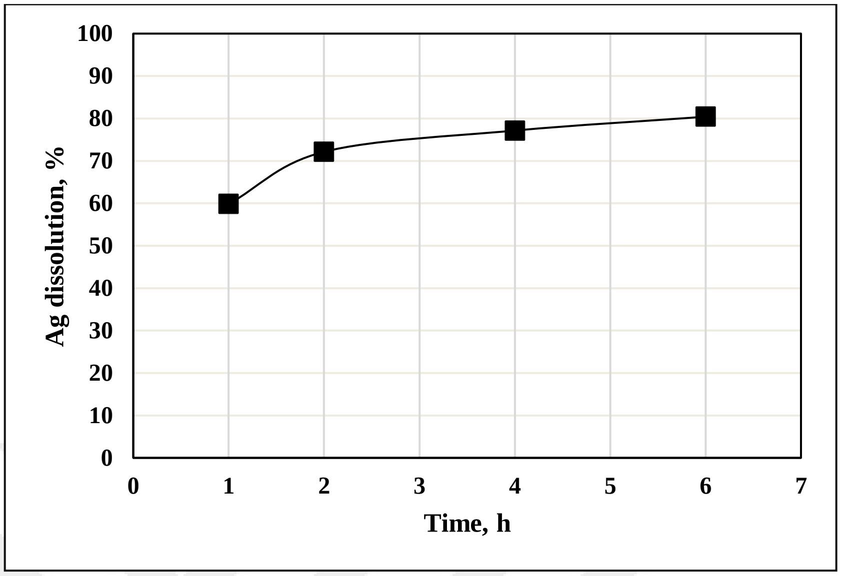

Figure 4.91. Ag dissolution with 20 g/L ammonium thiosulfate and 0.5 g/L copper sulfate at 25 °C and pH: 10.5.

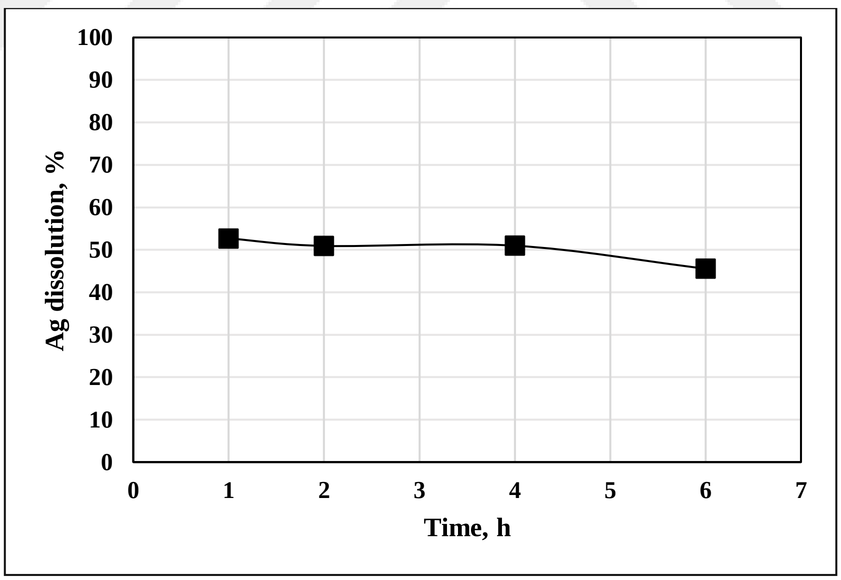

Figure 4.92. Ag dissolution with 20 g/L sodium thiosulfate and 0.5 g/L copper sulfate at 25 °C and pH: 10.5.

4.3.1.2. The effect of ammonium thiosulfate concentration and leaching time on silver dissolution

Figures 4.93-4.95 indicate the effect of ammonium thiosulfate concentration on the dissolution of Ag as a function of the time with $CuSO_4$ concentration of 0.5 g/L, S/L: 1/10 and leaching temperature of 25 °C. With increasing ammonium thiosulfate concentration, silver dissolution increases, which is similar with the findings of Bae et al., 2020. Figure 4.93 shows that when 30 g/L ammonium thiosulfate was used, Ag dissolution increased dramatically for 4 hours and then remained reasonably stable; in particular, 87.6 % Ag dissolution was seen at 30 g/L ammonium thiosulfate concentration for 4 hours. There is no favorable effect of leaching time on the dissolution of Ag in the case of 40 and 50 g/L ammonium thiosulfate concentrations, as Ag dissolution was less influenced than that of 30 g/L ammonium thiosulfate concentration over the first 1 h post-leaching of silver (Figure 4.94-4.95). According to Ficeriova et al., 2005 silver dissolution from the concentrate of complex sulphide using ammonium thiosulfate with no mechanochemical pre-treatment determined 52% with 74 g/L ammonium thiosulfate, 10 g/L copper sulfate, 1 h leaching time, pH of 5.0 and 70 ºC leaching temperature. Because of these observations, it is obvious that 30 g/L ammonium thiosulfate and a 4 hour leaching time are sufficient to dissolve over 85% Ag in this system. It was also discovered that ammonium thiosulfate produced less than 90% Ag dissolution. This is most likely due to Ag being trapped in quartz mineral phases (Bae et al., 2020; Ficeriová et al., 2005).

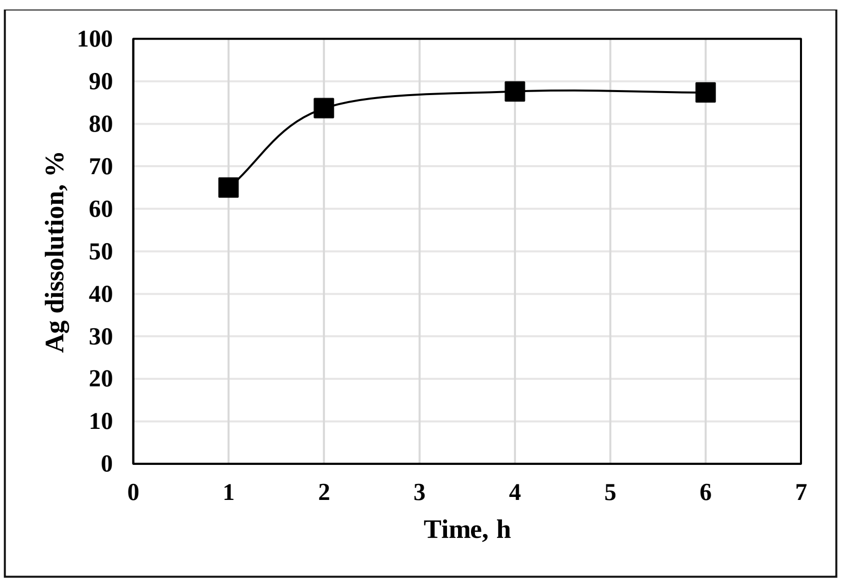

Figure 4.93. Ag dissolution with 30 g/L ammonium thiosulfate and 0.5 g/L copper sulfate, 25 °C, pH: 10.5.

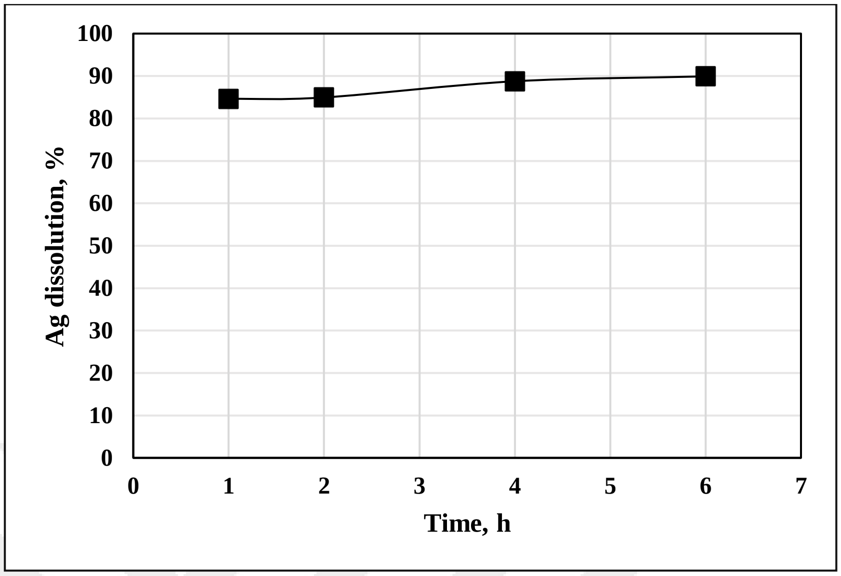

Figure 4.94. Ag dissolution with 40 g/L ammonium thiosulfate and 0.5 g/L copper sulfate, 25 °C, pH: 10.5.

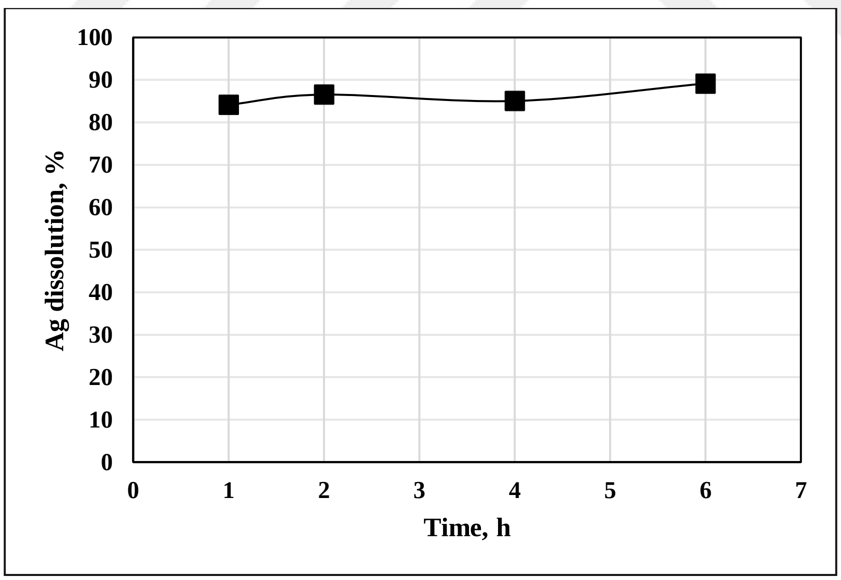

Figure 4.95. Ag dissolution with 50 g/L ammonium thiosulfate and 0.5 g/L copper sulfate, 25 °C, pH: 10.5.

4.3.1.3. The effect of copper sulfate concentration on silver dissolution

Figure 4.96 shows Ag dissolution as copper sulfate concentration varies. The experiments were carried out for 4 hours at a temperature of 25 °C with a solid-to-liquid ratio of 1/10 and a concentration of 30 g/L ammonium thiosulfate. According to Figure 4.96 up to 0.5 g/L $CuSO_4$ concentration, Ag dissolution increased slightly from 82.5 % to 87.6 %, and thereafter gradually increased. According to Bae et al., 2020, the dissolution of silver from concentrated sulphide ore increased as copper sulfate concentration increased. The 90.6% Ag dissolution was accomplished at a copper sulfate concentration of 1 g/L. The silver dissolution was determined to be 87.8% at 0.75 g/L copper sulfate concentration. The silver dissolution was found to be less impacted by changes in copper sulfate than the concentration of ammonium thiosulfate. As a result, in this investigation, the 0.5 g/L $CuSO_4$ concentration was shown to be appropriate for third step leaching for silver dissolution.

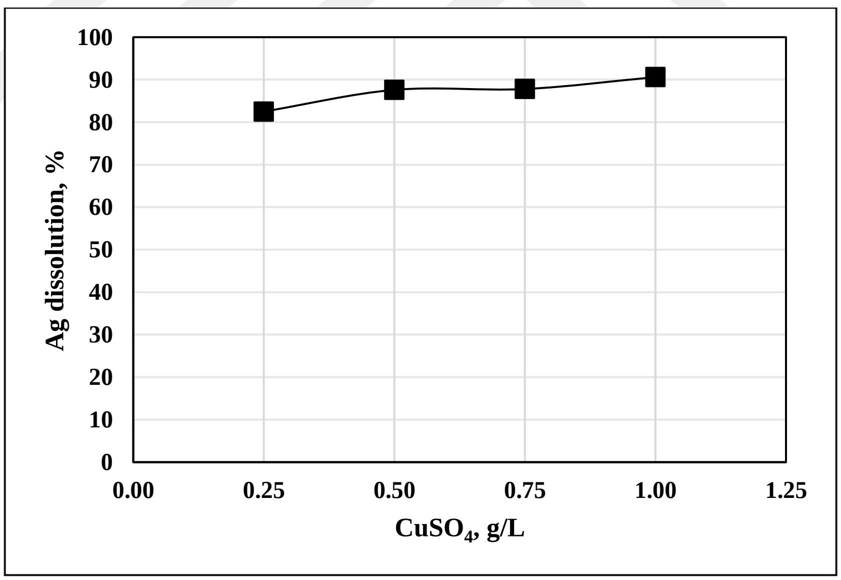

Figure 4.96. Ag dissolution with 30 g/L ammonium thiosulfate in different $CuSO_4$ concentrations at 25 °C, pH: 10.5, 4 h.

4.3.1.4. The effect of leaching temperature on the dissolution of silver

Figure 4.97 shows the effect of temperature on the dissolution of silver by ammonium thiosulfate solutions. The temperature of the leaching solution was varied from 25 to 60 °C with

30 g/L ammonium thiosulfate and 0.5 g/L copper sulfate a S/L: 1/10 for 4 hours and a pH of 10.5. As seen in Figure 4.97, the dissolution of silver grew gradually up to 40 °C of reaction temperature before stabilizing at a generally constant level. At 25 °C for 4 hours, 87.6% Ag dissolution was obtained, according to the current findings. In contrast to our findings, Li et al., 2018 discovered that when the sodium thiosulfate concentration was 75 g/L, the pH was 5.0, and the leaching time was 2 h, the recovery of silver decreased as the leaching temperature was increased from 25 to 60 ºC. The temperature of the third step leaching was set at 25 °C based on the findings of the experiments (Li et al., 2018).

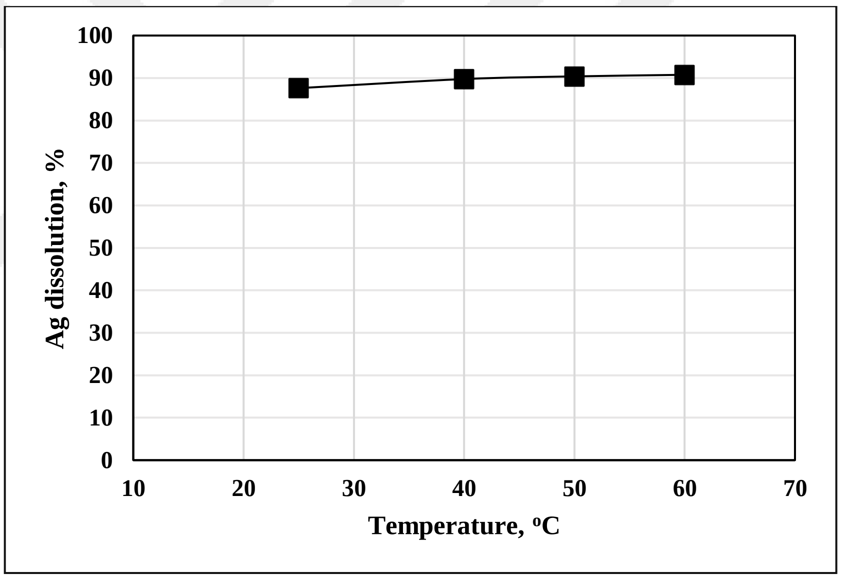

Figure 4.97. Ag dissolution with 30 g/L ammonium thiosulfate and 0.5 g/L $CuSO_4$ in pH: 10.5, 4 h leaching time.

4.3.2. Third step leaching of citric acid leach residue studies

After two-step leaching with citric acid followed by sodium potassium tartrate, the leach residue was collected for third-step leaching investigations using the cupric-ammonium thiosulfate system. The feed sample (the second step leaching residue) had a mean content of 267 ppm Ag, 17250 ppm Zn,100 ppm Cr, 400 ppm Cu, 25400 ppm Pb, 9950 ppm Ba, 13350 ppm As and 26.1 % Fe, according to the chemical analysis. In the third stage of Ag leaching, the citric acid leach residue was leached at different times at pH 9.5, 10.5 and 11.5 with a concentration of 20 g/L ammonium thiosulfate and 0.5 g/L copper sulfate. Figure 4.98 illustrates Ag dissolution of citric acid waste at a concentration of 20 g/L ammonium thiosulfate as a function of pH and leaching time at a concentration of 20 g/L ammonium thiosulfate. The dissolution of silver ranged from 84% to 92%. After 4 hours of leaching at pH 9.5, a maximum of 92 % Ag dissolution was achieved. As a result, silver dissolution decreased as the pH increased, and as the leaching time increased until 4 h, silver dissolution increased, but then observed slightly decreasing.

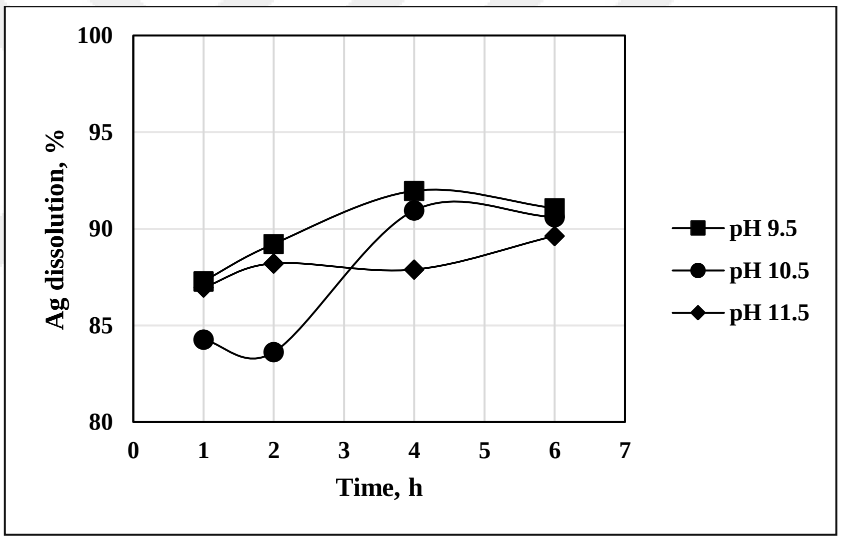

Figure 4.98. Ag dissolution with 20 g/L ammonium thiosulfate and 0.5 g/L $CuSO_4$ at different pH and leaching time.

4.3.3. Third step leaching of malic acid leach residue studies

The leach residue was collected for third-step leaching research utilizing the cupric-ammonium thiosulfate system after two-step leaching with malic acid and sodium potassium tartrate. According to chemical analysis, the feed sample (second step leaching residue) contained 176 ppm Ag, 20600 ppm Zn, 80 ppm Cr, 320 ppm Cu, 23800 ppm Pb, 10760 ppm Ba, 16100 ppm As, and 29.7 % Fe. In the third stage of Ag leaching, malic acid leaching residue was leached at different times at pH 9.5, 10.5 and 11.5 with a concentration of 20 g/L ammonium thiosulfate and 0.5 g/L copper sulfate. At a concentration of 20 g/L ammonium thiosulfate, Figure 4.99 illustrates the pH and leaching time dependent Ag dissolution of malic acid residue. Ag dissolution ranged from 84.2% to 93.2%. After 6 hours of leaching at pH 9.5, a maximum of 93.2% Ag dissolution was achieved. As a result, silver dissolution increases when the leaching time increases, but Ag dissolution decreases as the pH increase.

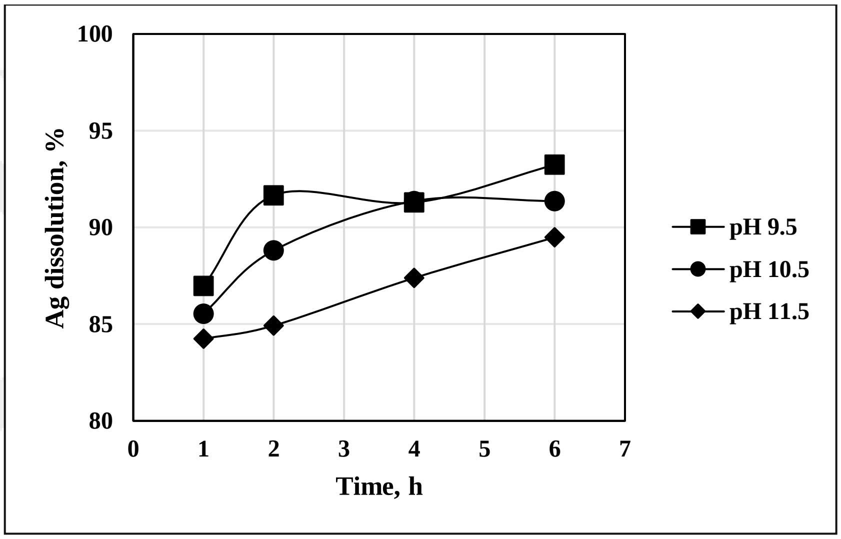

Figure 4.99. Ag dissolution with 20 g/L ammonium thiosulfate and 0.5 g/L $CuSO_4$ at different pH and leaching time.

4.4. Purification of Leach Solutions Study

The leach solution purification is very critical in the conventional hydrometallurgical route for the production of Zn metal. Various purification methods are used in practice to achieve high quality neutral electrolyte with minimum levels of impurities. There two steps for the purification of impurities in leach solution, precipitation and cementation.

4.4.1. Precipitation of impurities from leach solution

4.4.1.1. Precipitation of impurities from sulfuric acid leach solution

As we know, most impurities in our leach solution are Fe and As. the hydrolytic precipitation of Fe and As from pregnant leach solution (PLS) of H_2SO_4 leaching was carried out. According to chemical analysis feed grade were 2.98 g/L Fe, 1.85 g/L As, 11.65 g/L Zn, 0.206 g/L Al and 0.0462 g/L Cd.

- **The effect of pH and oxidant on precipitation of impurities**

The experiments were done using alkaline 5.0 M NaOH with and without H_2O_2 as oxidant as a precipitant between pH values 2.5 and 3.5 at 50 ^oC for 60 min. The effect of pH on the Fe, As, Cd, Al impurities along with Zn using NaOH is shown in Figure 4.100. As the pH increases precipitation of all five metal increases. However, As and Fe precipitation are much higher than Al, Zn and Cd. At pH 2.5, 69% Fe and 91% As and at pH 3.5, 93% Fe and 99% As precipitated. Metal precipitation order was As > Fe > Al > Zn> Cd. Zn and Cd precipitation were less than 10%. With NaOH, the best As and Fe precipitation pH was 3.5. Figure 4.101 shows the effect of 2.0 ml/L H_2O_2 addition to NaOH. Addition of small amount H_2O_2 significantly increased both As and Fe precipitation at pH 2.5 and 3.0. Rudnik, 2019 used 2.0 ml/L H_2O_2 as an oxidant in a precipitation test and found that it had a significant effect. At pH 3.5 both As and Fe precipitation were more than 99% at less than 10% Zn, Al and Cd precipitation. Tsakiridis et al.(2010) were determined 5% zinc losses in precipitation test at pH 3.5. Precipitation increase for Fe is faster than As in the investigated pH range. Presence of H_2O_2 both increased Fe removal and decreased Al removal. In addition, Antunano et al.(2013) discovered that pH 4 is the best pH for removing impurities from zinc leach solution. It's worth noting that Fe(II) ions can be oxidized with MnO_2 alone (Krupka et al., 2000) or in a mixture with H_2O_2 (Antuñano et al., 2013), air, or oxygen gas (Svens, 2010), or H_2O_2 (Herrero et al., 2010; Rudnik, 2019b) as is done in industry. The other hand ferric ion precipitates easily in the pH range 4.0 – 5.0, the ferrous ion remains stable. It is, therefore, important to oxidize the ferrous ion to ferric ion (Eq 4.36). Hydrogen peroxide is a very efficient oxidizer although the introduction of H_2O_2 decreases the pH owing to the production of hydrogen ion as the result of the oxidized product as given Eq 4.36-4.40 (Antuñano et al., 2013; Güler and Seyrankaya, 2016; Mbedzi et al., 2017; Rudnik, 2019a, 2019b; Tsakiridis et al., 2010).

$$2Fe^{+2} + H_2O_2 + 2H^+ \rightarrow 2Fe^{+3} + H_2O \qquad (4.36)$$

$$\text{Goethite: } 2Fe^{2+} + 1/2O_2 + 3H_2O \rightarrow 2FeOOH + 4H^+ \qquad (4.37)$$

$$\text{Jarosite: } 12Fe^{2+} + 8SO^{-}_4 + 3O_2 + 4XOH + 14H_2O \rightarrow 4XFe_3(SO_4)_2(OH)_6 + 8H^+ \text{ (X: Na, K, etc.)} \qquad (4.38)$$

$$\text{Hematite: } 2Fe^{2+} + 1/2O_2 + 2H_2O \rightarrow Fe_2O_3 + 4H^+ \qquad (4.39)$$

$$\text{Ferrihydrite: } 4Fe^{2+} + 3O_2 + 22H_2O \rightarrow 2Fe_2O_5{:}9H_2O + 8H^+ \qquad (4.40)$$

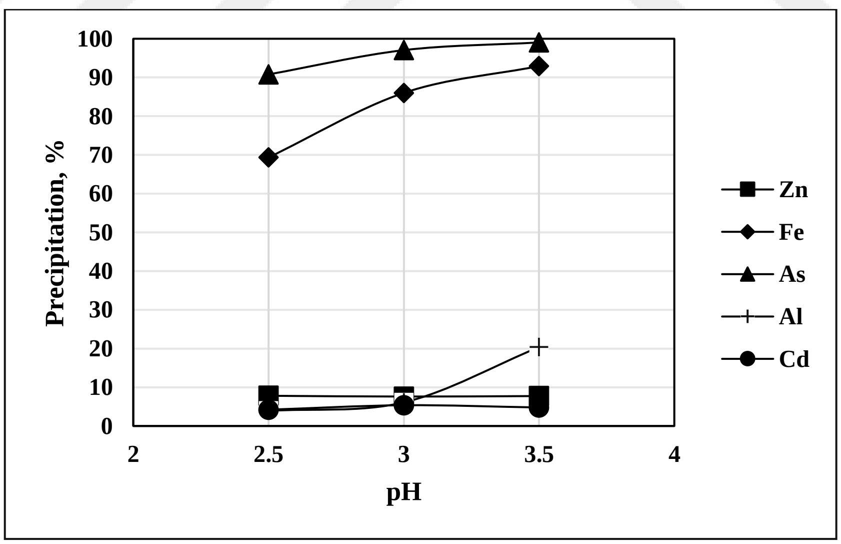

Figure 4.100. The effect of pH on the precipitation of impurities with 5.0 M NaOH at 50 °C and 60 min.

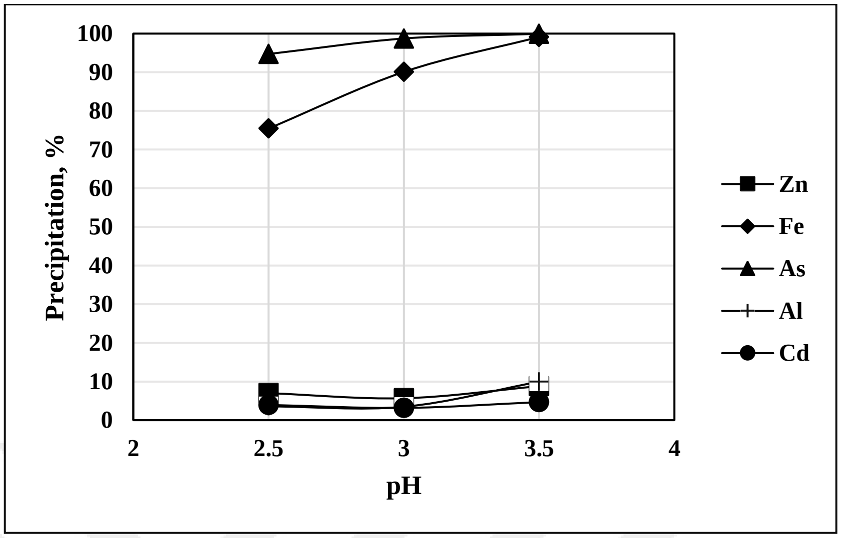

Figure 4.101. The effect of pH on the precipitation of impurities using 5.0 M NaOH 0.2 ml H_2O_2 at 50 ^oC and 60 min.

- **The effect of $NH_4(OH)$ on precipitation of impurities**

Instead of NaOH, $NH_4(OH)$ with 0.2 mL H_2O_2 was also tested for As and Fe precipitation (Figure 4.102). At pH 2.5, 92.1% As and 67.1% Fe; at pH 3.0 96.6% As and 82.1% Fe; and at pH 3.5 99.9% As and 98.9% Fe precipitation were achieved. Both NaOH + H_2O_2 and $NH_4(OH)$ + H_2O_2 gave similar results for As and Fe precipitation. pH 3.5 achieved almost full As and Fe precipitations with NaOH or $NH_4(OH)$ in the presence of H_2O_2.

These tests showed that the best pH for Fe and As precipitation is 3.5. This pH value is compatible with previous literature studies. Tsakiridis et al., (2010) also precipitated 99.9% Fe as aggregates of Jarosite crystallites at pH 3.5.

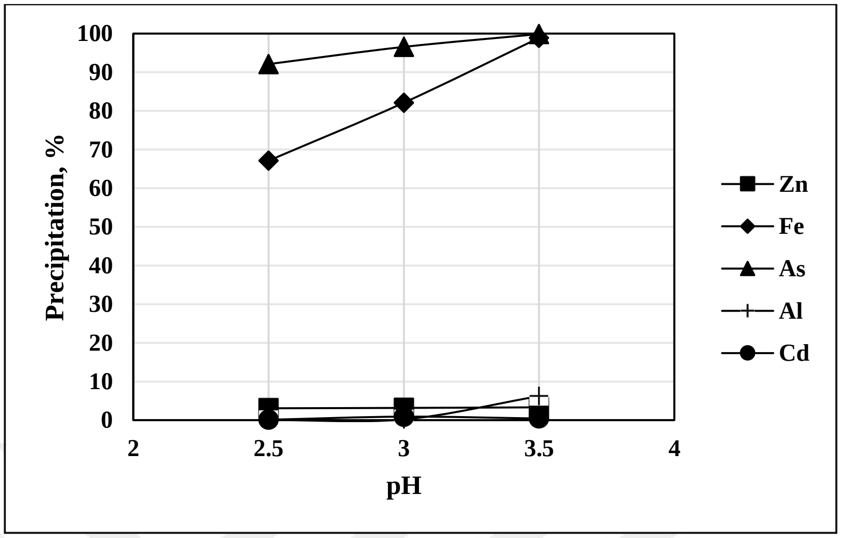

Figure 4.102. The effect of pH on precipitation of impurities using $NH_4(OH)$ and 0.2 ml H_2O_2 at 50 ^oC and 60 min.

❖ **The effect of temperature on the precipitation with NaOH and H_2O_2**

In the first stage purification, more than 99% Fe and As were removed in pH 3.5, 50 ^oC and 60 min. these conditions. Then, the effect of the precipitation temperature was studied at 25 ^oC and 75 ^oC temperatures between pH 2.5 and 3.5 for 60 minutes. According to the results, increasing the temperature has a significant effect on the precipitation of Fe and As, Other hand precipitation of Al starting at pH 3.0 and reaching over 60% at pH 3.5. The optimum conditions for precipitation was chosen as 50 ^oC temperature and pH 3.5. Figures 4.103 and 4.104 show the precipitation of impurities with NaOH and H_2O_2 at 25 and 75 ^oC.

Figure 4.105 shows the XRD spectra of precipitation residue from the optimum conditions. According to the XRD spectra Goethite (FeO(OH)) was formed in the precipitation experiment at the optimum pH. Guler and Seyrankaya (2016) observed goethite in the XRD results at higher ph (4.0-4.5) and they found jarosite peak in lower pH (3.0-3.5). It could be because the precipitation test was conducted at 90˚C. Tsakiridis et al.(2010) observed the same results. They carried out the precipitation tests in 95 ^oC and found jarosite in the XRD results. Rudnik (2019a) reported jarosite (90–100 °C, pH 1.5–1.8), goethite (80–90 °C, pH 2–3), and hematite (over 185 °C, in oxidizing atmosphere) are formed by precipitation processes. According to Babacan(1971), stability of hematite, goethite, ferric hydroxide and hydroxyl salts (e.g. jarosite) depending on temperature and pH is given in Figure 4.106. (Güler and Seyrankaya, 2016; Rudnik, 2019a; Tsakiridis et al., 2010; Babacan 1971).

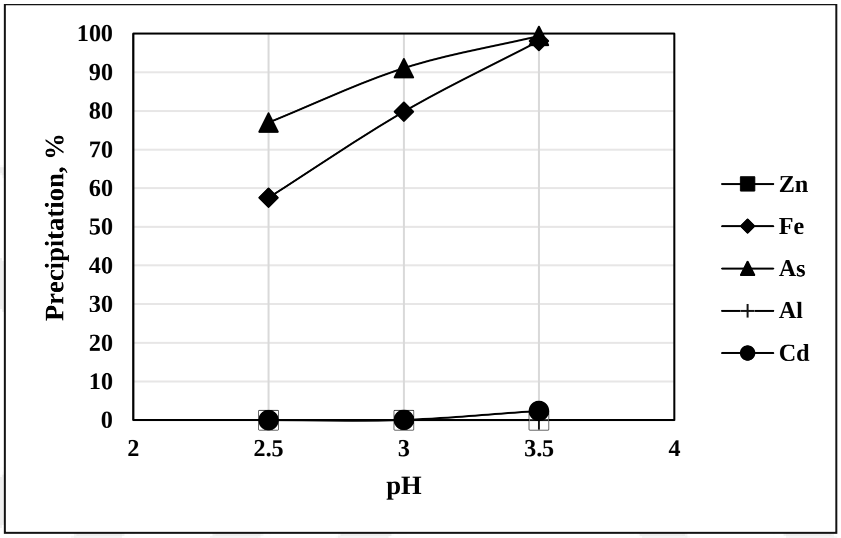

Figure 4.103. The precipitation of impurities with NaOH and H_2O_2 at pH 3.5, 25 ºC and 60 min.

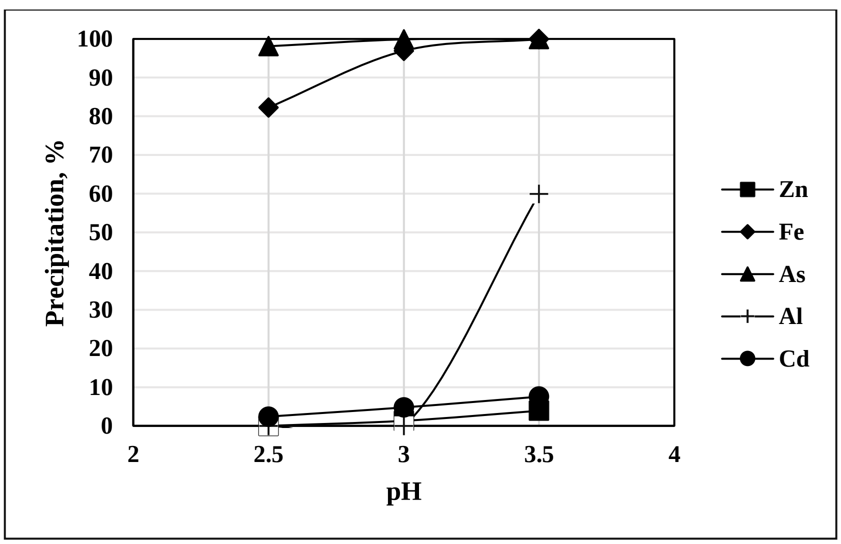

Figure 4.104. The precipitation of impurities with NaOH and H_2O_2 at pH 3.5, 75 ºC and 60 min.

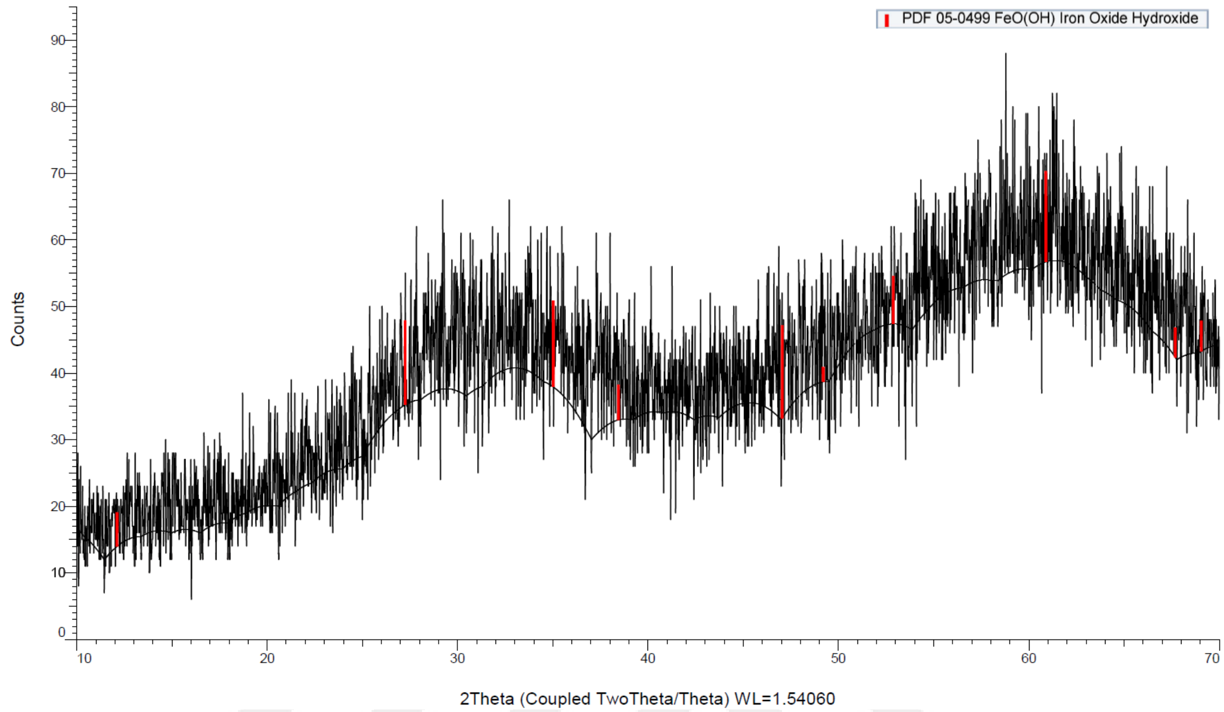

Figure 4.105. The XRD spectra of precipitation residue at pH 3.5, 50 ^{o}C and 60 min.

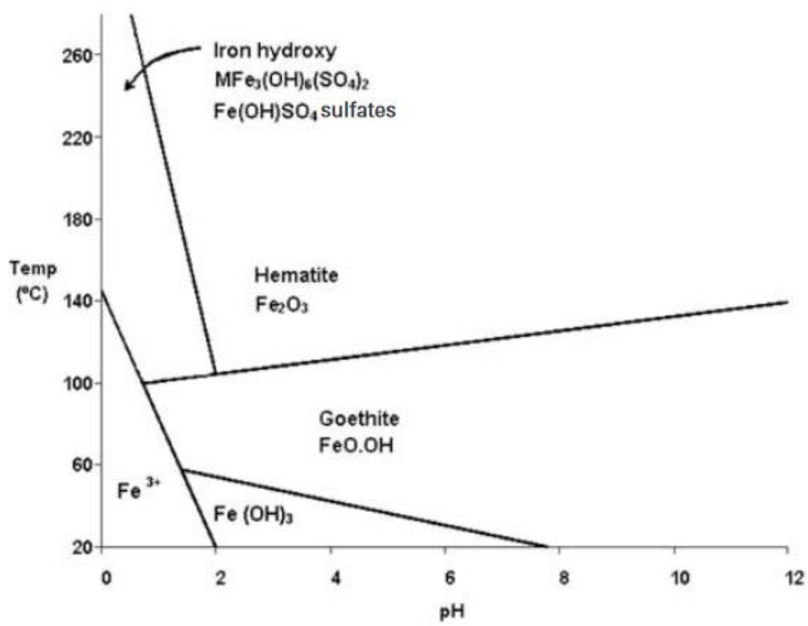

Figure 4.106. Solubility of goethite, hematite, ferric hydroxide and hydroxyl salt (e.g. jarosite) depending on temperature and pH (Babacan, 1971).

4.4.2. Cementation of impurities from leach solution

2 g/L Zn dust was used to precipitate other impurity metals from Fe and As removed Zn-rich PLS solution at 200 rpm mixing speed and 50^{o}C precipitation temperature and 60 min. precipitation time. D_{80} of Zn dust was 35 microns. pH of the medium was adjusted with NaOH addition. The main goal of the cementation process is to remove metallic impurities with substantially larger reduction potentials than zinc, such as lead, copper, or cadmium which in Cu, Cd, Sn, Mn and Al metals are in our solution (Herrero et al., 2010). Second stage purification feed contains 9160 mg/L Zn, 101.5-152 mg/L Al, 33.3-35.2 mg/L Mn, 32.9-37.4 mg/L Cd, 8.82 mg/L Cu and 0.4 mg/L Sn.

4.4.2.1. The effect of pH on the cementation of remaining impurities with zinc dust

Figure 4.107 shows the precipitation of remaining metals from the first step precipitation tests without Zn dust at 50 ^{o}C and 200 rpm mixing speed for 1 h from pH 4.0 to 5.0. In absence of Zn dust, high pH significantly increased precipitation of Al and Cu. Al precipitation increased from 45% at pH: 4.0 to 96% at pH: 5.0 and Cu precipitation from 0% at pH: 4.0 to 53% at pH: 5.0. Sn removal was constant around 17% between pH 4.0 and 5.0. Mn and Zn removal were almost zero percent. In the second step precipitation, the best pH was 5.0 for removing 96% Al and 53% Cu. Figure 4.108 shows the cementation of remaining metals from the first stage precipitation tests using Zn dust at 50 ^{o}C and 200 rpm mixing speed for 1 h from pH 4.0 to 5.0. As results Zn dust and high pH significantly precipitated Cu and Cd and increasing rate Al. More than 99% Cu and 96% Cd precipitated at pH 4.0 Increase of pH to 5.0, slightly improved both Cu and Cd precipitation. However, increasing pH from 4.0 to 5.0 increased Al precipitation from 30% to 97%. Zinc dust cemented the impurities found in the filtrate after iron and arsenic removal (Eqs 4.41-4.43).

$$Zn + Cd^{2+} \rightarrow Zn^{2+} + Cd \quad (4.41)$$

$$Zn + Cu^{2+} \rightarrow Zn^{2+} + Cu \quad (4.42)$$

$$Zn + Sn^{2+} \rightarrow Zn^{2+} + Sn \quad (4.43)$$

According to Song et al., 2019 copper's activity was lower than that of cadmium. The copper ions in the solution were first cemented by zinc dust, which then interacted with the cadmium ions. Other hand they observed heating at low temperatures accelerated the process, but at 50 °C, the effect of temperature was no longer significant. They removed 99% copper and cadmium in pH 5.0 and 30 min. These findings are consistent with the results we have obtained.(Song et al., 2019). After the cementation test 9070 g/L, 0.015 mg/L Cu, 0.3 mg/L Sn, 1.84 mg/L Al, 0.15 mg/L Cd and 36.4 mg/L Mn remained in the solution. According to Yaghoubi 2021 The presence of (1–3) g/L manganese decreases the rate of lead anode corrosion and the contamination of zinc products with lead. This is based on the depolarizing impact of the MnO_2 layer on the anode. Herrero et al., 2010 determined almost 130 mg/L of the main impurities remained in their solution. The results we obtained have less impurities compared to their findings (Herrero et al., 2010; Yaghoubi, 2021).

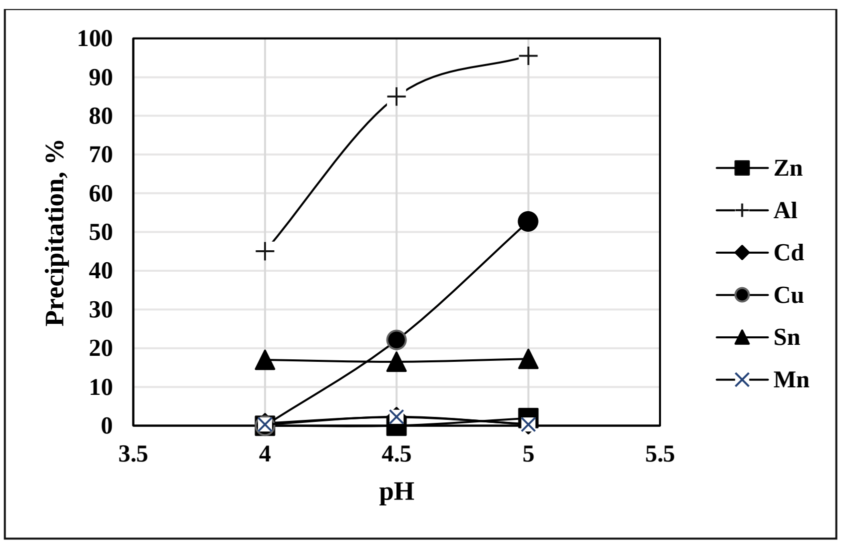

Figure 4.107. The second step of precipitation with NaOH at 50 ^{o}C and 60 min.

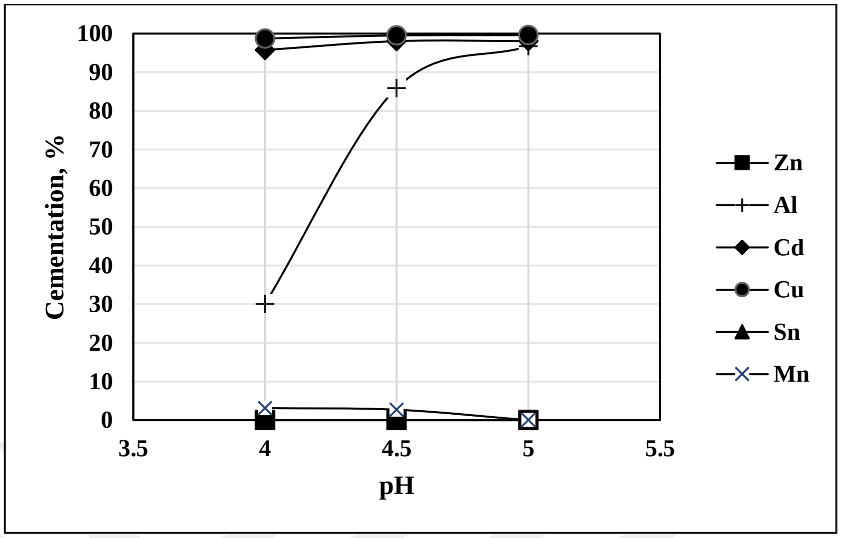

Figure 4.108. The cementation of impurities with 2 g/L Zn dust at 50 ^{o}C and 60 min.

4.4.3. Precipitation of PbS from the second step NaOH+KNaTartarte leach solutions with Na_2S

Studies were conducted on precipitation of Pb from the second stage NaOH+KNa-Tartrate leach PLS as PbS with Na_2S.

<u>4.4.3.1. Precipitation of PbS from sulfuric acid leach solution</u>

First stage sulfuric acid leach residue was second stage leached with NaOH+KNa-tartrate and the lead was precipitated with 0.5 M and 1.0 M Na_2S at 50 ^{o}C for 10, 30 and 60 min. The feed material in this stage contains 8270 mg/L Pb, 248 mg/L Zn and 5630 mg/L Fe. Figures 4.109-4.112 show the effect of Na_2S addition from 5 to 40 ml, molarity of Na_2S and time on Pb, Zn and Fe precipitation. The starting pH for 0.5 M and 1.0 M Na_2S precipitation was around 12.82 and 12.49 for 30 min. and 12.78 and 13.32 for 60 min. respectively. Final precipitation pH changed between 11.2 and 12.5. With increasing both leaching time and Na_2S addition amount, the amount of precipitated PbS increases. At the beginning of precipitation, pH was between 12.5 and 13.3 and at the end of precipitation, pH decreased between 11.2 and 12.5. Figure 4.113 shows Zn, Pb and Fe precipitation at 1.0 M Na_2S for 10 min. precipitation time at

50 ^oC. Staring pH changed between 11.8 and 12.0 and final pH changed from 11.9 and 12.5. using 10 ml Na_2S for 100 mL PLS decreased 8.27 g/L Pb concentration and 0.25 g/L Zn concentration to zero in 10 min. at 30.7% Fe co-precipitation. There is not much effect of precipitation time on Pb, Zn and Fe precipitation. After 10 mL of Na_2S, addition almost full Pb/Zn precipitation was achieved. Therefore, 10 min. precipitation is enough.

Precipitation order with Na_2S is Pb > Zn > Fe. According to Zhang et al.(2014), the solubility products of PbS and ZnS are KspPbS=9.3×10^{-28} and K_{sp}ZnS = 8.9×10^{-22}, respectively. When sulfur ions are injected to a solution containing lead ions and zinc ions, it is known that lead sulfide will precipitate before zinc sulfide as Eqs. 4.44 and 4.45 show (Zhang et al., 2014):

$$Pb^{2+} + S^{2-} \rightarrow PbS \downarrow \tag{4.44}$$

$$Zn^{2+} + S^{2-} \rightarrow ZnS \downarrow \tag{4.45}$$

Full Pb and Zn precipitations with 0.5 M Na_2S is possible by adding 20 mL Na_2S for 60 min. precipitation time and with 1.0 M Na_2S is possible by adding 10 mL Na_2S. It seems there is no effect of precipitation time. Fe precipitation also increases with increasing Na_2S volume. Maximum 67% Fe precipitation with 0.5 M Na_2S concentration and 89.5% Fe precipitation with 1.0 M Na_2S concentration were obtained. At 0.5 M Na_2S concentration, 20 mL Na_2S addition precipitated 99.7% Pb, 100% Zn and 44.4% Fe for 30 min. At 1.0 M Na_2S concentration, 10 mL Na_2S addition achieved 99.7% Pb, 100% Zn and 38% Fe precipitation. These dosages were assumed optimum for PbS precipitation. Liu et al. (2019), Zhao and Stanforth (2000) and Erdem and Yurten, (2015), obtained the similar result, they precipitated more than 99% lead with 0.5 M Na_2S. Although Zhang et al.(2014) removed 95% lead from solution with 0.5M Na_2S. The amount ratio of Na_2S to Pb ions was determined with a value of 2.9. Our result is slightly different from other researches. For example, Zhao and Stanforth(2000), Erdem, and Yurten (2015) obtained weight ratio of Na_2S to Pb 1.8 and 1.5

respectively. Although Zhang et al. (2014) found this number 4.36. It could be owing to a high lead concentration in our solution (Erdem and Yurten, 2015; Liu et al., 2019; Zhang et al., 2014; Zhao and Stanforth, 2000).

Figure 4.114 shows the effect of temperature on Zn, Pb and Fe precipitation with 1.0M Na_2S for 30 min. precipitation time at 25 ^oC. After 10 mL Na_2S addition, almost full Pb/Zn precipitation was obtained for both precipitation times. Fe precipitation was higher at 50 ^oC than 25 ^oC. Thus, 25 ^oC was chosen the best precipitation temperature. Figure 4.115 shows XRD patterns of 0.5 M Na_2S, 20 mL addition for 30 min. Figure 4.116 shows XRD patterns of 1.0M Na_2S, 10 mL addition for 30 min. All precipitates were PbS for both cases.

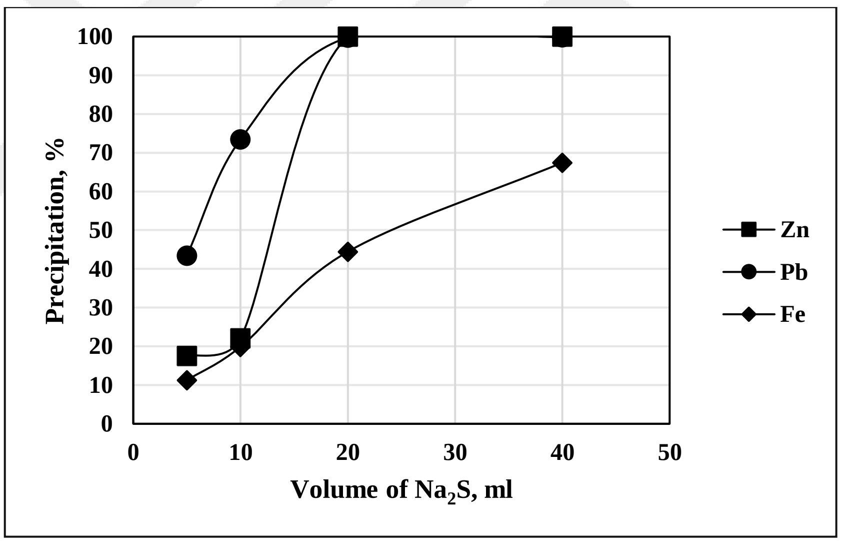

Figure 4.109. The effect of Na_2S volume on precipitation at 50 ^oC, 0.5 M Na_2S and 30 min.

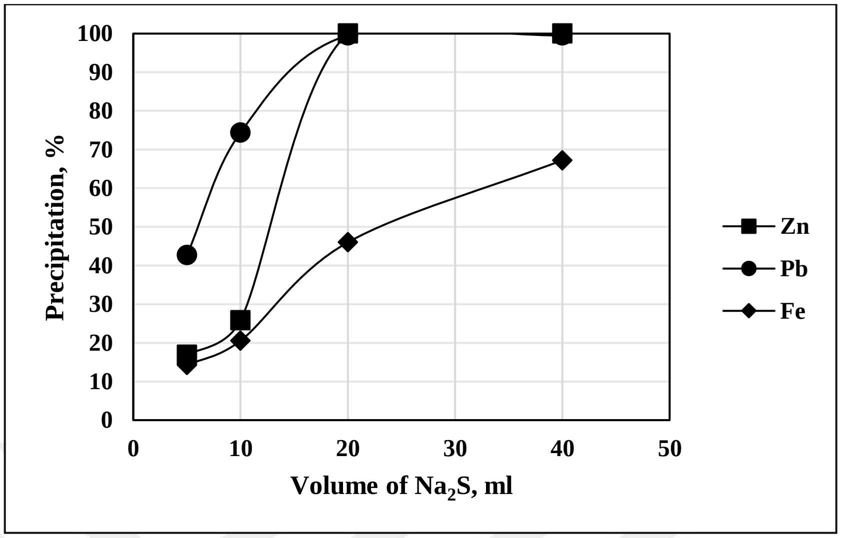

Figure 4.110. The effect of Na_2S volume on precipitation at 50 ^oC, 0.5 M Na_2S and 60 min.

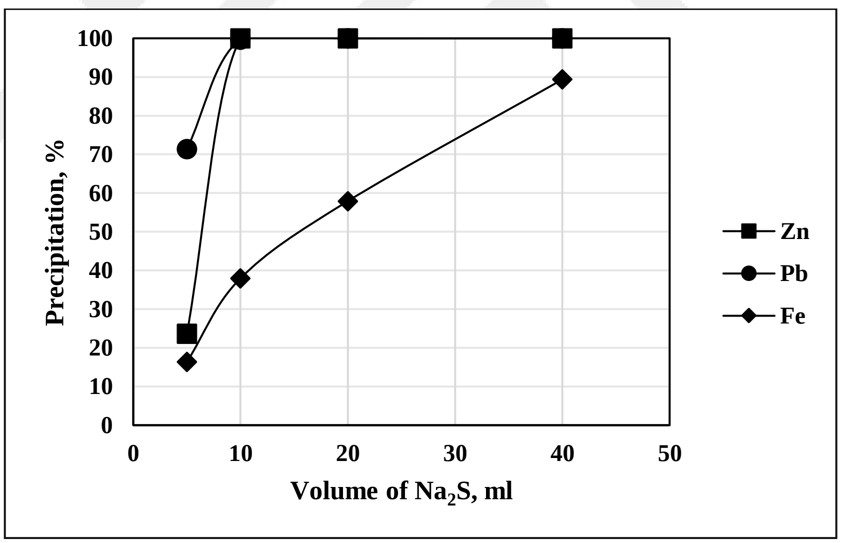

Figure 4.111. The effect of Na_2S volume on precipitation at 50 ^oC, 1.0 M Na_2S and 30 min.

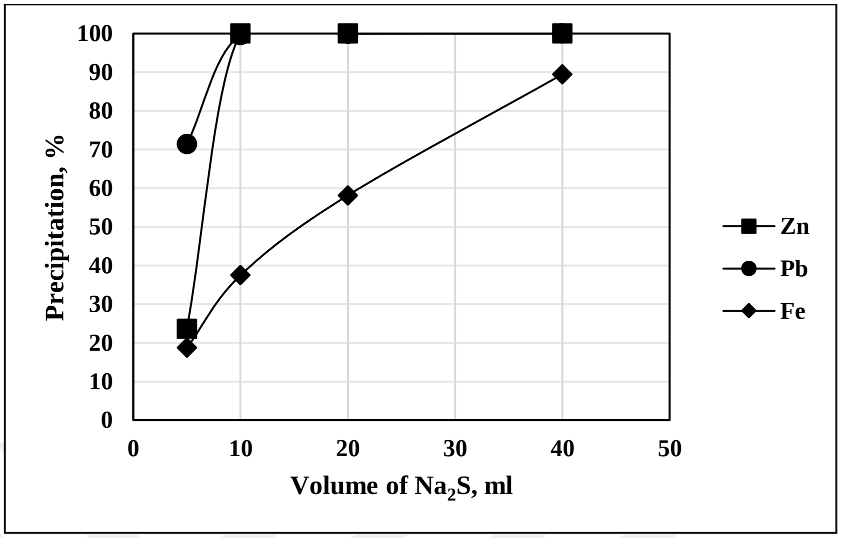

Figure 4.112. The effect of Na_2S volume on precipitation at 50 ^oC, 1.0 M Na_2S and 60 min.

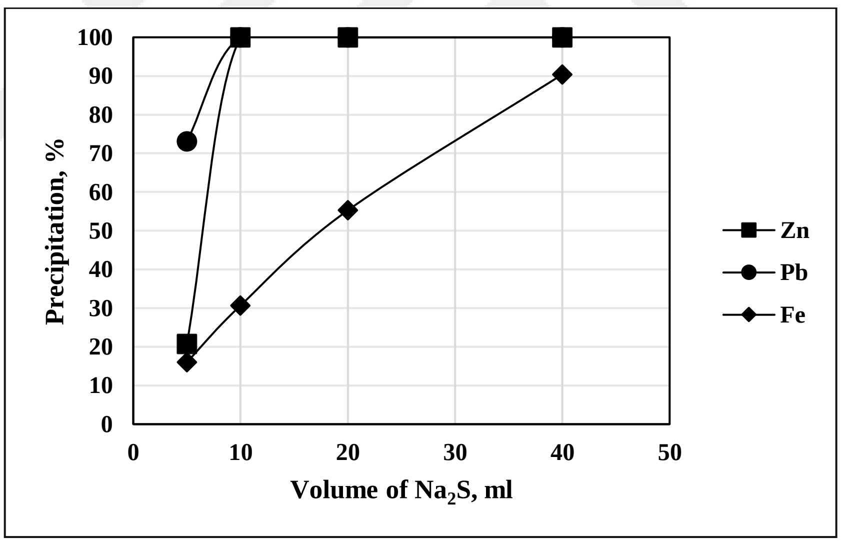

Figure 4.113. The effect of Na_2S volume on precipitation at 50 ^oC, 1.0 M Na_2S and 10 min.

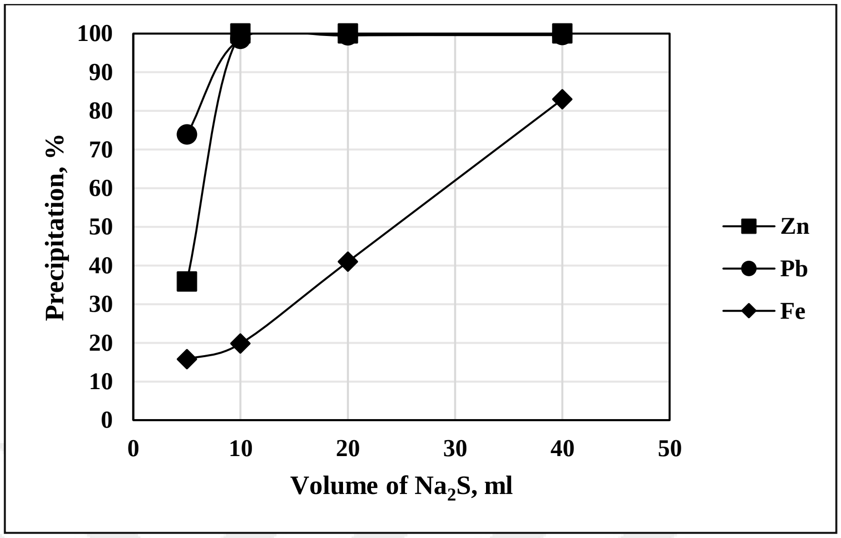

Figure 4.114. The effect of Na_2S volume on precipitation at 25 ^oC, 1.0 M Na_2S and 30 min.

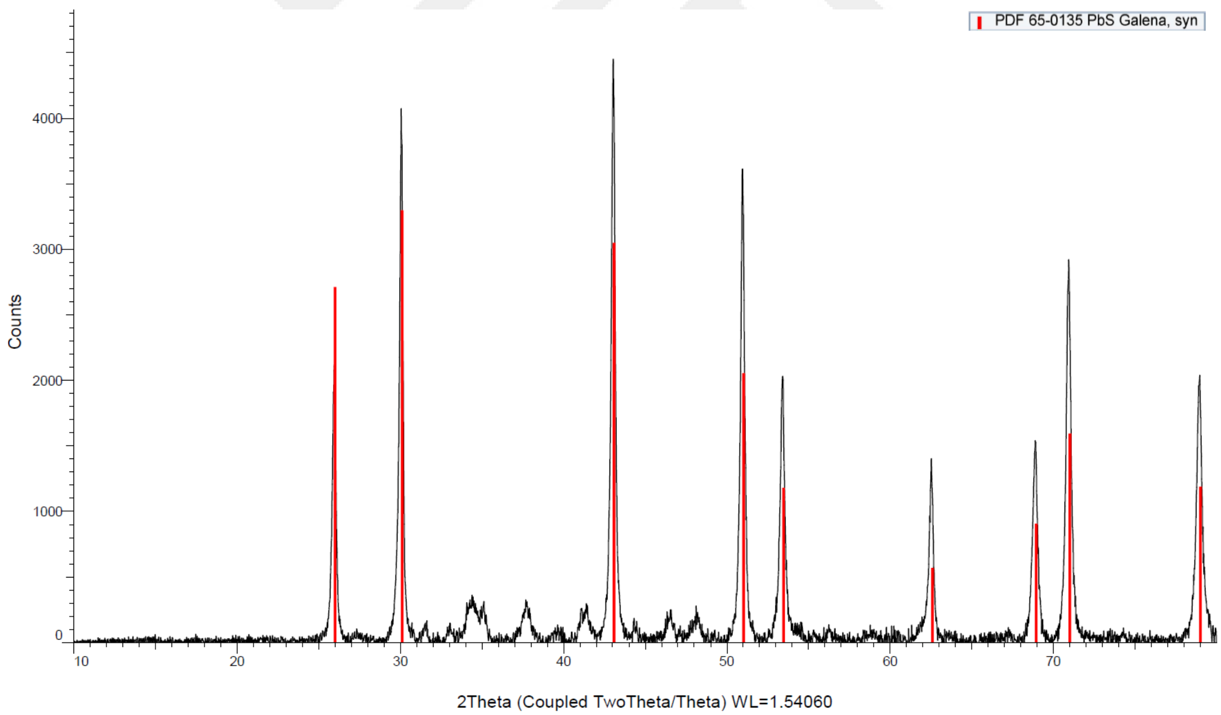

Figure 4.115. XRD pattern of PbS precipitated with 0.5 M Na_2S, 20 mL dosage for 30 min.

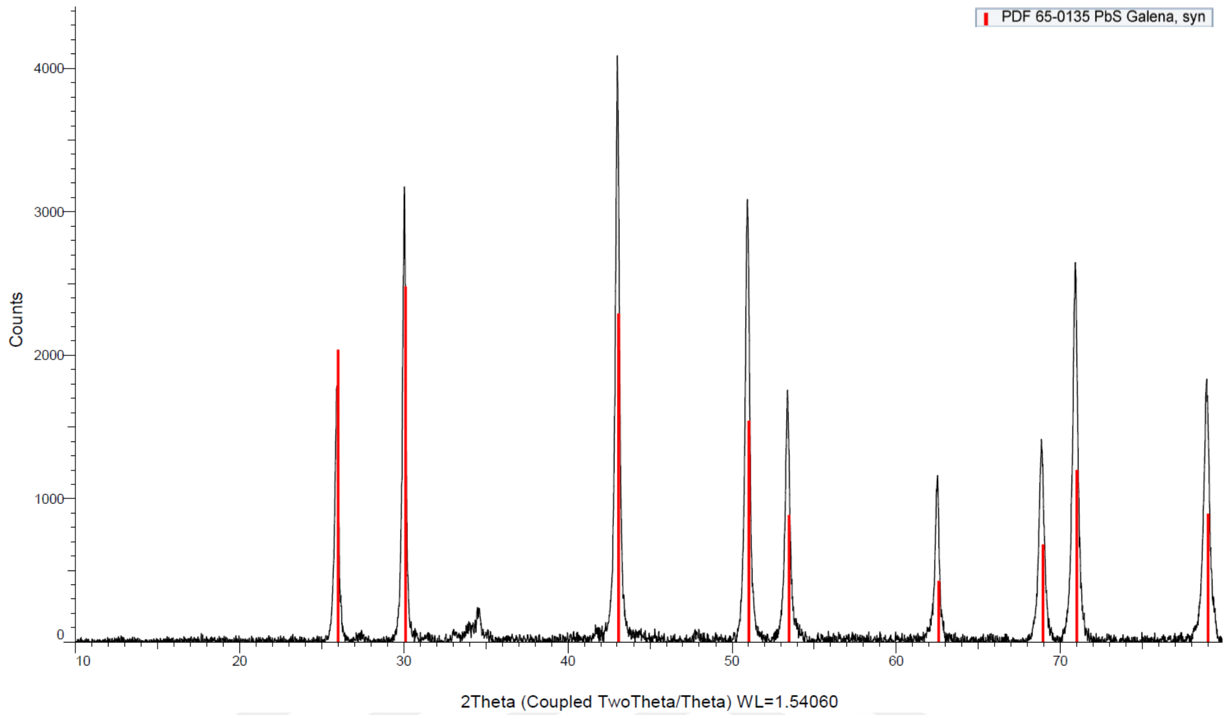

Figure 4.116. XRD pattern of PbS precipitated with 1.0 M Na_2S, 10 mL dosage for 30 min.

4.4.3.2. Precipitation of PbS from citric acid leach solution

Citric acid leach residue was leached with NaOH+NaK-Tartrate and then the leach PLS was precipitated 0.5 and 1.0M Na_2S at 50 °C for 10 and 30 min. 0.1 mL PLS precipitated with 5 to 40 mL Na_2S solutions under 200 rpm mixing conditions. The feed material in this stage contains 8420 mg/L Pb, 457 mg/L Zn and 6570 mg/L Fe. For 0.5 M Na_2S addition, precipitation staring pH was between 11.31 and 11.4 and the final pH was between 11.63 and 11.97. With increasing the addition amount of Na_2S increased the PbS precipitation. Na_2S precipitation also slightly increased the medium pH at the end of 30 min. precipitation time. 100% Pb and Zn precipitation, and 28% Fe precipitation were achieved with 20 mL 0.5M Na_2S addition in 30 min. 100% Pb and Zn precipitation, and 27% Fe precipitation were also achieved with 10 mL 1.0M Na_2S addition in 30 min. Increase in Na_2S addition amount increases Fe co-precipitation. Figure 4.117 and 4.118 show the precipitation of PbS in 0.5 M and 1.0M at 50 °C for 30 min.

The effect of precipitation time was investigated using 1.0 M Na_2S concentration at 50 ^oC for 10 min. precipitation time (Figure 4.119). PbS precipitation increased with increasing Na_2S addition. 99.1% Pb precipitation and full Zn precipitation was achieved at 28.1% Fe co-precipitation at 10 mL Na_2S addition. Full Pb and Zn precipitations were achieved at 27.1% Fe co-precipitation at 10 mL Na_2S addition. Increase in Na_2S addition amount significantly increase Fe co-precipitation up to 80%. For citric acid PLS 10 min, precipitation time again was better than 30 min.

The effect of precipitation temperature was investigated using 1.0M Na_2S concentration for 30 min. precipitation time. At 25 ^oC precipitation temperature, PbS precipitation increased with increasing Na_2S addition. 99% Pb precipitation and full Zn precipitation was achieved at 29.4% Fe co-precipitation at 10 mL Na_2S addition. Increase in Na_2S addition amount significantly increases Fe co-precipitation up to 79.5%. In comparison to the 50 °C precipitation test, the 25 °C precipitation temperature performed better (Figure 4.120).

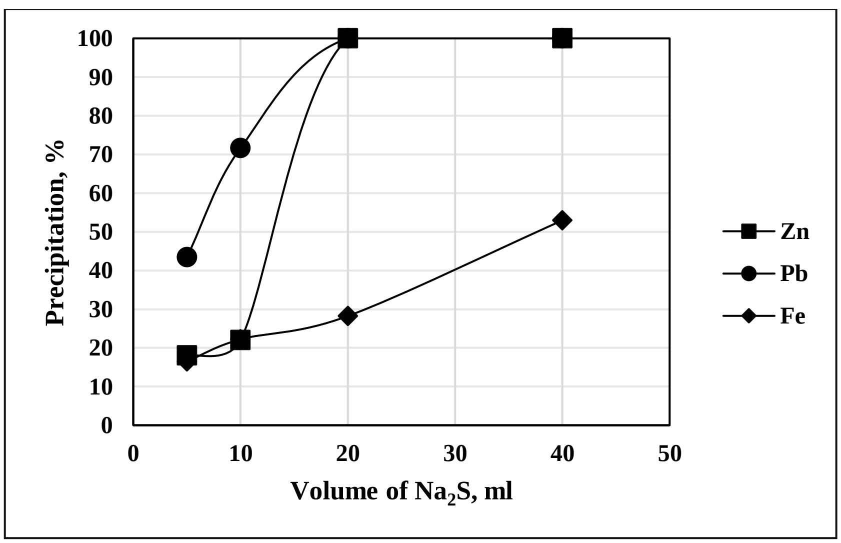

Figure 4.117. The effect of Na_2S volume on precipitation at 50 ^oC, 0.5 M Na_2S and 30 min.

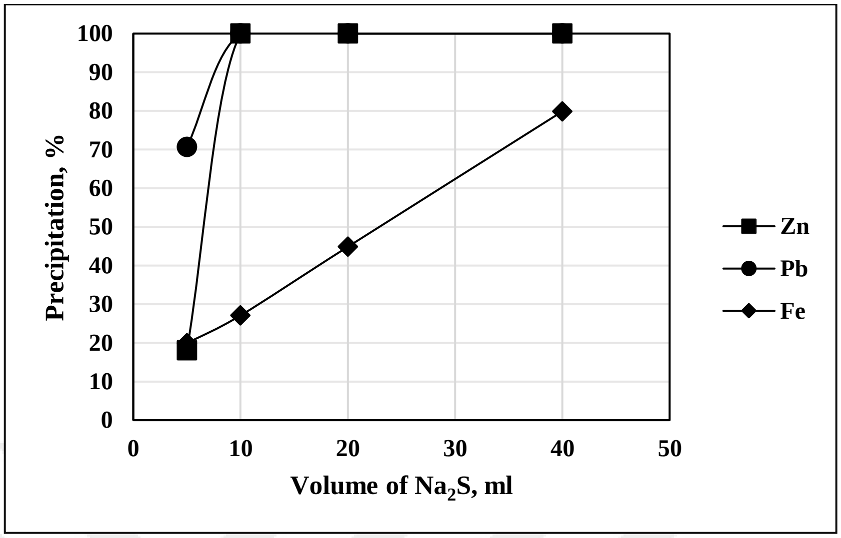

Figure 4.118. The effect of Na_2S volume on precipitation at 50 ^oC, 1.0 M Na_2S and 30 min.

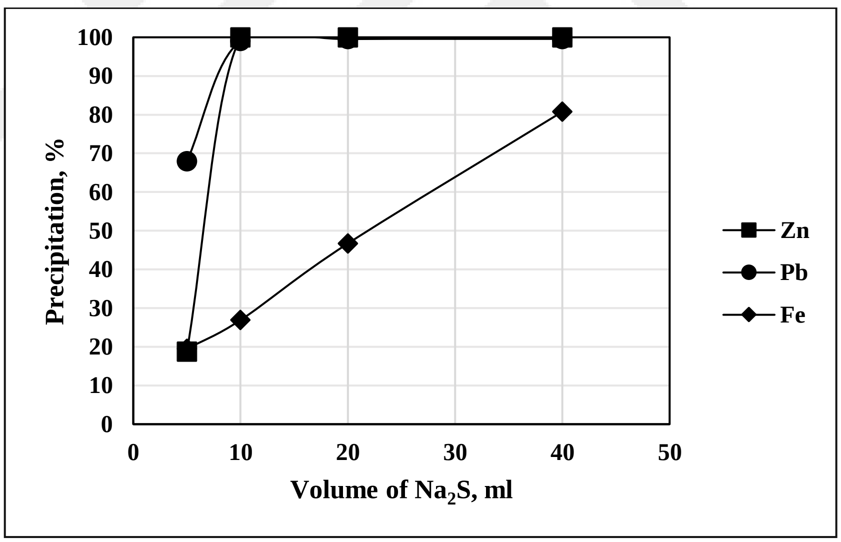

Figure 4.119. The effect of Na_2S volume on precipitation at 50 ^oC, 1.0 M Na_2S and 10 min.

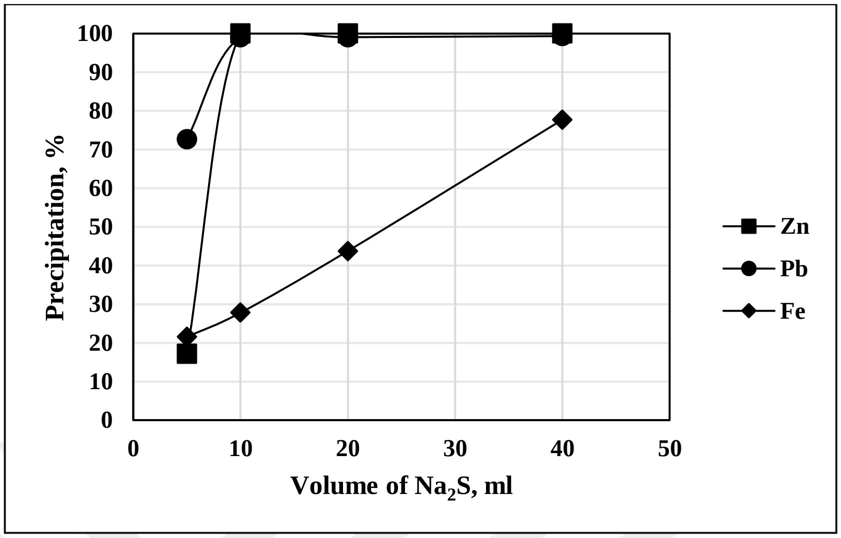

Figure 4.120. The effect of Na_2S volume on precipitation at 25 ^oC, 1.0 M Na_2S and 30 min.

4.4.3.3. Precipitation of PbS from malic acid leach solution

Malic acid leach residue was leached with NaOH+NaK-Tartrate and then the leach PLS was precipitated 0.5 and 1.0 M Na_2S at 25 and 50 ^oC for 10 and 30 min. The feed material in this stage contains 8100 mg/L Pb, 466 mg/L Zn and 6480 mg/L Fe Figures 4.121 and 4.122 show the effect of Na_2S addition on precipitation at 0.5M and 1.0 M Na_2S respectively, 30 min precipitation time and 50 ^oC. 100 mL PLS precipitated with 5 to 40 mL Na_2S solutions at 25 and 50 ^oC under 200 rpm mixing conditions. 99.5% Pb and full Zn precipitation, and 32.7% Fe co-precipitation were achieved with 20 mL 0.5M Na_2S addition in 30 min. 99.6% Pb and full Zn precipitation, and 28.1% Fe precipitation were also achieved with 10 mL 1.0M Na_2S addition in 30 min. Increase in Na_2S addition amount increases Fe co-precipitation up to 81%. Figure4.193 shows the effect of 1.0M Na_2S addition volume at 50 ^oC for 10 min precipitation time. With the increase in Na_2S addition amount, Pb, Zn and Fe precipitation increased. About 10 mL Na_2S addition was achieved almost full Pb and Zn precipitation around 20% Fe co-precipitation. At 50 ^oC using 10 mL 1.0M Na_2S concentration, 100% Zn, 99.1% Pb and 28.1% Fe were co-precipitated in 10 min. Full Pb and Zn, and 27.1% Fe were co-precipitated in 30 min. As results, 10 min. precipitation time is also selected for malic acid leach solution.

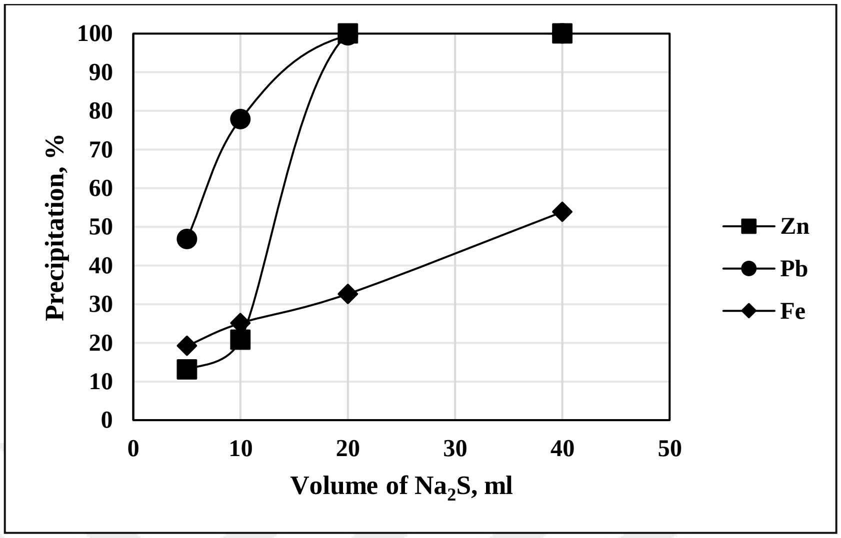

Figure 4.121. The effect of Na_2S volume on precipitation at 50 ^oC, 0.5 M Na_2S and 30 min.

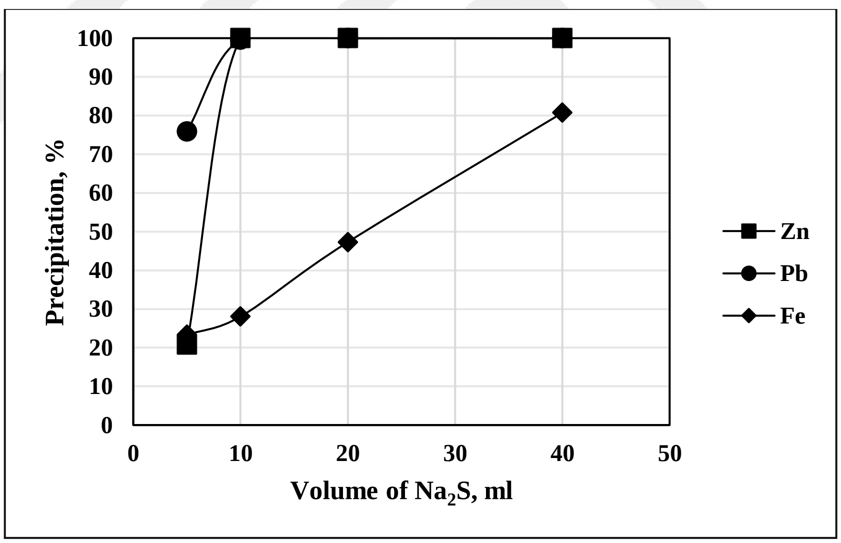

Figure 4.122. The effect of Na_2S volume on precipitation at 50 ^oC, 1.0 M Na_2S and 30 min.

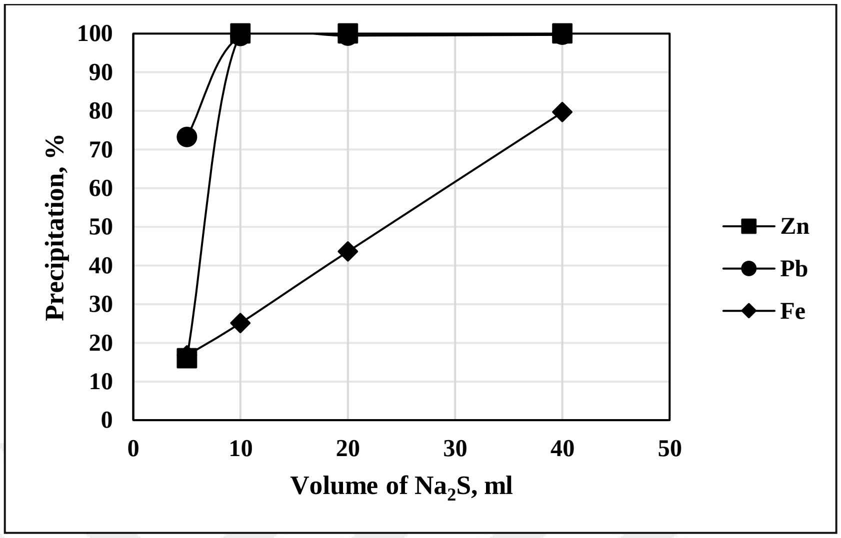

Figure 4.123. The effect of Na_2S volume on precipitation at 50 ^oC, 1.0 M Na_2S and 10 min.

4.5. Solvent extraction study

4.5.1. Solvent extraction of sulfuric acid leach solution

Two series of experiments were carried out in the extraction of zinc with D2EHPA.

4.5.1.1. First series of the solvent extraction experiments

- **Metal extraction with D2EHPA**

The first series experiments were done for determining the optimum pH of the zinc extradition. SX was applied to the first stage H_2SO_4 PLS after hydrolytic precipitation of Fe and As with NaOH and H_2O_2 (pH: 3.5, 50 ^oC, 60 min., and 200 rpm). Figure 4.124 shows the effect of pH on zinc extraction with 20% D2EHPA, 40 ^oC, 10 min and A/O: 1/1(25 mL/25mL). With increasing extraction pH from 1.15 to 3.58, Zn extraction increased from 27.8% to 100%. For 25 mL PLS SX, 9037 mg/L Zn concentration decreased to 232 mg/L at pH 2.6 with 97.1% extraction efficiency. At pH of 3.5, full Zn extraction efficiencies were obtained for 25 SX solutions. Considering the cost of NaOH, pH 2.6 was assumed the best extraction pH for H_2SO_4

PLS. Zn concentration decreased from 9038 to 232 mg/L in the aqueous phase at pH 2.19. The same results were observed by some researchers (Hollagh et al., 2010; Long et al., 2010; Pereira et al., 2007; Vahidi et al., 2009). They discovered that 20% D2EHPA is sufficient for zinc extraction of more than 99%.

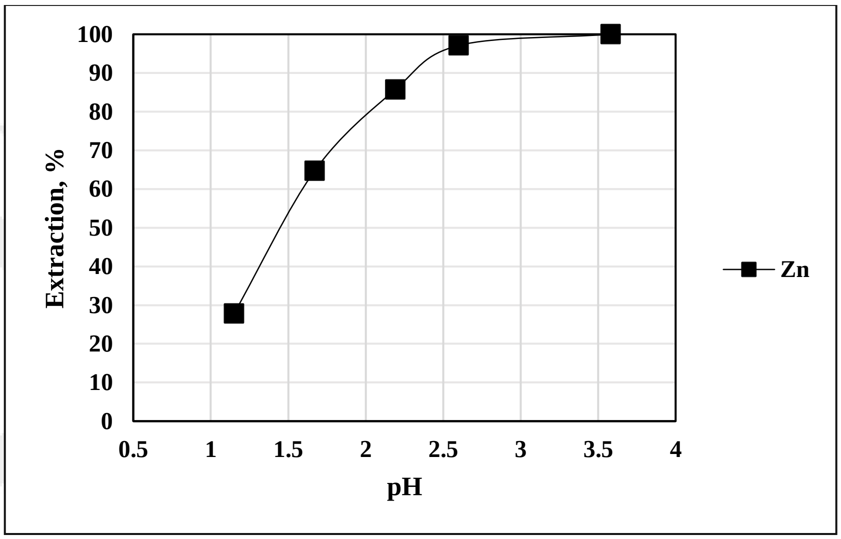

Figure 4.124. Effect of pH on Zn extraction using 20% D2EHPA at 40^oC temperature, 10 min.

❖ **Metal extraction with Cyanex 272**

Solvent extraction test was carried out with 20% Cyanex 272 at 40^oC, 10 min and A/O: 1/1 (25 mL/25mL) (Figure 4.125). Zn extraction to the organic phase was 11.9% at pH of 0.95 and increased up to 97.7% at pH of 3.7. 180 mg/L Zn concentration in the aqueous phase was remained at pH of 3.7. Zn extraction significantly increased especially after pH of 2.0. According to Figure 4.126 after pH of 3.53 a third phase formation was observed. Using modifier could have a significant effect in these experiments. Tsakiridis et al. (2010) and Tanong et al. (2017) with Cyanex 272 and TBP as a modifier extracted more than 99% zinc from the aqueous phase. D2EHPA was chosen as optimum extractant in this series of experiments(Tanong et al. 2017; Tsakiridis et al. 2010)).

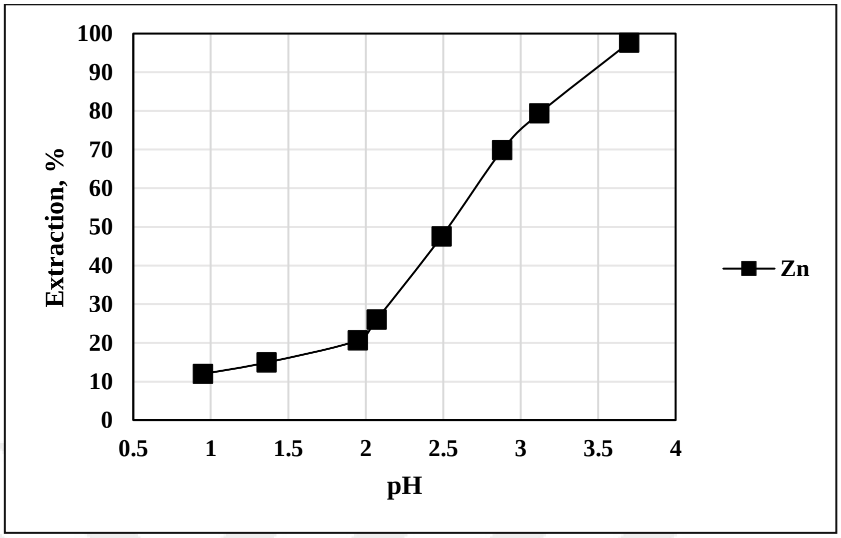

Figure 4.125. Effect of pH on Zn extraction using 20% Cyanex 272 at 40 ^{o}C temperature, 10 min.

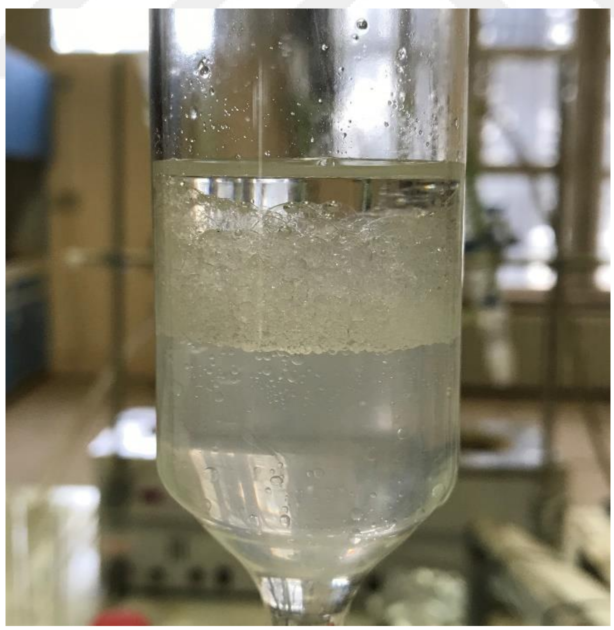

Figure 4.126. Third phase formation during zinc extraction with 20% Cyanex 272 at pH of 3.53

❖ **Stripping step of the loaded organic solution**

Stripping efficiency of Zn from organic phase to aqueous phase was performed using H_2SO_4 at 40 ºC for 10 min and A/O: 1. Figure 4.127 shows zinc stripped from organic phase in different pH. At optimum SX pH of 2.6, Zn concentration was 8773.12 mg/L. The effect of pH on Zn stripping efficiency was determined at five different pH values from 0.25 to 1.25. As the pH of the stripping decreases, the Zn stripping efficiency increases. At pH: 1.25, the stripping efficiency was about 17% and at pH 0.25 the Zn stripping efficiency was full.

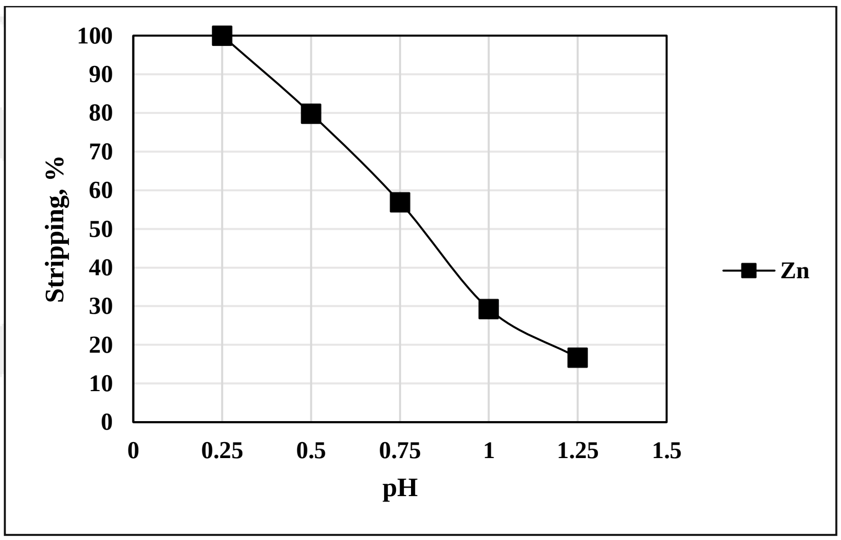

Figure 4.127. Effect of pH on zinc stripping from loaded organic.

<u>4.5.1.2. Second series of the solvent extraction experiments</u>

- **Metal extraction with D2EHPA**

In this series, the solvent extraction experiment was carried out with 20% D2EHPA at pH 3.5 because that was the optimum pH in the precipitation test. The experiments was done at 25 ºC, 10 min and A/O: 1. 99.8% zinc was loaded to organic phase. Zinc concentration decrease from 8936 mg/l to 13.3 mg/L in aqueous phase.

❖ **Stripping step of the loaded organic solution**

According to first series of the stripping experiments, pH 0.25 was chosen as an optimum pH for stripping experiments. As results 96.1% zinc stripped from loaded organic at 25 ^{o}C, 10 min and A/O: 2. 349 mg/L zinc stayed in the organic phase.

4.5.2. Solvent extraction of malic acid leach solution

Before the solvent extraction tests, the precipitation of lead were performed with 5.0 M sulfuric acid solution at a stirring speed of 200 rpm because lead was on of principle impurities in the malic acid leach solution.

4.5.2.1. Removal of lead from malic acid leach solution

Figure 4.128 illustrates metal ion precipitation as a function of pH. Lead precipitated when sulfuric acid was added, while the other metal ions remained entirely stable in the aqueous phase. At pH 0.25, the maximum lead precipitation (99.6%) was obtained within the tested experimental range. This pH level was confirmed to be ideal. Due to the low solubility of $PbSO_4$ in aqueous solutions, it was possible to separate lead from zinc by selective precipitation with sulphuric acid. The reaction product, $PbSO_4$ (anglesite), was verified by XRD characterization of the precipitate displayed in Figure 4.129. As a result, the overall precipitation process is (Halli et al., 2020; Hussaini et al., 2021b):

$$Pb^{2+}(aq) + H_2SO_4(aq) \rightarrow PbSO_4(s) + 2H^+ (aq) \qquad (4.46)$$

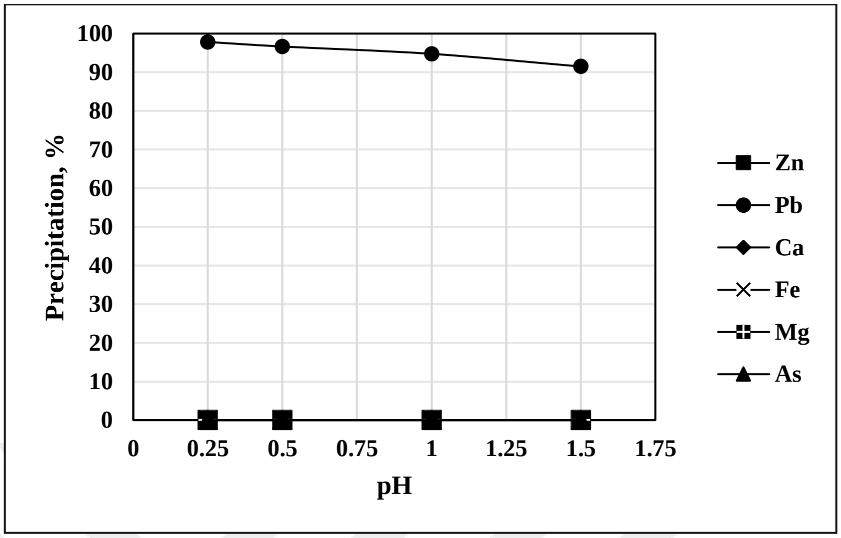

Figure 4.128. Metal precipitation with 5.0 M H_2SO_4 at different pH, 25 ºC and 30 min.

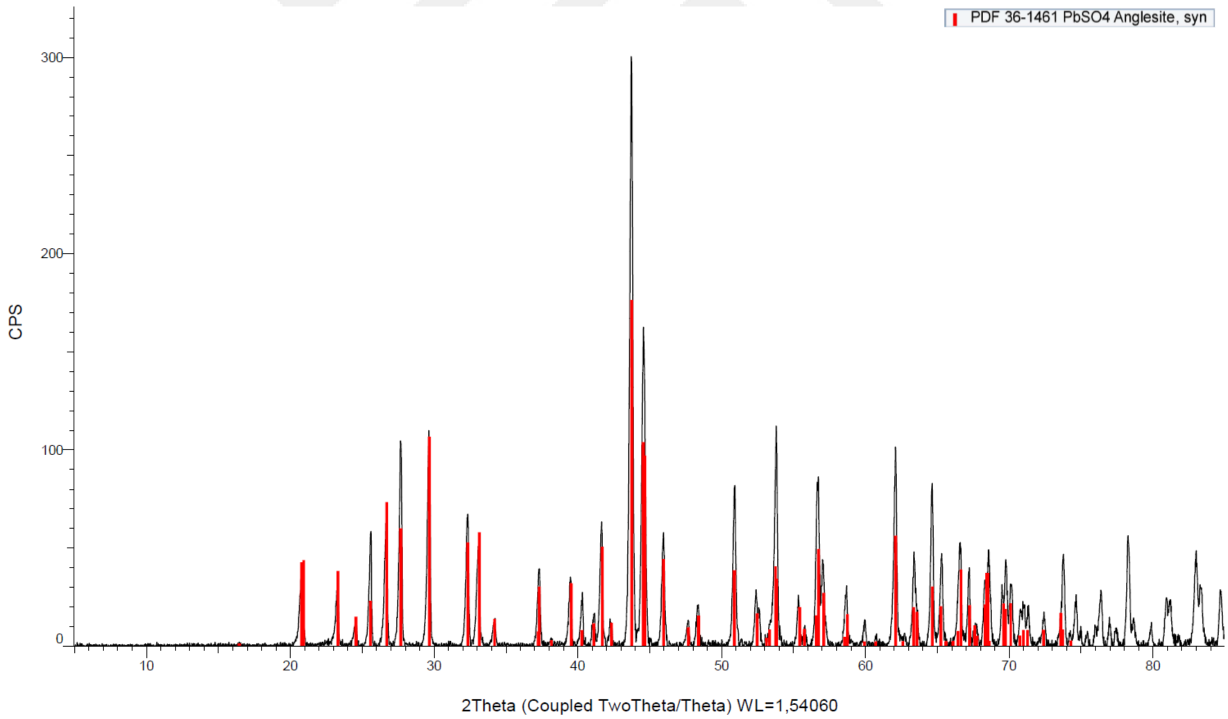

Figure 4.129. The XRD pattern of $PbSO_4$ precipitation at pH 0.25

4.5.2.2. Metal extraction with D2EHPA

After the lead precipitation procedure, the PLS was conducted to a solvent extraction process to remove Zn from the main impurities, including As, Fe, Mg, and Ca. For this objective, the extractant D2EHPA was studied. With exception of Pb, which was almost totally eliminated from the solution after precipitation, the chemical composition of the PLS remained largely unchanged (Table 4.20). Figures 4.130-4.132 show the metal extraction using 5, 10 and 15% D2EHPA as a function of pH. The pH ranges in the three figures differ because extractions at pH levels higher than those required for a quantitative Zn extraction were not performed. Zinc extraction normally increased with pH using different extractant concentration. This is a prevalent property of D2EHPA as an acidic extractant, as demonstrated by previous researchers who extracted Zn from different acidic aqueous solutions with D2EHPA (Amer et al., 1995; Cole and Sole, 2003; Deep and de Carvalho, 2008; Hosseini et al., 2010; Hussaini et al., 2021b; Vahidi et al., 2009). In all of the pH ranges examined, zinc extraction takes precedence over other impurities. Ca extraction followed a similar pattern to Zn extraction; however, Fe extraction followed a distinct pattern. When the pH was increased from 0.3 to 1.3 with 5% D2EHPA concentration, Fe extraction improved at first, but then reduced when the pH was raised to 5.4. In all of the measured ranges, the extractions of As and Mg were quite modest. The discovered Fe behavior was most likely owing to its interaction with the malate ions, which competed with the extractant-iron process. According to Hamada et al., 2005, Fe did not precipitate in the presence of malic acid at pHs ranging from 2.5 to 11.5 (Hamada et al., 2005). They reported that the malate ions were considered to operate as chelating ligands, keeping both the trivalent and divalent Fe ions in solution. The chelate effect makes the hydroxyl group participate in metal chelation, resulting in the formation of stable fused five and six-membered chelating rings. Their results are confirmed by the experimental findings of Vukosav et al (2010) that the soluble Fe species in malic acid are stable for at least a year at pH ranges of 1.5 to 11.5 in the aqueous phase (Vukosav et al., 2010).

Table 4.20. The chemical content of PLS after precipitation step at pH 0.25

Elements	Zn	Fe	Ca	As	Mg
Concentration (mg/L)	5020	1095	512	441	212

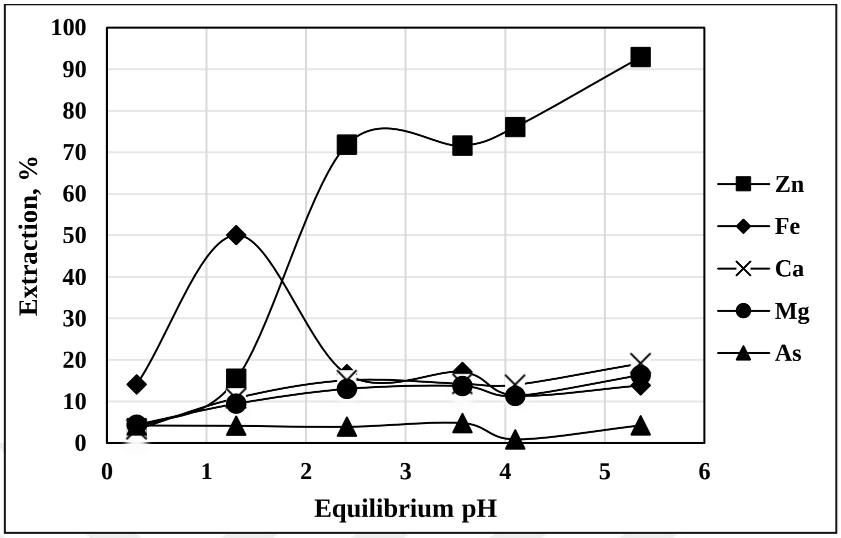

Figure 4.130. Metal extraction with 5% D2EHPA as a function of pH at 25 ^{o}C and 10 min.

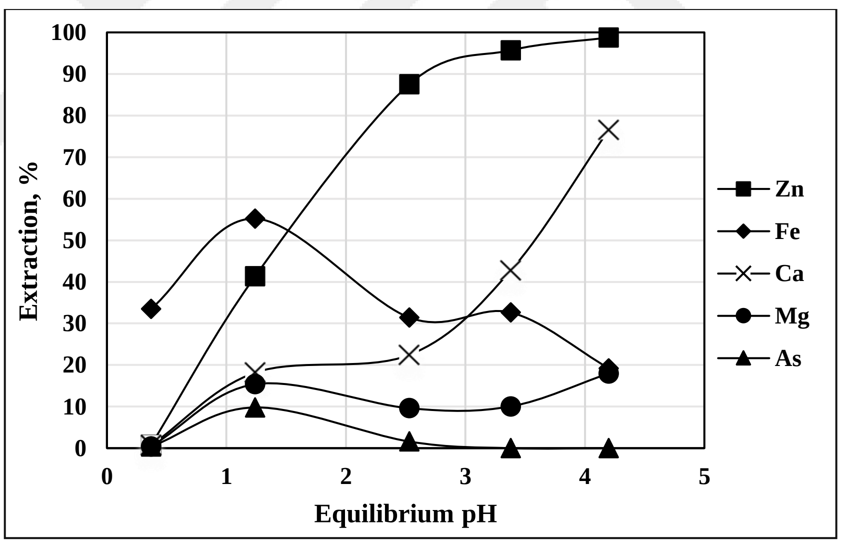

Figure 4.131. Metal extraction with 10% D2EHPA as a function of pH at 25 ^{o}C and 10 min.

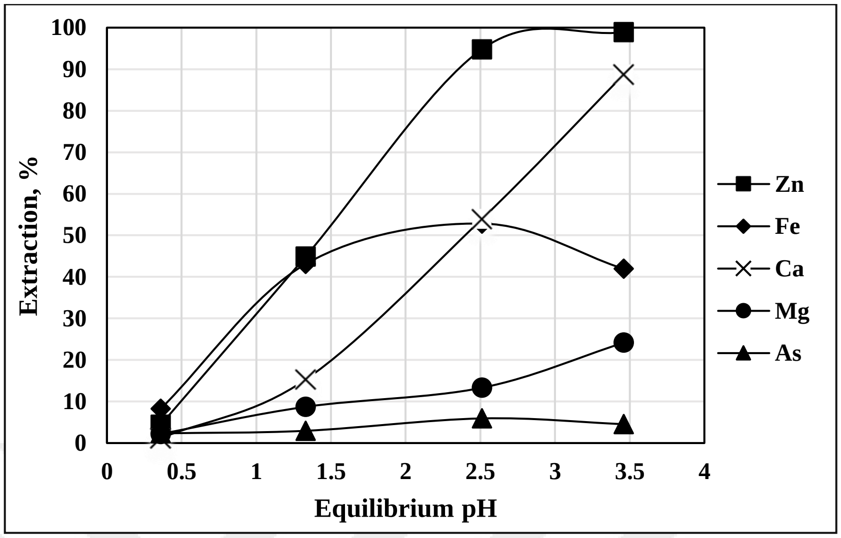

Figure 4.132. Metal extraction with 15% D2EHPA as a function of pH at 25 ºC and 10 min.

At the same pH, the extraction of Fe, Ca and Zn into the aqueous phase increased increasing the extractant concentration. This shows that the crowding effect may be to blame for the decreases in the extraction of Fe at pH levels greater than 2.5, as the extraction of Mg and Ca became more popular. While Ca extraction increased significantly as extractant concentrations increased, the extraction of Fe increased at a slower rate than Zn extraction, resulting in a higher separation factor (*β*) between Fe and Zn (Table 4.21). At pH 4.2, the maximum separation factor ($\beta_{Zn/Fe}$ = 597) was achieved by using 10% D2EHPA concentration. Ca has no detrimental effect on zinc electrowinning at low concentrations (Qin et al., 2003), and As was not extracted under these conditions. As a result, it was discovered that using a 10% extractant concentration and a pH of 4.2 to extract 99.3% of Zn together with 19.2% of Fe, 76.6% of Ca, and 18% of Mg in a single contact was optimal for extraction of Zn from the PLS.

Table 4.21. The separation factor of zinc with respect to iron with D2EHPA in malic acid leach solution

5% D2EHPA		10% D2EHPA		15% D2EHPA	
pH	βZn/Fe	pH	βZn/Fe	pH	βZn/Fe
2.41	12.8	2.53	15.3	1.33	1.1
3.57	12.2	3.38	46	2.51	16.3
4.1	24.5	4.2	597	3.46	124
5.36	81				

❖ **Effect of the contact time on metal extraction**

Figure 4.133 illustrates metal extraction as a function of time with 10% D2EHPA at a pH of 4.2 and 25°C as a temperature. The metal extractions after the first 3 minutes and 20 minutes of contact time were nearly identical, indicating that the majority of the extraction reactions took place in less than 3 minutes. However, the staggered extraction percentages of the metal ions, especially those of Mg and As, indicate that equilibrium has not yet been achieved after 20 minutes of contact time. Because less impurities were carried into the organic phase together with Zn, the unstable extractions of Mg and As appeared to be helpful (Hussaini et al., 2021b).

❖ **Effect of the temperature on metal extraction**

Figure 4.134 shows the effect of temperature on metal extraction using 10% D2EHPA, pH of 4.2 and 10 min contact time. According Figure 4.134 when the contact time was adjusted to 10 min, As extraction were continuously below 1%, even at various operational temperatures ranging from 25 to 40 ^{o}C. This demonstrates the value of using a 10 min contact time to reduce impurity extraction. When the temperature was raised to 40 °C., the extractions of Fe and Mg increased. The calcium extraction with D2EHPA from the malic acid solution, on the other hand, decreased as the temperature increased, indicating that the calcium extraction with D2EHPA from the malic acid solution was exothermic reaction driven (Hussaini et al., 2021b). The zinc extraction, on the other hand, was rather consistent across all of the studied ranges. Because there was no actual benefit from increasing the temperature, a temperature of 25 °C with a contact time of 10 minutes was chosen to be optimal. Figure 4.135 shows the image of loaded organic and raffinate in the optimum conditions.

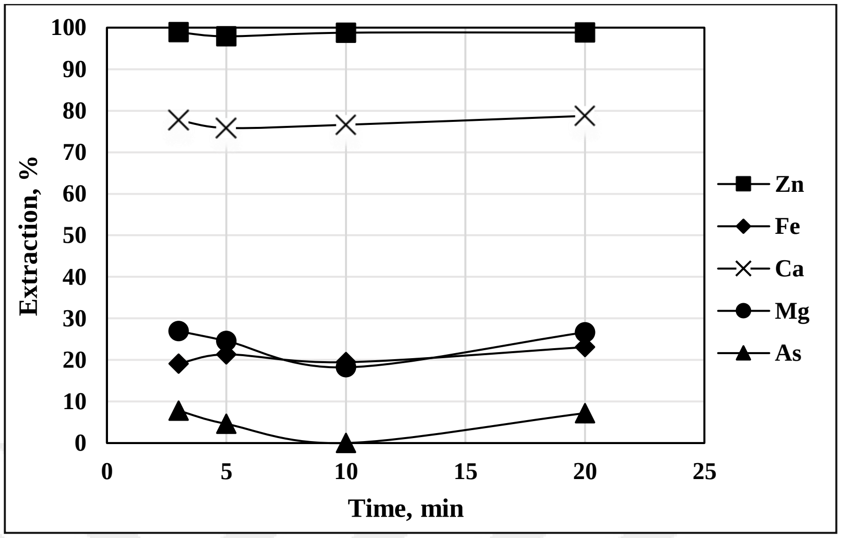

Figure 4.133. Metal extraction in different time with 10% D2EHPA, pH 4.2 and 25 ^{o}C.

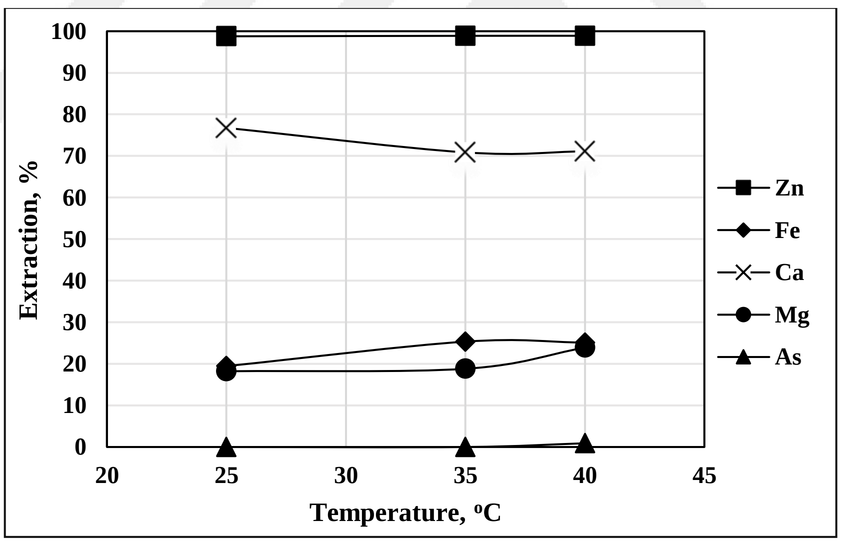

Figure 4.134. Metal extraction in different temperature with 10% D2EHPA, pH 4.2 and 10 min.

Figure 4.135. The image of loaded organic and raffinate phases using 10% D2EHPA at pH 4.2, 10 min 25 ^{o}C.

- **McCabe-Thiele diagram drawing for zinc extraction using D2EHPA**

A series of solvent extraction experiments were carried out for determining that zinc with how many stages would be loaded in to organic phase using 10% D2EHPA at various A/O ratios (1, 2, 3, 4, 5 and 6). The results are given in Figure 4.136 and Table 4.22. With one theoretical counter-current stage at an operating line unity, Zn was almost entirely loaded into the organic phase. A feed solution containing 5020 mg/L of Zn formed an organic phase containing 4984 mg/L of Zn. After a single-stage extraction at an A/O ratio of 1.0, 25 °C and pH 4.2, the organic phase was loaded with 4984 mg/L of Zn, 210 mg/L of Fe, 392 mg/L of Ca, , and 38 mg/L of Mg.

Table 4.22. The obtained results for the McCabe-Thiele diagram drawing at pH 4.2 at various A/O ratios.

A/O ratio	Zn in organic (g/L)	Zn in aqueous (g/L)
1	4.99	0.02
2	8.52	0.54
3	8.83	1.47
4	9.23	1.91
5	9.40	2.21
6	9.92	2.41

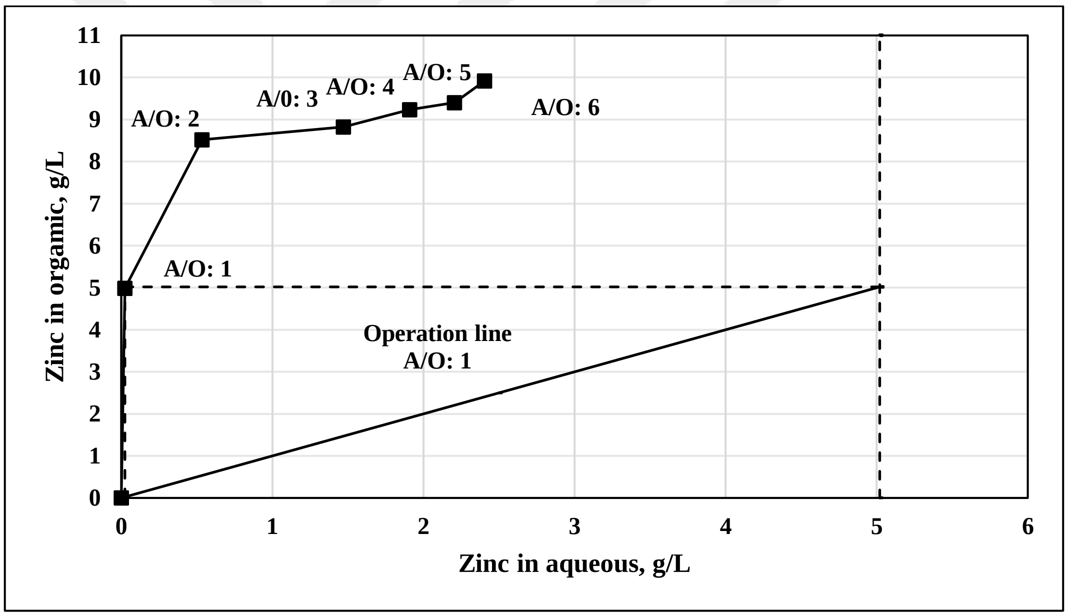

Figure 4.136. McCabe-Thiele diagram for zinc extraction with 10% D2EHPA, 25 ^oC and 10 min.

❖ **Stripping step of the loaded organic**

The metals that remained in the organic solution were stripped. The pH of deionized water was adjusted at 0.25, 0.5, 0.75, 1.0 and 1.25 with sulfuric acid and the experiments werecarried out in A/O: 1.0, 25 ^oC and 10 min. Figure 4.137 shows the stripped metals from the loaded organic phase as a function of pH. According the results at pHs ranging from 0.25 to 0.5, Zn was fully stripped from the loaded organic phase. At the pH ranges investigated, the stripping percentages of the other metal ions remained rather stable, with Ca at 100%, Mg at around 50% and Fe at 0%. Because iron and D2EHPA form a strong complex, it is difficult for an inorganic acid to strip it. Yu et al, 1989 suggested, this is thought to be because iron and D2EHPA form octagonal complexes. The complex's hydrophobic end will be driven towards the organic phase, while acid anions of inorganic and hydrogen ions are highly hydrophilic (Hussaini et al., 2021b; Yu et al., 1989). As a result, the extracted complexes have low concentrations, and the inorganic acids are present at the interface, allowing Fe to be stripped from the organic phase. According to Hu et al., 2014, Fe stripping was slow, and even with 4.0 mol/L sulphuric acid, only around 40% of Fe was removed from Fe-loaded D2EHPA solution (Hu et al., 2014). They, however, demonstrate that reductive stripping with a 7% oxalic acid solution may completely stripping Fe from the organic phase, allowing the D2EHPA solution to be recycled. Other methods involving the reduction of Fe from its trivalent to divalent states, such as so-called galvanic stripping by, for example, adding Zn metal as a reductant when contacting the loaded organic solution with mild sulphuric acid solution, have also been shown to be capable of completely stripping Fe from loaded D2EHPA solution (Chia Aquije, 1993; Gu et al., 2000).

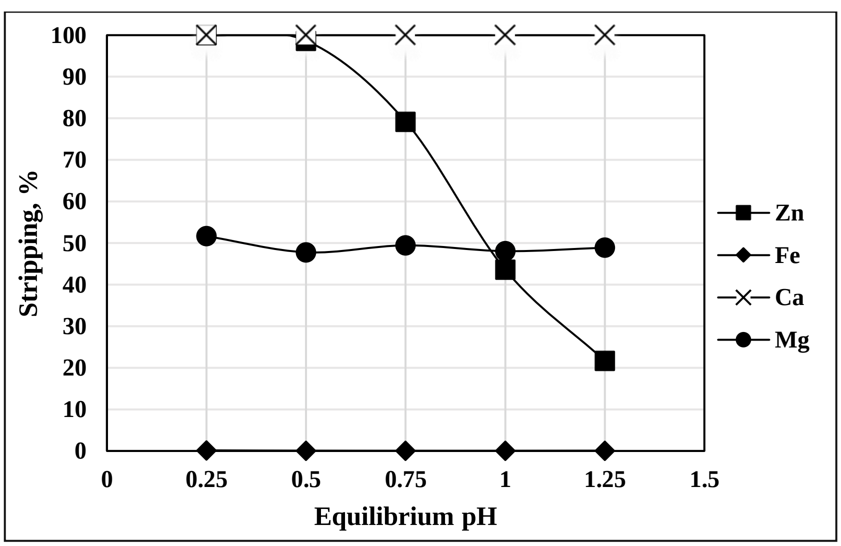

Figure 4.137. Metal stripping from the loaded organic phase at different pHs, 25 ^{o}C and 10 min

❖ McCabe-Thiele diagram drawing for zinc stripping

For this set of experiments, the SX experiment were performed with 10% D2EHPA at pH: 4.2. The loaded organic solution was used for stripping experiments at pH 0.5 in different O/A ratios. The phase ratio between the organic and aqueous phases (O/A) was varied from 1:1 to 6:1 to create a McCabe-Thiele diagram for Zn stripping. The results are given in Figure 4.138 and Table 4.23. According to the diagram, two counter-current contacting stages were required at a 2:1 (O/A ratio) working line to totally strip Zn from organic solution at a pH of 0.5, resulting in a Zn concentration of 9968 mg/L in the loaded strip solution (Hussaini et al., 2021b).

Table 4.23. The obtained results for the McCabe-Thiele diagram drawing at pH 0.5 at various O/A ratios.

O/A ratio	Zn in organic (g/L)	Zn in aqueous (g/L)
1	0.00	4.98
2	0.41	9.14
3	1.28	11.12
4	2.04	11.76
5	2.57	12.09
6	2.95	12.20

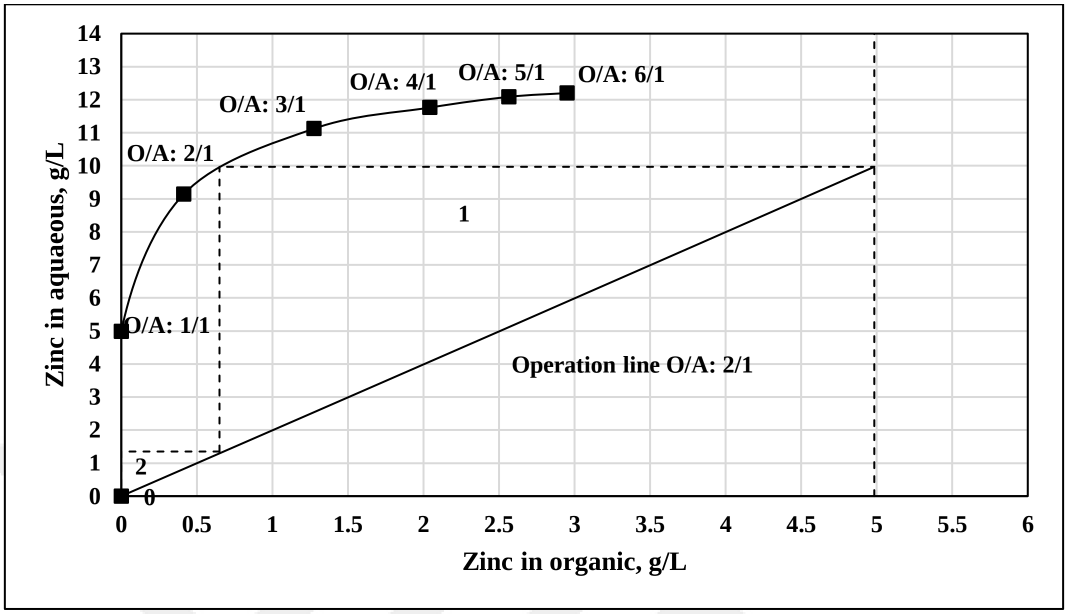

Figure 4.138. Diagram of McCabe-Thiele for zinc stripping at pH 0.5, 25 ^{o}C and 10 min.

4.5.2.3. Metal extraction with Cyanex 272

According to Figure 4.139, the solvent extraction experiments with Cyanex 272 was not beneficial for the extraction of zinc because of third phase formation. Using modifiers such as TBP could be useful for the extraction of zinc with Cyanex 272.

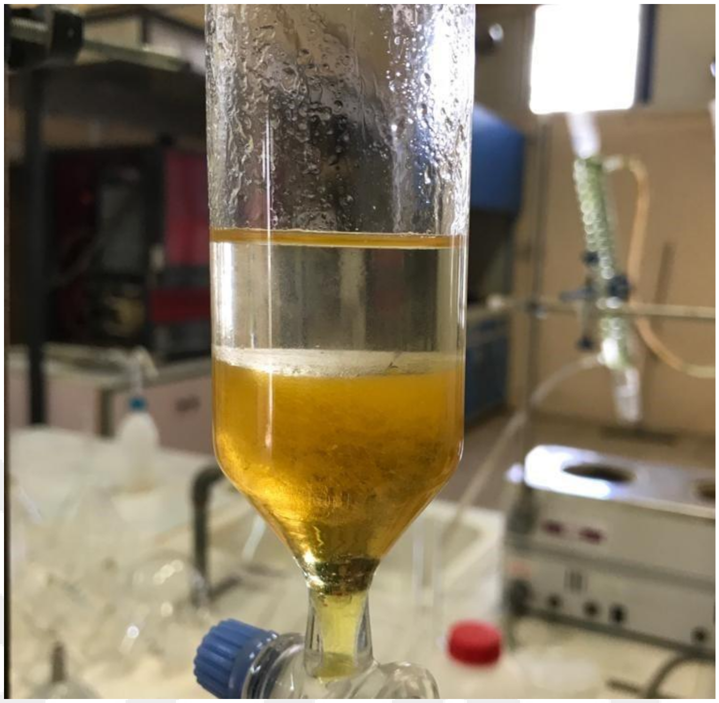

Figure 4.139. Third phase formation during zinc extraction with 10% Cyanex 272.

4.5.3. Solvent extraction of citric acid leach solution

4.5.3.1. Removal of lead from citric acid leach solution

For this experiment 50 ml citric acid PLS was tried to precipitated using 5.0 M H_2SO_4 at four different pH values (0.25, 0.5, 1.0 and 1.5) at 25 ^oC for 30 miniute. Lead precipitation increased from 97.1% to 99.3% and Ca precipitation from 61.5% to 77.6% without any precipitation of Fe, Zn, Mg, As and Al. Optimum pH was assumed to be 1.0 where 98.9% Pb was precipitated. The metal precipitation in different pH is shown in Figure 4.140. Because $PbSO_4$ is insoluble in aqueous solutions due to its low solubility, it was possible to separate zinc from lead by selective precipitation with sulfuric acid (Eq 4.47). XRD analysis of the precipitate at the optimum condition confirmed the reaction products, $PbSO_4$ (anglesite) and $CaSO_4$ (gypsum), as shown in Figure 4.112. Fusi et al. (2015) reported, dissolved sulfate ions SO_4^{2-} seek out and bind with available Ca^{2+} ions to form calcium sulfate $CaSO_4$, as shown in equation

4.48 (Fusi et al., 2015). According to Figure 4.141, where the malic leach PLS was precipitated, and the XRD findings revealed that there was no $CaSO_4$ in the precipitate, unlike in precipitation experiment of citric leach solution. We detected a high percentage of $CaSO_4$ in the precipitate, which is cause for concern because it was one of the study's major impurities. As a result, we can write the overall precipitation reaction as:

$$Pb^{2+}(aq) + H_2SO_4(aq) = PbSO_4(s) + 2H^+(aq) \tag{4.47}$$

$$Ca^{2+}(aq) + H_2SO_4(aq) = CaSO_4(s) + 2H^+(aq) \tag{4.48}$$

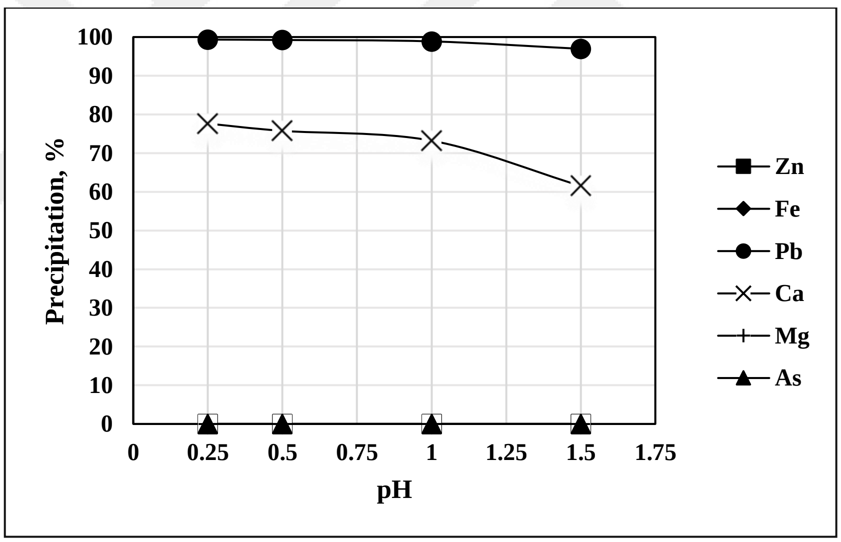

Figure 4.140. Metal precipitation with 5.0 M H_2SO_4 at different pH, 25 °C and 30 min.

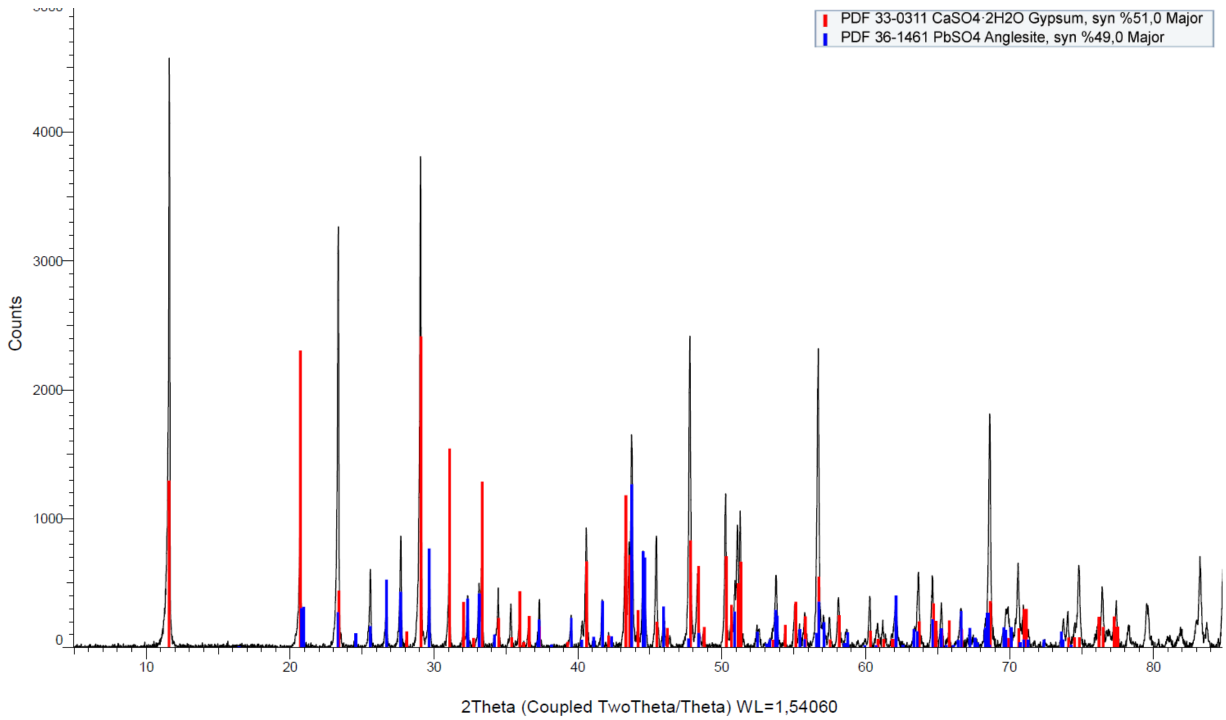

Figure 4.141. XRD pattern of precipitated sample at pH 1.0.

4.5.3.2. Metal extraction with D2EHPA

The PLS was treated with an SX process after the lead precipitation technique to extract zinc from the main impurities, which comprised As, Fe, Ca and Mg. The solvent extraction experiments were started with D2EHPA. The chemical composition of the PLS remained almost unchanged following precipitation, with the exception of Pb, which was almost completely removed from the solution (Table 4.24).

Table 4.24. The chemical content of PLS after precipitation step (pH: 1.0).

Elements	Zn	Fe	As	Ca	Mg
Concentration (mg/L)	10350	7990	1560	503	457

Figure 4.142-4.144 show the effect of D2EHPA concentrations ranging from 10% to 20% on metal extraction at various pH levels. Because extractions at pH levels higher than those

required for a practically significant zinc extraction were not performed, the pH ranges in the three figures differ. Zinc is extracted before the other impurities in all of the pH ranges studied. The extraction of Ca followed the same trend as that of zinc. iron, on the other hand, followed a clear pattern. Iron extraction decreased at first when the pH was increased from 1.0 to 1.9 at a 10% D2EHPA concentration, but subsequently stayed constant when the pH was raised to 3.6. This activity could be explained by the complex formation of iron with citrate ions. According to literature, the stability constant for the Fe citrate complex is 11–15 (Field et al., 1974; Halli et al., 2020; Nischwitz and Michalke, 2009). The extractions of arsenic were low in all of the studied ranges, while Mg extractions increase as pH rises, at 15% and 20% D2EHPA, respectively. In aqueous solution, iron-citrate speciation diagrams reveal that iron can form reasonably stable neutral species. This shows that acidic extractant reject the formation of stable iron-citrate complexes, resulting in a decrease in iron extraction as pH increases (Zhang et al., 2020).

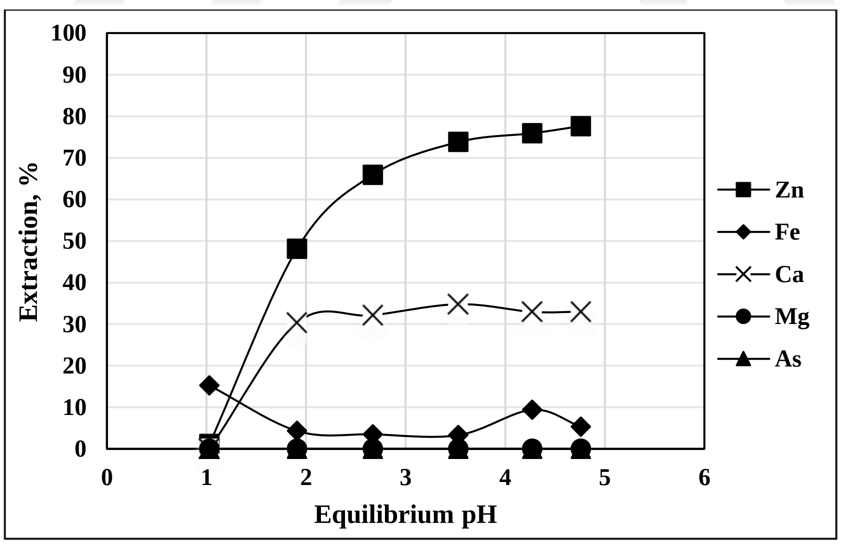

Figure 4.142. Metal extraction as a function of pH with 10% D2EHPA, 25 ^{o}C and 10 min.

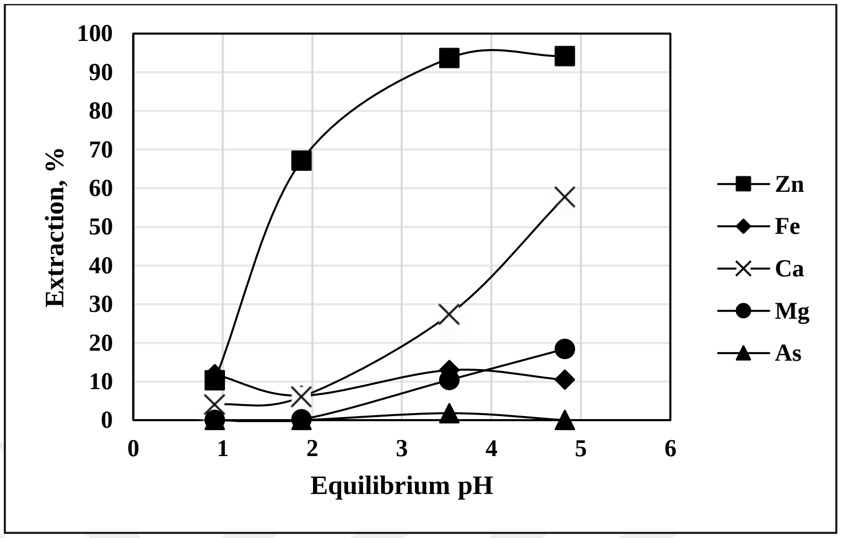

Figure 4.143. Metal extraction as a function of pH with 15% D2EHPA, 25 ^{o}C and 10 min.

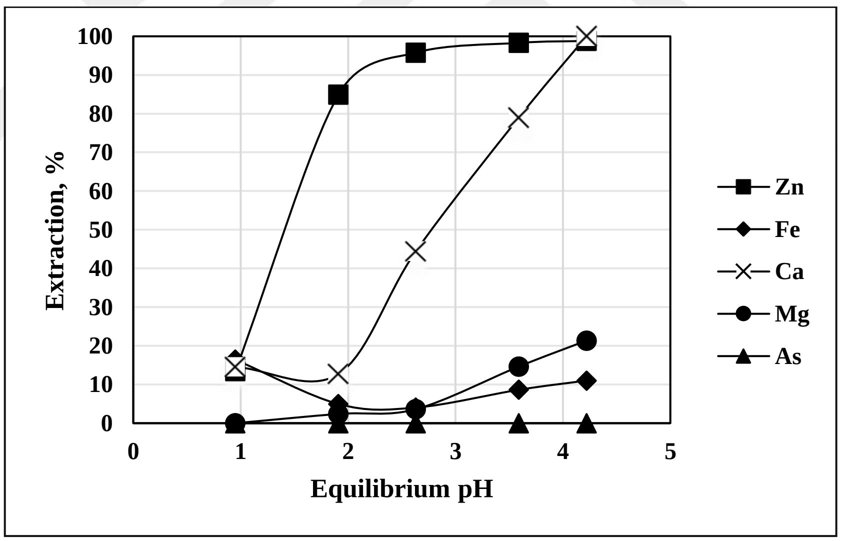

Figure 4.144. Metal extraction as a function of pH with 20% D2EHPA, 25 ^{o}C and 10 min.

At the same pH, increasing the extractant concentration increased the extraction of calcium, iron, and zinc into the aqueous phase. As magnesium and calcium extraction became more prevalent, the crowding effect may have been to blame for the drop in iron extraction at pH levels higher than 2.0. While calcium extraction increased dramatically as extractant concentrations, increased, iron extraction grew at a slower rate than zinc extraction, resulting in a higher Fe-Zn separation factor (β). According to Table 4.25, with a 20% D2EHPA concentration at pH 3.6, the greatest separation factor (Zn/Fe = 613) was achieved. At low concentrations, calcium, in particular, has no harmful effect on zinc electrowinning (Kagambega et al., 2017; Qin et al., 2007), and no As was extracted under these conditions. According to result, it was determined that extracting 98.3% of Zn, 79% of Ca, 18% of Mg, and 8.6% of Fe in a single contact with a 20% D2EHPA concentration and a pH of 3.6 was ideal for separating impurities and zinc.

Table 4.25. Zinc separation factors in a citric acid solution using D2EHPA in relation to iron.

10% D2EHPA		15% D2EHPA		20% D2EHPA	
pH	β Zn/Fe	pH	β Zn/Fe	pH	β Zn/Fe
2.41	0.1	0.91	0.9	0.95	0.8
1.91	20.6	1.88	30.2	1.91	107.7
2.67	53.4	3.53	99.0	2.63	537.4
4.76	61.7	4.82	138.3	3.59	612.7

- **Effect of the contact time on metal extraction**

Figure 4.145 indicates the effects of contact time on metal extraction using 20% D2EHPA and a pH of 3.6 at a temperature of 25 °C. After 3 minutes and 20 minutes of contact time, metal extractions were remarkably similar, indicating that the majority of the extraction reactions took place in within 3 minutes. Although, after 20 minutes of contact time, the staggered extraction percentages of the metal ions, particularly those of magnesium and arsenic, suggest that equilibrium has not yet been reached. The irregularity of magnesium and arsenic extractions appeared to be beneficial since less impurities were transferred into the organic phase with the zinc. As results, 10 min contact time was selected as optimum for extraction procedure.

- **Effect of the temperature on metal extraction**

Figure 4.146 shows the effect of temperature on metal extraction using 20% D2EHPA, pH of 3.6 and 10 min contact time. Even at a variety of operation temperatures ranging from 25 to 40 °C, arsenic extractions were insignificant when the contact time was limited to 10 minutes, as shown in Figure 4.146. This highlights the need of a 10-minute contact time for reducing impurity extraction. The extractions of iron and magnesium remained consistent when the temperature was raised to 40 ^{o}C. However, when the temperature increases, the calcium extraction with D2EHPA from the citric acid solution decreased, indicating that the extraction of calcium with D2EHPA from the citric acid solution was driven exothermically. The same results were observed in solvent extraction from malic acid leach solution (Hussaini et al., 2021b). On the other hand, the zinc extraction was rather consistent throughout all of the ranges investigated. Because there was no evident effect from increasing the temperature, a temperature of 25°C with a contact time of 10 minutes was chosen as the best. Figure 4.147 shows the image of loaded organic and raffinate in the optimum conditions.

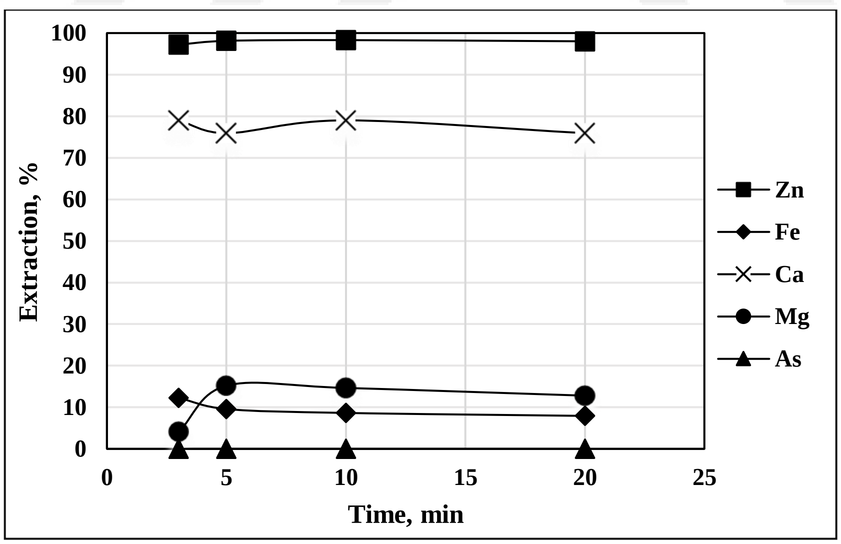

Figure 4.145. Metal extraction in different time with 20% D2EHPA, pH 3.6 and 25 ^{o}C.

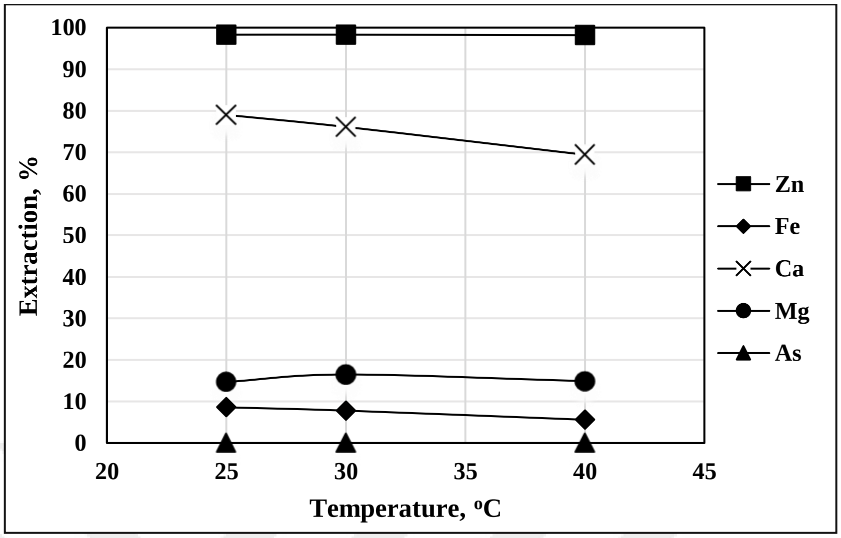

Figure 4.146. Metal dissolution at different temperature with 20% D2EHPA, pH 3.6 and 10 min.

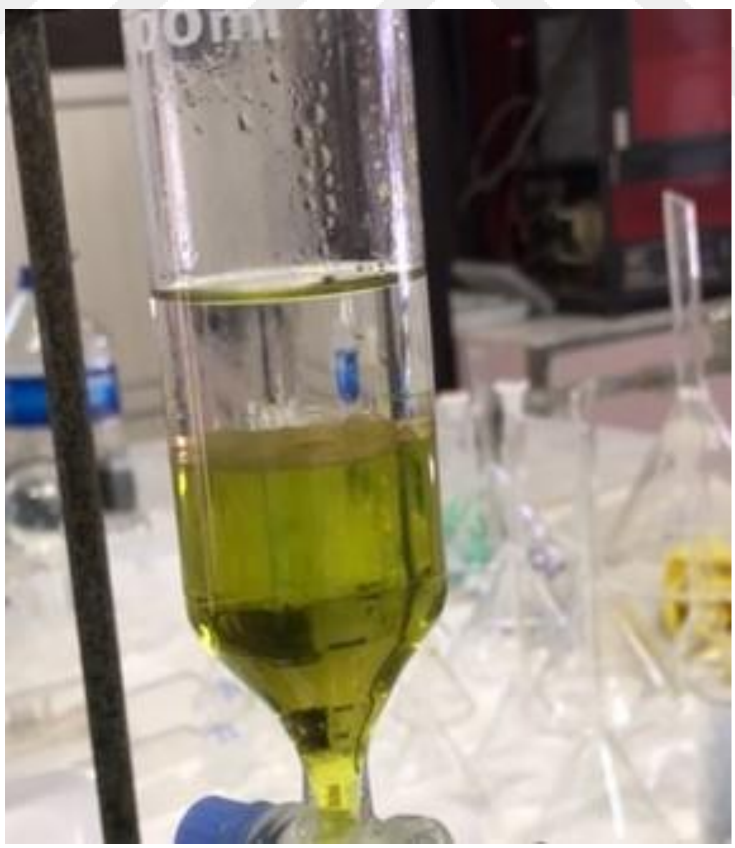

Figure 4.147. The image of loaded organic and raffinate phases using 20% D2EHPA at pH 3.6, 10 min 25 ºC.

❖ McCabe-Thiele diagram drawing for zinc extraction using D2EHPA

A series of solvent extraction experiments were carried out for determining that zinc with how many stages would be loaded in to organic phase using 20% D2EHPA at various A/O ratios (1, 2, 3 and 4). The results are given in Figure 4.148 and Table 4.26. With one theoretical counter-current stage at an operating line unity, zinc was nearly completely loaded into the organic phase. An organic phase containing 10247 mg/L of zinc was obtained from a feed solution containing 10350 mg/L of zinc. The scrubbing studies were carried out on the organic phase, which had been loaded with 10247 mg/L of zinc, 875 mg/L of Fe, 397 mg/L of Ca and 73 mg/L of Mg, which extracted in a single stage at pH 3.6, 1/1 O/A ratio, and 25 °C.

Table 4.26. The obtained results for the McCabe-Thiele diagram drawing at pH 3.6 at various A/O ratios.

A/O ratio	Zn in organic (g/L)	Zn in aqueous (g/L)
1	10.25	0.10
2	15.22	2.74
3	16.22	4.94
4	18.66	5.69

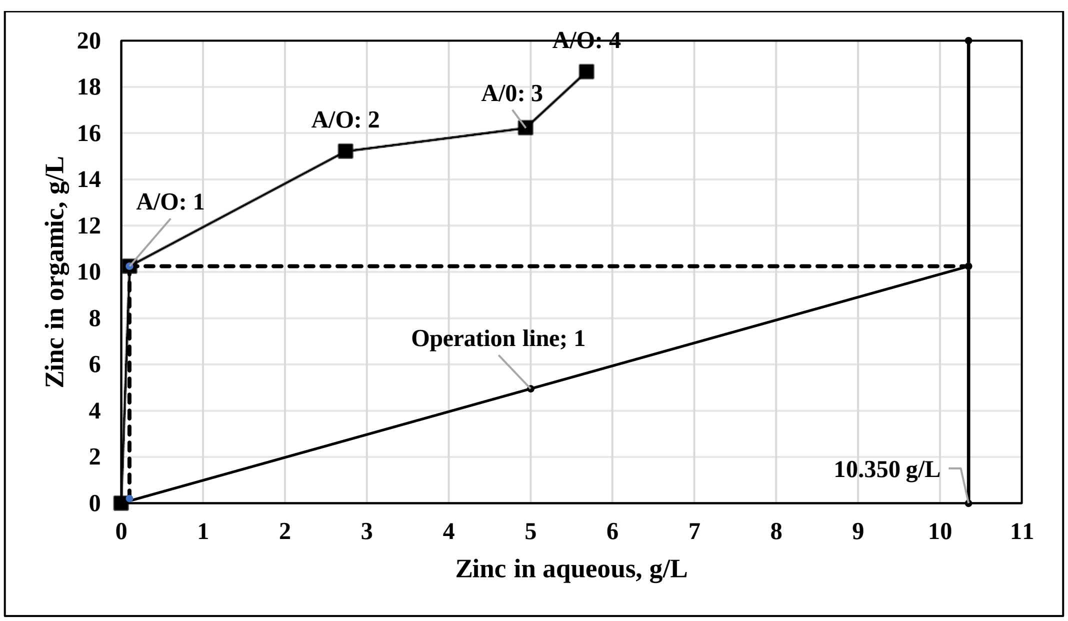

Figure 4.148. McCabe-Thiele diagram for zinc extraction with 20% D2EHPA, 25 ^{o}C and 10 min.

❖ **Scrubbing step of loaded organic with synthetic zinc solution**

All of these experiments indicate that after the extraction phases, a scrubbing step is required to remove impurities from the organic phase. Scrubbing experiments were done on the loaded organic solutions produced from the extraction experiments at previously defined optimum conditions in order to remove magnesium and calcium from the loaded organic solutions and obtain a final zinc product with the high purity. Scrubbing tests were carried out with an A/O ratio of one and pH levels of 4.5, 5, and 5.5 (Figure 4.149). The loaded organic was contacted with a synthetic zinc solution comprising 20 g/L of zinc (Kursunoglu et al., 2017; Ritcey 2006). The Zn in the aqueous phase displaced calcium and magnesium from loaded organic phase. The organic phase will have a higher zinc loading as a result of this procedure. Eq. 4.49 illustrates the mechanism of displacement. According to Figure 4.149, The scrubbing efficiency is unaffected by pH. Calcium was scrubbed from the loaded organic solution at a rate of over 90%, but magnesium-scrubbing effectiveness was just 34%.

$$(C_{16}H_{35}O_4P)(Ca, Mg) + ZnSO_4 \leftrightharpoons (C_{16}H_{35}O_4P)Zn + (Ca, Mg)\ SO_4 \qquad (4.49)$$

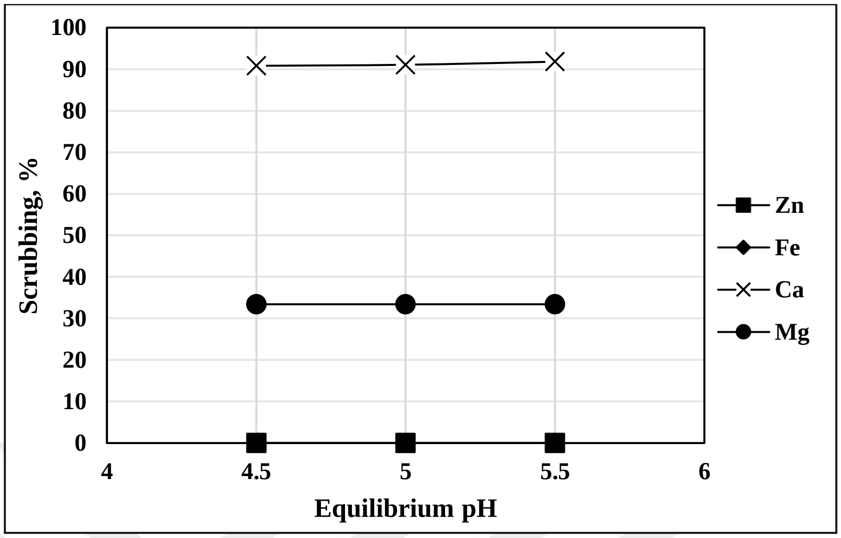

Figure 4.149. Scrubbing of the loaded organic solution with synthetic zinc solution at different pHs, 25°C and 10 min.

❖ **Stripping step of the loaded organic solution**

At a pH range of 0.25 to 1, Zn was stripped from the loaded organic using sulfuric acid solutions at room temperature and a 10-minute stripping duration. Figure 4.150 illustrates the results of metal concentration stripped from the loaded organic phase in different pHs. At pHs varied from 0.25 to 1, the stripping efficiency of Zn from the loaded organic solution increased, reaching 91.3 % at pH 0.25. With a 1.0 M sulfuric acid solution, Halli et al. (2020) achieved about 93% stripping efficiency. It indicates that a second stage of stripping is required to completely transfer the zinc. As a result, the second step of stripping was done at pH 0.25 (Table 4.27) (Halli et al., 2020).

The percentages of iron and magnesium stripped were minor at the pH ranges studied, whereas the percentage of calcium stripped increased with decreasing pH. Iron forms a strong bond with D2EHPA, which is difficult to break down using an inorganic acid. The same results were observed in solvent extraction experiments for malic leach solution. Removal of iron from a stripped organic solution with HCl at pHs 4, 5, and 6 is shown in Figure 4.151. According to the findings, iron was almost fully removed from solution at pH 5, but calcium and magnesium removal reduced as pH increased. The regenerated solution can be used to recover residual HCl, providing a concentrated $FeCl_3$ liquor that can be neutralized before being dumped in tailings (Cole and Sole, 2003).

Table 4.27. Stripping steps of the loaded organic solution at pH 0.25.

Concentration in organic (mg/L)				
	Zn	Fe	Ca	Mg
Feed for stripping	13581	875	37	64
Step 1	1181	874	29	64
Step 2	0	874	24	63

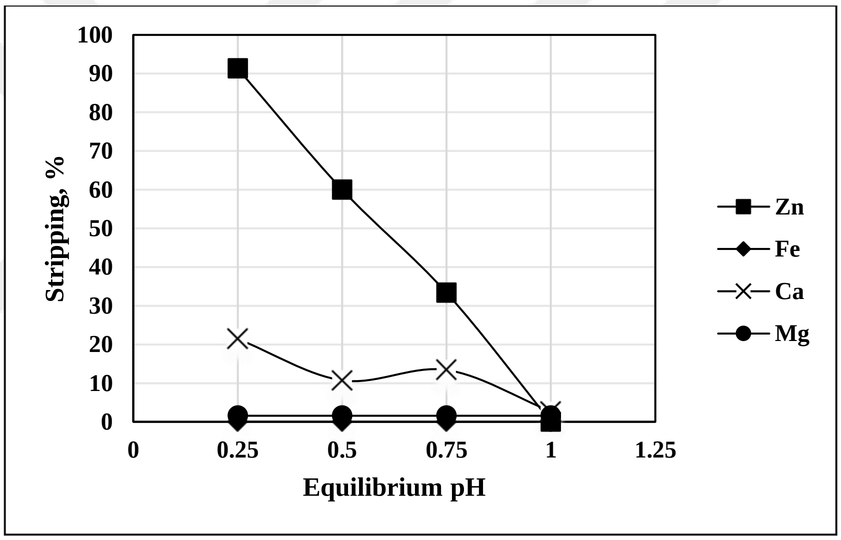

Figure 4.150. Metal stripping from the loaded organic solution with sulfuric acid at different pHs, 25 ^oC and 10 min.

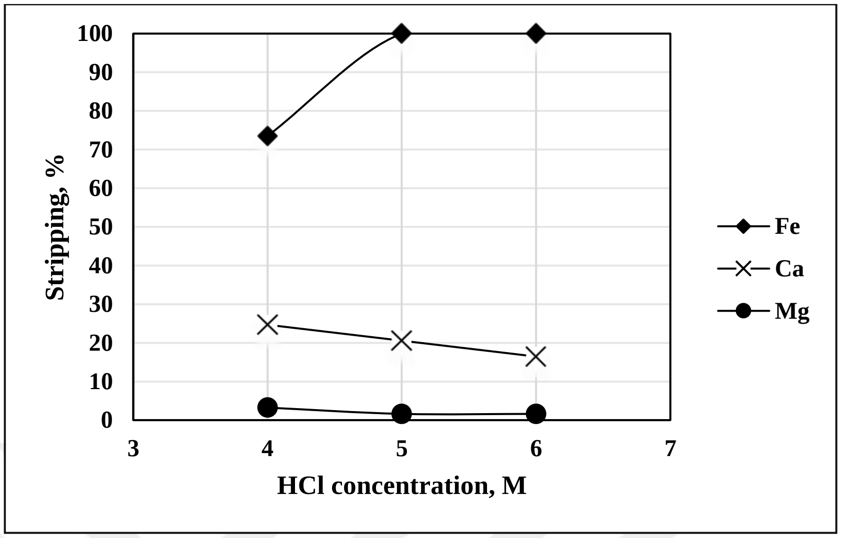

Figure 4.151. Stripping of the stripped organic solution at different pHs with HCl, 25 ^oC and 10 min.

4.5.3.3. Metal extraction with Cyanex 272

Following the solvent extraction using D2EHPA, some studies with Cyanex 272 were carried out to determine the effect of various extractant on metal extraction at 25 ^oC and 10 min. Figure 4.152-4.154 show the effect of Cyanex 272 concentrations ranging from 10% to 20% on metal extraction at various pH levels. In all of the pH ranges investigated, zinc is extracted before the other impurities. The extraction of calcium was not seen with Cyanex 272 in comparison to D2EHPA findings. According to Tsakiridis et al, 2010, calcium was rejected using Cyanex 272 as an extractant. When the Cyanex 272 concentration was increased, the extraction of magnesium increased after pH 4.7. Magnesium extraction with 20% Cyanex 272 increases from 6.6 at pH 4.7 to 16.7 at pH 5.92. Guinaraes and Mansur, 2017; Tsakiridis et al, 2010 observed the same results, with the extraction of magnesium increasing after 4.5 utilizing Cyanex 272 (Guimarães and Mansur, 2017; Tsakiridis et al., 2010). Iron extraction slightly increased with the Cyanex 272 concentration increased. Using 20% Cyanex 272, iron extraction reached 10% with increased pH until 5.92. The complex formation of iron with citrate ions could explain this behavior. In all of the ranges studied, arsenic extractions were negligible. As a result, the experiments with Cyanex 272 obtained the same findings in terms of iron and arsenic extraction with D2EHPA. With increasing concentration of Cyanex 272, zinc extraction increased. 97.4% zinc was obtained with 20% Cyanex 272 at pH 5.92, 25ºC and 10 min. the concentration of extractant observed, that was the same result with D2EHPA but the zinc extracted at high pHs with 20% Cyanex 272. It could be due to the extraction of zinc from citrates solution with Cyanex 272 required decomposition of zinc-citrate complex in high pHs. On the other hand, a higher concentration of Cyanex 272 is likely to have a significant effect on zinc extraction at low pHs. According to the literature, Cyanex 272 could extract zinc from sulfate and chlorate leach solutions at pHs of 2.5-3.5 (Baba and Adekola, 2011; Salgado, 2003; Tanong et al., 2017; Tsakiridis et al., 2010).

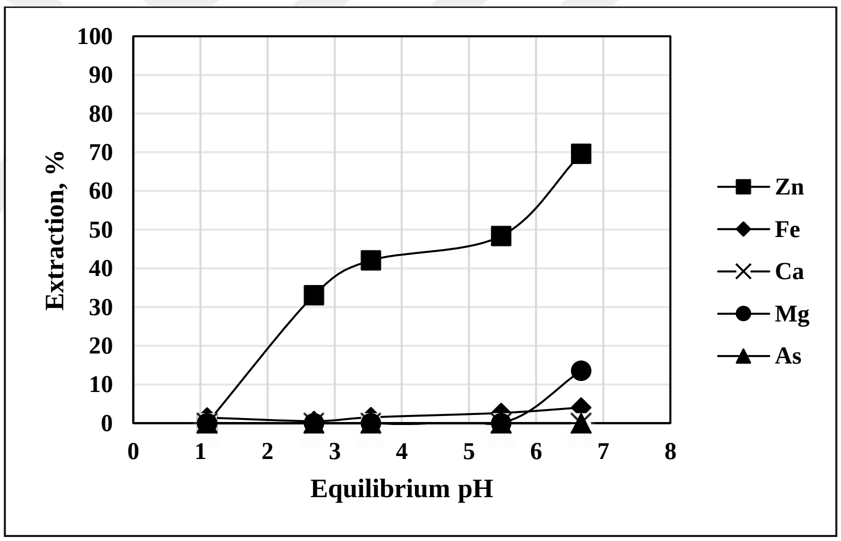

Figure 4.152. Metal extraction as a function of pH with 10% Cyanex 272, 25 ºC and 10 min.

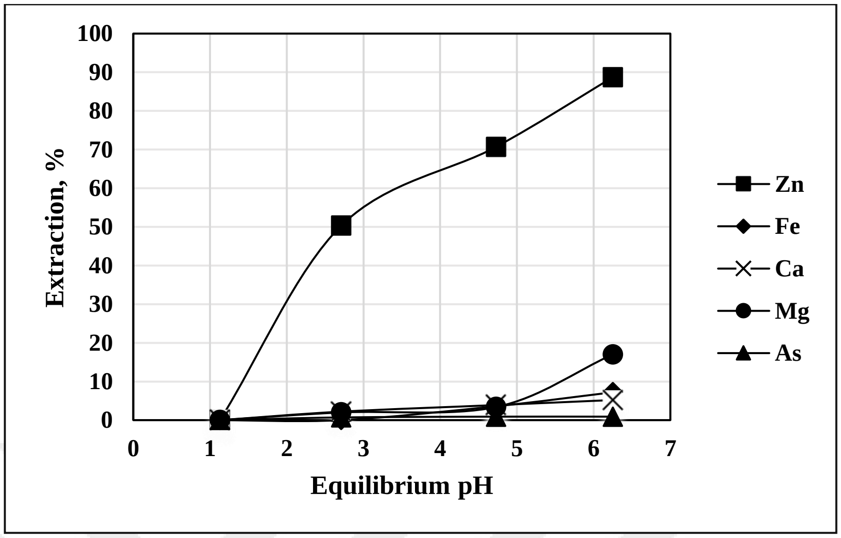

Figure 4.153. Metal extraction as a function of pH with 15% Cyanex 272, 25 ºC and 10 min.

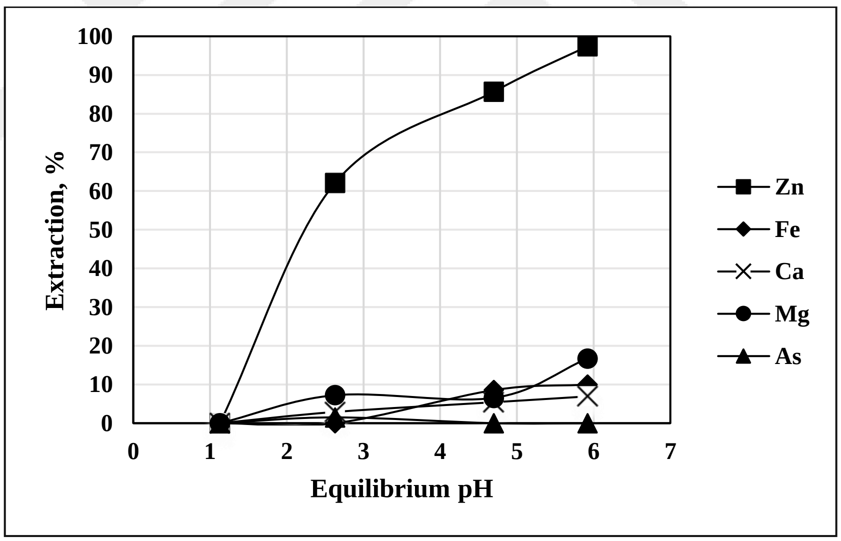

Figure 4.154. Metal extraction as a function of pH with 20% Cyanex 272, 25 ºC and 10 min.

4.6. Electrowinning study

4.6.1. Electrowinning of sulfuric acid leach solution after solvent extraction

Electrowinning was carried out using 0.25-1.0 A current and 200-700 A/m^2 current density at 20 ºC and different time in a beaker. According to literature, Pb plate and Al plate were used as a anode and cathode in EW experiments(Lins et al., 2010; Lu et al., 2013; Xu et al., 2020). The Al plate was prepared from old automobile plates with a 13.5 cm^2 area, and the Pb plate was the same area at a constant distance of 35 mm from the cathode. The solution was used for these experiments obtained from the stripped zinc solution after the solvent extraction experiment. Zinc concentration of solution was 4414 mg/L. The relevant reactions occur on the anode and cathode surfaces when current passes to cause the decomposition of stripped solution (Eqs. 4.50 and 4.51).

$$\text{Cathode: } Zn^{2+}\,(aq) + e^{-} = Zn(s),\ E^{o} = -0.76\ V \tag{4.50}$$

$$\text{Anode: } H_2O\,(l) = 1/2O_2\,(g) + 2H^{+}\,(aq) + 2e^{-},\ E^{o} = -1.23\ V \tag{4.51}$$

According to Figure 4.155, Zn recovery on the cathode increased with both increasing EW time and EW current. At 0.25 A current (200 A/m^2), Zn recovery was 69.1% at 120 min. and 86.1% at 240 min. At 1.0 A current (700 A/m^2), Zn recovery was 90.1% at 120 min. and 100% at 240 min. Increasing current from 0.25 A to 1.0 A increased Zn recovery from 69.1% more than 100% in 240 min. As a result, the optimum of EW experiments was found to be 0.75 A (500 A/m^2 current density) and 240 minutes. In these conditions, zinc was recovered at a rate of 99.7%. Tsakiridis et al, 2010 found the same results. On the cathode surface, the deposited zinc was crystalline, gray in color, compact, and fine-grained (Figure 4.156). A high-quality cathode product was obtained, according to XRD analysis (Figures 4.157).

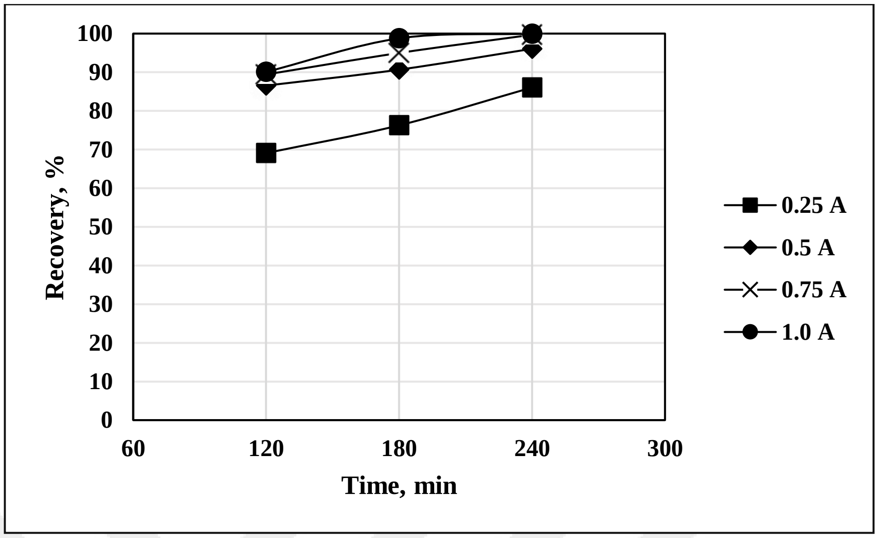

Figure 4.155. Effect of EW time and current on Zn recovery from sulfuric leach solution.

Figure 4.156. The deposited zinc on Al cathode sheet after.

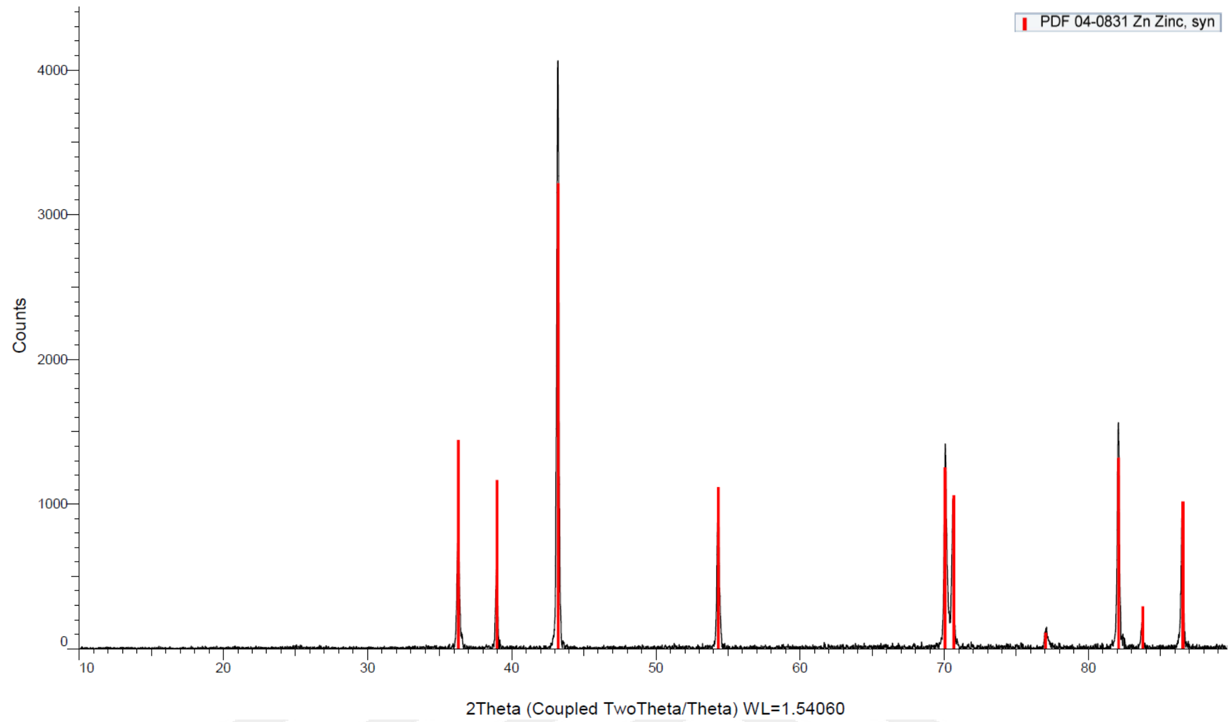

Figure 4.157. XRD spectra of deposited Zn on Al cathode sheet.

4.6.2. Electrowinning of citric acid leach solution after solvent extraction

Electrowinning experiments were carried out using 0.25-1.0 A current and 200-700 A/m^2 current density at 20 ^oC and different time in a beaker. The solution used in EW experiments was obtained after the stripping experiment. The metal concentration of solution was 5213 mg/L Zn, under 1 mg/L Fe, under 1 mg/L As, under 1 mg/L Mg and 5 mg/L Ca. According to Figure 4.158, Zn recovery on the cathode increased with both increasing EW time and EW current. At 0.25 A current (200 A/m^2), Zn recovery was 50.6% at 120 min. and 67.3/7% at 240 min. At 1.0 A current (700 A/m^2), Zn recovery was 91.4% at 120 min. and 99.3 % at 240 min. As a result, the optimum of EW experiments was found to be 1.0 A (700 A/m^2 current density) and 240 minutes.

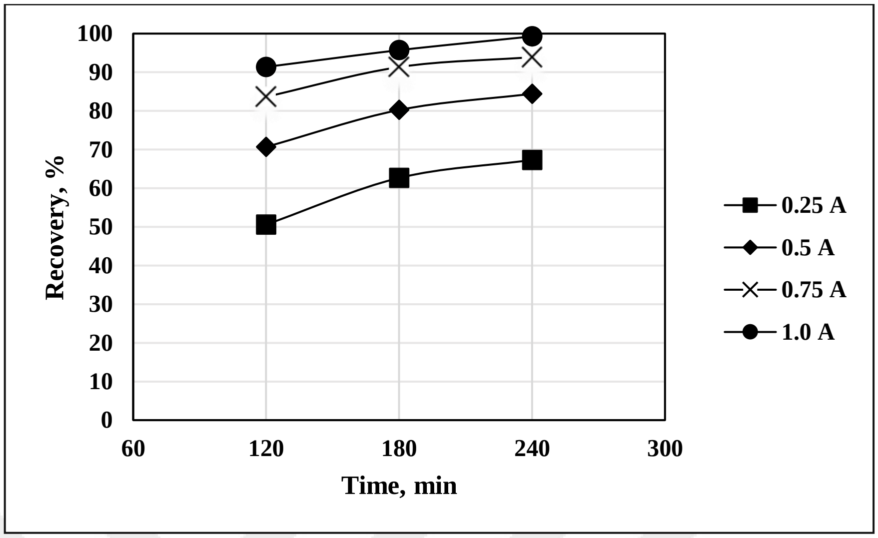

Figure 4.158. Effect of EW time and current on Zn recovery from citric leach solution.

4.6.3. Electrowinning of malic acid leach solution after solvent extraction

Electrowinning studies were carried out in a beaker with a current of 0.5-1.0 A and 350-700 A/m^2 current density at 20 ºC for various periods. After the stripping experiment, the solution for EW experiments was obtained. The metal concentration of solution were 4984 mg/L Zn, 0.3 mg/L Fe, 0.1 mg/L As, under 17.20 mg/L Mg and 289 mg/L Ca. According to Qin et al, 2003; Adhia 1969 and Hussaini et al, 2021, the magnesium and calcium impurities in the solution had no negative effect on the electrowinning process of zinc. Figure 4.159 shows the effect of current and time on zinc recovery in EW process. As results, with increasing EW duration and current, Zn recovery on the cathode increased. Zn recovery at 0.5 A current (350 A/m^2) was 85.5% after 120 min and 90.8 % at 240 min. Zn recovery at 1.0 A current (700 A/m^2) was 91.6 % after 120 min and 96 % after 240 min (Adhia, 1969; Hussaini et al., 2021b; Qin et al., 2003).

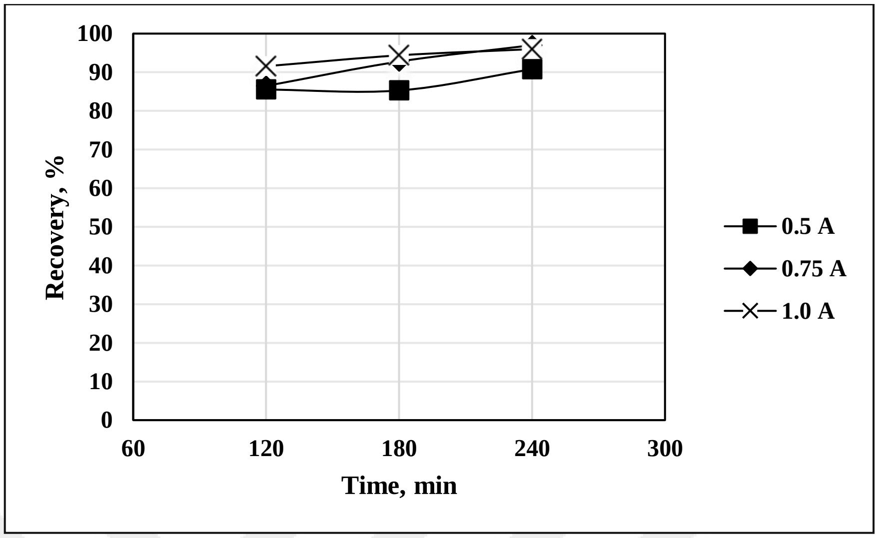

Figure 4.159. Effect of EW time and current on Zn recovery from malic leach solution.

Figures 4.160-4.162 presents a proposed process to recover lead, zinc from sulfuric, citric, and malic acid leach solution of our sample by precipitation, solvent extraction and electrowinning.

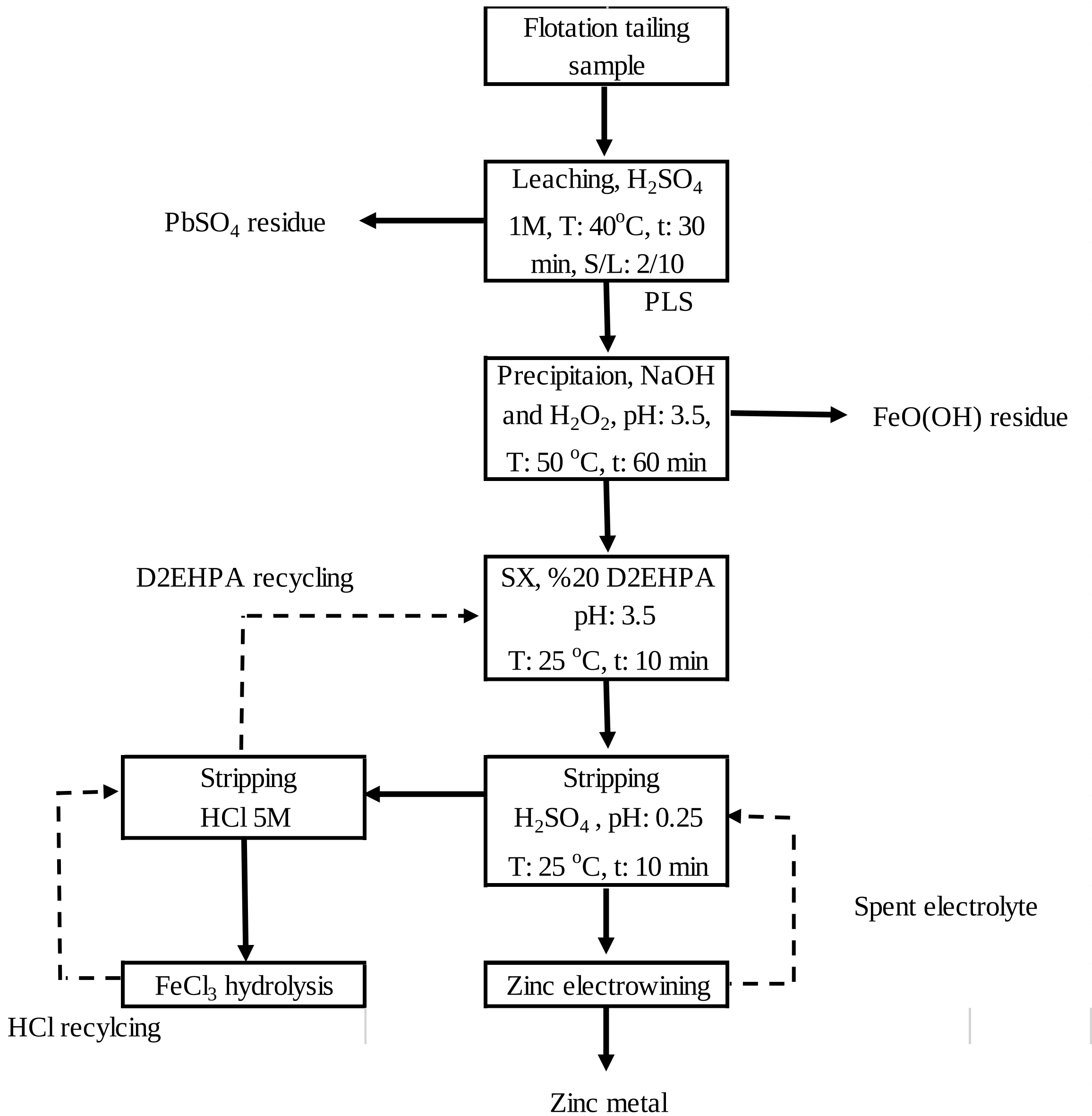

Figure 4.160. Proposed flowsheet for the Pb-Zn recovery from a sulfuric acid leach solution.

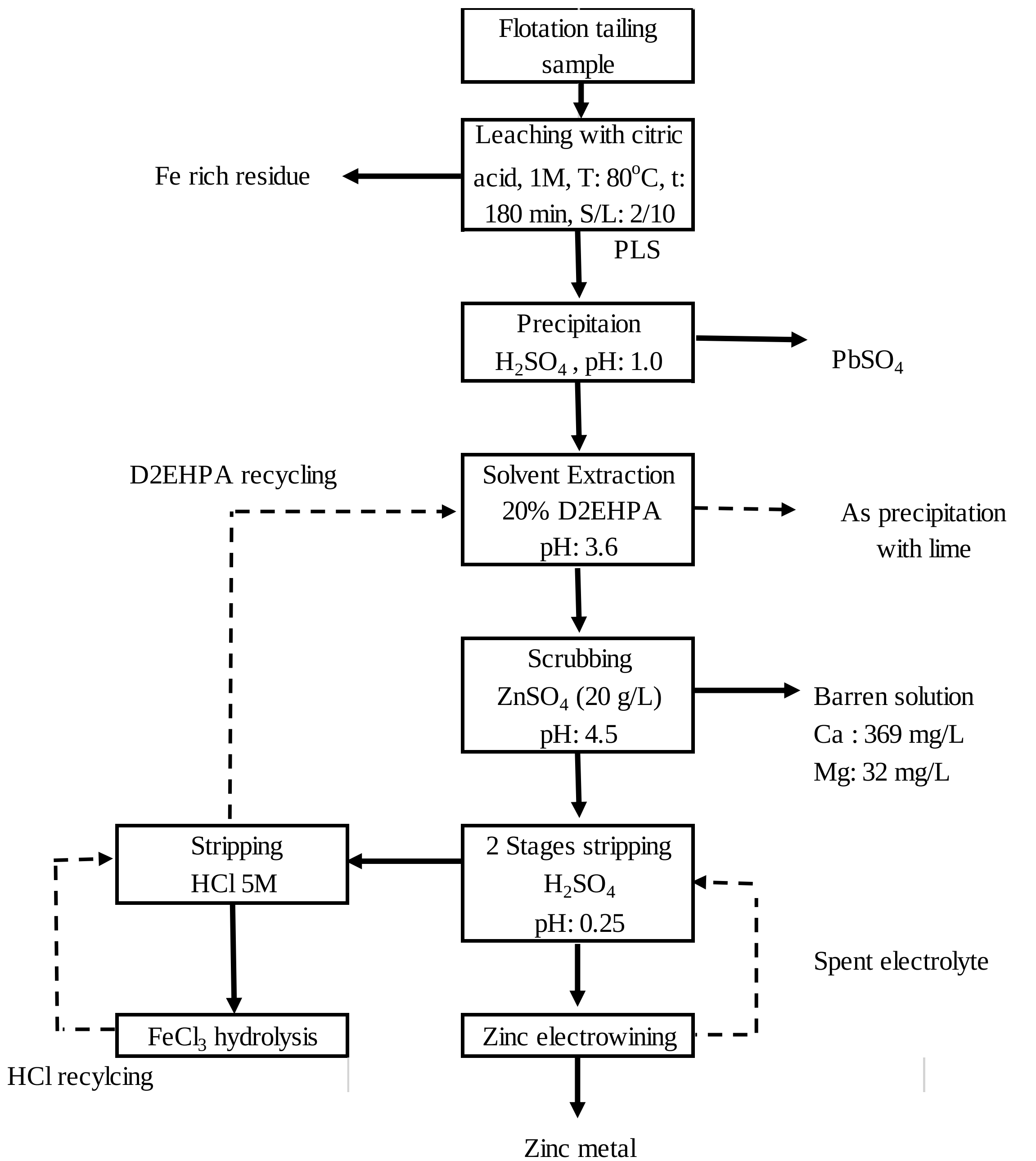

Figure 4.161. Proposed flowsheet for the Pb-Zn recovery from a citric leach solution.

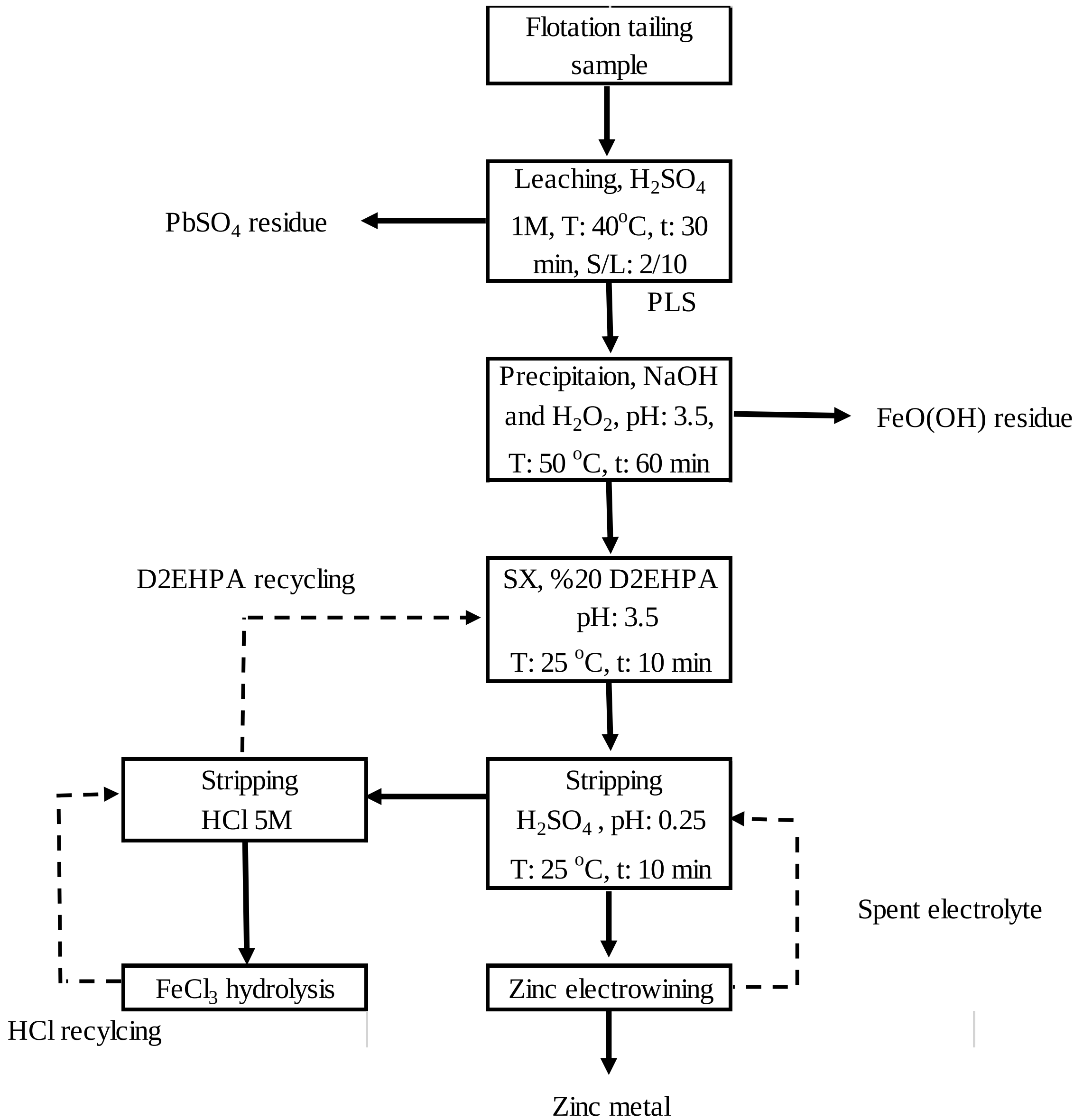

Figure 4.162. Proposed flowsheet for the Pb-Zn recovery from a malic leach solution.

5. CONCLUSIONS AND RECOMMENDATIONS

For this thesis, a representative sample was taken from the tails of the Oreks Mining Company in Yahyalı-Kayseri from the oxidized Pb-Zn flotation plant. The sample properties (moisture content, particle size distribution, chemical and mineralogical analyses, thermal analysis, surface morphology and surface area) were determined. Oreks flotation tailings are very fine (50% -13µm) in size. While cerusite, smithsonite, goethite, corkite and bodantite are the main minerals, calcite and quartz have been found to be secondary gangue minerals. Oreks flotation tailings mainly contain 5.77% Zn, 7.5% Pb, 21.3% Fe, 5.6% As and 101 ppm Ag. The samples have a very fine distribution, porous, complex and finely distributed structure. The specific surface area is 1.9 m^2/g.

In this thesis, three-stage leaching experiments were carried out on a laboratory scale. Leaching tests were carried out in a 500 mL glass balloon heated and spiral condenser reactor at a rate of 1/10 solid/liquid (S/L) with a representative sample of at least 25 g. During the leaching, 5 mL of liquid samples were taken at certain intervals and analyzed by ICP (in ALS-Izmir) and/or AAS (in ESOGÜ and/or AGÜ). In leaching tests, the effects of parameters such as reagent type, reagent concentration, leaching temperature, leaching, duration, S/L ratio were examined by keeping the part size and mixing speed constant at 400 rpm and optimized for reagent selection and maximum metal dissolution.

5.1. Conclusions

The aim of the first stage leaching is to obtain the maximum Zn dissolution (≥90%) and the minimum Pb, Fe and As dissolution. At this stage, four inorganic acids (H_2SO_4, HCl, HNO_3, and $HClO_4$), six organic acids (citric, oxalic, ascorbic, tartaric, malic and formic acids) two alkaline solutions (caustic soda and ammonium chloride) and five chelating reagents (EDTA, ammonium acetate, sulfate, chloride and oxalate) has been used. As our target, at least 90% Zn dissolution, 1.0 M H_2SO_4 concentration, 40 ^oC leaching temperature, 30 min. the leaching time was obtained at a rate of 2/10 S/L. In leaching with H_2SO_4, Pb and Ag are insoluble and remain in the residue as a compound. The selectivity between Zn and Pb is more than 90%, and selectivity between Zn and Fe is between 71% and 80%.

As a results of leaching experiment with HCl, 91% Zn and 10% Pb were obtained with a 72% Zn-Fe selectivity difference with 1.0 M concentration, 1/10 S/L ratio, 80 ^{o}C temperature and 30 min. leaching time. 1.0 M HNO_3, on the other hand, can only dissolve 70% Zn. 1.0 M $HClO_4$ dissolves 89.3% Zn and 7.4% Pb. H_2SO_4 has been selected as the best reagent for Zn dissolution from inorganic mineral acids and obtaining the best Zn-Pb and Zn-Fe selectivity.

The optimal dosage of citric acid is 1.0 M concentration, which 91% Zn was obtained in 80 ^{o}C leaching temperature, 180 min. time leaching and at a rate of 2/10 S/L. Zn-Pb selectivity is 72%, Zn-As selectivity is 76%, and Zn-Fe selectivity is 72%. With 1.0 M malic acid, 92% Zn, 8% Pb and 3% Fe were dissolved in 80 ^{o}C temperature, 60 min. leaching time and 1/10 S/L ratio. Oxalic acid does not dissolve Zn and Pb. With 1.0 M oxalic acid, 96% Fe and 69% As were dissolved in 180 minutes at 60 ^{o}C, with very low Zn and Pb solubility during leaching and at a rate of 1/10 S/L. 1.0 M formic acid was obtained selectively Zn by a maximum of 82% without dissolution of Pb and Fe.

With 0.375 M EDTA concentration, 95% Zn with 28% Pb were achieved in 80 ^{o}C leaching temperature, 120 min. leaching time and at a rate of 1/10 S/L. The selectivity of Zn-Fe is 82%. The sequence of metal dissolution is Zn>Pb>Fe.

Under the tested conditions, ascorbic acid, ammonium acetate, ammonium hydroxide, ammonium sulfate, ammonium oxalate, tartaric acid, glycerin dissolve the desired base metals lower than our target value. Ammonium chloride dissolved both Zn and Ag, and alkali NaOH dissolved both Zn and Pb together. It dissolves Zn and Pb simultaneously without Fe. with 5.0 M NaOH alkali 81.4% Zn and 47% Pb obtained in 80 ^{o}C leaching temperature and 180 min. during the leaching and rate of 1/10 S/L. 50% NH_4OH was dissolved 61.3% Zn at a rate of 1/10 S/L, at a leaching temperature of 80 ^{o}C and at a leaching rate of 180 min. The dissolution of metals is significantly increased with a decrease in pH, the addition of chelate reagent, which binds to the metal in a balanced, annular coordinated complex. Increases in leaching temperature and time generally had a positive effect on metal dissolution as expected.

It is possible to use environmentally friendly organic 1.0 M citric and malic acids together with 1.0 M H_2SO_4 in the first stage Zn leaching. Since organic acids are weaker acids, they usually require higher temperatures and leaching time in both organic acids. it gives the highest Zn dissolution and high Fe and As solubility at a leaching temperature of 80 ^oC and 180 min during leaching. Organic acids slightly dissolve Pb, while H_2SO_4 does not.

The maximum 95% Pb, 10% Zn and 27.4% Fe impurity were obtained from H_2SO_4 residues at a leaching temperature of 40 ^oC at a concentration of 3.75 M NaOH + 1.88 M KNa-tartrate at a leaching time of 120 min and a rate of 1/10 S/L.

It was obtained a maximum of 86.6% Pb, 30.9% Zn and 29.9% Fe impurities from citric acid residues at a concentration of 3.75 M NaOH + 1.88 M KNa-tartrate at a leaching temperature of 25 ^oC at a leaching time of 120 min and at a rate of 1/10 S/L.

It was obtained a maximum of 85% Pb, 19% Zn and 28.3% Fe impurities from malic acid residues at a leaching temperature of 25 ^oC at a concentration of 3.75 M NaOH + 1.88 M KNa-tartrate at a leaching time of 120 min and at a rate of 1/10 S/L.

8420 mg/L Pb was obtained from citric acid, 8270 mg/L Pb was obtained from H_2SO_4 and 8100 mg/L Pb was obtained from malic acid leaching residue. The second stage is the sequence of H_2SO_4 > malic acid > citric acid residue in terms of both Pb-Zn and Pb-Fe selectivity in Pb leaching.

The second stage Pb leaching residues were subjected to the third stage Ag leaching at different pH and times at room temperature with ammonium thiosulfate/sodium thiosulfate + $CuSO_4.5H_2O$. The concentration of 30 g/L $(NH_4)_2S_2O_3$ was determined to be the best reagent dosage. A solution of 87.6% Ag at pH: 10.5 in 4 hours was obtained from H_2SO_4 residue, 92% Ag at pH: 9.5 in 4 hours from citric acid residue, and 91.4% Ag at pH: 9.5 in 4 hours from malic acid residue.

Hydrolytic Fe and As impurities were removed by precipitating more than 99% with $NaOH+H_2O_2$ at a temperature of 50 ^oC, pH: 3.5 and in 1 hour. A collapse has formed in the amorphous structure in the form of $Fe(OH)_3$, jarosite and goethite. Citric and malic acid PLS did not respond to hydrolytic precipitation. With H_2SO_4, the Pb impurity was precipitated at room temperature and for 30 min. It was precipitated from citric acid PLS in the form of 98.9% Pb at pH: 1.0 and malic acid PLS in the form of 96.7% Pb lead sulfate at pH: 0.5.

After the second step of leaching studies with NaOH and KNaTartrate for Pb dissolution, another stage of experiments was carried out using 1.0 M Na_2S with H_2SO_4, citric acid, and malic acid PLS for PbS and ZnS precipitation at room temperature for 30 minutes. While Zn was precipitated 100% from all PLS, Pb was precipitated 98.6% from H_2SO_4 PLS, 99% from citric acid PLS and 98.8% from malic acid PLS. The liquid product obtained from sediment filtration contains the by-product Na_2SO_4.

After the precipitation test in H_2SO_4 PLS, the solvent extraction experiments carried out using 20% D2EHPA+Hexane. 98% Zn extracted in pH: 2.6, the ratio of organic/liquid (O/A) 1/1, 10 min, 400 rpm and 25 ^oC. The loaded organic stripped with diluted sulfuric acid at pH 0.25 in two steps, 10 min and 25 ^oC.

D2EHPA and Cyanex272 were used for the solvent extraction experiment of citric acid PLS. 20% D2EHPA was selected as an optimum organic and concentration after the different concentration of the organic were tested. From the solvent extraction experiments of citric acid PLS, 98.3% Zn, a substantial amount of Ca (79%) and a small amount of Mg (14.7%), as well as a small amount of Fe (8.6 %), was transferred to organic phase with 20% D2EHPA at pH: 3.6, 10 min, 25 ^oC and A/O: 1/1. The greatest separation factor (β) between Fe and Zn was discovered to be 613.

According to McCabe-Thiele findings, 10247 mg/L of Zinc was loaded in organic solution at a 1:1 operating line (O/A) in one counter-current stage under ideal solvent extraction conditions. At pH 4.5, the loaded organic solution was carried to the scrubbing stage, where a 20 g/L Zinc solution was utilized to remove around 91% Ca and 34% Mg. The loaded organic phase was stripped of 100% Zn and 27 % Ca for 10 minutes at pH 0.25 and a one-to-one O/A ratio. Minerals observed in the loaded strip solution, calcium and magnesium, had no reversible effect on the zinc electrowinning process. HCl was used to remove Fe from a stripped organic solution at pHs 4, 5, and 6. As the results demonstrate, Fe was almost totally removed from solution at pH 5, and Ca and Mg removal reduced as pH increased.

The solvent extraction of malic leach solution was studied with different concentration of D2EHPA and Cyanex272. With 10% D2EHPA, 99.3% zinc was transferred into the organic phase, along with a significant amount of 76.6% Ca and a little amount of 19.2% Fe and 18% Mg, at pH 4.2, A/O ratio of 1.0 at 25 °C for 10 minutes. At pH 0.5, most of Zn and Ca with 47.8% of Mg, were removed from the loaded organic phase.

In the electrowinning of the stripped solution, 99.7% Zn was achieved from the H_2SO_4 PLS with current of 0.75A (500 A/m^2 current density) using Pb anode and an Al cathode electrode for 4 hours. With 1.0 A current (700 A/m^2 current density) 99.3% Zn was achieved from stripped citric acid PLS in 4 hours. a maximum of 97% Zn was obtained from malic acid PLS in 0.75 A current (500 A/m^2 current density) in 4 hours. . On the cathode surface, the deposited zinc was crystalline, gray in color, compact, and fine-grained.

If the base and precious metals in the flotation tailing are recovered with 100% efficiency, 57.7 kg Zn, 75 kg Pb and 101 g Ag can be recovered from 1 ton of processed waste. When these were evaluated with the price of the London Metal Exchange, the value of 1 ton of waste was found to be $ 437. Three companies in Kayseri sell these wastes to China and/or Iran for $30-50/t. The absence of Au in flotation tailing is a disadvantage. However, the hydrometallurgical recycling of these hazardous wastes is very important for environmental protection, secondary metal production and for job creation.

Due to the fact that this flotation tailing is a complex and carbonated waste and does not contain any gold in it, the use of bulk leaching instead of mixed tank leaching in the leaching process can provide a significant advantage in operating costs.

5.2. Recommendations

The goal of this study was to find the best process factors for recovering base and precious metals. The following subjects may be of interest to academics interested in working on this issue.

- The effect of particle size on the leaching can be studied.
- The effect of the ultrasonic treatment technic in the leaching can be researched. According to literature, this can improve metal extraction.
- The effect of adding HCl to the leaching media in the brine leaching can be investigated for increasing Pb dissolution.
- Using brine leaching and HCl in the third step leaching for recovery of silver could be studied.
- The effect of pH and reagent concentration can be studied in the third step leaching for recovery of silver from citric and malic leach residue.
- Recovery of Fe from oxalic acid leach solution can be investigated.
- Precipitation experiments in H_2SO_4 PLS at temperatures above 95 °C produce hematite instead of amorphous goethite. Hematite can be used for steel production if Fe grade is more than 50%.
- In the solvent extraction experiments with Cyanex272 in H_2SO_4 PLS using TBP as a modifier can be helpful for zinc extraction.
- D2EHPA and Cyanex 272 can be used in a synergistic solvent extraction system for extraction of zinc without any impurities.
- At high synthetic Zn concentration, the effect of the SX current efficiency in electrowinning should be studied.

REFERENCES

Abali, Y., Bayca, S.U., Gumus, R., 2017. Dissolution kinetics of smithsonite in boric acid solutions. Physicochem. Probl. Miner. Process. ISSN 2084-4735 538 kB. https://doi.org/10.5277/PPMP170113

Abdel-Aal, E.A., 2000. Kinetics of sulfuric acid leaching of low-grade zinc silicate ore. Hydrometallurgy 55, 247–254. https://doi.org/10.1016/S0304-386X(00)00059-1

Abdel-Aal, E.-S.A., Rashad, M.M., El-Shazly, A.N., Ibrahim, I.A., El-Shahat, M.F., 2016. Hydrometallurgical treatment of non-sulfide zinc ore for precipitation of zinc oxide nanoparticles. Physicochem. Probl. Miner. Process. ISSN 2084-4735 556 kB. https://doi.org/10.5277/PPMP160217

Abkhoshk, E., Jorjani, E., Al-Harahsheh, M.S., Rashchi, F., Naazeri, M., 2014. Review of the hydrometallurgical processing of non-sulfide zinc ores. Hydrometallurgy 149, 153–167. https://doi.org/10.1016/j.hydromet.2014.08.001

Addemir O., Açma E., Arslan C., 1994, ÇİNKO, Sistem Yayıncılık.

Adhia, J.D., 1969. Effect and control of impurities in electrolytic zinc production 10.

Alizadeh, R., Rashchi, F., Vahidi, E., 2011. Recovery of zinc from leach residues with minimum iron dissolution using oxidative leaching. Waste Manag. Res. J. Sustain. Circ. Econ. 29, 165–171. https://doi.org/10.1177/0734242X10372661

Amer, S., Figueiredo, J.M., Luis, A., 1995. The recovery of zinc from the leach liquors of the CENIM-LNETI process by solvent extraction with di(-2-ethylhexyl)phosphoric acid. Hydrometallurgy 37, 323–337. https://doi.org/10.1016/0304-386X(94)00040-A

Antonijević, M.M., Dimitrijević, M.D., Stevanović, Z.O., Serbula, S.M., Bogdanovic, G.D., 2008. Investigation of the possibility of copper recovery from the flotation tailings by acid leaching. J. Hazard. Mater. 158, 23–34. https://doi.org/10.1016/j.jhazmat.2008.01.063

REFERENCES (continued)

Antuñano, N., Herrero, D., Arias, P.L., Cambra, J.F., 2013. Electrowinning studies for metallic zinc production from double leached Waelz oxide. Process Saf. Environ. Prot. 91, 495–502. https://doi.org/10.1016/j.psep.2012.10.014

Asadi, T., Azizi, A., Lee, J., Jahani, M., 2017. Leaching of zinc from a lead-zinc flotation tailing sample using ferric sulphate and sulfuric acid media. J. Environ. Chem. Eng. 5, 4769–4775. https://doi.org/10.1016/j.jece.2017.09.005

Ashtari, P., Pourghahramani, P., 2015. Selective mechanochemical alkaline leaching of zinc from zinc plant residue. Hydrometallurgy 156, 165–172. https://doi.org/10.1016/j.hydromet.2015.03.017

Aykac, Y., 2006, Recovery of zinc from lead-zinc flotation tailings of oxide-sulfide Pb-Zn ores by hydrometallurgical processes, M.Sc. Thesis, Istanbul Technic University, 59p.

Aylmore, M.G., Muir, D.M., 2001. Thiosulfate leaching of gold—A review. Miner. Eng. 14, 135–174. https://doi.org/10.1016/S0892-6875(00)00172-2

Azizi, A., Ghasemi, S.M.S., 2017. A comparative analysis of the dissolution kinetics of lead from low grade oxide ores in HCl, H_2SO_4, HNO_3 and citric acid solutions. Metall. Res. Technol. 114, 406. https://doi.org/10.1051/metal/2017014

Baba, A.A., Adekola, F.A., 2011. Beneficiation of a Nigerian sphalerite mineral: Solvent extraction of zinc by Cyanex®272 in hydrochloric acid. Hydrometallurgy 109, 187–193. https://doi.org/10.1016/j.hydromet.2011.06.004

Babcan, J., 1971, “Synthesis of jarosite, KFe3(SO4)2(OH)6,” Geol Zb., Vol 22, No. 2, pp. 299-304.

Badanoiu, G., Buzatu, T., Buzatu, M., Butu, M., 2013. Study Concerning PbO Solubility in NaOH Solution for the Treatment of Sulfate-oxide Pastes Obtained from Dismantling used Lead-acid Batteries. REV CHIM 8.

REFERENCES (continued)

Bae, M., Kim, S., Sohn, J., Yang, D., Lee, H., 2020. Leaching Behavior of Gold and Silver from Concentrated Sulfide Ore Using Ammonium Thiosulfate. Metals 10, 1029. https://doi.org/10.3390/met10081029

Banijamali, S.H., Raygan, S., Amadeh, A.A., 2021. Leaching behavior of silver sulfide in the sodium thiosulfate-copper sulfate- sodium metabisulfite system. Miner. Eng. 174, 107275. https://doi.org/10.1016/j.mineng.2021.107275

Behnajady, B., Moghaddam, J., 2017. Selective leaching of zinc from hazardous As-bearing zinc plant purification filter cake. Chem. Eng. Res. Des. 117, 564–574. https://doi.org/10.1016/j.cherd.2016.11.019

Behnajady, B., Moghaddam, J., Behnajady, M.A., Rashchi, F., 2012. Determination of the Optimum Conditions for the Leaching of Lead from Zinc Plant Residues in NaCl–H_2SO_4–$Ca(OH)_2$ Media by the Taguchi Method. Ind. Eng. Chem. Res. 51, 3887–3894. https://doi.org/10.1021/ie202571x

Boni, M., Coppola, V., Dejonghe, L., Fedele, L., 2005. Willemite in the Belgian nonsulfide zinc deposits: a fluid inclusion study. Periodico di Mineralogia, 74, 87–100.

Bond, A.M., 1999. 200 years of practical electroanalytical chemistry: past, present and future directions illustrated by reference to the on-line, on-stream and off-line determination of trace metals in zinc plant electrolyte by voltammetric and potentiometric techniques, Anal. Chim. Acta. 400, pp. 333–379.

Boukerche, I., Djerad, S., Larba, R., Benmansour, L., Tifouti, L., 2018. Dissolution behavior of metallic zinc in organic acid. Environ. Res. 1, 8.

Canbazoğlu, M., Kaya, Ö., Kulaksız, M., Nizamoglu, Y., 2009, Zinc Recovery from Flotation Tailings with Sulphuric Acid Leaching, The XII International Mineral Processing Symposium, Nevşahir, 581- 587.

Chen, A., Zhao, Z. wei, Jia, X., Long, S., Huo, G., Chen, X., 2009. Alkaline leaching Zn and its concomitant metals from refractory hemimorphite zinc oxide ore. Hydrometallurgy 97, 228–232. https://doi.org/10.1016/j.hydromet.2009.01.005

REFERENCES (continued)

Chen, C.-S., Shih, Y.-J., Huang, Y.-H., 2016. Recovery of lead from smelting fly ash of waste lead-acid battery by leaching and electrowinning. Waste Manag. 52, 212–220. https://doi.org/10.1016/j.wasman.2016.03.056

Chia Aquije, L., 1993. Galvanic stripping of Fe^{+3} and Pb^{+2} ions and dissolution of metallic Fe, Zn, Pb and Cd using Di(2-ethylhexyl)phosphoric acid. Dr. Diss.

Chmielewski, T., Gibas, K., Borowski, K., Adamski, Z., Wozniak, B., Muszer, A., 2017. Chloride leaching of silver and lead from a solid residue after atmospheric leaching of flotation copper concentrates. Physicochem. Probl. Miner. Process. ISSN 2084-4735 472 kB. https://doi.org/10.5277/PPMP170218

Cole, P.M., Sole, K.C., 2003. Zinc solvent extraction in the process industries. Miner. Process. Extr. Metall. Rev. 24, 91–137. https://doi.org/10.1080/08827500306897

Cornell, R.M., Schwertmann, U., 1996. The Iron Oxides. VCH Publishers, New York (USA), p. 175.

Deep, A., de Carvalho, J.M.R., 2008. Review on the Recent Developments in the Solvent Extraction of Zinc. Solvent Extr. Ion Exch. 26, 375–404. https://doi.org/10.1080/07366290802179267

Demir, F., Laçin, O., Dönmez, B., 2006. Leaching Kinetics of Calcined Magnesite in Citric Acid Solutions. Ind. Eng. Chem. Res. 45, 1307–1311. https://doi.org/10.1021/ie0507629

Deng, J., Wen, S., Yin, Q., Wu, D., Sun, Q., 2017. Leaching of malachite using 5-sulfosalicylic acid. J. Taiwan Inst. Chem. Eng. 71, 20–27. https://doi.org/10.1016/j.jtice.2016.11.013

Deng, Jiushuai, Sun, Q., Lin, P., Song, G., Wen, S., Deng, Jianying, Wu, D., 2015. Dissolution Kinetics of Zinc Oxide Ore with an Organic Acid. Int. J. Metall. Mater. Eng. 1. https://doi.org/10.15344/2455-2372/2015/109

REFERENCES (continued)

Dhawan, N., Safarzadeh, M.S., Birinci, M., 2011. Kinetics of hydrochloric acid leaching of smithsonite. Russ. J. Non-Ferr. Met. 52, 209–216. https://doi.org/10.3103/S1067821211030059

Ding, Z., Yin, Z., Hu, H., Chen, Q., 2010. Dissolution kinetics of zinc silicate (hemimorphite) in ammoniacal solution. Hydrometallurgy 104, 201–206. https://doi.org/10.1016/j.hydromet.2010.06.004

Dou, A.C., Yang, T.Z., Yang, J.X., Wu, J.H., Wang, A., 2011. Leaching of low-grade zinc oxide ores in Ida2− −H2O system. Trans. Nonferrous Met. Soc, China 21, 2548-2553

Ehsani, I., Ucyildiz, A., Obut, A., 2018. Leaching behaviour of zinc from a smithsonite ore in sodium hydroxide solutions. Physicochem. Probl. Miner. Process. ISSN 2084-4735. https://doi.org/10.5277/PPMP18150

Erdem, M., Yurten, M., 2015. Kinetics of Pb and Zn leaching from zinc plant residue by sodium hydroxide. J. Min. Metall. Sect. B Metall. 51, 89–95. https://doi.org/10.2298/JMMB140503012E

Espiari, S., Rashchi, F., Sadrnezhaad, S.K., 2006. Hydrometallurgical treatment of tailings with high zinc content. Hydrometallurgy 82, 54–62. https://doi.org/10.1016/j.hydromet.2006.01.005

Farahmand, F., Moradkhani, D., Safarzadeh, M.S., Rashchi, F., 2009. Brine leaching of lead-bearing zinc plant residues: Process optimization using orthogonal array design methodology. Hydrometallurgy 95, 316–324. https://doi.org/10.1016/j.hydromet.2008.07.012

Feng, L., Yang, X., Shen, Q., Xu, M., Jin, B., 2007. Pelletizing and alkaline leaching of powdery low grade zinc oxide ores. Hydrometallurgy 89, 305–310. https://doi.org/10.1016/j.hydromet.2007.08.002

REFERENCES (continued)

Ferracin, L.C., Chácon-Sanhueza, A.E., Davoglio, R.A., Rocha, L.O., Caffeu, D.J., Fontanetti, A.R., Rocha-Filho, R.C., Biaggio, S.R., Bocchi, N., 2002. Lead recovery from a typical Brazilian sludge of exhausted lead-acid batteries using an electrohydrometallurgical process. Hydrometallurgy 65, 137–144. https://doi.org/10.1016/S0304-386X(02)00087-7

Ficeriová, J., Baláž, P., Leon Villachica, C., 2005. Thiosulfate leaching of silver, gold and bismuth from a complex sulfide concentrates. Hydrometallurgy 77, 35–39. https://doi.org/10.1016/j.hydromet.2004.09.010

Field, T.B., McCourt, J.L., McBryde, W.A.E., 1974. Composition and Stability of Iron and Copper Citrate Complexes in Aqueous Solution. Can. J. Chem. 52, 3119–3124. https://doi.org/10.1139/v74-458

Free, M,. 2013, Hydrometallurgy Fundamentals and Applications. Hoboken, NJ: John Wiley & Sons Inc.

Fusi, L., Primicerio, M., Monti, A., 2015. A model for calcium carbonate neutralization in the presence of armoring. Appl. Math. Model. 39, 348–362. https://doi.org/10.1016/j.apm.2014.05.037

Gilg, H.A., Boni, M., Balassone, G., Allen, C.R., Banks, D., Moore, F., 2006. Marble-hosted sulfide ores in the Angouran Zn-(Pb–Ag) deposit, NW Iran: interaction of sedimentary brines with a metamorphic core complex. Miner. Deposita 41, 1–16. https://doi.org/10.1007/s00126-005-0035-5

Gu, H., Chang, C.-M., Barrera-Godínez, J.A., O'Keefe, T.J., 2000. Preliminary design of a solvent extraction process for the galvanic stripping of iron from D2EHPA. Min. Metall. Explor. 17, 16–22. https://doi.org/10.1007/BF03402824

Guimarães, A.S., Mansur, M.B., 2017. Solvent extraction of calcium and magnesium from concentrate nickel sulfate solutions using D2HEPA and Cyanex 272 extractants. Hydrometallurgy 173, 91–97. https://doi.org/10.1016/j.hydromet.2017.08.005

REFERENCES (continued)

Güler, E., Seyrankaya, A., 2016. Precipitation of impurity ions from zinc leach solutions with high iron contents - A special emphasis on cobalt precipitation. Hydrometallurgy 164, 118–124. https://doi.org/10.1016/j.hydromet.2016.06.010

Guler, E., Seyrankaya, A., Tufan, E., Coren, I., 2014, Removal of impurities ions from zinc sulfate solution by cementation, 14th International Mineral Symposium, Kusadasi, Turkey, 537-543.

Güler, E., Seyrankaya, A., Cöcen, I., 2011. Hydrometallurgical Evaluation of Zinc Leach Plant Residue. Asian J Chem 23, 10.

Guo, Z., Pan, F., Xiao, X., Zhang, L., Jiang, K., 2010. Optimization of brine leaching of metals from hydrometallurgical residue. Trans. Nonferrous Met. Soc. China 20, 2000–2005. https://doi.org/10.1016/S1003-6326(09)60408-8

Gupta, C.K., Mukherjee, T.K., 2020. Hydrometallurgy in Extraction Processes. CRC Press, Boca Raton. https://doi.org/10.1201/9780203751404

Gutknecht, T., Colombus, Y., Steenari, B.-M., 2017. Recycling Zinc from Metal Oxide Varistors Through Leaching and Cementation of Cobalt and Nickel. J. Sustain. Metall. 3, 239–250. https://doi.org/10.1007/s40831-016-0072-6

Habashi, F., 1970. Principles of extractive metallurgy. Vol3,. Gordon and Breach Science Publishers, New York.

Halli, P., Agarwal, V., Partinen, J., Lundström, M., 2020. Recovery of Pb and Zn from a citrate leach liquor of a roasted EAF dust using precipitation and solvent extraction. Sep. Purif. Technol. 236, 116264. https://doi.org/10.1016/j.seppur.2019.116264

Halli, P., Hamuyuni, J., Leikola, M., Lundström, M., 2018. Developing a sustainable solution for recycling electric arc furnace dust via organic acid leaching. Miner. Eng. 124, 1–9. https://doi.org/10.1016/j.mineng.2018.05.011

REFERENCES (continued)

Halli, P., Hamuyuni, J., Revitzer, H., Lundström, M., 2017. Selection of leaching media for metal dissolution from electric arc furnace dust. J. Clean. Prod. 164, 265–276. https://doi.org/10.1016/j.jclepro.2017.06.212

Hamada, Y.Z., Carlson, B., Dangberg, J., 2005. Interaction of Malate and Lactate with Chromium(III) and Iron(III) in Aqueous Solutions. Synth. React. Inorg. Met.-Org. Nano-Met. Chem. 35, 515–522. https://doi.org/10.1080/15533170500198887

Harmer, S.L., Goncharova, L.V., Kolarova, R., Lennard, W.N., Muñoz-Márquez, M.A., Mitchell, I.V., Nesbitt, H.W., 2007. Surface structure of sphalerite studied by medium energy ion scattering and XPS. Surf. Sci. 601, 352–361. https://doi.org/10.1016/j.susc.2006.10.001

Havlik, T., Souza, B., Bernardes, A., Schneider, I., Miskufova, A., 2006. Hydrometallurgical processing of carbon steel EAF dust. J. Hazard. Mater. 135, 311–318. https://doi.org/10.1016/j.jhazmat.2005.11.067

He, D., Yang, C., Wu, Y., Liu, X., Xie, W., Yang, J., 2017. PbSO4 Leaching in Citric Acid/Sodium Citrate Solution and Subsequent Yielding Lead Citrate via Controlled Crystallization. Minerals 7, 93. https://doi.org/10.3390/min7060093

Herrero, D., Arias, P.L., Cambra, J.F., Antuñano, N., 2011. Studies on impurity iron removal from zinc electrolyte using MnO2–H2O2. Hydrometallurgy 105, 370–373. https://doi.org/10.1016/j.hydromet.2010.11.010

Herrero, D., Arias, P.L., Güemez, B., Barrio, V.L., Cambra, J.F., Requies, J., 2010. Hydrometallurgical process development for the production of a zinc sulphate liquor suitable for electrowinning. Miner. Eng. 23, 511–517. https://doi.org/10.1016/j.mineng.2010.01.010

Hitzman, M.W., Reynolds, N.A., Sangster, D.F., Allen, C.R., Carman, C.E., 2003, Classification, genesis, and exploration guides for nonsulfide zinc deposits, Econ. Geol, 98, 685–714.

REFERENCES (continued)

Hollagh, A.R.E., Darvishi, D., Alamdari, E.K., Moradkhani, D., 2010. PROCESSING FOR EXTRACTION OF VALUABLE METALS FROM ZINC PLANT RESIDUE 12.

Hosseini, T., Rashchi, F., Vahidi, E., Mostoufi, N., 2010. Investigating the Synergistic Effect of D2EHPA and Cyanex 302 on Zinc and Manganese Separation. Sep. Sci. Technol. 45, 1158–1164. https://doi.org/10.1080/01496391003727908

Hu, G., Chen, D., Wang, L., Liu, J., Zhao, H., Liu, Y., Qi, T., Zhang, C., Yu, P., 2014. Extraction of vanadium from chloride solution with high concentration of iron by solvent extraction using D2EHPA. Sep. Purif. Technol. 125, 59–65. https://doi.org/10.1016/j.seppur.2014.01.031

Hurşit, M., Laçin, O., Saraç, H., 2009. Dissolution kinetics of smithsonite ore as an alternative zinc source with an organic leach reagent. J. Taiwan Inst. Chem. Eng. 40, 6–12. https://doi.org/10.1016/j.jtice.2008.07.003

Hussaini, S., Kursunoglu, S., Top, S., Ichlas, Z.T., Kaya, M., 2021a. Testing of 17-different leaching agents for the recovery of zinc from a carbonate-type Pb-Zn ore flotation tailing. Miner. Eng. 168, 106935. https://doi.org/10.1016/j.mineng.2021.106935

Hussaini, S., Tita, A.M., Kursunoglu, S., Top, S., Ichlas, Z.T., Kar, U., Kaya, M., 2021b. Pb-Zn recovery from a malic leach solution of a carbonate type ore flotation tailing by precipitation and solvent extraction. Sep. Purif. Technol. 272, 118963. https://doi.org/10.1016/j.seppur.2021.118963

Irannajad, M., Meshkini, M., Azadmehr, A.R., 2013. Leaching of zinc from low grade oxide ore using organic acid. Physicochem. Probl. Miner. Process. 49 547-555 ISSN 2084-4735. https://doi.org/10.5277/PPMP130215

ILZSG, 2020, Lead and zinc statistics monthly bulletin of the international lead zinc study group, www.ilzsg.org

IZA, 2011, International Zinc Association. http://www.zinc.org/basics/zinc_uses

REFERENCES (continued)

Jandová, J., Maixner, J., Grygar, T., 2002. Reprocessing Of Zinc Galvanic Waste Sludge by Selective Precipitation 4.

Jha, M.K., Kumar, V., Singh, R.J., 2001. Review of hydrometallurgical recovery of zinc from industrial wastes. Resour. Conserv. Recycl. 33, 1–22. https://doi.org/10.1016/S0921-3449(00)00095-1

Jia, N., Wang, H., Zhang, M., Guo, M., 2016. Selective and Efficient Extraction of Zinc from Mixed Sulfide–oxide Zinc and Lead Ore. Miner. Process. Extr. Metall. Rev. 37, 418–426. https://doi.org/10.1080/08827508.2016.1233874

Jiang, G., Peng, B., Liang, Y., Chai, L., Wang, Q., Li, Q., Hu, M., 2017. Recovery of valuable metals from zinc leaching residue by sulfate roasting and water leaching. Trans. Nonferrous Met. Soc. China 27, 1180–1187. https://doi.org/10.1016/S1003-6326(17)60138-9

Ju, S., Motang, T., Shenghai, Y., Yingnian, L., 2005. Dissolution kinetics of smithsonite ore in ammonium chloride solution. Hydrometallurgy 80, 67–74. https://doi.org/10.1016/j.hydromet.2005.07.003

Kagambega, N., Galvez, R., Ouattara, A., 2017. Three Commercial organic Acids for the Leaching of Metals from Tailings 10.

Karlsson, T., Cao, Y., Colombus, Y., Steenari, B.-M., 2018. Investigation of the kinetics and the morphology of cementation products formed during purification of a synthetic zinc sulfate electrolyte. Hydrometallurgy 181, 169–179. https://doi.org/10.1016/j.hydromet.2018.09.007

Kaya, M., Gul, E., Kursunoglu, S., Hussaini, S., 2019, Leaching of Oxidized Turkish Pb-Zn Flotation Tails by Inorganic Acids. 1st International Mineral Processing Congress (IMPC-EURASIA) 2019, Antalya, Turkey.

REFERENCES (continued)

Kaya, M., Hussaini, S., Kursunoglu, S., 2020a. Critical review on secondary zinc resources and their recycling technologies. Hydrometallurgy 195, 105362. https://doi.org/10.1016/j.hydromet.2020.105362

Kaya, M., Kursunoglu, S., Hussaini, S., Gül, E., 2020b. Leaching of Turkish Oxidized Pb-Zn Flotation Tails by Inorganic and Organic Acids 13.

Kaya, Ö., SeriN Çakir, F., 2019. Recovery of Zinc from Zinc Oxide Ore by Sulfuric Acid Leaching. Cumhur. Sci. J. https://doi.org/10.17776/csj.463775

Krupka, D., Ochab, B., Miernik, J., 2000. The Boleslaw Electrolytic Zinc Plant, in: Lead-Zinc 2000. John Wiley & Sons, Ltd, pp. 277–286. https://doi.org/10.1002/9781118805558.ch16

Kukurugya, F., Vindt, T., Havlík, T., 2015. Behavior of zinc, iron and calcium from electric arc furnace (EAF) dust in hydrometallurgical processing in sulfuric acid solutions: Thermodynamic and kinetic aspects. Hydrometallurgy 154, 20–32. https://doi.org/10.1016/j.hydromet.2015.03.008

Kursun, I., Ozdemir, O., Eskibalci, M.F., Hacifazlioglu, H., Terzi, M., 2017. Dissolution of Lead from Lead-Zinc Tailings with Nitric Acid 8.

Kursunoglu, S., Ichlas, Z.T., Kaya, M., 2017. Solvent extraction process for the recovery of nickel and cobalt from Caldag laterite leach solution: The first bench scale study. Hydrometallurgy 169, 135–141. https://doi.org/10.1016/j.hydromet.2017.01.001

Kursunoglu, S., Kursunoglu, N., Hussaini, S., Kaya, M., 2021. Selection of an appropriate acid type for the recovery of zinc from a flotation tailing by the analytic hierarchy process. J. Clean. Prod. 283, 124659. https://doi.org/10.1016/j.jclepro.2020.124659

Langová, Š. Riplová, J., Vallová, S., 2007. Atmospheric leaching of steel-making wastes and the precipitation of goethite from the ferric sulphate solution. Hydrometallurgy 87, 157–162. https://doi.org/10.1016/j.hydromet.2007.03.002

REFERENCES (continued)

Larba, R., Boukerche, I., Alane, N., Habbache, N., Djerad, S., Tifouti, L., 2013. Citric acid as an alternative lixiviant for zinc oxide dissolution. Hydrometallurgy 134–135, 117–123. https://doi.org/10.1016/j.hydromet.2013.02.002

Large, D., 2001, the geology of non-sulphide zinc deposits—an overview, Erzmetall, 54, 264–276.

Li, H., Li, S., Srinivasakannan, C., Zhang, L., Yin, S., Yang, K., Xie, H., 2018. Efficient cleaning extraction of silver from spent symbiosis lead-zinc mine assisted by ultrasound in sodium thiosulfate system. Ultrason. Sonochem. 49, 118–127. https://doi.org/10.1016/j.ultsonch.2018.07.034

Li, L., Xu, Z., Wu, J., Tian, G., 2010. Bioaccumulation of heavy metals in the earthworm Eisenia fetida in relation to bioavailable metal concentrations in pig manure. Bioresour. Technol. 101, 3430–3436. https://doi.org/10.1016/j.biortech.2009.12.085

Li, M., Yang, J., Liang, S., Hou, H., Hu, J., Liu, B., Kumar, R.V., 2019. Review on clean recovery of discarded/spent lead-acid battery and trends of recycled products. J. Power Sources 436, 226853. https://doi.org/10.1016/j.jpowsour.2019.226853

Li, Q., Zhang, B., Min, X., Shen, W., 2013. Acid leaching kinetics of zinc plant purification residue. Trans. Nonferrous Met. Soc. China 23, 2786–2791. https://doi.org/10.1016/S1003-6326(13)62798-3

Lide, D.R., 1978, Handbook of Chemistry and physics, The Chemical Co.

Lins, V. de F.C., Abelha, R., Castro, M. das M.R. de, Souza, M.M.D. de, Moraes, L.L. de, Araújo, C.R., Matencio, T., 2010. Effect of iron on energy consumption and current efficiency of zinc electrowinning from sulfate solutions. Tecnol. Em Metal. E Mater. 7, 61–66. https://doi.org/10.4322/tmm.00701011

Liu, Q., Yang, S., Chen, Y., He, J., Xue, H., 2014. Selective recovery of lead from zinc oxide dust with alkaline Na2EDTA solution. Trans. Nonferrous Met. Soc. China 24, 1179–1186. https://doi.org/10.1016/S1003-6326(14)63177-0

REFERENCES (continued)

Liu, Q., Zhao, Y., Zhao, G., 2011. Production of zinc and lead concentrates from lean oxidized zinc ores by alkaline leaching followed by two-step precipitation using sulfides. Hydrometallurgy 110, 79–84. https://doi.org/10.1016/j.hydromet.2011.08.009

Liu, W., Li, W., Han, J., Wu, D., Li, Z., Gu, K., Qin, W., 2019. Preparation of calcium stannate from lead refining slag by alkaline leaching-purification-causticization process. Sep. Purif. Technol. 212, 119–125. https://doi.org/10.1016/j.seppur.2018.11.024

Long, H., Chai, L., Qin, W., Tang, S., 2010. Solvent extraction of zinc from zinc sulfate solution. J. Cent. South Univ. Technol. 17, 760–764. https://doi.org/10.1007/s11771-010-0553-x

Lottering, C., 2006. Leaching Of Secondary Zinc Oxides Using Sulphuric Acid. Master thesis, Stellenbosch University.

Lu, J., Guo, H., Dreisinger, D., Downing, B., 2013. Effects of Current Density and Nickel as an Impurity on Zinc Electrowinning. J. Metall. Eng. 2, 9.

Ma, C., Shu, Y., Chen, H., 2015. Recycling lead from spent lead pastes using oxalate and sodium oxalate and preparation of novel lead oxide for lead-acid batteries. RSC Adv. 5, 94895–94902. https://doi.org/10.1039/C5RA18627G

Mackinnon, D.J., Brannen, J.M., Morrison, R.M., 1983. Zinc electrowinning from aqueous chloride electrolytes. J. Appl. Electrochem. 13, 39–53. https://doi.org/10.1007/BF00615886

Majima, H., Awakura, Y., Tsugui, K., Peters, E., 1990. Fundamental studies on chlorine behavior as related to zinc electrowinning from aqueous chloride electrolytes. Metall. Trans. B 21, 251–258. https://doi.org/10.1007/BF02664192

Martín, D., Díaz, G., García, M.A., Sánchez, F., 2002. Extending zinc production possibilities through solvent extraction 6.

REFERENCES (continued)

Mbedzi, N., Ibana, D., Dyer, L., Browner, R., 2017. The effect of oxidant addition on ferrous iron removal from multi-element acidic sulphate solutions. Presented at the Proceedings Of The 1st International Process Metallurgy Conference (IPMC 2016), West Java, Indonesia, p. 030002. https://doi.org/10.1063/1.4974413

Mirza, A., 2016. Corrosion of lead anodes in base metals electrowinning. J. South. Afr. Inst. Min. Metall. 116, 533–538. https://doi.org/10.17159/2411-9717/2016/v116n6a7

Moghaddam, J., Sarraf-Mamoory, R., Yamini, Y., Abdollahy, M., 2005. Determination of the Optimum Conditions for the Leaching of Nonsulfide Zinc Ores (High-SiO_2) in Ammonium Carbonate Media. Ind. Eng. Chem. Res. 44, 8952–8958. https://doi.org/10.1021/ie050479+

Montenegro, V., Agatzini-Leonardou, S., Oustadakis, P., Tsakiridis, P., 2016. Hydrometallurgical Treatment of EAF Dust by Direct Sulphuric Acid Leaching at Atmospheric Pressure. Waste Biomass Valorization 7, 1531–1548. https://doi.org/10.1007/s12649-016-9543-z

Moradi, S., Monhemius, A.J., 2011. Mixed sulphide–oxide lead and zinc ores: Problems and solutions. Miner. Eng. 24, 1062–1076. https://doi.org/10.1016/j.mineng.2011.05.014

Najiba, S., 2009. Recovery of Zinc from Ash of Galvanizing Plant by Hydrometallurgical Route 92.

Nischwitz, V., Michalke, B., 2009. Electrospray ionisation with selected reaction monitoring for the determination of Mn-citrate, Fe-citrate, Cu-citrate and Zn-citrate. Rapid Commun. Mass Spectrom. 23, 2338–2346. https://doi.org/10.1002/rcm.4156

Nworie, O., Qin, J., Lin, C., 2017. Differential Effects of Low-Molecular-Weight Organic Acids on the Mobilization of Soil-Borne Arsenic and Trace Metals. Toxics 5, 18. https://doi.org/10.3390/toxics5030018

Onal, G, 1998 Turkey lead inventory, Istanbul exporters association, 16p.

REFERENCES (continued)

Oustadakis, P., Tsakiridis, P.E., Katsiapi, A., Agatzini-Leonardou, S., 2010. Hydrometallurgical process for zinc recovery from electric arc furnace dust (EAFD). J. Hazard. Mater. 179, 1–7. https://doi.org/10.1016/j.jhazmat.2010.01.059

Pakarinen, J., Paatero, E., 2011. Recovery of manganese from iron containing sulfate solutions by precipitation. Miner. Eng. 24, 1421–1429. https://doi.org/10.1016/j.mineng.2011.06.004

Peng, N., Peng, B., Chai, L., Liu, W., Li, M., Yuan, Y., Yan, H., Hou, D.-K., 2012. Decomposition of Zinc Ferrite in Zinc Leaching Residue by Reduction Roasting. Procedia Environ. Sci. 16, 705–714. https://doi.org/10.1016/j.proenv.2012.10.097

Pereira, D., Rocha, S., Mansur, M., 2007. Recovery of zinc sulphate from industrial effluents by liquid–liquid extraction using D2EHPA (di-2-ethylhexyl phosphoric acid). Sep. Purif. Technol. 53, 89–96. https://doi.org/10.1016/j.seppur.2006.06.013

Ppourbaix, M, 1974, Atlas of Electrochemical Equilibria in - Aqueous Solutions, NACE International Cebelcor.

Qin, W., Lan, Z., Li, W., 2003. Recovery of zinc from low-grade zinc oxide ores by solvent extraction. J. Cent. South Univ. Technol. 10, 98–102. https://doi.org/10.1007/s11771-003-0047-1

Qin, W., Li, W., Lan, Z., Qiu, G., 2007. Simulated small-scale pilot plant heap leaching of low-grade oxide zinc ore with integrated selective extraction of zinc. Miner. Eng. 20, 694–700. https://doi.org/10.1016/j.mineng.2007.01.004

Rao, S., Yang, T., Zhang, D., Liu, W., Chen, L., Hao, Z., Xiao, Q., Wen, J., 2015. Leaching of low grade zinc oxide ores in NH4Cl–NH3 solutions with nitrilotriacetic acid as complexing agents. Hydrometallurgy 158, 101–106. https://doi.org/10.1016/j.hydromet.2015.10.013

REFERENCES (continued)

Ritcey, G.M., Ashbrook, A.W., 1979. Solvent extraction : principles and applications to process metallurgy. undefined.

Ritcey, G. M. Solvent Extraction, Principles and Applications to Process Metallurgy; 2nd ed.; Ritcey & Associates Inc.: Ottawa, Canada, 2006; Vol. 1 and 2.

Rudnik, E., 2019a. Recovery of zinc from zinc ash by leaching in sulphuric acid and electrowinning. Hydrometallurgy 188, 256–263. https://doi.org/10.1016/j.hydromet.2019.07.006

Rudnik, E., 2019b. Investigation of industrial waste materials for hydrometallurgical recovery of zinc. Miner. Eng. 139, 105871. https://doi.org/10.1016/j.mineng.2019.105871

Rusen, A., 2007. Recovery of zinc and lead from çinkur leach residues by using hydrometallurgical techniques. A Thesis Submitted To The Graduate School Of Natural And Applied Sciences Of Middle East Technical University 114.

Ruşen, A., Sunkar, A.S., Topkaya, Y.A., 2008. Zinc and lead extraction from Çinkur leach residues by using hydrometallurgical method. Hydrometallurgy 93, 45–50. https://doi.org/10.1016/j.hydromet.2008.02.018

Şahin, M., Erdem, M., 2015. Cleaning of high lead-bearing zinc leaching residue by recovery of lead with alkaline leaching. Hydrometallurgy 153, 170–178. https://doi.org/10.1016/j.hydromet.2015.03.003

Salgado, A., 2003. Recovery of zinc and manganese from spent alkaline batteries by liquid–liquid extraction with Cyanex 272. J. Power Sources 115, 367–373. https://doi.org/10.1016/S0378-7753(03)00025-9

Sami, V., 2013, Hydrometallurgical recovery of valuable metals from secondary raw material, PhD Thesis, Lappeenranta University of Technology.

Sethurajan, M., 2015, Metallurgical sludges – Bio/leaching and heavy metals recovery (Zn & Cu), PhD Thesis, University of Paris-Est, 232p.

REFERENCES (continued)

Santos, F.M.F., Pina, P.S., Porcaro, R., Oliveira, V.A., Silva, C.A., Leão, V.A., 2010. The kinetics of zinc silicate leaching in sodium hydroxide. Hydrometallurgy 102, 43–49. https://doi.org/10.1016/j.hydromet.2010.01.010

Seyed Ghasemi, S.M., Azizi, A., 2018. Alkaline leaching of lead and zinc by sodium hydroxide: kinetics modeling. J. Mater. Res. Technol. 7, 118–125. https://doi.org/10.1016/j.jmrt.2017.03.005

Seyed Ghasemi, S.M., Azizi, A., 2016. Investigation of leaching kinetics of zinc from a low-grade ore in organic and inorganic acids. J. Min. Environ. https://doi.org/10.22044/jme.2016.767

Shawabkeh, R.A., 2010. Hydrometallurgical extraction of zinc from Jordanian electric arc furnace dust. Hydrometallurgy 104, 61–65. https://doi.org/10.1016/j.hydromet.2010.04.014

Singh, V., 1996. Technological innovation in the zinc electrolyte purification process of a hydrometallurgical zinc plant through reduction in zinc dust consumption. Hydrometallurgy 40, 247–262. https://doi.org/10.1016/0304-386X(94)00054-7

Song, B.X., West Chester, W., 2004. Process of preparing in-situ water-soluble zinc salt for use in automatic dishwashing compositions. Pat. US 2004, A1.

Song, K., Yuan, J., Shen, P., Li, Jialei, Li, Jianmin, liu, D., 2018. Research on Leaching Performance of Low Grade Zinc Oxide Ore in the System of $(NH_4)_2SO_4$-NH_3-H_2O. IOP Conf. Ser. Earth Environ. Sci. 170, 022114. https://doi.org/10.1088/1755-1315/170/2/022114

Song, S., Sun, W., Wang, L., Liu, R., Han, H., Hu, Y., Yang, Y., 2019. Recovery of cobalt and zinc from the leaching solution of zinc smelting slag. J. Environ. Chem. Eng. 7, 102777. https://doi.org/10.1016/j.jece.2018.11.022

SOP, 2001, Specialization Commission Metallic Mines Sub-Commission Lead-Zinc-Cadmium Study Group Report, Ankara.

REFERENCES (continued)

Sun, B., Zhao, F.J., Lombi, E., McGrath, S.P., 2001. Leaching of heavy metals from contaminated soils using EDTA. Environ. Pollut. 113, 111–120. https://doi.org/10.1016/S0269-7491(00)00176-7

Sunkar, A.S., 2005, Investigation and development of possible leaching processes for recovery of zinc and lead from çinkur leach residues, M.Sc Thesis, Middle East Technical University, 87p.

Svens, K., 2010. Outotec atmospheric zinc concentrate direct leaching process - Past, present and future. World Metall. - ERZMETALL 63, 136–144.

Talan, D., Atalay, M.Ü., Altun, N.E., 2017. Extraction of Zinc from Smithsonite by Ammonia Leaching. Presented at the The 3rd World Congress on Mechanical, Chemical, and Material Engineering. https://doi.org/10.11159/mmme17.130

Tanong, K., Tran, L.-H., Mercier, G., Blais, J.-F., 2017. Recovery of Zn (II), Mn (II), Cd (II) and Ni (II) from the unsorted spent batteries using solvent extraction, electrodeposition and precipitation methods. J. Clean. Prod. 148, 233–244. https://doi.org/10.1016/j.jclepro.2017.01.158

Thompson, M., 2006, Base Metal Handbook, Third ed. Wood Head Publishing Limited, Cambridge, England.

Tripathy, B.C., Das, S.C., Misra, V.N., 2003. Effect of antimony(III) on the electrocrystallisation of zinc from sulphate solutions containing SLS. Hydrometallurgy 69, 81–88. https://doi.org/10.1016/S0304-386X(02)00204-9

Tsakiridis, P.E., Oustadakis, P., Katsiapi, A., Agatzini-Leonardou, S., 2010. Hydrometallurgical process for zinc recovery from electric arc furnace dust (EAFD). Part II: Downstream processing and zinc recovery by electrowinning. J. Hazard. Mater. 179, 8–14. https://doi.org/10.1016/j.jhazmat.2010.04.004

Turan, M.D., Altundoğan, H.S., Tümen, F., 2004. Recovery of zinc and lead from zinc plant residue. Hydrometallurgy 75, 169–176. https://doi.org/10.1016/j.hydromet.2004.07.008

REFERENCES (continued)

U.S.Geological Survey, 2020, Mineral commodity summaries, https://pubs.usgs.gov/periodicals/mcs2020/mcs202-zinc.pdf.

U.S.Geological Survey, 2020, Minerla commodity summaries. https://pubs.usgs.gov/periodicals/mcs2020/mcs202-lead.pdf.

Vahidi, E., Rashchi, F., Moradkhani, D., 2009. Recovery of zinc from an industrial zinc leach residue by solvent extraction using D2EHPA. Miner. Eng. 22, 204–206. https://doi.org/10.1016/j.mineng.2008.05.002

Volpe, M., Oliveri, D., Ferrara, G., Salvaggio, M., Piazza, S., Italiano, S., Sunseri, C., 2009. Metallic lead recovery from lead-acid battery paste by urea acetate dissolution and cementation on iron. Hydrometallurgy 96, 123–131. https://doi.org/10.1016/j.hydromet.2008.09.001

Vukosav, P., Tomišić, V., Mlakar, M., 2010. Iron(III)-Complexes Engaged in the Biochemical Processes in Seawater. II. Voltammetry of Fe(III)-Malate Complexes in Model Aqueous Solution. Electroanalysis 22, 2179–2186. https://doi.org/10.1002/elan.200900632

Wang, L., Mu, W., Shen, H., Liu, S., Zhai, Y., 2015. Leaching of lead from zinc leach residue in acidic calcium chloride aqueous solution. Int. J. Miner. Metall. Mater. 22, 460–466. https://doi.org/10.1007/s12613-015-1094-y

Wang, R., Tang, M., Yang, S., Zhagn, W., Tang, C., He, J., Yang, J., 2008. Leaching kinetics of low grade zinc oxide ore in NH3-NH4Cl-H2O system. J. Cent. South Univ. Technol. 15, 679–683. https://doi.org/10.1007/s11771-008-0126-4

Warner, N.A., 2009, Towards zinc metal at McArthur River. Miner. Eng, 22, pp727–741

Wikipedia, 2020, The Free Encyclopedia, Zinc, Last Accessed: 2020, http://en.wikipedia.org/wiki/Zinc

Wikipedia, 2020, https://en.m.wikipedia.org/wiki/Lead

REFERENCES (continued)

Wu, D.D., Wen, S.M., Yang, J., Deng, J.S., 2015. Investigation of dissolution kinetics of zinc from smithsonite in 5-sulphosalicylic acid solution. Can. Metall. Q. 54, 51–57. https://doi.org/10.1179/1879139514Y.0000000150

Xia, Z., Zhang, X., Huang, X., Yang, S., Chen, Y., Ye, L., 2020. Hydrometallurgical stepwise recovery of copper and zinc from smelting slag of waste brass in ammonium chloride solution. Hydrometallurgy 197, 105475. https://doi.org/10.1016/j.hydromet.2020.105475

Xie, H., Zhang, L., Li, H., Koppala, S., Yin, S., Li, S., Yang, K., Zhu, F., 2019. Efficient recycling of Pb from zinc leaching residues by using the hydrometallurgical method. Mater. Res. Express 6, 075505. https://doi.org/10.1088/2053-1591/ab11b9

Xing, P., Wang, C., Wang, L., Ma, B., Chen, Y., 2019. Hydrometallurgical recovery of lead from spent lead-acid battery paste via leaching and electrowinning in chloride solution. Hydrometallurgy 189, 105134. https://doi.org/10.1016/j.hydromet.2019.105134

Xu, X., Li, D., Chen, L., Liu, M., Liu, C., Jia, J., 2020. Improve the energy efficiency: Effects of additives on longtime zinc electrowinning. Hydrometallurgy 193, 105326. https://doi.org/10.1016/j.hydromet.2020.105326

Yaghoubi, M, 2021, Mn control in zinc electrowinning process by electrochemical means using Pb-Ag anode, M.Sc thesis, University of Laval.

Yan, H., Chai, L., Peng, B., Li, M., Peng, N., Hou, D., 2014. A novel method to recover zinc and iron from zinc leaching residue. Miner. Eng. 55, 103–110. https://doi.org/10.1016/j.mineng.2013.09.015

Yang, K., Zhang, L., Lv, C., Peng, J., Li, S., Ma, A., Chen, W., Xie, F., 2017. Role of sodium citrate in leaching of low-grade and multiphase zinc oxide ore in ammonia–ammonium sulfate solution. Hydrometallurgy 169, 534–541. https://doi.org/10.1016/j.hydromet.2017.03.013

REFERENCES (continued)

Yang, T., Rao, S., Zhang, D., Wen, J., Liu, W., Chen, L., Zhang, X., 2016. Leaching of low grade zinc oxide ores in nitrilotriacetic acid solutions. Hydrometallurgy 161, 107–111. https://doi.org/10.1016/j.hydromet.2016.01.024

Yang, T., Xie, B., Liu, W., Zhang, D., Chen, L., 2020. An environment-friendly process of lead recovery from spent lead paste. Sep. Purif. Technol. 233, 116035. https://doi.org/10.1016/j.seppur.2019.116035

Ye, M., Yan, P., Sun, S., Han, D., Xiao, X., Zheng, L., Huang, S., Chen, Y., Zhuang, S., 2017. Bioleaching combined brine leaching of heavy metals from lead-zinc mine tailings: Transformations during the leaching process. Chemosphere 168, 1115–1125. https://doi.org/10.1016/j.chemosphere.2016.10.095

Yoshida, T., 2003. Leaching of Zinc Oxide in Acidic Solution. Mater. Trans. 44, 2489–2493. https://doi.org/10.2320/matertrans.44.2489

Youcai, Z., Stanforth, R., 2001. Selective Separation of Lead from Alkaline Zinc Solution by Sulfide Precipitation. Sep. Sci. Technol. 36, 2561–2570. https://doi.org/10.1081/SS-100106110

Youcai, Z., Stanforth, R., 2000. Extraction of zinc from zinc ferrites by fusion with caustic soda. Miner. Eng. 13, 1417–1421. https://doi.org/10.1016/S0892-6875(00)00123-0

Yu, S., Chen, J., Chen, C., 1989. Stripping of Fe(III) extracted by di-2-ethylhexyl phosphoric acid from sulfate solutions with sulfuric acid. Hydrometallurgy 22, 267–272. https://doi.org/10.1016/0304-386X(89)90057-1

Yu, W., Zhang, P., Yang, J., Li, M., Hu, Y., Liang, S., Wang, J., Li, S., Xiao, K., Hou, H., Hu, J., Kumar, R.V., 2019. A low-emission strategy to recover lead compound products directly from spent lead-acid battery paste: Key issue of impurities removal. J. Clean. Prod. 210, 1534–1544. https://doi.org/10.1016/j.jclepro.2018.11.133

Zhang, W., Cheng, C.Y., 2007. Manganese metallurgy review. Part II: Manganese separation and recovery from solution. Hydrometallurgy 89, 160–177. https://doi.org/10.1016/j.hydromet.2007.08.009

REFERENCES (continued)

Zhang, Y., Deng, J., Chen, J., Yu, R., Xing, X., 2014. A low-cost and large-scale synthesis of nano-zinc oxide from smithsonite. Inorg. Chem. Commun. 43, 138–141. https://doi.org/10.1016/j.inoche.2014.02.032

Zhang, Y., Deng, J., Chen, J., Yu, R., Xing, X., 2013. Leaching of zinc from calcined smithsonite using sodium hydroxide. Hydrometallurgy 131–132, 89–92. https://doi.org/10.1016/j.hydromet.2012.10.007

Zhang, Y., Hua, Y., Gao, X., Xu, C., Li, J., Li, Y., Zhang, Q., Xiong, L., Su, Z., Wang, M., Ru, J., 2016. Recovery of zinc from a low-grade zinc oxide ore with high silicon by sulfuric acid curing and water leaching. Hydrometallurgy 166, 16–21. https://doi.org/10.1016/j.hydromet.2016.08.010

Zhang, Y., Jin, B., Huang, Y., Song, Q., Wang, C., 2019. Two-stage leaching of zinc and copper from arsenic-rich copper smelting hazardous dusts after alkali leaching of arsenic. Sep. Purif. Technol. 220, 250–258. https://doi.org/10.1016/j.seppur.2019.03.067

Zhang, Z., Li, W., Zhan, J., Li, G., Zhao, Z., Hwang, J.-Y., 2020. A Novel Technology for the Recovery of Zinc from the Zinc Leaching Residue by the Bottom-blown Reduction. Miner. Process. Extr. Metall. Rev. 1–8. https://doi.org/10.1080/08827508.2020.1793143

Zhao, Y., Stanforth, R., 2000. Production of Zn powder by alkaline treatment of smithsonite Zn–Pb ores. Hydrometallurgy 56, 237–249. https://doi.org/10.1016/S0304-386X(00)00079-7

Zhu, X., He, X., Yang, J., Gao, L., Liu, J., Yang, D., Sun, X., Zhang, W., Wang, Q., Kumar, R.V., 2013. Leaching of spent lead acid battery paste components by sodium citrate and acetic acid. J. Hazard. Mater. 250–251, 387–396. https://doi.org/10.1016/j.jhazmat.2013.02.018

Zhu, X., Zhang, W., Zhang, L., Zuo, Q., Yang, J., Han, L., 2019. A green recycling process of the spent lead paste from discarded lead–acid battery by a hydrometallurgical process. Waste Manag. Res. J. Sustain. Circ. Econ. 37, 508–515. https://doi.org/10.1177/0734242X19830175

REFERENCES (continued)

Zipperian, D., Raghavan, S., Wilson, J.P., 1988. Gold and silver extraction by ammoniacal thiosulfate leaching from a rhyolite ore. Hydrometallurgy 19, 361–375. https://doi.org/10.1016/0304-386X(88)90041-2